



The University of
Nottingham

UNITED KINGDOM · CHINA · MALAYSIA

Virus life cycle and the pathogenesis of malignant catarrhal fever

By

Osama Kumati

BVSc & MSc

**Thesis submitted to the University of Nottingham for
the degree of Doctorate of Philosophy**

**Division of Infection and Immunity
School of Veterinary Medicine and Science
The University of Nottingham**

May 2016

Abstract

Malignant catarrhal fever (MCF) is caused by two closely associated gamma herpes viruses namely alcelaphine herpesvirus 1 (AIHV-1) and ovine herpesvirus 2 (OvHV-2) and characterised with lymphocyte infiltration in non-lymphoid tissues, vasculitis and epithelial damage. The mechanism by which the viruses cause the disease is not fully understood. The hypothesis of this project was that MCF is initiated by aberrant gene expression in endothelium, epithelium and infected T cells of susceptible animals, because they are not the natural hosts for the viruses and the viruses will not have evolved in them. The first goal was to examine whether rabbit epithelium and bovine endothelium can be infected *in vitro* and *in vivo* with AIHV-1 using q PCR and, if infected whether viral transcripts could be identified in these tissue cells using q PCR and *in situ* hybridisation (ISH). The results revealed that endothelium and epithelium can be infected and latent infection can be established in them. This suggests the likelihood of establishing a similar type of infection *in vivo*. Secondly, the trial to identify latency-associated transcripts using 5-azacitidine treatment on bovine turbinate fibroblast (BT) cells and rabbit large granular lymphocytes (LGLs) was only partially successful. However, pan T antigen was expressed in 5-azacitidine treated but not untreated LGLs cells. This may indicate a function of the drug either directly or

through the latency state. Transcriptome analysis in the infected and treated LGLs and BT cells showed that several pathways were affected by 5-aza although a possible latency (low transcript levels) was only seen in the BTs. Transcriptome analysis revealed similar pathways to those described for MCF in the tissues *in vivo*, and an effect of 5-aza on these. Viral transcripts analysis showed that genes related to productive/lytic cycles were higher than latent ones on day 17 of the *in vivo* experiment demonstrating that the virus may replicate at this stage of the disease. The attempt to localize the viral transcripts on the rabbit infected tissues using ISH was unsuccessful due to a lack of time.

Declaration

I declare that the work in this dissertation was carried out in accordance with the regulations of the University of Nottingham.

The work is original and has not been submitted for any other degree at the University of Nottingham or elsewhere.

Name: Osama Kumati

Signature:

Date:

Conferences, posters, and oral presentations:

- Postgraduate (PG) research forum: a Research Poster presented; Faculty of Medicine, University of Nottingham, QMC. 15th June 2013.
- Research Day (first year); Oral Presentation, in Veterinary Medicine and Science; 15th July 2012.
- Research Day (second year); Oral Presentation, in Veterinary Medicine and Science; 13th February 2014.
- Research Day (third year); Oral Presentation, in Veterinary Medicine and Science; 18th June 2015.

Acknowledgements

I would like to express my sincere gratitude to my supervisors Professor. David Haig and Dr. Robbin Flynn for their scientific supervision and support. I am immensely grateful for opportunities you have given me. Your guidance helped me in all time of research and writing of this thesis. Many thanks for supervision and input.

I am also very grateful to Dr George Russell of the Moredun Research Institute for his involvement in the project and providing BT cells. I would also like to thank Professor. James Stewart of Liverpool University for giving me opportunity to be trained on ISH technique in his laboratory.

I would like to acknowledge the members of ADAC group at the University of Nottingham for their help and support with special thanks to Dr. Tom Giles. I'm also grateful to the staff, technician and postgraduate communities within the school for their help, interactions, support and advice.

Many sincere thanks go to Dr. Nivethitha Parameswaran and technician Belinda Wang for their technical knowledge during the research time. Without their invaluable input it would be difficult to carry out this research.

I wish to express my deepest gratitude to my late parents, also my wife and children for their patience and support and my family especially my sisters for their moral and financial support during my hardship.

Table of contents

1.1 Malignant catarrhal fever (MCF).....	1
1.1.1 General comments:	1
1.2 Aetiology of MCF.....	4
1.2.1 Herpes viruses	4
1.3 Malignant catarrhal fever viruses (MCFV)	8
1.4 Genomic structure of AIHV-1 and gene function	11
1.5 AIHV-1 genome sequence classification	14
1.6 AIHV-1 genome sequence	15
1.7 Spliced genes in AIHV-1 virus	16
1.8 Functions of non-conserved genes	17
1.9 Gene similarities to other herpes viruses	20
1.10 Gene expression of the MCF viral genome, latency and lytic cycles	21
1.11 Virulent and attenuated forms of AIHV-1	23
1.12 Virus life cycle	25
1.13 Latency	29
1.14 Symptoms and pathology of MCF	31
1.14.1 Clinical signs	31
1.14.2 Pathology of MCF	32
1.15 Epidemiology of MCF	34
1.15.1 MCF Transmission	34
1.15.2 Geographical distribution	35
1.15.3 Susceptible species	36
1.16 Disease Impact.....	37
1.17 Diagnosis of MCF	39
1.18 Treatment and prevention.....	41
1.19 Prospective vaccine development.....	43
1.20 Chemicals for the experiments.....	45
1.20.1 5-azacitidine.....	45
1.20.2 Cyclosporine A	45
1.21 Pathogenesis	46
1.21.1 Direct versus indirect mechanism of MCF	46
1.21.2 Experimental MCF	48
1.21.3 Large granular lymphocytes in MCF and their phenotype.	49
1.21.4 The role of cytokines in MCF pathogenesis	50
1.21.5 The site of infection and MCF pathogenesis	52
1.21.6 Recombinant AIHV-1	54
1.22 Hypothesis	55
1.23 Objectives.....	55
2.1 Introduction	57
2.2 Tissue culture.....	57

2.2.1 Large granular lymphocytes	58
2.2.2 Counting cells	59
2.2.3 Cryopreservation of cells	59
2.2.4 AIHV-1 virus stocks	60
2.2.5 Virus titration : 50% tissue culture infective dose (TCID50)	63
2.3 Molecular techniques.....	66
2.3.1 DNA extraction	66
2.3.2 RNA extraction	68
2.4 Nucleic acid amplification and quantitation	69
2.4.1 Complementary DNA (cDNA) synthesis.....	69
2.4.2 Polymerase chain reaction (PCR)	71
2.4.2.1 PCR condition.....	71
2.4.2.2 Agarose gel electrophoresis	71
2.4.3 Viral load measurement.....	73
2.4.4 Quantitative real-time PCR (q RT-PCR)	74
2.4.5 Quantification of DNA and RNA by spectrophotometer	78
2.5 Flow cytometry.....	79
2.5.1 Direct Immunofluorescence labelling of cells	81
2.5.2 Indirect Immunofluorescence labelling of cells.....	81
2.5.3 Flow cytometry analysis of labelled cells	82
2.6 Animals	82
2.6.1 Inoculation	83
2.6.2 Experiment (1) design.....	83
2.6.3 Experiment (2) design.....	84
2.6.4 Sample collection.....	84
2.7 Histology	85
2.7.1 Paraffin embedding	86
2.7.2 Tissue sectioning and staining	86
2.8.1 RNA <i>in situ</i> hybridisation	87
2.8.1.1 Preparation of riboprobes for virus gene transcripts.....	88
2.8.1.2 Primers design.....	88
2.8.1.3 Polymerase chain reaction (PCR) amplification.....	88
2.8.1.4 Gel extraction for ORF65 product	90
2.8.2 Plasmid cloning, transformation and bacterial culture	91
2.8.2.1 Plasmid purification	92
2.8.2.1.1 Minimum isolation of plasmid DNA (Mini-prep).....	92
2.8.2.1.2 Maximum isolation of plasmid DNA (maxi-prep).....	93

2.8.2.1.3 DNA sequencing	94
2.8.2.1.4 Restriction digestion for plasmid DNA preparation....	94
2.8.2.1.5 In vitro transcription of digoxigenin (dig)-labelled RNA probes	95
2.8.2.1.6 Dot blot analysis of generated probes.....	96
2.8.3 Deparaffinisation, proteolysis, and acetylation of tissue sections	98
2.8.4 Hybridisation of probes	99
2.8.5 Anti-DIG labelling for probe detection	100
2.9 RNA quality measurement using Agilent Bio-analyser Nano 6000 kit.....	102
2.10 RNA sequencing (RNA-Seq) methods.....	104
2.10.1 RNA poly (A) library	104
2.11 Illumina machine NextSeq500 sequencing platform work flow	106
2.12 Bioinformatics tools.....	107
2.12.1 Blast like alignment tool (BLAT)	107
2.12.2 Scythe-a Bayesian adapter trimmer	108
2.12.3 Sickle- a windowed adaptive trimming tool for FASTQ files using quality	108
2.12.4 HISAT	109
2.12.5 Sequence alignment map (SAM) tool.....	110
2.12.6 String Tie assembler tool	110
2.12.7 Ballgown.....	111
2.13 Statistical analysis	113
3.1 Abstract	114
3.2 Introduction	116
3.3 Materials and methods	118
3.3.1 Virus	118
3.3.2 Virus dose	118
3.4 In vitro infection.....	119
3.4.1 Direct virus infection.....	119
3.5 Results	121
3.5.1 Infection of the epithelial and endothelial cell lines.....	121
3.5.2 BAE endothelial cells	121
3.5.3 SIRC epithelial cells	123
3.5.4 Detection of viral DNA in the infected cells.....	125
3.5.5 Viral gene expression in the infected cells.....	127
3.6 Discussion	132
4.1 Abstract	136

4.2 Introduction	138
4.3 Materials and methods	139
4.3.1 Samples collection	139
4.3.2 Tissue culture and infection.....	139
4.3.3 Drug treatments.....	139
4.3.4 Flow cytometry.....	140
4.4 Results	141
4.4.1 Viral DNA detection.....	141
4.4.2 Viral DNA load in LGLs.....	143
4.4.3 The effect of 5-azacitidine on BT cells.....	144
4.4.4 Measuring viral gene transcripts	145
4.4.5 Flow cytometry analysis of LGL.....	148
4.5 Discussion	151
5.1 Abstract	158
5.2 Introduction	160
5.3 Materials and methods	162
5.3.1 Tissue and infection	162
5.3.2 RNA extraction	162
5.3.3 RNA quality measurement using utilizing Agilent Bio-analyser Nano 6000 kit.....	162
5.3.4 Complimentary (cDNA) DNA Library preparation and sequencing.....	163
5.3.5 Sequence analysis, bioinformatics and statistics	163
5.4 Results	165
5.4.1 Viral DNA load in LGLs.....	165
5.4.2 RNA Integrity Number (RIN) measurement	165
5.4.3 Mapping results.....	168
5.4.4 Differentially expressed host genes	171
5.4.5 Differentially-expressed virus genes detected by RNA-Seq	206
5.4.6 David clustering	208
5.4.7 IPA results	210
5.5 Discussion	215
6.1 Abstract	221
6.2 Introduction	222
6.3 Materials and methods	224
6.3.1 Animals.....	224
6.3.2 Inoculum	224
6.3.3 Experimental design.....	224

6.3.6 Molecular techniques.....	224
6.3.4 Samples collection	224
6.3.5 Histology	224
6.3.7 <i>In situ</i> Hybridization.....	224
6.4 Results	225
6.4.1 Experiment (1) results	225
6.4.1.1 Clinical signs	225
6.4.1.2 Gross appearance of MCF lesions.....	227
6.4.1.3 Viral DNA load measurement	227
6.4.1.4 Histological analysis of AIHV-1 in rabbits	229
6.4.1.5 Gene expression.....	236
6.4.1.6 <i>In situ</i> Hybridisation.....	239
6.4.2 Experiment (2) results	240
6.5 Discussion	243
7.1 General discussion	246
7.1.1 Conclusion and recommendations	257
7.1.2 Project summary	259
8.1 SOLUTIONS	261
8.1.1 DEPC water.....	261
8.1.2 ddH ₂ O	261
8.1.3 TrisHCl	261
8.1.4 CaCl ₂	261
8.1.5 MgCl ₂ -hexahydrate	262
8.1.6 NaCl.....	262
8.1.7 0.2 M HCl (Sterilize prior to use; not 2 N HCl)	262
8.1.8 PIPES.....	262
8.1.9 10x PBS	262
8.1.10 Buffer 1, pH 7,5.....	263
8.1.11 Buffer 3, pH 9.5.....	263
8.1.12 Buffer 4, pH 8.0.....	263
8.1.13 1x PBS + 5 mM MgCl ₂	264
8.1.14 2x SSC + 5 mM EDTA-Na ₂	264
8.1.15 0.2% Glycine in 1x PBS	264
8.1.16 4% paraformaldehyde (PFA)	264
8.1.17 50x Denhardt`s solution	265
8.1.18 20x hybridisation salts.....	265
8.1.19 Prehybridisation mix (PHB-Mix)	265

8.1.20 50x TAE Electrophoresis Buffer	266
8.1.21 1x TAE Electrophoresis Buffer	266
8.1.22 ssDNA	267
8.1.23 Proteinase K solution:.....	267
8.1.25 RNA stock solution	267
8.1.26 Dye solution	267
8.2 Rabbit DAVID cluster.....	269
8.3 Cattle DAVID clusters	283
8.4 Rabbit IPA analysis	298
8.5 Cattle IPA analysis	304
8.6 Rabbit to human with gene description	310
8.7 Rabbit DAVID analysis 1	312
8.8 Cattle to human with gene description.....	315
8.9 Cattle DAVID analysis 1	317
8.10 Scripts.....	320
8.10.1 EdgeR	320
8.10.2 Ballgown.....	323
8.10.3 Hisat	325
References	339

List of tables

Table 1 shows malignant catarrhal fever viruses and their resevoir and susceptible species (Li et al., 2014).....	9
Table 2 Function of unique genes in AIHV-1 and OvHV-2 (Russell et al., 2009).....	19
Table 3 example of virus titration	65
Table 4 primers and probes used for target and reference genes throughout the study.....	76
Table 5 Labelling steps.....	80
Table 6 shows AIHV-1 ORF65 and ORF A9.5 primer sequences and amplicon size.....	88
Table 7 Viral gene transcripts representing either productive or latent cycle or involved in the virus life cycle.	120
Table 8 Summary of results.....	131
Table 9 sample number, sample name, RNA concentrations and RNA integrity numbers (RIN) for LGL and BT samples sent for RNA-Seq analysis.	166
Table 10 conserved gene matrix of rabbit LGLs differentially expressed genes in the presence of 5-azacitidine in comparison to infected only control.	174
Table 11 conserved gene matrix of cattle's differentially expressed genes in the presence of 5-azacitidine in comparison to infected control.....	176
Table 12 up-regulated and down regulated of rabbit gene transcripts involved in lipid bio-synthesis	178
Table 13 up-regulated and down regulated LGL transcripts involved in the nuclear lumen pathway	179
Table 14 up-regulated and down regulated of LGL transcripts involved in the DNA repair pathway.....	183
Table 15 up-regulated and down regulated LGL transcripts involved in cellular death and apoptosis pathway	186
Table 16 up-regulated and down regulated LGL transcripts involved in the cell cycle pathway	189
Table 17 up-regulated and down regulated of cattle BT transcripts involved in the mitochondrion integrity pathway	192
Table 18 up-regulated and down regulated of cattle BT transcripts involved in endosomal pathways	197
Table 19 up-regulated and down regulated of cattle BT gene transcripts involved in the organelle lumen pathway.....	199
Table 20 up-regulated and down regulated of cattle BT gene transcripts involved in lysosomal pathways.....	203
Table 21 up-regulated and down regulated of cattle BT gene transcripts involved in purine and pyrimidine biosynthesis pathways	204

Table 22 summary of viral gene transcripts and viral DNA load in rabbit LGL and cattle BT cells in the presence and absence of 5-azacitidine as measured by qPCR and PCR approaches.....	207
Table 23 summary of ingenuity pathway analysis of rabbit LGLs in the presence of 5-azacitidine	212
Table 24 summary of ingenuity pathway analysis of bovine turbinate (BT) cells in the presence of 5-azacitidine	213
Table 25 shows the design of two rabbit's experiments infected and treated with cyclosporine A as long as pathological changes	226
Table 26 cyclosporine A experiment: AIHV-1 MCF histology on lymphoid and non-lymphoid tissues.....	230

List of Figures

Figure 1 schematic figure illustrates the simple structure of the herpes virus virion (stdgen.northwestern.edu/stdgen/bacteria/hhv2/herpes.html).....	5
Figure 2 demonstrates the genome structure of AIHV-1 and OvHV-2.	13
Figure 3 schematic map shows the changes in genes due to passage resulting in attenuation (Wright et al., 2003).	25
Figure 4 illustrates the herpesvirus life cycle steps from entry to egress. The entry happens when virus glycoprotein attaches to specific cell receptors. Un-coating of the virus takes place in the cytoplasm and linear DNA transferred to the nucleus where the replication and transcription occur. The virus is transported to the cytoplasm through inter-nuclear pore (INP) from the nucleus where complete assembly of the progeny virus takes place. The release of the Herpes virion occurs by budding.	27
Figure 5 snapshot of q RT-PCR amplification curve.	77
Figure 6 snapshot of q RT-PCR standard curve.	77
Figure 7 AIHV-1 PCR products for ORF A9.5 and ORF65 genes. ...	89
Figure 8 dot blot analysis of AIHV-1 ORF A9.5 RNA probe	97
Figure 9 shows the Agilent 6000 Nano chip appearance and its different loading wells	103
Figure 10 infection of bovine turbinate fibroblast (BT) cells	121
Figure 11 Infection of bovine aortic endothelial (BAE) cells	122
Figure 12 Infection of bovine turbinate BT cells with infected BAE123	123
Figure 13 Infection of SIRC epithelial cells	124
Figure 14 Infection of bovine turbinate BT cells with infected SIRC	125
Figure 15 qPCR products for low-pass AIHV-1 ORF3 gene visualised on agarose gel.	125
Figure 16 qPCR products for high-pass AIHV-1 ORF3 gene visualised on agarose gel	126
Figure 17 qPCR products for low and high pass AIHV-1 ORF3 gene visualised on agarose gel. Infected BT cells and controls uninfected BT, SIRC and BAE cells	127
Figure 18 AIHV-1 transcripts in infected BT cells	128
Figure 19 AIHV-1 transcripts in infected endothelial cells	129
Figure 20 AIHV-1 transcripts in infected epithelial cells	130
Figure 21 Q PCR and PCR products for AIHV-1 ORF3 gene	141
Figure 22 Q PCR and PCR products for AIHV-1 ORF3 gene	142
Figure 23 Q PCR and PCR products of AIHV-1 ORF A3 gene.....	143
Figure 24 AIHV-1 DNA copy number in rabbits' large granular lymphocytes.	144
Figure 25 BT cells infected with AIHV-1 C500 strain and infected and treated with 5-azacitidine.....	145
Figure 26 viral gene transcripts of AIHV-1 C500 in rabbit LGLs ...	147

Figure 27 viral gene transcripts of AIHV-1 C500 strain in BT cells	148
Figure 28 flow cytometry analysis of mononuclear cells in LGL non-treated and treated with 5-azacitidine.....	150
Figure 29 flow cytometry analysis of LGL double stained with two fluorescence antibodies in 5-azacitidine treated and non-treated IYDY cell lines	151
Figure 30 AIHV-1 DNA copy number in rabbit large granular lymphocytes	167
Figure 31 RNA Integrity Number.	168
Figure 32 genome coverage for rabbits (<i>Oryctolagus cuniculus</i> 2) and cattle (<i>Bos taurus</i> 8).....	169
Figure 33 mapping percentage for rabbits (<i>Oryctolagus cuniculus</i> 2) and cattle (<i>Bos taurus</i> 8) genomes.	170
Figure 34 differentially expressed AIHV-1 virus in rabbits' LGLs and BT cells.....	208
Figure 35 viral DNA load in lymph nodes and blood from rabbits tissues infected and treated with cyclosporine and infected only control animals.	228
Figure 36 viral DNA load in rabbits' tissues infected and treated with cyclosporine A and infected only controls.....	228
Figure 37 haematoxylin and eosin stain of rabbits' kidney	232
Figure 38 haematoxylin and eosin stain of rabbit's liver.....	233
Figure 39 haematoxylin and eosin stain of rabbit's lung.....	234
Figure 40 haematoxylin and eosin stain of rabbit's appendix.....	235
Figure 41 haematoxylin and eosin stain of rabbit's spleen.....	236
Figure 42 viral transcripts of six AIHV-1 genes in rabbits' tissues	238
Figure 43 haematoxylin and eosin stain in rabbit's liver (1)	241
Figure 44 viral DNA load in tissues in infected only and infected and treated with cyclosporine A group animals (1)	242

List of abbreviations

µl	Microliter
5-aza	5-azacitidine
AIHV-1	Alcelaphine herpes virus 1
APHA	Animal and plant health agency
BAC	Bacterial artificial chromosome
BAE	Bovine aortic endothelium
BLAT	Blast-like alignment tool
BT	Bovine turbinate fibroblast cells
CPE	Cytopathic effect
CpHV-2	Caprine herpes virus 2
CsA	Cyclosporine A
DEFRA	Department of environment, food and rural affairs
DEPC	Diethyl bicarbonate
DMSO	Dimethyl sulfoxide
DNA	Deoxyribonucleic acid
EBV	Epstein-Barr virus
ECACC	European Collection of Authenticated Cell Cultures
EHV-1	Equine herpesvirus 1
ELIZA	enzyme-linked immunosorbent assay
EM	Electron microscope
ET	Electron tomography

H-DNA	High guanine-cytosine (GC) content of DNA
HVS	Herpes virus saimiri
IFA	Immunofluorescence assay
IFN- γ	Interferon gamma
IL-2	Interleukin-2
IPA	Ingenuity Pathway Analysis
ISH	In situ hybridisation
Kbp	Kilo base pair
KSHV	Kaposi sarcoma-associated herpes virus
LANA	Latency associated nuclear antigen
LATs	Latency associated transcripts
L-DNA	Low guanine-cytosine (GC) content of DNA
LGLs	Large granular lymphocytes
MCF	Malignant catarrhal fever
MCFV	Malignant catarrhal fever virus
MCF-WTD	Malignant catarrhal fever- white tailed deer
ml	Millilitre
mRNA	Messenger Ribonucleic acid
NK	Natural killer cells
ORF	Open reading frame
OvHV-2	Ovine herpes virus 2
PCR	Polymerase chain reaction
RNA	Ribonucleic acid

RTA	R trans-activator protein
RT-PCR	Reverse- transcriptase PCR
SA-MCF	Sheep associated malignant catarrhal fever
SIRC	Serum institute rabbit cornea
TCR	T cell receptor
TGN	Transit Golgi network
WA-MCF	Wildebeest associated malignant catarrhal fever

Chapter 1

Introduction

1.1 Malignant catarrhal fever (MCF)

1.1.1 General comments:

Malignant catarrhal fever (MCF) is acute, systemic, lethal lymphoproliferative disease of cattle and even-toed ungulates including pigs, deer, and bison (Buxton, 1984; Plowright, 1960; Schultheiss, 2000). The disease is caused by group of viruses belonging to the *Herpesviridae* family, subfamily *Gammaherpesvirinae*, genus *Macavirus* (Li et al., 2005). Two viruses of this group that are known to cause MCF, alcelaphine herpes virus 1 (AIHV-1) and ovine herpes virus 2 (OvHV-2), are widely distributed and extensively studied (Russell et al., 2009). Wildebeest (*Connochaetes taurinus*) is the reservoir host for AIHV-1 in the sub-Saharan area, hence the name wildebeest-associated MCF (WA-MCF) for disease susceptible-animals that contract MCF from wildebeest. Sheep (*Ovis aries*) are the reservoir host for OvHV-2 worldwide; hence the name sheep associated MCF (SA-MCF) (Dewals et al., 2008, Russell et al., 2009). There are no clinical signs of MCF in the reservoir hosts, however, often-fatal MCF is seen when virus is transmitted to the disease-susceptible species (cattle, deer, bison, pigs and water buffalo) (Russell et al., 2009). The clinical signs of MCF range from per-acute to mild form and the outcome are usually fatal although recovery has been recorded. The most common symptoms recorded are high fever; salivation, nasal and ocular discharge, diarrhoea, and enlarged lymph nodes.

Pathologically, the disease is characterised with erosions and haemorrhages in the intestinal tract, vasculitis, and infiltration of lymphoid cells in non-lymphoid organs (kidney, lung, and liver) (CFSP, 2012, OIE, 2013). The importance of MCF lies in the fact that the disease is a major cause of death in many disease-susceptible animals worldwide that come into contact with reservoir hosts. It is also a serious welfare issue (Lankester et al., 2015a, Li et al., 2014). MCF occurs worldwide wherever reservoir and disease-susceptible animals are close to each other, and can affect a wide range of naturally-susceptible species within the Artiodactyl families Cervidae, Suidae, Bovidae, and Geravidae. Most of the well-adapted carrying hosts are within the subfamilies Hippotraginae, Alcellaphinae, and Caprinae, containing roan antelope, wildebeest, sheep, and goats (Li et al., 2005, Russell et al., 2009). Based on their susceptibility to MCF, animals can be classified as relatively resistant (such as European cattle to OvHV-2 MCF) intermediate susceptibility (e.g. water buffalo and most deer) to the highly susceptible ones like Pere David's deer, bison and Bali cattle (CFSP, 2012). Transmission of MCF is brought about by wildebeest calves and lambs between two to nine months through aerosol and close contacts (Li et al., 2011a, Mushi et al., 1981). MCF is associated with a high mortality rate (often 100% in outbreaks where clinical signs are observed) and low morbidity rate (sporadic) (Schultheiss et al., 1998). Rabbits and hamsters are good animal models for the

disease as they show similar clinical signs and pathological changes to those exhibited in the susceptible animals (Anderson et al., 2007, Buxton and Reid, 1980, Buxton et al., 1984).

Gross diagnosis of MCF can be achieved through noting the characteristic clinical signs and pathological changes. Nevertheless, an accurate (specific) diagnosis is necessary as well. Molecular tools such as the polymerase chain reaction (PCR) and serological tests like the enzyme-linked immunosorbent assay (ELISA) have become bench standards for detecting MCF viral DNA and antigen/antibody respectively (Fraser et al., 2006, Li et al., 2001). To date, there is no effective treatment for MCF (Li et al., 2014, Russell et al., 2009). However, there have been vaccine trials by several researchers most without success (Mirangi, 1991, Rossiter et al., 1977) until recently (Haig et al., 2008). Despite the fact that the disease is generally sporadic (affecting small numbers of animals) the incidence of MCF fluctuates year on year and continues to be a problem (Anderson et al., 2007). In some outbreaks MCF can affect up to 40 % of a herd (Russell et al., 2009). The details of the virus life cycle and the pathogenesis (the mechanism by which the disease happens) of MCF is still not well understood (Russell et al., 2009).

1.2 Aetiology of MCF

1.2.1 Herpes viruses

Herpes viruses comprise a large family of DNA viruses that induce disease in both animals and humans (Mettenleiter et al., 2009). The herpesvirion, an infectious virus particle, comprises an icosahedral capsid (Figure 1) consisting of 162 capsomeres (Mettenleiter et al., 2009) which contain a large double stranded linear DNA genome (125 to 240 kilo base pair Kbp), and encircled with an envelope holding glycoprotein spikes on its surface. The structure between the capsid and the envelope is called the tegument which is made up of proteins that are related to the capsid proteins (Pellett and Roziman, 2007). The aim of the productive/lytic infection is to produce progeny virions that are able to spread and infect new cells. In this type of infection, there are regulated viral genes expressions, and genome replication, virion assembly, egress and transmission. Early in this cycle, successive sets of genes are transcribed including α immediate early (IE) that are involved in initiation of virus DNA replication, β early (E) genes that act to DNA replication and control cellular activities such as RNA polymerase II (Estes *et al.*, 2007). After that, the transcription program switches to γ late genes expressing γ proteins. The newly replicated viral DNA is integrated into immature capsids and tegument proteins in the nucleus (Mettenleiter & Minson, 2006). The virus also gets its primary envelope in the nucleus, nuclear membranes play role in virus

capsid nuclear egress (Peng *et al.*, 2010). The virus gains its secondary membrane when buds through Golgi apparatus derived vesicles (Mettenleiter *et al.*, 2006). Eventually, mature virion fuse with the cell membrane and buds to the extracellular spaces (Mettenleiter, 2006).

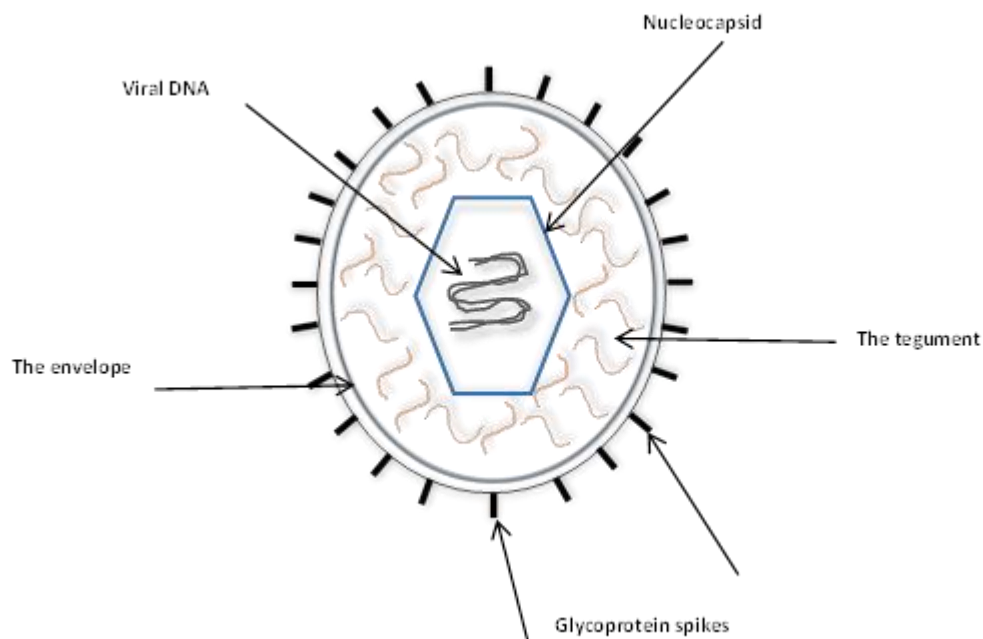


Figure 1 schematic figure illustrates the simple structure of the herpes virus virion (stdgen.northwestern.edu/stdgen/bacteria/hhv2/herpes.html).

The viruses of the family Herpesviridae have common biological features, i.e. they contain groups of enzymes that are implicated in metabolizing nucleic acid, DNA synthesis, and processing of proteins as well as the ability to establish latent infection in their natural hosts (Pellett and Roziman, 2007). The family Herpesviridae is classified into three subfamilies (*Alphaherpesvirinae*, *Betaherpesvirinae*, and *Gamaherpesvirinae*) according to their

biological properties and the viruses within these subfamilies further categorised to genera on the basis of resemblances in the DNA sequence (Pellett and Roizman, 2007).

Herpesviridae are well distributed in nature in a way that most animals have at least one herpesvirus and some viruses have more than one definitive host. To date more than 200 herpesviruses have been recognized, nine of which are human viruses (Pellett & Roizman, 2013). Viruses of veterinary importance are found in mammals, birds and fish. The range of diseases caused by herpesvirus infections is quite large. Moreover, the same virus can provoke different diseases, depending on the viral strain, the age of the animal or the route of infection. Bovine herpesvirus 1 (BHV-1) and Suid herpesvirus 1 (SHV-1) are good examples: BHV-1 infection of cattle causes rhinotracheitis, vulvovaginitis, conjunctivitis, abortion in pregnant cows, encephalitis in young calves, metritis; BHV-1 is also associated with enteritis and mastitis (Pastoret et al., 1982). SHV-1 infection of pigs is followed by abortion in pregnant sows, by septicaemia in neonates, by encephalomyelitis in piglets or by respiratory diseases in young pigs and adults. In domestic animals, clinical disease is usually produced following a primary infection; recrudescence disease, i.e. caused by a reactivated virus, seems to be rare. The situation differs in humans: labial and genital recrudescence lesions are commonly observed in humans infected with herpes simplex virus type 1 and 2 (HSV 1 and 2), even in the

presence of a high level of specific immunity (Nahmias et al., 1981). Shingles is a painful expression of reactivation of varicella-zoster virus, another human herpesvirus.

1.3 Malignant catarrhal fever viruses (MCFV)

Malignant catarrhal fever viruses (MCFV) belong to the genus *Macavirus* in the subfamily *Gammaherpesvirinae* within the family *Herpesviridae* (Davison et al., 2009, Gasper et al., 2012). The classification of these viruses within the genus *Macavirus* came after being categorised previously under the genus *Rhadinovirus*, and is based on the existence of the 15A antigenic epitope and also due to the resemblance in the conserved regions of the DNA polymerase gene among MCFV (Li et al., 2003, Russell et al., 2009). At least two of these viruses within the MCFV can give rise to the disease in naturally susceptible species and have been studied in detail- AIHV-1 and OvHV-2 (Davison et al., 2009). The MCFV group comprises ten viruses (Table 1). Six of these viruses have been recognised as pathogenic (capable of inducing disease in the susceptible host) (Li et al., 2003). The pathogenic ones consist of alcelaphine herpes virus 1 (AIHV-1), ovine herpes virus 2 (OvHV-2), alcelaphine herpes virus 2 (AIHV-2), ibex-MCFV, caprine herpes virus 2 (CpHV-2), and MCF- white tailed deer (WTD) (Gasper et al., 2012, Li et al., 2003). Wildebeest associated MCF (WA-MCF) caused by AIHV-1 poses an important problem in cattle in Eastern and Southern Africa and zoos where natural and susceptible species are kept together in the same vicinity. Sheep associated MCF (SA-MCF) is considered as a major problem in many parts of the world, in particular, to the highly vulnerable animals, like Bali cattle, Pere David's deer, and bison as

well as in zoological collections where sheep and susceptible animals co-mingle (Heuschele, 1988, Plowright et al., 1960, Schultheiss et al., 1998).

Table 1 shows malignant catarrhal fever viruses and their reservoir and susceptible species (Li et al., 2014).

The virus	Disease documented	natural host	Susceptible host
AIHV-1	√	Wildebeest	cattle
AIHV-2	√	Hartebeest	Deer and bison
OvHV-2	√	Sheep	Cattle, deer, bison, pigs, and giraffe
CpHV-2	√	Goat	Sika deer and white tailed deer
Ibex-MCF	√	Ibex	Bongo and anoa
MCF-WTD	√	Unknown	White tailed deer
HiHV-1	X	Roan antelope	Unknown
Oryx-MCF	X	Oryx	Unknown
Muskox-MCF	X	Muskox	Unknown
Aoudad-MCF	X	Aoudad	Unknown

Abbreviations: AIHV-1, alcelaphine herpes virus 1. AIHV-2; alcelaphine herpes virus 2. OvHV-2; ovine herpes virus 2, CpHV-2; caprine herpes virus 2, Ibex-MCF; ibex9-malignant catarrhal fever, MCF-WTD; MCF-white tailed deer, HiHV-1; hippotrogine herpes virus 1, Oryx-MCF; Oryx-malignant catarrhal fever, Muskox-MCF; Muskox-malignant catarrhal fever, Aoudad-MCF; Aoudad-malignant catarrhal fever. √: Yes, X: NO.

The reservoir host for MCFV-WTD is still unidentified. However, the virus can infect and give rise to MCF in white tailed deer in North America and the virus was found to be genetically closely related to AIHV-1 and OvHV-2 (Li et al., 2000). Domestic and wild goats are

the reservoir hosts for CpHV-2 and the virus is endemic in them. In addition, it has been reported that the virus can cause MCF in a wide range of species including pronghorn antelope, white tailed deer, and sika deer. The most common symptoms associated with the CpHV-2 MCF are emaciation, alopecia, and dermatitis (Keel et al., 2003, Li et al., 2011b). AIHV-2, initially, was classified as apathogenic under natural circumstances. Nevertheless, the virus was isolated from Jackson's hartebeest which induced MCF in Barbary red deer leading to the observation that the virus can be pathogenic (Klieforth et al., 2002, Li et al., 2003, Li et al., 2005). Ibex MCF virus found in ibex is capable of inducing MCF in bongo, an American forest antelope and in anoa (midget buffalo) (Li et al., 2011b). The non-pathogenic MCFV are Hippotragine herpes virus 1 (HiHV-1) and Oryx-MCFV in roan antelope and Oryx respectively with no recognisable susceptible hosts as well as Muskox and Aoudad MCFV in Muskox and Aoudad also with no susceptible hosts recognised to date (Li et al., 2005).

1.4 Genomic structure of AIHV-1 and gene function

AIHV-1 can easily be grown in cell culture. In contrast, it has been difficult to propagate OvHV-2 *in vitro*. This has hindered the study of OvHV-2 virology, infection, and pathogenesis. However, the use of T-lympho-blastoid cell lines with the morphology of large granular lymphocytes (LGL) derived from organs from MCF-affected animals has enabled researchers to study the host-virus communication (Hart et al., 2007a). These large granular lymphocytes are large lymphoblasts that can grow in the absence of exogenous cytokines and are indiscriminately cytotoxic, killing various target cells in a non-MHC-dependent manner (swa et al., 2001). The two viruses have had their genomes sequenced (Figure 2) (Ensser et al., 1997a, Hart et al., 2007a). The OvHV-2 genome is very similar to that of AIHV-1 and herpesvirus saimiri (HVS), a *gama*herpesvirus categorised under the genus Rhadinovirus. Both viruses have a unique sequence of around 131 kbp and these are flanked by terminal repeats of 4.2 kbp and 1.1 kbp for OvHV-2 and AIHV-1 respectively. OvHV-2 has 73 open reading frames (ORFs), 62 of which have homologues in other *gama*herpesviruses whereas AIHV-1 contains 70 ORFs, 61 of which are conserved among other *gama*herpesviruses. Eight out of the 10 unique genes, designated A1 to A10 in AIHV-1, have homologues in OvHV-2 while OvHV-2 includes 3 completely unique ORFs, i.e. Ov2.5, Ov3.5, and Ov8.5 (Ensser et al., 1997a, Hart et al., 2007a). All ORFs of the two

viruses were named after those within the other *gama*herpesviruses. As such, ORFs with similarity in herpesvirus saimiri were given the number of the related herpesvirus saimiri gene. Those which are unique to each virus were designated prefixes with A and Ov for AIHV-1 and OvHV-1 respectively followed by numbers one to ten. The unique genes of OvHV-2 assigned a nomenclature showing the relative position of the adjacent genes, for example, Ov2.5 locates between OV2 and Ov3 and so on and so forth for the other genes (Hart et al., 2007a, Russell et al., 2009).

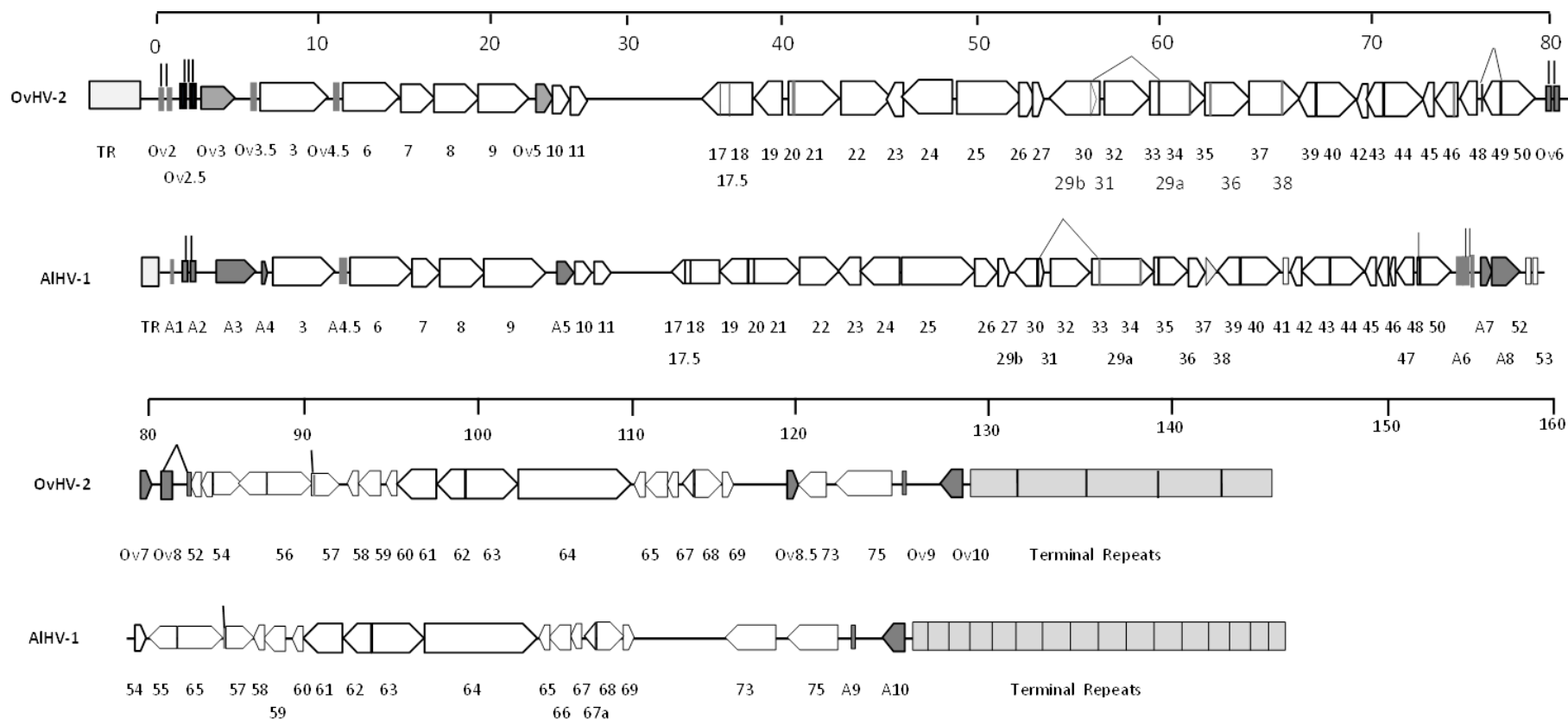


Figure 2 demonstrates the genome structure of AIHV-1 and OvHV-2. Genes are shown as block arrows representing their orientation and position of open reading frames. Gene designations are written below according to the numbering system adopted in Herpes virus saimiri. The unique genes in both viruses are shaded grey and named beneath each gene with a prefix A for AIHV-1 virus and Ov for OvHV-2 whereas conserved genes are shown as white arrows. The terminal repeats (TR) are given grey shaded blocks. (Russell et al., 2009).

1.5 AIHV-1 genome sequence classification

Following the complete AIHV-1 DNA genome characterized by Ensser and co-researchers in 1997, Coulter et al. (2001) arranged the Herpesvirus genome sequences in five blocks, designated the roman numbers, based on the gene similarity among the viruses within this family. Blocks I, II, IV include ORFs that are conserved within all herpesviruses subfamilies while blocks III and V comprise ORFs that are conserved between the subfamily *Gamaherpesvirus* only. Block I contains ORFs 6 to 9. Block II contains ORFs 17 to 47. Block III contains ORFs 48 to 50. Block IV contains ORFs 52 to 69. Block V contains ORF75.

There are changeable areas which can be assigned A-F disseminated between these conserved blocks of genes throughout the family of Herpesviruses. In AIHV-1 area A comprises A1 to A4 and ORF3. Area B comprises A5 and ORFs 10 and 11. Area D/E comprises A6, A7, A8, ORFs 73, 75, A9, and A10 (Coulter et al., 2001).

1.6 AIHV-1 genome sequence

As in Herpesvirus saimiri, the low guanine-cytosine (GC) content (L-DNA) (46.17%) in AIHV-1, which contains the coding ORFs is surrounded by high GC content area of nucleotide repeats (H-DNA) (71.83%) which is considered as predominately a non-coding region (Ensser et al., 1997a). The L-DNA region of around 131,000 Kbp nucleotide sequence comprises (Figure 2) 70 ORFs as previously found by Ensser et al. (1997a). However, Mills et al. (2003) and Russell et al. (2013) discovered two new ORFs in AIHV-1 virus located in the inter-genic spaces between ORF 6 and ORF3 (designated ORF A4.5) and between ORF A9 and ORF A10 which is assigned ORF A9.5. This brings the number of open reading frames in the L-DNA region to 72 ORFs instead of 70 as previously stated. Consequently, the number of the unique genes (shared by AIHV-1 and OvHV-2 plus unique to AIHV-1) in AIHV-1 virus is twelve to date. Ten of these have homologues in OvHV-2 and two are unique to AIHV-1. Ovine herpes virus genes Ov2 and Ov3 which have homologues in AIHV-1 lie in the left end of the unique region whereas Ov2.5 and Ov3.5 locate in the same area but with no homology with AIHV-1 genes (Hart et al., 2007a, Russell et al., 2009).

The ORFs A1 to A4 are located at the left end of L-DNA genome and at the right end of the H-DNA region whereas ORF A4.5 and Ov4.5 lie between ORF3 and ORF6 (Coulter et al., 2001, Hart et al., 2007a,

Russell et al., 2009). ORF A5 and Ov5 locate between ORFs 9 and 10 (Coulter et al., 2001, Hart et al., 2007a). ORFs A6, A7, A8 and Ov6, Ov7, and Ov8 locate amongst ORF50 and ORF52. Ovine herpes virus Ov8.5 with no homology in AIHV-1 locates between ORF73 and ORF69 (Hart et al., 2007a, Russell et al., 2009). ORF A9 and Ov9 locate after ORF75 towards the right H-DNA genome while A10 and Ov10 locate adjacent to and to the left of the right H-DNA repeat (Coulter et al., 2001, Hart et al., 2007a, Russell et al., 2009). ORF A9.5 and its homologues Ov9.5 lie between A9 and A10, and Ov9 and Ov10 respectively (Russell et al., 2014, Russell et al., 2013). Figure 2 shows the location of the unique genes on both AIHV-1 and OVHV-2 genomes.

1.7 Spliced genes in AIHV-1 virus

Splicing is a process that happens in the nucleus after transcription to RNA in which the introns are removed and the exons are joined together to make mRNA which can then be translated to a protein within the ribosomes (House, 2008; Poulos, 2011). This process is important as it removes the introns (non-coding sequence) and joins exons (coding-sequence) to produce mature mRNA.

In the two MCF viruses that have been sequenced (AIHV-1 and OvHV-2) splicing takes place in both conserved and unique ORFs (Ensser et al., 1997a, Hart et al., 2007a). ORF A2 encodes a spliced product and ORF50 the R-transactivator gene is expected to show

splicing due to the fact that herpesviruses equivalent genes exhibit splicing (Ensser et al., 1997a).

1.8 Functions of non-conserved genes

ORF A1 has no homology to other herpes virus ORFs and its putative protein product is not similar to any known proteins with no known function. It is therefore assumed to be non-functional or a pseudogene (Russell et al., 2009). Table 2 lists the known and predicted functions of the twelve unique genes of AIHV-1. ORF A2 and ORF Ov2 are similar to ATF3 which is considered as stress-induced transcription factor. A2 gene and its product is a member of the basic leucine zipper proteins implicated in altering host genes expressions. Therefore, they may play a role as transcription factor (Hart et al., 2007a, Parameswaran et al., 2014). Nevertheless, AIHV-1 ORFA2 is dispensable for the induction of MCF (Parameswaran et al., 2014). Semaphorins are huge family of glycoproteins that are found in all vertebrates and invertebrate's species in addition to viruses (Jongbloets et al., 2013). It has been found that these proteins are involved in many biological activities like cancer, bone haemostasis, and immune system (Xu et al., 1998). Semaphorin 7A (SEMA7A) is encoded by AIHV-1 ORF A3 and OvHV-2 ORF Ov3 homologue (Myster et al., 2015). However, AIHV-1 ORF A3 has not been implicated in lymphocytes infiltration in MCF but is essential for avoiding immune evasion (Myster et al., 2015).

Ovine herpes virus Ov3.5 is a unique gene with no similarity to any other viral genes encoding a putative signal peptide. Therefore, it thought to be secreted by the infected cells (Hart et al., 2007a, Thonur et al., 2006). ORF A4 has no obvious role with no homology to other herpes virus ORFs (Russell et al., 2009). ORF A4.5 is similar to OvHV-2 Ov4.5 which encodes a protein similar to Epstein-Barr virus EBV BALF1 and cellular B-cell lymphoma genes of the Bcl-2 family that regulate programmed cell death (apoptosis). It seems therefore that this gene may be involved in inhibiting/supporting cell death, hence encouraging cell survival and establishment of productive and / or latent infection cycles (Hart et al., 2007a, Russell et al., 2009).

Table 2 Function of unique genes in AIHV-1 and OvHV-2 (Russell et al., 2009).

AIHV-1 ORF	OvHV-2 ORF	Function
A1		Unknown
A2	Ov2	Leucine zipper protein; transcription regulation
	Ov2.5	Viral IL-10
A3	Ov3	Semaphorin homologue; intracellular signalling
	Ov3.5	Unknown, signal peptide
A4		Unknown
A4.5	Ov4.5	Bcl-2 homologue; cell death regulators
A5	Ov5	GPCR (G-protein coupled receptor); intracellular signalling
A6	Ov6	Similar to Epstein-Barr virus BZLF1; viral transactivator
A7	Ov7	Virus glycoprotein
A8	Ov8	Virus glycoprotein
	Ov8.5	Unknown
A9	Ov9	Bcl-2 homologue; cell death regulators
A9.5	Ov9.5	Secreted glycoprotein with unknown function
A10	Ov10	Unknown, glycoprotein

ORF A5 is similar to OvHV-2 Ov5 encodes a G protein-coupled-receptors orthologue (GPCRs), hence it may play a role in modulating the host immune defence or any of the other functions of this diverse family of molecules (Ensser et al., 1997a, Hart et al., 2007a). However, the role of this ORF was investigated using the bacterial artificial chromosome AIHV-1BAC to produce a recombinant virus with a deleted A5 gene. Animals infected with this clone developed MCF-like syndrome indicating that A5 has no function in the development of MCF (Boudry et al., 2007). ORF A6 is similar to OV6 encodes a protein similar to EBV BZLF1 which encodes a protein considered as a transcriptional factor that is responsible for

the activation of early genes leading to latent / lytic cycle switch (Coulter et al., 2001, Hart et al., 2007a). ORF A7 and A8 and their homology Ov7 and Ov8 in OvHV-2 virus are viral glycoproteins and may have a role in cell attachment and entry to the host cell (Coulter et al., 2001, Hart et al., 2007a, Russell et al., 2009). ORF A9 and Ov9 has similar predicted function to ORF A4.5 as it has homology to bcl-2 anti-apoptosis family genes and therefore may inhibit/induce the host cell death (Coulter et al., 2001, Russell et al., 2009) to enhance productive and /lytic infections. ORF A10 is putative (unknown gene function) glycoprotein and may be involved in cell attachment and entry to the host cell (Coulter et al., 2001). ORF A10, similar to Ov10, is putative (unknown gene function) glycoprotein and may be involved in cell attachment and entry to the host cell (Coulter et al., 2001, Hart et al., 2007a, Russell et al., 2009). Ovine herpes virus Ov8.5 with no similarity to any genes in AIHV-1 genome has no identified function (Hart et al., 2007a, Thonur et al., 2006). ORF A9.5 is similar to Ov9.5 encoding secreted glycoprotein that is similar to IL-4 (Lankester et al., 2015b, Russell et al., 2014, Russell et al., 2013). However, the role of this gene in inducing MCF is still unknown.

1.9 Gene similarities to other herpes viruses

AIHV-1 ORF73, encodes latency associated nuclear antigen (LANA), is homologous to latency associated transcripts of other herpes

viruses including HHV-8- also known as Kaposi's sarcoma-associated herpesvirus (KSHV LANA) ORF73 (Palmeira et al., 2013, Taus et al., 2007), herpes saimiri ORF73 (Blake, 2010), And EBV Epstein Barr nuclear antigen (EBNA1) (Blake, 2010). These are important for the viral latency cycle (Hu et al., 2002). It looks likely therefore that AIHV-1 ORF73 has the same function (Dewals et al., 2008, Palmeira et al., 2013). The R transactivator (RTA) ORF50 has a role in switching from latency to lytic replication responsible for the productive life cycle (Frame and Dalziel, 2008, Goodwin et al., 2001, Staudt and Dittmer., 2007). ORF 25 homologue is conserved in all herpesviruses and encodes a major capsid protein (Ensser et al., 1997a). This ORF product is expressed during the lytic cycle demonstrating viral replication (Cunha et al., 2008, Dewals et al., 2008). ORF63 is conserved among other herpes viruses and encodes a tegument structural protein (Boyle and Monie, 2012, Ensser et al., 1997a). The presence of these proteins is associated with the expression of ORF50/ORF25 responsible for productive/lytic cycle (Gailbreath et al., 2008, Meier-Trummer et al., 2009b).

1.10 Gene expression of the MCF viral genome, latency and lytic cycles

Based on the genome sequence of OvHV-2, Thonur et al. (2006) studied the transcription of OvHV-2 genes and its conformation in lymphocytes from both natural (wildebeest and sheep) and

susceptible hosts (cattle, bison, pigs, deer, water buffalo). OvHV-2 viral genome from peripheral blood mononuclear cells derived from sheep (natural host reservoir species) was primarily circular as measured using Gardella gel analysis, indicating a latent conformation and mRNA for only Ov3.5 unique gene, encoding a putative signal peptide which thought to be secreted by the infected cells, was identified. In contrast, cultured large granular lymphocytes (LGL), have natural killer (NK)/T cells morphology, contain enriched-population of infected cells and are good source to study virus-host interaction, from the rabbit (a MCF-susceptible species following experimental infection) had mainly a linear viral genome indicating productive cycle whereas bovine (natural disease-susceptible host) LGL cultures contained mainly circular viral DNA indicating latency dominance. Both these susceptible species genomes expressed nearly all of the virus unique genes. Their expression in this experiment indicates that they may be involved some way in MCF pathogenesis. Treating the LGLs from the susceptible species with doxorubicin, a drug used for cancer treatment that drives the productive life cycle (AbuHammad and Zihlif, 2013, Feng et al., 2004, Rahman et al., 2001), stimulated predominantly linear genome from latent circular ones, while treatment with 5-azacytidine, a drug utilised to stimulate latency in EBV-infected tissues (Feng et al., 2004, Mossman et al., 1989, Schaefer et al., 1997), supported circular genome production in LGL

lines and a range of putative latency transcripts (Thonur et al., 2006). In spite of productive cycle gene expression, no virions were detected by electron microscopy (EM) in the cultures, indicating an incomplete virus life cycle (Thonur et al., 2006). These results are in agreement with the previous work of Rosbottom and co-researchers who made the same conclusion (Rosbottom et al., 2002).

In particular, OvHV-2 and AIHV-1 gene expression in the tissues of infected cattle or rabbits indicated that the latency transcript ORF 73 could be detected, leading to a belief that MCF is a disease of latency (Meier-Trummer et al., 2009a, Palmeira et al., 2013). In contrast, other researchers have shown evidence of viral replication and productive virus associated with this (Cunha et al., 2012, Cunha et al., 2013, Li et al., 2008a, Nelson et al., 2013). The structural viral proteins (as mRNA transcripts) were identified in organs within SA-MCF virus-infected rabbits indicating viral replication was occurring (Gailbreath et al., 2008). In addition, it was found that there was low expression of ORF50 in lymphoid tissues extracted from WA-MCF-affected rabbits, which might indicate productive infection (Dewals et al., 2008).

1.11 Virulent and attenuated forms of AIHV-1

AIHV-1 C500 strain derived from a cow (Plowright et al., 1960, Plowright et al., 1975) that developed MCF can be cultured in bovine turbinate (BT) cells (Handley et al., 1995). After several passages

(up to 5 times) the virus exists as free virus that is virulent and can cause disease when injected into MCF-susceptible animals (Dewals et al., 2011, Haig et al., 2008, Palmeira et al., 2013, Parameswaran et al., 2014) but as culture passages proceed, the proportion of virus that is attenuated (i.e. cannot induce disease when injected into MCF-susceptible animals) increases. Virus can exist as free in culture or as a proportion that is cell-associated and not excreted into the cultures (Wright et al., 2003). Handley et al. (1995) conducted the first study of these changes. They found out that an area in the middle of AIHV-1 DNA was deleted that results in virus attenuation. This region contains the distal part of ORF 50b, proximal part of A6 and distal part of A10.

The AIHV-1 C500 strain was completely sequenced by Ensser et al., (1997a), allowing more detailed study. Wright et al. (2003) discovered that after multiple passages *in vitro* there was evidence of gene deletion, translocation, and duplication that could be involved in attenuation process. Candidate ORFs included ORF50 and ORF A6 that were truncated and translocated (distal part of ORF 50b, proximal part of A6 and distal part of A10). ORF48 and ORF A7 might have been affected which locate to either side of the translocated fragments (Figure 3) (Wright et al., 2003).

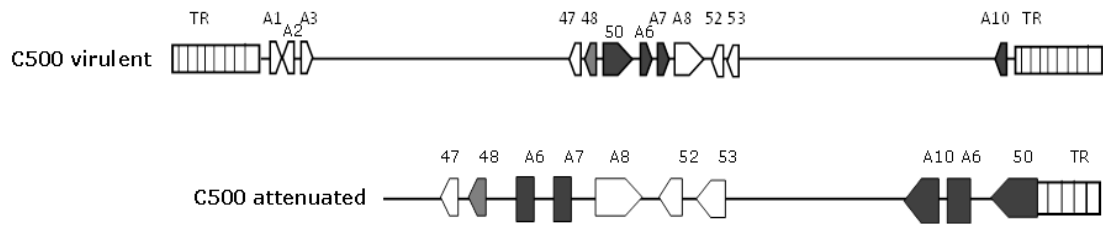


Figure 3 schematic map shows the changes in genes due to passage resulting in attenuation (Wright et al., 2003).

A further proteomic study identified differences in protein expression between the virulent and attenuated forms of AIHV-1 (Dry et al., 2008). This revealed that 23 virus proteins were expressed in both virus forms. This means that there was no change in the structural composition of the virulent and attenuated viruses detectable by this method. It was concluded therefore that the attenuation of the virus was not due to the virus particle structure, but perhaps a result of altered viral gene expression in the infected cell (Dry et al., 2008).

1.12 Virus life cycle

The life cycle (Figure 4) of viruses of the herpesvirus family is initiated when the virus engages with the host cell surface, binding to specific receptors, for example, it was shown that gD of herpes simplex virus-1 (HSV-1) bound to the herpes virus entry mediator A (HveA receptor) whereas gp42 of Epstein-Barr virus (EBV) bound to HLA-DR (Flint et al., 2009). The receptors used by MCF-related viruses to enter the host cell are still not known (Russell et al., 2009). After binding of viral envelope glycoproteins to cell

membrane receptors, entry is brought about by membrane fusion proteins. By contrast, a study carried out to identify the different stages of *Gammaherpesvirus* life cycle using murine gammaherpesvirus 68 (MHV 68) and utilizing dual-axis electron tomography (ET) revealed that the entry occurs by endocytosis (Peng et al., 2010). Once the virion is internalised, un-coating or disassembling occurs and the DNA genome is released and then transported *via* transit Golgi network (TGN) to the nucleus where the linear double stranded DNA genome is circularised by covalent bonds before replication. After that, viral DNA is transcribed into early mRNAs which are then transported to the cytoplasm for early protein synthesis. These early proteins are imported into the nucleus and promote viral DNA replication. The viral DNA is then transcribed into the late mRNAs which are responsible for late viral protein synthesis (capsid and envelope proteins). The viral envelope proteins are processed in the endoplasmic reticulum (ER) and Golgi complex. The capsid proteins are imported into the nucleus and then encapsidate the newly replicated genomes. The assembly of the progeny virions partially occurs in the nucleus and in the cytoplasm by the Golgi membranes. The release of the enveloped virus from the host cell occurs by budding (Flint et al., 2009).

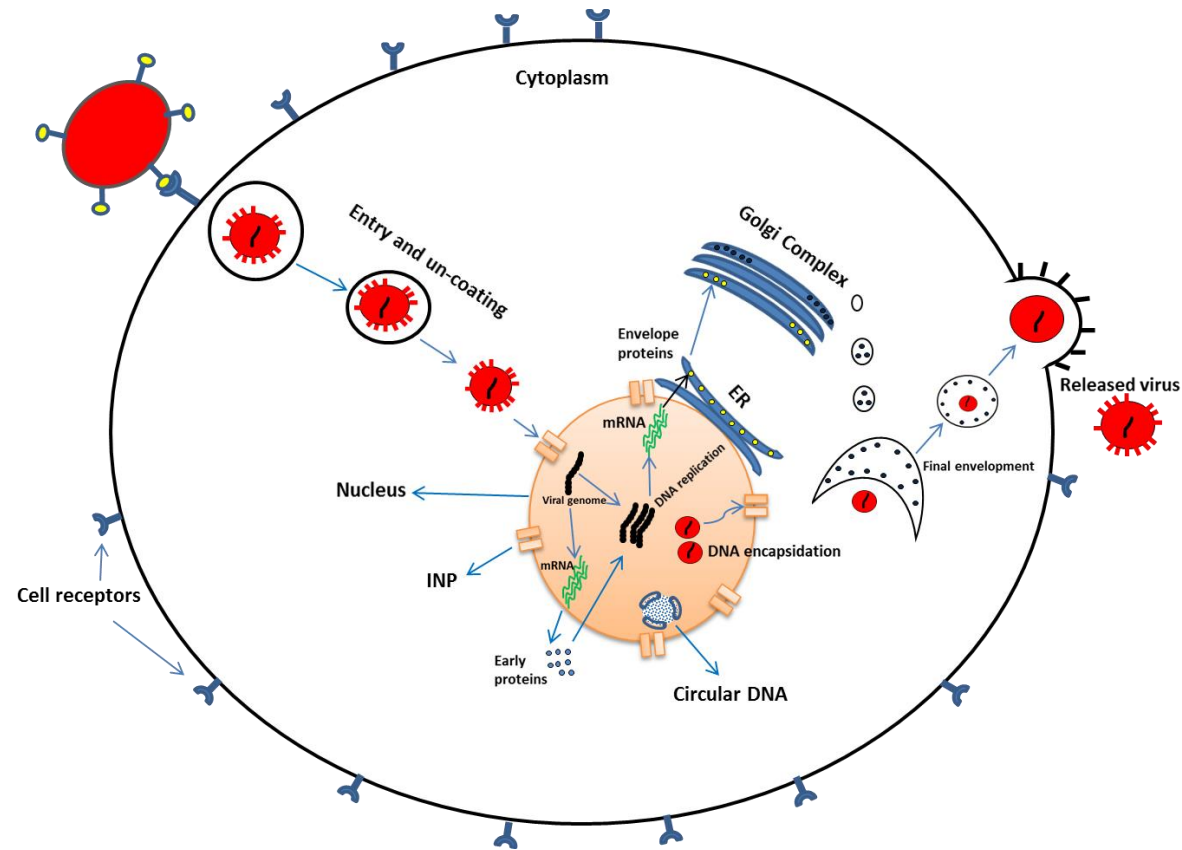


Figure 4 illustrates the herpesvirus life cycle steps from entry to egress. The entry happens when virus glycoprotein attaches to specific cell receptors. Un-coating of the virus takes place in the cytoplasm and linear DNA transferred to the nucleus where the replication and transcription occur. The virus is transported to the cytoplasm through inter-nuclear pore (INP) from the nucleus where complete assembly of the progeny virus takes place. The release of the Herpes virion occurs by budding.

There have been studies carried out on MCF viruses' replication, in particular, OvHV-2. These studies were able to identify the stages through which OvHV-2 replicate in both reservoir and susceptible host (Li et al., 2008a, Rosbottom et al., 2002, Taus et al., 2010). In sheep, the reservoir host for SA-MCF, the virus initially replicates in particular in the alveolar epithelium of the lung. This takes place in the early stage of the disease course. Afterwards, the virus disseminates into the blood (tropism) favouring the lymphocytes where it can establish latent infection (Li et al., 2008a, Taus et al., 2010). Ultimately, the virus targets the respiratory system, especially the lung and nasal sinuses where it departs the host in a cell-free form (Cunha et al., 2012). In susceptible species such as rabbits and bison that have been experimentally infected, the pattern of infection, initially, is similar to the reservoir host where the virus replicates in the lung tissue and then disseminates into the blood. However, the pattern here varies from the one in the reservoir host. The expression of ORF50, ORF25, and ORF73 is marked in most of the tissues (Cunha et al., 2012). The expression of ORF63 and ORF43 genes encoding structural proteins in the tissues of the susceptible species supports the incidence of viral replication (Meier-Trummer et al., 2009b). With regard to AIHV-1 virus, the details of virus life cycle are still unknown. Nonetheless, recent work has shown that the virus replicates in the lung of the susceptible species in very early clinical stage and then disseminate

into the blood where it establishes latency in T lymphocytes (mainly CD8⁺ T lymphocyte) (Myster et al., 2015, Palmeira et al., 2013).

1.13 Latency

MCF-associated viruses (AIHV-1 and OvHV-2) are assumed similar to the viruses of the family *Herpesviridae* in terms of their ability to become latent. The herpes viruses are able to establish latency in natural host tissues and sometimes in tissue culture (Flint et al., 2009). The hallmark of this stage is that the viral genome is preserved as a circular episome inside the nucleus, few viral genes are expressed (Virgin et al., 1999), and no virions produced. Moreover, the cytopathic effects (cell lysis due to the lytic virus cycle) are inhibited and the virus can avoid the host immune control (Blake, 2010). Reactivation occurs when the host immune system is stressed or compromised (Russell et al., 2009). Different herpesviruses have the ability to establish latency in certain cells. For example, Herpes simplex virus (HSV) remains latent in peripheral sensory ganglia (Flint et al., 2009) whereas the Epstein-Barr virus undergoes latency in B lymphocytes and epithelial cells (Mesri et al., 1996). In regard to the MCF-associated viruses AIHV-1 or OvHV-2, the site in which the viruses establish latency it is still unknown (Russell et al., 2009).

The mechanism by which Herpes viruses establish latency is complex and not completely known (Flint et al., 2009, Nicoll et al.,

2012). In herpes simplex virus 1 (HSV 1), supporting of latency goes through two important steps. In the first one the virus suppresses the expression of lytic cycle genes and secondly prevent programmed cell death (apoptosis) (Nicoll et al., 2012). The expression of latency associated transcripts (LAT) is important in establishing latency in HSV1 and HSV 2 (Nicoll et al., 2012). LAT is a set of RNAs encoded from the virus genome resulting in the construction of minor LAT transcripts. These transcripts inhibit the immediate early genes (IE), such as ICP0 (transcriptional activator) and ICP4 (transcriptional regulator), required to initiate lytic/productive cycle in the host cell (Nicoll et al., 2012). In addition, LATs are involved in repression of proteins production such as glycoprotein gD and gJ, ICP27 (transcriptional factor), ICP10 (apoptotic regulator), which is responsible for the promotion of cell survival (Nicoll et al., 2012).

The role of micro-RNA (miRNA) in regulating viral latency has been highlighted. Micro-RNA is non-coding sequence belongs to the RNA family and found in plants, animals, algae and viruses (Griffiths-Jones, 2008). EBV and KSHV which belong to *gammaherpes* virus subfamily, have been found to encode miRNAs (Pfeffer, 2005) that are associated with immune response (Grundhoff, 2011) and also have anti-apoptotic role (Seto, 2010).

1.14 Symptoms and pathology of MCF

1.14.1 Clinical signs

Animals affected include cattle, deer, bison, and pigs. The signs are similar for AIHV-1 and OvHV-2 MCF. The clinical signs of MCF are diverse as the disease can affect many systems of the infected animals including the digestive system, respiratory system, head and eye, nervous system, and uro-genital system (Liggitt and DeMartini, 1980a, Liggitt and DeMartini, 1980b, Russell et al., 2009). MCF has many forms ranging from peracute to mild stages. The symptoms are few in the peracute phase, which is characterised by sudden death. However, depression, weakness, dysentery may develop 12 to 24 hours before the onset of death. This is mostly seen in the highly susceptible species (CSFH, 2012; OIE, 2013). In the acute form, the clinical signs are more obvious and are associated with the emergence of high fever, inappetence, lachrymation, nasal discharge which progresses to mucopurulent, corneal opacity, decrease in milk production, and skin lesions in the form of ulceration and exudation that are mainly found in perineum, udder and teats. Salivation, erosions of the tongue and the buccal papillae are detected. Superficial lymph nodes are enlarged and limb joints may be swollen. Head pressing, hyperesthesia, tremors and nystagmus are the most obvious nervous signs of the MCF (Russell et al., 2009, Zemljic et al., 2012). The severity of the disease depends on the causative agent, species infected and the course of

disease (Russell et al., 2009). Although the clinical signs are similar in other species to those found in cattle, there is some variance in some aspects. For instance, in bison, the animals usually die in the acute stage without developing the head and eye form, diarrhoea, neurological signs as well as lymph nodes only slightly enlarged. Acute MCF is predominant; however, chronic disease and recovery of some cases have also been documented (Milne and Reid, 1990, O'Toole et al., 1997).

1.14.2 Pathology of MCF

The macroscopic pathological changes are commonly diffuse and mirror the intensity of the clinical signs, and may include most body systems (OIE, 2013). Erosions and petechial haemorrhages are seen in the gastrointestinal tract and echymotic haemorrhages (a haemorrhagic spots forming rounded and irregular patch) of the gall bladder epithelium. In the respiratory tract the development of a diphtheric membrane and erosions are often recognized. Lymph nodes are enlarged, in particular in cattle and can be solid, and white when cut. Kidneys' surfaces are, generally, characterised by the presence of white foci (OIE, 2013; CSFH, 2012; Russell et al, 2009).

Epithelial degeneration, vasculitis, hyperplasia and necrosis of lymphoid organs, and the accumulation of lymphoid cells in nonlymphoid organs are the main obvious microscopic appearances

in MCF (OIE, 2013). Vascular lesions exist and are obvious in the arterioles, venules, arteries and veins of tissues including the brain. They are identified by the infiltration of the lymphoid cells in the tunica adventia and media of the blood vessels. The accumulation of the lymphoid cells is pronounced, especially, in the renal cortex, periportal regions of the liver, and extremely large in the kidney (OIE, 2013).

The infiltration of lymphoid cells in both SA-MCF and WA-MCF are mostly T cells, the majority of which are CD8⁺ T cells along with very small numbers of CD4⁺ T cell (Anderson et al., 2007, Dewals et al., 2008).

1.15 Epidemiology of MCF

1.15.1 MCF Transmission

Although MCF viruses (AIHV-1 and OvHV-2) show no clinical signs in the reservoir host, they can induce the disease in susceptible species. Both viruses can be propagated horizontally from reservoir to susceptible host by either direct contact or respiratory route, mostly from lambs and wildebeest calves under 12 months old (Li et al., 1998, Mushi and Rurangirwa, 1981, Mushi et al., 1980). The horizontal transmission between the susceptible hosts does not occur and they are considered as dead end hosts (Ackermann 2006). Nonetheless, some cases of transmission among infected deer were documented (Reid et al., 1986). Also, it has been shown that the inability of animals to transmit the disease horizontally is owing to the cell-associated trait of the viruses as well as the failure to shed cell-free viruses by the animals (Li et al., 2014). However, vertical transmission has been documented in susceptible host animals. In study carried out by Plowright et al, (1972) a cow was inoculated with AIHV-1. After 84 months the cow was killed and the virus was grown in a culture from its organs. It was found that four out of the six calves that the cow yielded throughout its life were infected with the virus after parturition. In addition, OvHV-2 genome was identified in specimens of digestive tract, respiratory and urogenital tract of a sheep as well as semen of rams (Hussy et al, 2001; CFSPH, 2012). These observations have defined a possible

role for vertical transmission for passing the infection to the progeny after birth. Although the presence of both reservoir and susceptible hosts within the same vicinity is fundamentally required to transmit MCF, some cases of infection have been recorded when both types of hosts were at some distance up to five Km (CFSPH, 2012). The role of external parasites (Plowright, 1965) and urine (Michel, 1993) in transmitting MCF is ruled out.

1.15.2 Geographical distribution

Malignant catarrhal fever is distributed all over the globe; however, the incidence of the disease is dependent on both the causative agent and the susceptible host (CFSPH, 2012). WA-MCF is found in the sub-Saharan region in Africa when cattle and wildebeest are reared together in the same proximity. In addition, many cases of WA-MCF have been reported from wild parks and zoological gatherings (Russell et al., 2009). Sheep associated malignant catarrhal fever is found mainly in Europe and North America (Russell et al., 2009). However, the disease has been reported from various areas of the world in the Middle East (Abu Elzein et al., 2003) in New Zealand (Russell et al., 2009). Moreover, the disease is considered as a serious problem in Bali cattle in Indonesia (Wiyono et al., 1994).

1.15.3 Susceptible species

Malignant catarrhal fever viruses can infect a wide range of animals worldwide and exhibit clinical signs in these species. These animals belong to subfamily Bovinae including, cattle, bison, and water buffalo as well as family Cervidae containing, deer and moose. It has also been found that MCF viruses can induce the disease in animals belong to other species such as pigs and giraffes (Russell et al, 2009; CSFH, 2012). Some species are more sensitive to the infection of certain type of MCF virus than other species. For example, European cattle are more easily infected with OvHV-2 and are somewhat more resistant to AIHV-1. In contrast, animals such as Pere David's deer, wild-tailed deer, and bison are extremely susceptible to OvHV-2 infection (CFSPH, 2012).

1.16 Disease Impact

The lack of an effective reporting approach along with misdiagnosis of the clinical MCF has almost certainly led to the under-diagnosis of MCF (O'Toole et al., 1997). The significance of MCF lies in the fact that the disease is considered as a major cause of death in farmed bison in North America (Li et al., 2006), farmed deer and Bali cattle as well as a cause of death wherever the reservoir and host species for the virus cohabit. In the USA, an outbreak of MCF in 2003 led to the death of about 800 bison resulting in a loss of millions of dollars to the owners (Li et al., 2006). This has led the United States department of agriculture (USDA) placing MCF research in its priority programme. MCF is also reported as a serious problem in farmed deer in variety of locations and Bali cattle in Indonesia (Wiyono et al., 1994). The disease is mainly sporadic in Europe and the UK. However, outbreaks range (60-300) occurs annually in the UK. In addition, MCF may contribute to Bovine respiratory disease (Parameswaran et al., 2014). This has led organisations such as Animal and Plant Health Agency (APHA), Department for Environment, Food and Rural Affairs (DEFRA), and Global Alliance for Livestock Veterinary Medicines (GALVMED) to support research on MCF control (personal comment, David Haig). In Africa, it has been estimated that about 7% of the cattle exposed to wildebeest calves during migration perish due to MCF (Cleaveland et al., 2001). Consequently, MCF has been placed as one of the most significant

cattle diseases in certain parts of eastern and southern Africa (Cleaveland et al., 2001). MCF is a major cause of death in zoological gatherings where susceptible and reservoir hosts cohabit, hence loss of some expensive animals (Russell et al., 2009). The significance of MCF does not only lie on the fact that the disease can cause death in many animals around the world but also due to serious welfare issues that this brings and also socio-economic problems for farmers and pastoralists (Li et al., 2014, Palmeira et al., 2013). Eventually, the research on MCF and studying the virus life cycle and how it reacts with the host may contribute scientifically towards opening opportunities for researchers studying herpes viruses to gain more knowledge about the virus behaviour.

1.17 Diagnosis of MCF

Diagnosis of MCF depends, initially, on the clinical signs and the pathology of the disease (Li et al., 2011b). The existence of the susceptible species close to the reservoir hosts in the same vicinity could be a valuable approach for diagnosing MCF (CFSP, 2012). Tissues such as liver, kidney, intestines, lung, spleen, and lymph nodes should be collected from animals developing MCF clinical signs for diagnostics (Anderson et al., 2007, Parameswaran et al., 2014). Histologically, lesions such as vasculitis and accumulation of lymphocytes in the lymphoid tissues are suggestive of MCF incidence (Anderson et al., 2007, Cunha et al., 2012, Palmeira et al., 2013). MCF should be differentiated from other viral diseases such as mucosal disease, bovine viral diarrhoea virus, and infectious bovine rhinotracheitis (OIE, 2013; CFSP, 2012). One of the effective methods for diagnosing MCF with regard to AIHV-1 virus infection is to infect bovine turbinate fibroblast (BT) cells with the isolated virus and monitor any cytopathic effect (CPE) development. This is characterized by the absence of monolayer and the accumulation of cell debris (Wright et al., 2003). However, the advent of molecular based techniques like the polymerase chain reaction (PCR) assays has considerably enhanced MCF laboratory diagnostics (Li et al., 2011a, Russell et al., 2009). Especially, real time quantitative PCR (RT q-PCR) and nested PCR which are considered powerful and reliable tools for detecting viral DNA in the samples of MCF infected

animals (Hussy et al., 2001, Traul et al., 2005). This is due the fact that MCF affected animals have detectable levels of Viral DNA in their blood (at certain stages of the disease) and organs at post-mortem (Dewals et al., 2008). There are serological approaches to detecting MCF virus antibodies including the virus_neutralisation test (VN), enzyme-linked immunosorbent assay (ELISA), immunoperoxidase test (IPT), immunofluorescence assay (IFA) and immunoblotting introduced for the diagnosis of MCF (OIE, 2013). These techniques depend upon identifying antibodies for specific MCF virus antigens (CSFH, 2012). Neutralisation test (VN) could be effective for detecting antibodies from animals infected with AIHV-1 virus or viruses associated with AIHV-1 such as AIHV-2 and HiHV-1 whereas it is non-specific for detecting antibodies in animals infected with OvHV-2 or other related viruses (CSFH, 2012). The use of competitive enzyme-linked immunosorbent assay (cELISA), monoclonal antibody based technique utilizing 15A antibody targeting a conserved epitope among all MCF viruses or an indirect ELISA using virus extract are the methods of choice for identifying antibodies in MCF affected animals (Fraser et al., 2006, Li et al., 1994).

1.18 Treatment and prevention

There is currently no effective remedy or licensed vaccination for treating or preventing MCF (Russell et al., 2012b, Russell et al., 2009). The only current approach to control the disease is to separate the reservoir host from the susceptible species (CSFH, 2012; OIE, 2013). The efficiency of this method depends upon the reservoir host, susceptible species, separation distance as well as the age of the carrying host (CSFH, 2012; OIE, 2013). With regard to WA-MCF, separation of cattle from wildebeest is crucially important in preventing MCF transmission especially around the calving season whereas in SA-MCF this approach is of less significance in particular in the European cattle, the relatively resistant species (CSFH, 2012; OIE, 2013). However, isolation of highly susceptible animals to SA-MCF such as bison, Pere David's deer, and Bali cattle is highly recommended (CSFH, 2012; OIE, 2013). The MCF viruses can be transmitted over several km (Li et al., 2008b), with one report of disease in bison located 5km from the nearest sheep farm (CFSH, 2012). The age of wildebeest calves and lambs should be avoided ranges from two to nine months as these animals have higher cell-free virus titrations in their nasal secretions (CSFH, 2012; OIE, 2013). Avoiding stress factors such as starvation, high stock density, travelling could be effective in controlling MCF as such factors can induce virus reactivation (CSFH, 2012; OIE, 2013). Equine herpesvirus 1 (EHV-1) latently infected

horses can reactivate if the appropriate conditions such as stress, immunosuppression, transportation, sale barns and competitions appear (Dunowska., 2014).

1.19 Prospective vaccine development

The lack of effective treatment for MCF has encouraged scientists to develop a strategic vaccination approaches to protect susceptible species against the disease. Therefore, many studies (Plowright et al., 1975, Ferris et al., 1976, Edington and Plowright, 1980, Haig et al., 2008, Russell et al., 2012a) have been carried out in order to fulfil this target. The first trial to protect cattle utilising live or attenuated WC11 strain of AIHV-1 was not effective (Plowright et al., 1975). Similarly, study using inactivated cell free virulent C500 AIHV-1 virus in rabbits challenged parentally to generate immunity against cell free virus did not provide complete protection (Russell, 1980). However, another study using rabbits inoculated systemically with cell-associated virus and vaccinated with live cell-associated virus produced protection against the virus while inactivated cell-associated vaccination did not generate immunity (Edington and Plowright, 1980).

In order to examine whether cattle immunised with AIHV-1 C500 strain naturally and challenged with the attenuated virus could develop protective immunity Haig et al. (2008) conducted a study to address this hypothesis. In this trial cattle challenged with virulent cell-free virus naturally (intranasal inoculation) and immunised with attenuated AIHV-1 C500 strain in Freund's adjuvant (intramuscular route). The data obtained revealed that nine out of ten of the cattle systemically administrated developed a high level of neutralizing

antibodies in their nasal discharges as well as generating protective immunity. Moreover, animals challenged systemically did not develop protection against the virus (Haig et al., 2008).

The role of licensed adjuvant (Emulsigen, MVP Technologies) in helping protective immunity in cattle challenged with AIHV-1 (intranasal route) has been examined. The results indicated that considerable number of cattle were protected from the virulent virus at around three months post immunisation, however, the disease is developed when cattle further challenged at later time from 26 to 39 weeks post primary immunisation (Russell et al., 2012a). In addition, the high level of neutralising antibodies in the nasal secretions and blood from vaccinated and survived animals highlighted their role as a mucosal barrier for blocking the virus entry (Russell et al., 2012a).

The bulk of the vaccine development work has been done on AIHV-1 rather than OvHV-2. This is due to the absence of an effective propagating system for OvHV-2 in culture (Hart et al., 2007b). However, there are many factors such as the high similarity between AIHV-1 and OvHV-2 (Hart et al., 2007b, Ensser et al., 1997b), the existence of good reliable experimental animals (Anderson et al., 2007), and the use of large granular lymphocytes (LGLs) generated from the tissues of infected animals (Thonur et al., 2006), which can pave the way for researchers to develop a promising vaccine for MCF protection.

1.20 Chemicals for the experiments

1.20.1 5-azacitidine

5-azacitidine is a chemical analogue of cytidine, a nucleotide in DNA and RNA. The drug is a chemotherapeutic agent and used in the treatment of cancer (Brodovsky et al., 2013). The drug works through two mechanisms- at low doses, by inhibiting of DNA methyltransferases leading to hypo methylation of DNA, and high doses through its incorporation to the nucleic acids causing cell death (Kaur et al., 2014). The drug has wide spectrum of side effects ranging from anaemia, renal failure, foetal damage, fever, vomiting, and diarrhoea. Due to its hypo methylation activity, it has been found that 5-azacitidine can reduce the stability of silencing signals (stabilized by methylation) and hence affecting gene expression (Navada et al., 2014).

1.20.2 Cyclosporine A

Cyclosporine A is an immunosuppressant agent used in organ transplantation to prevent tissue rejection (Mott, Zhang et al. 2004). The drug decreases the activity of the immune system by interfering with the development and activity of T cells. Beside its use in tissue transplantation, it has been used for the treatment of rheumatoid arthritis, acute ulcerative colitis, and dry eyes. The adverse effects of cyclosporine A include fever, diarrhoea, vomiting, convulsions, hypertension, thrombosis in renal vasculature and

weakening the immune response through lowering the growth of T cells (Henry et al., 1995, Robert et al., 2010). The mechanism of action of cyclosporine A is not well known but it is thought that cyclosporine binds to cyclophilin of T cells. This cyclosporine and cyclophilin complex inhibits calcineurin required for the transcription of IL-2 (Youn et al., 2002).

1.21 Pathogenesis

Malignant catarrhal fever is a lymphoproliferative disease characterised by the proliferation of lymphocytes in lymphoid tissues (lymph nodes, spleen, and appendix) and interstitial infiltration of lymphoid cells in non-lymphoid organs (Liver, kidney, and lung) and this is often connected with tissue necrosis (Buxton et al., 1984). Many hypotheses have been suggested and many studies have been conducted in order to interpret the pathogenesis (mechanism by which the disease occurs) of MCF (Dewals et al., 2008, Anderson et al., 2007, Buxton et al., 1984). However, it is yet unknown.

1.21.1 Direct versus indirect mechanism of MCF

Buxton et al. (1984) infected rabbits with sheep-associated malignant catarrhal fever virus (SA-MCF) in lymphoid cells intravenously; it was found that the systemic pathological changes were analogous to those found in rabbits similarly infected with WA-MCF virus. It was also discovered that there was augmentation in T-

lymphocytes which was due to hyperplasia instead of neoplasia. Moreover, after treating the infected rabbits with cyclosporine (lymphocyte proliferation suppressor), the T cell proliferation ceased but areas of necrosis and disease were unaffected suggesting to the authors that tissue necrosis was due to autoimmunity induced by cytotoxic activity of uninfected cells under the control of a small number of infected cells. This indicated that the development of MCF was not associated with cell infiltration as such but to the tissue necrotic lesions. This hypothesis was strengthened by the paucity of virus or viral antigen in infected tissues, supporting this indirect mechanism (Bridgen et al., 1992). However, further studies have shown that both viruses induce lymphoid cell accumulations comprised mainly of T-lymphocytes, of which CD8⁺ T-cells predominate (Anderson et al., 2007, Simon et al., 2003). Using *in situ* PCR, Simon et al. (2003) confirmed that larger numbers of the CD8⁺ T-cells were infected with OvHV-2 in the brain of a cow and bison than previously thought indicating that the pathogenesis of MCF may not be by bystander cell activity after all.

Dewals and Vanderplassen continued examining the pathogenesis of WA-MCF (AIHV-1) in rabbits using multi-colour flow cytometry staining to phenotype mononuclear leucocytes in both lymphoid (during the infection and at time of euthanasia) and lymphoid tissues (at time of euthanasia). They found that the prevalent T cell subsets were CD3⁺ CD8⁺ CD4⁻ and the majority of these cells

produced gamma interferon (IFN- γ) and perforin (Dewals and Vanderplasschen, 2011). In addition, the identification of CD8 perforin⁺ $\gamma\delta^-$ T cells has been reported (Nelson et al., 2010) in the perivascular spaces throughout experimental SA-MCF (OvHV-2) in bison. These outcomes show that MCF is associated with the extension and infiltration of infected activated and cytotoxic CD8⁺ T cells expressing high levels of IFN- γ and perforin.

1.21.2 Experimental MCF

The use of rabbits as experimental animals has facilitated the study of the pathogenesis of MCF as they develop the same symptoms and systemic changes that occur in the naturally-susceptible hosts (Anderson et al., 2007, Buxton et al., 1984, Cunha et al., 2013, Gailbreath et al., 2008). These studies have demonstrated certain variations between MCF caused by AIHV-1 and OvHV-2. AIHV-1-related lesions were more abundant in the peripheral lymph nodes, while lesions associated with OvHV-2 were more obvious in visceral lymph nodes such as mesenteric lymph nodes. Moreover, AIHV-1-associated lesions showed less necrotic regions than those seen in OvHV-2 (Anderson et al., 2007, Buxton et al., 1984).

In an experiment carried out by Gailbreath et al. (2008) cell-free OvHV-2 removed from nasal secretions of virus-shedding sheep was inoculated by intranasal nebulisation into eight rabbits. Five of these, developed clinical signs and systemic pathological changes

which were similar to those changes in rabbits infected intravenously by cell-associated OvHV-2 in earlier studies.

1.21.3 Large granular lymphocytes in MCF and their phenotype

Large granular lymphocytes (LGL) are the T/NK cells that grow in culture from the tissues (usually lymphoid tissue) of MCF-affected animals. They are enriched for virus-infected cells that are difficult to detect *in vivo*. They possess cytotoxic activity and seem to express either natural killer or T cell phenotypes (Burrells and Reid, 1991). The phenotype of LGLs has been studied in cells from various species infected with either OvHV-2 or AIHV-1 (Burrells and Reid, 1991, Schock et al., 1998, Schock and Reid, 1996). Schock et al. (1998) examined the phenotype of LGLs in five different cell lines derived from some cattle infected with OvHV-2. It was shown that surface antigen CD2 and CD5 expressed on greater than 97.5 % of cells in all cell lines. CD4 was expressed on the majority of cells in three cell lines while CD8⁺ was expressed on one cell line. However, CD8⁺ T cell was the predominant cell type accumulated in the brain of a cow and bison infected with OvHV-2 (Simon et al., 2003). It was also demonstrated that CD25, the interleukin-2 (IL-2) alpha chain receptor, was expressed on all the cell lines. The growth of LGLs infected with OvHV-2 is enhanced in the presence of IL-2 and

high cell density (Schock et al., 1998). However, these cells can develop in IL-2-free culture (Swa et al., 2001).

Greater than 90% of LGL cell lines are virus infected as identified by immunocytochemistry or by *in situ* hybridisation for viral DNA or mRNA, despite the scarcity of cells containing virus in MCF affected organs *in vivo*. LGL cell lines are able to induce MCF when transferred to rabbits (Russell et al., 2009). LGLs are able to destroy tissue cells in an MHC-unrestricted manner and do not grow after stimulation with mitogens, while control T cells do (Schock et al., 1998, Swa et al., 2001). The interpretation of the activated cytotoxic phenotype of infected LGLs, in IL-2 free culture, includes constitutively activated Lck and Fyn kinases. These kinases are normally significant for the primary stimulation of T cells via the T cell receptor and co-receptors on the cell surface (Swa et al., 2001). LGLs produce various cytokines including TNF-alpha, IFN-gamma but are usually deficient in IL-2 either before or after stimulation by mitogen (Schock et al., 1998). LGLs have been used intensively to study the pathogenesis of MCF *in vitro* (Hart et al., 2007a, Thonur et al., 2006).

1.21.4 The role of cytokines in MCF pathogenesis

The role of cytokines, in particular, interleukin 15 (IL-15) and interleukin 2 (IL-2) in the pathogenesis of MCF has been examined (Anderson et al., 2008, Meier-Trummer et al., 2009a) IL-15 is a

cytokine which has a structural resemblance with IL-2. It is secreted by a wide range of cells and tissues containing, monocytes, macrophages, dendritic cells (DC), epithelium, and endothelium (Grabstein et al., 1994). Its function is to recruit, activate the proliferation of, and regulate cytotoxic cells including CD8⁺ cytotoxic T lymphocytes, natural killer cells (NK), NK T cells, and CD4⁺ cytotoxic lymphocytes. Therefore, it plays a significant role in both innate and adaptive immunity. Also, it has an anti-apoptotic function (Anderson et al., 2008, Lodolce et al., 2002). Moreover, the involvement of IL-15 in the pathogenesis of various autoimmune diseases has been documented. It has been found that, in mouse paradigms of autoimmunity, inhibiting IL-15 abolished the intensity of the diseases (Smith et al., 2000).

It was discovered; utilizing *in situ* hybridisation, after infecting rabbits with either AIHV-1 or OvHV-2 that IL-15 was abundant in the lymphoid tissues. The abundance of IL-15 is associated with tissue lesions indicating that the cytokine may be implicated in the pathogenesis of MCF (Anderson et al., 2008). In addition, it was found in the same experiment that the intensity of BLT esterase, (that detects tryptase) measuring cytotoxicity, was preserved in LGLs when stimulated with IL-15 in comparison with IL-2. These observations demonstrate that IL-15 may play a role in the regulation of the active cytotoxic cells in MCF (Anderson et al., 2008).

IL-2 is a cytokine which plays a significant role in the growth of T cells as well as the development of T regulatory cells (Tregs). It is expressed by T cells, mainly CD4⁺ T lymphocytes during immune responses (Boyman and Sprent, 2012, Meier-Trummer et al., 2009a). IL-2 transcript abundance was low in lymphoid tissues derived from cows infected with OvHV-2 using microarray RNAseq assay. Although, the abundance of CD28 and T cell receptor (TCR), co-stimulatory enhancer for IL-2 production, was very high. It was also demonstrated that the ratio of CD4⁺ was less than CD8⁺ lymphocytes. These observations indicate that IL-2 deficiency may have a significant role in the pathogenesis origin of MCF (Meier-Trummer et al., 2009a).

1.21.5 The site of infection and MCF pathogenesis

A reverse-transcription PCR was used as the technique to detect OvHV-2 in organs in which OvHV-2 replication takes place *in-vivo*. Samples (turbinate, lungs, and trachea) were collected from naturally-infected sheep (reservoir species) and samples including kidney, bladder, brain, and intestine were obtained from cattle and bison infected with OvHV-2. OvHV-2 major capsid protein gene (ORF25) was utilised as a marker of viral replication. The data obtained revealed that the ORF25 transcript was present in 30% of the respiratory tract-related samples, 66% of which were turbinate, in sheep, indicating that this is the site of virus production in the

reservoir host. In contrast, most of the bovine and bison samples contained ORF25 transcripts indicating that replication or at least partial productive cycle appears to take place in most tissues (Cunha et al., 2008). Of course in the MCF-susceptible animals this productive cycle is incomplete as discussed above. *In situ* hybridisation and immuno-histochemistry using antibodies for capsid and tegument structural proteins (ORF43 and ORF63) of OvHV-2 were used to identify regions of viral replication in six OvHV-2 infected rabbits. The results showed that all infected rabbits developed pathological lesions in the samples. However, virus structural proteins were identified solely in the appendix, in particular, in the epithelial cells and M-cells, while ORF63 mRNA was only found in the epithelial cells but not in the M-cells suggesting that these cells may have a role in the pathogenesis of MCF and may represent an entry site for the virus (Meier-Trummer et al., 2009b).

It may be worth mentioning that the researchers in both experiments have used different techniques, different virus administration approaches (intravenous and aerosol), and different viral strains. This may have an impact on the data obtained as, for example, the OvHV-2 virus used was from European and American strains (Meier-Trummer et al., 2009b). Although it has been found in earlier work that the two strains are highly similar 94-100% (Hart et al., 2007b, Taus et al., 2007), variations in the genomic

sequences between the two strains may interpret their biological diversity (Meier-Trummer et al., 2009b).

1.21.6 Recombinant AIHV-1

In order to study the role of virus genes in pathogenesis, Researchers have exploited the availability of virulent AIHV-1 virus in low passage tissue culture to construct a stable virus genome as a bacterial artificial chromosome (BAC), for this, a modified *loxP*-flanked BAC cassette was integrated in one of the two large non-coding sites of AIHV-1 DNA. The integration led to the generation of an AIHV-1 BAC clone in bacteria and capable of producing infectious particles when transfected into permissive cells. AIHV-1 virions originated from BAC were able to replicate and generate MCF in rabbits that were similar to that of the AIHV-1 virulent parental strain. This discovery will greatly assist our understanding of MCF pathogenesis by allowing gene knockout and reinsertion recombinant viruses to be made (Dewals et al., 2006a).

1.22 Hypothesis

Malignant catarrhal fever is initiated by aberrant gene expression in infected T cells, epithelium and endothelium.

1.23 Objectives

1. **Objective 1:** To determine whether bovine endothelium and rabbit epithelium can be infected with AIHV-1 C500 strain *in vitro* (cell lines, rabbit and cattle) and *in vivo* (in rabbits detected by *in situ* hybridisation). Also to determine the life cycle stage of the virus in the infected cells (by RT-qPCR and *in situ* hybridisation) using known latent and lytic transcript analysis.
2. **Objective 2:** to attempt to switch the virus life cycle from lytic to latent in large granular lymphocytes (LGLs, mixed latency and lytic cycle) and BT fibroblasts (lytic cycle only) infected with AIHV-1 C500 strain after treatment with 5-azacitidine (a drug used to support latency). In addition, RNAseq will be used to map the host and viral gene transcripts in these cells to look for pathways associated with latency and the lytic cycle.
3. **Objective 3:** To determine viral gene expression in the tissues of animals infected with AIHV-1 and treated with cyclosporine-A (CSA) to attempt removal of the infiltrating

infected T cells. The effect of this on disease outcome and virus gene expression will be monitored.

Chapter 2

**General materials and
methods**

2.1 Introduction

This chapter describes the approaches which have been done in most of the work and common for all of the chapters while more specific methodology will be described in the results chapters.

Virus: The C500 strain (Plowright et al., 1960, Plowright et al., 1975) was used. For preparation of virus stocks, see section (2.2.4) below.

2.2 Tissue culture

Three types of cultured plate adherent cells were grown for the study; bovine turbinate fibroblast (BT) cells were kindly donated by Dr George Russell of Moredun institute (Palmeira et al., 2013, Parameswaran et al., 2014), bovine aortic endothelium (BAE) cells (cat# 87022601, ECACC) the official name is BFA but BAE is used throughout the project, (Pollock et al., 1991), and statens seruminstitut rabbit cornea (SIRC) cells (Cat# 89090404, ECACC), (Parameswaran et al., 2014). The media used were Iscove's Modified Dulbecco's Medium (IMDM, Gibco® ThermoFisher Scientific, UK) for the growth of BT cells and Dulbecco's Modified Eagle Media (DMEM, Gibco® ThermoFisher Scientific, UK) for the culture of BAE and SIRC. All the manipulations were undertaken under aseptic conditions in a laminar air flow tissue culture hood. The cells were split when they reached 80% confluence using 1%

trypsin in phosphate buffer saline (PBS) for up to 10 minutes (2ml for a 25 cm² flask and 4ml for a 75cm² flask) in 37° C, 5% CO₂ in air incubator. Trypsin reaction was stopped by adding the same volume of warmed media containing 10% foetal calf serum (FCS). Supernatant was removed by centrifugation at the 1500 rpm for 5 minutes at 21 °C. The cell pellet was re-suspended by adding media (5ml for 25 cm² and 14 ml for 75 cm² flasks). Cells were incubated at 37 °C, 5% CO₂ in air and checked regularly (every 3 days) until cells become confluent.

2.2.1 Large granular lymphocytes

Large granular lymphocytes (LGLs) derived from rabbit mesenteric or popliteal lymph nodes are used in the study. Briefly, lymph node tissues were teased apart using sterile forceps and scissors. To give a single cell suspension the tissues were then passed through a 70 µm filter using PBS (using back of 2ml syringe and 50ml centrifuge tube). The cells were washed twice with IMDM medium (containing Glutamax, 10% FCS, 100µg/ml penicillin, 50µg/ streptomycin). All manipulations were undertaken using sterile solutions, equipment and aseptic technique under the laminar flow hood. Cells were culture in upright 25cm² flasks at 37°C, in 5% CO₂ in air. For maintaining the cultures, the cells were fed with fresh IMDM media (contain 10% special FCS and 50 µl interleukin-2 (IL-2) 50ng/ml media (Cat# 202-IL, Recombinant Human IL-2, R&D Systems))

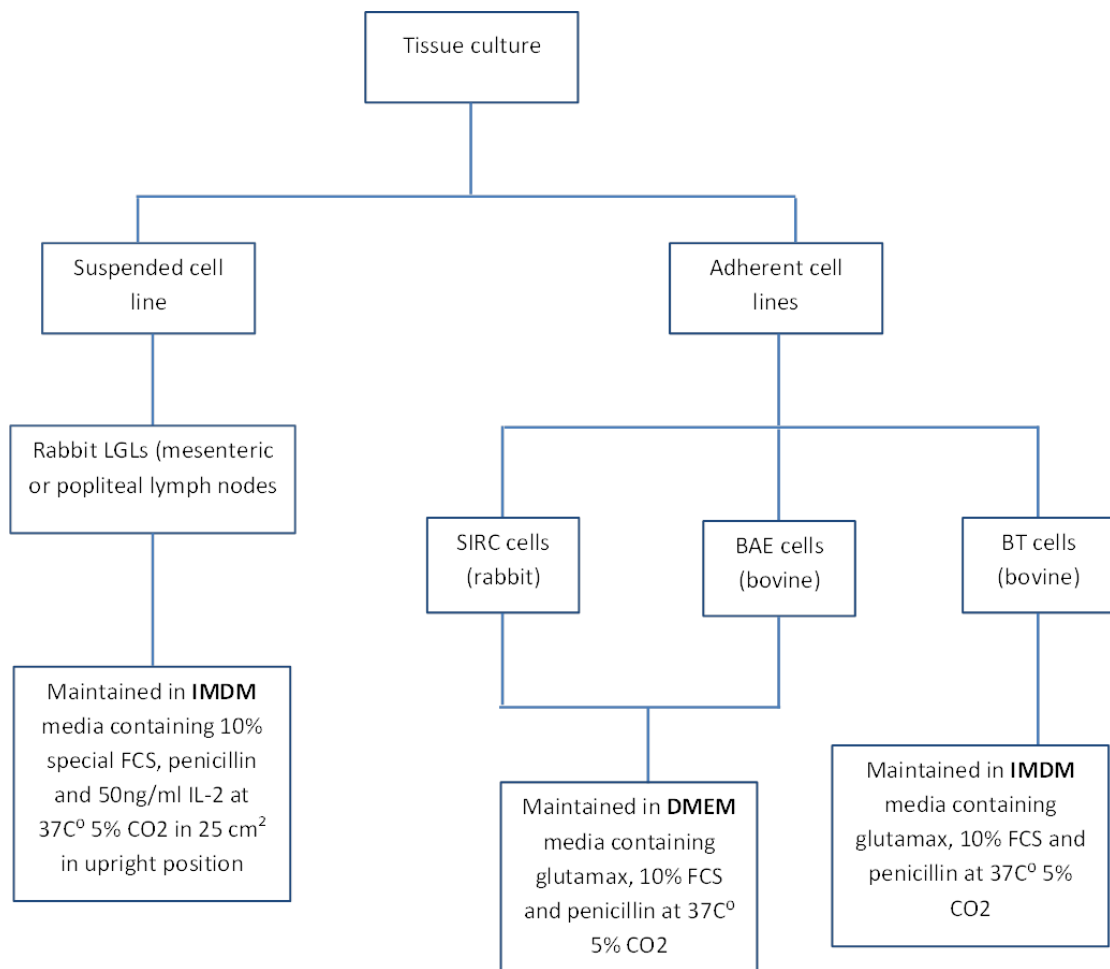
added up to 10 ml total volume of media by remixing the top ~one third of culture medium where most of the cells are at the bottom region of the flasks)) when the medium colour changes to yellow/orange or once every seven days. After that, cells are checked under the microscope for growth and stored back in the incubator in the upright position.

2.2.2 Counting cells

A haemocytometer was used to count cells and trypan blue exclusion used as a measure of cell viability.

2.2.3 Cryopreservation of cells

Adherent cells (BT, BAE and SIRC) were cryopreserved at 5×10^6 - 1×10^7 cells per ml medium containing 50% FCS in 10% v/v dimethyl sulfoxide (DMSO) (Cat# 472301, Sigma-Aldrich) and the LGLs and lymphoid cells at 1×10^7 - 1×10^8 cells per ml. Adherent cells were detached from cultured plates by adding 1% trypsin in 1xPBS, centrifuged at 1200 rpm for 5 min. The cell pellet was re-suspended in freezing medium consists of 90% IMDM or DMEM media (containing 10% FCS, 1% penicillin/streptomycin) and 10% filtered (DMSO) according to the type of the cells. The cell suspension was then transferred to labelled cryo-tubes, placed in Mr frosty (freezing container, ThermoFisher Scientific, UK) in -80 °C freezer overnight and then in liquid nitrogen.



2.2.4 AIHV-1 virus stocks

Low culture pass (virulent) AIHV-1 C500 strain (Plowright et al., 1975) virus stock was obtained from infected rabbit lymphoid cells incubated with BT cells where a mixture of cell-associated virulent and cell-free virulent viruses obtained from up to five passages in BT cells were harvested and frozen away as stock virus. The AIHV-1 C500 strain used to infect BT cells to make the virus stock was obtained from AIHV-1 infected rabbit's mesenteric lymph node (MLN) cells. The approach applied was as follows: All the

manipulations undertaken were under aseptic conditions in the laminar flow hood. BT cells were washed twice with PBS. Vials of infected rabbits MLN cells were taken out of the liquid Nitrogen storage and placed on dry ice. The vials were thawed and the MLN cells were added to a centrifuge tube containing 15 ml IMDM media and centrifuged then re-suspended two and half millilitres of the medium were added to each flask of BT cells (4 flasks in total) and one left as a BT only control. The flasks were incubated at 37 °C, in 5% CO₂ in air incubator overnight.

The following day, the media were discarded and the cells were washed with 1xPBS twice. Fifteen millilitres of IMDM media were added to each flask and then kept at 37 °C, in a 5% CO₂ air incubator. The cells were monitored daily for any cytopathic effect (CPE) which is characterised by the accumulation of cell debris and the absence of monolayer.

The supernatant from the cultures were collected when the BT cells showed approximately 50% CPE, centrifuged and the pellet re-suspended in 4 ml medium. The supernatant collected in 75 cm² flask and placed on Ice. Four ml 1xPBS was added to the attached cells which were mechanically detached from all the flasks, centrifuged and the pellet mixed with the previously obtained pellet. The mixture was then freeze-thaw three times in liquid nitrogen and spun down. The supernatant carefully collected and finally mixed with the supernatant initially collected in 75 cm² flask. The

supernatant was aliquot in labelled cryo-tubes (1ml each), placed in -80 °C freezer overnight and then stored in liquid nitrogen. Applying the same technique P₁, P₂, P₃, and P₄ were finally made. With regard to high pass attenuated AIHV-1 virus stock was made by passaging the virus in BT cells more than 5 times up to thirty passages.

2.2.5 Virus titration : 50% tissue culture infective dose (TCID₅₀)

TCID₅₀ is the approach used to measure virus titration. This measure the infective dose of the virus required to kill 50 % of infected BT cells measured as a cytopathic effect (CPE).

The procedure was undertaken under aseptic conditions in the laminar flow hood. Seven Eppendorf tubes were labelled 10¹ to 10⁷ for the virus to be titrated. A volume of 100 µl of BT cell suspension (2x10⁵ cells/ml in IMDM medium containing 10% FCS) was added to wells of a 96-well plate designated A1-4 to H1-4 (Figure 5). The plate was kept at 37 °C, in 5% CO₂ in air in an incubator overnight. The following day the media were discarded and the cells were washed twice with 1xPBS. A volume of 900 µl serum-free IMDM medium was loaded into each labelled Eppendorf tubes. AIHV-1 C500 virus for titration was thawed from frozen storage. A volume of 100 µl of neat AIHV-1 virus was added to the tube labelled 10¹, and mixed thoroughly. A volume of 100 µl of 10¹ dilutions was then transferred to 10² Eppendorf tube and so on up to the 10⁷ tube giving a number of serially diluted samples. A volume of 100 µl of dilution 10¹ was added to the wells B1-4 and dilution 10² to wells C1-4 and so on to H1-4. A volume of 100 µl of serum free medium was added to the wells A1-4 used as control (Figure 5).

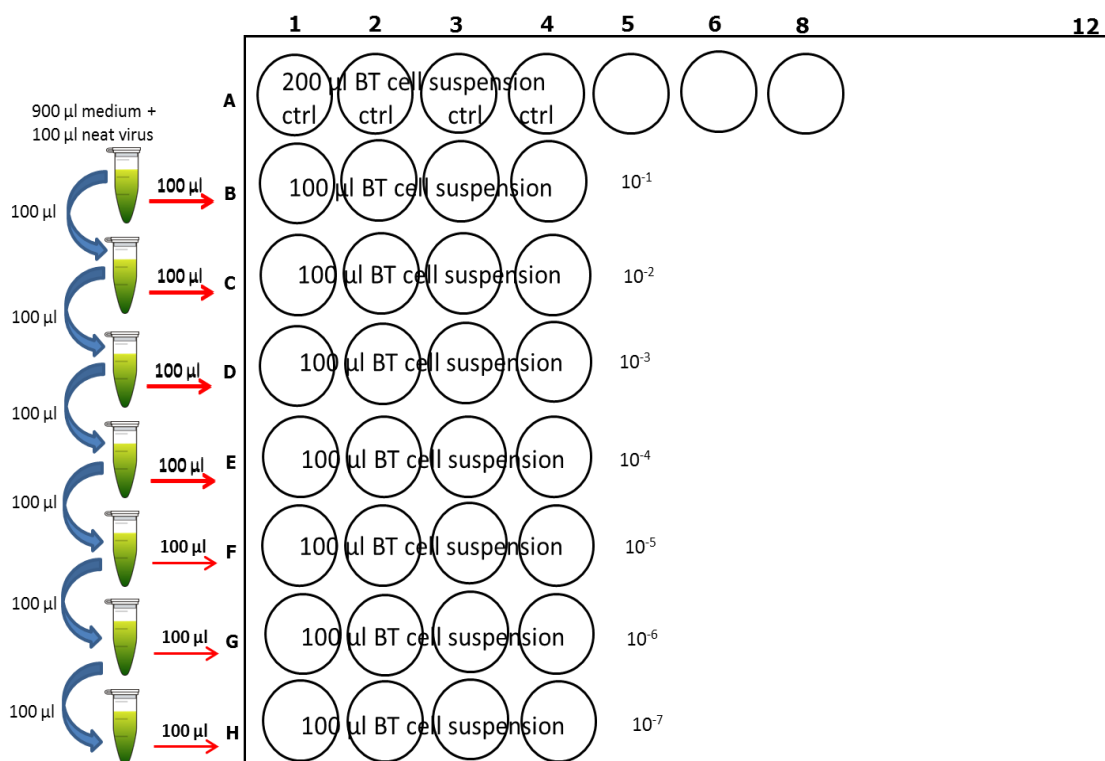


Figure 5 Virus titration: 50% tissue culture infective dose (TCID₅₀). The figure shows the steps were taken to carry out TCID₅₀ for virus titration.

The plate was finally placed in the 37 °C, 5% CO₂ incubator for two hours. After two hours, all the wells including the control were topped up with 100 µl IMDM medium containing 10% FCS. The plate was then placed in the 37 °C, 5% CO₂ incubator and read for % CPE after 4-5 days.

Wells were positive if CPE was present. The virus titre is calculated by Spearman/Karber (<http://www.cureffi.org/2015/09/20/the-math-behind-spearman-karber-analysis/>) Calculation as follows: Log TCID₅₀-L-d (S-0.5) where

L = negative log of lowest dilution

D = difference between log dilution steps

S = sum of proportion of positive tests (wells showing CPE from virus infection)

Example of virus titration

Table 3 example of virus titration

Virus dilution	Positive wells				Proportion of infected culture
10⁻¹	+	+	+	+	4/4 = 1
10⁻²	+	+	+	+	4/4 = 1
10⁻³	+	+	+	+	4/4 = 1
10⁻⁴	+	+	-	-	2/4 = 0.5
10⁻⁵	-	-	+	-	1/4 = 0.25
10⁻⁶	-	-	-	-	0/4 = 0
					<u>3.75</u>

2.3 Molecular techniques

2.3.1 DNA extraction

The total cellular and viral DNA was extracted using DNeasy blood and tissue kit (cat# 69506, Qiagen) according to manufacturer's instructions. DNA was extracted from different tissues, blood and cultured cells.

Cultured cells: appropriate number of cells was centrifuged (maximum 5×10^6) for 5 min at 300 g. The pellet was re-suspended in 200 μ l phosphate buffered saline (PBS) and 20 μ l proteinase K was added. A volume of 200 μ l of buffer AL was added, mixed thoroughly by vortexing, and then incubated at 56 °C for 10 min. After that, 200 μ l of absolute ethanol was added to the sample and mixed thoroughly by vortexing. The mixture was then pipetted into DNeasy Mini spin column placed in a 2 ml collection tube, centrifuged at 6000g for 1 min, and the flow-through and the collection tube were completely discarded. The DNeasy Mini spin column was placed in a new 2 ml collection tube, 500 μ l of buffer AW1 was added and centrifuged at 6000 g for 1 min. The flow-through and the collection tube were discarded. The DNeasy Mini spin column was placed in a new 2 ml collection tube, 500 μ l of buffer AW2 was added and centrifuged at 20,000 g for 3 min. The flow-through and the collection tube were discarded. The DNeasy Mini spin column was placed in a clean 1.5 ml, 100 μ l of buffer AE was directly loaded onto DNeasy membrane, incubated at room

temperature for 1 min, and then centrifuged for 1 min at 6000 g to elute.

From blood: A volume of 20 μ l of proteinase K was loaded into a 1.5 ml Eppendorf tube. A volume of 50-100 μ l anti-coagulated blood was added and the volume was adjusted to 220 μ l with PBS. A volume of 200 μ l of buffer AL was added, mixed thoroughly by vortexing, and then incubated at 56 °C for 10 min. After that, the steps were exactly similar to the ones done for cultured cells.

Animal tissues: A piece of 25mg tissue was cut into small pieces, and then placed in a 2 ml micro-centrifuge tube. A volume of 200 μ l of buffer ATL was then added. A stainless steel bead was added to the tube and the tube was placed in a tissue lyser (TissueLyser II Qiagen, Uk) to help disrupting the tissue. A volume of 20 μ l of proteinase K was added, mixed thoroughly by vortexing, and incubated at 56 °C until the tissue is completely lysed. The next steps are similar to the ones done for cultured tissues.

2.3.2 RNA extraction

Total RNA was extracted using RNeasy Plus mini kit (cat# 74134, Qiagen). A maximum of 1×10^7 cells were harvested and appropriate volume (600 μ l) of Buffer RLT Plus was added and mixed by vortexing for 30 s. The homogenised lysate was transferred to a gDNA Eliminator spin column placed in a 2 ml collection tube and centrifuged for 30 s at 8000 g. the column was discarded and the flow-through was saved. One volume (600 μ l) of 70% ethanol was added to the flow-through and mixed well by pipetting. Up to 700 μ l of the sample was transferred to an RNeasy spin column placed in a 2 ml collection tube and centrifuged for 15 s at 8000 g. the flow-through was discarded. A volume of 350 Buffer RWT was added to the RNeasy spin column and was centrifuged for 15 s at 8000 g to wash the membrane. The flow-through was discarded. A volume of 10 μ l DNase I stock (cat# 79254, Qiagen) solution was added to 70 μ l Buffer RDD (cat# 79254, Qiagen), mixed gently by inverting the tube, and centrifuged briefly. The DNase incubation mix (80) was directly added to the RNeasy spin column membrane, and placed on the benchtop for 15 min. A volume of 350 Buffer RWT was added to the RNeasy spin column and was centrifuged for 15 s at 8000 g to wash the membrane. The flow-through was discarded. A volume of 500 μ l Buffer RPE was added to RNeasy spin column, and centrifuged for 15 s at 8000 g to wash the membrane. The flow-through was discarded. A volume of 500 μ l Buffer RPE was added

to RNeasy spin column, and centrifuged for 2 min at 8000 g to wash the membrane. The RNeasy spin column was placed in a new 1.5 ml collection tube. A volume of 30 μ l RNase-free water was directly added to the spin column membrane, centrifuged for 1 min at 8000 g to elute the RNA.

Animal tissues: a piece of an animal tissue (less than 50 mg) was excised and loaded into a 2 ml collection tube. 600 μ l of Buffer RLT Plus were added and a stainless steel bead was added to the tube and the tube was placed in a tissue-Lyser (Tissue Lyser II, Qiagen, UK) to disrupt the tissue. The tube containing the lysate was placed on the benchtop at room temperature for 5 min. The next steps are similar to the ones done for extraction of the RNA from the cultured cells.

2.4 Nucleic acid amplification and quantitation

2.4.1 Complementary DNA (cDNA) synthesis

Complementary DNA was synthesised using the Transcriptor First Strand cDNA Synthesis Kit (cat # 04897030001, Roche Applied Sciences, UK). The template-primer mixture for 20 μ l reaction was prepared in a sterile, nuclease-free, thin-walled PCR tube on ice by adding the components in the following order; the equivalent of 1 μ g total RNA, 2 μ l random hexamer primer, and up to 13 μ l RNase free water. After that, the RT (reverse transcriptase) mix was prepared by adding the following reagents; 4 μ l Transcriptor Reverse

Transcriptase Buffer, 0.5 μ l Protector RNase Inhibitor, 2 μ l Deoxynucleotide Mix, and 0.5 μ l Transcriptor Reverse Transcriptase (storage buffer; 200 mM potassium phosphate, 2 mM dithiothreitol, 0.2 % Triton X-100 (v/v), 50% glycerol (v/v), pH approx. 7.2). The RT mix was then added to the tube containing the template-primer mix. The mixture was mixed carefully by flicking the tube, centrifuged briefly, and finally placed in a thermal block cycler with a heated lid for 10 min at 25 °C followed by 35 min at 55 °C. The Transcriptor Reverse Transcriptase was inactivated by heating to 55 °C for 5 min using XP Thermal Cycler (Bioer, UK). The reaction was stopped by placing the tube on ice and sample was stored at -20 °C.

2.4.2 Polymerase chain reaction (PCR)

2.4.2.1 PCR condition

The procedure was undertaken under aseptic conditions in the ultra violet cabinet. The equipment (pipettes, tips, and nuclease-free water) were exposed to ultra violet light for 15 min. All the reagents except the Taq polymerase were thawed and placed into the ice box. The master mix mixture for 24 μ l reactions was prepared in a sterile, nuclease-free, thin-walled PCR tube on ice by adding the components in the following order; 17,875 μ l nuclease free water, 2.5 μ l 10x buffer, 1 μ l MgCl₂ (25mM), 0.5 μ l dNTPs (10mM), 1 μ l forward primer (5pmol/ μ l), 1 μ l reverse primer (5pmol/ μ l), and 0.125 μ l Taq polymerase (5 u/ μ l). A volume of 1 μ l sample/s was added to the tube containing the master mix mixture outside the UV hood. The tube was centrifuged and placed in the PCR machine to run according to the following programme; 1 cycle (initializing) x 94 °C, 35 (denaturation) x 94 °C for 1 min, 60 °C (annealing) for 1 min, 72 °C (elongation) for 1 min, and 1x 4 °C hold.

2.4.2.2 Agarose gel electrophoresis

The PCR products were resolved to agarose gel (Sigma-Aldrich, UK). Certain amount of agarose powder, according to the concentration required, was dissolved in 100 ml 1xTAE buffer in a beaker. The beaker was then heated in the microwave oven for sometimes until completely dissolved, cooled down, and 3.8 μ l Nancy-520 (nucleic

acid stain) (Sigma-Aldrich, Uk) was added. The gel solution was slowly poured into the gel tray and the air bubbles were removed using disposable tips. The gel was left for sometimes to set. The gel tray was placed in the gel tank and 1xTAE buffer (Tris base, acetic acid and EDTA) was added to the gel tank until the wells were covered. A volume of 1 μ l 6% loading dye (New England BioLabs) was thoroughly mixed with 5 μ l sample and then loaded into the gel wells along with 6 μ l DNA ladder (New England BioLabs). The voltage was adjusted to 110 V for 1 hour and the DNA was viewed by the UV illuminator (ImageQuant 300 imager, GE healthcare, UK).

2.4.3 Viral load measurement

Viral load is used to quantify the viral copy number in specific cells and tissues. q PCR is the device by which the viral load is identified. AIHV-1 virus copy number is measured by comparing the C_T value with standard curve by normalizing AIHV-1 ORF3 gene with 10^5 copy number of rabbit β globin used as a reference gene as described in (Boudry, 2007). The forward primer sequence for ORF3 used 5'-GGGCTAATTTGTGCAGTTTGTGA-3' and reverse primer 5'-AGGTGTTTCTGAAAAGAGGGGAA-3' and the probe used for the assay was FAMAIHV-1 6FAM ACAGGCTCCTCGTCCTCGTCGTGT TAMRA. The rabbit β globin forward primer used 5'-GGTATCCTTTTTACAGCACAAC-3' and the reverse primer 5'-CAGGTCCCCAAAGGACTCG-3', in the presence of the fluorescent probe 5'-FAM-CCTGGGCTGTTTTTCATTTTCTCAGG-TAMRA-3'.

AIHV-1 BAC plasmid was utilized as standard as described in (Dewals et al., 2006a). The data obtained analysed using the absolute quantitative approach utilizing Light Cycler 480 software analysis.

2.4.4 Quantitative real-time PCR (q RT-PCR)

The quantitative PCR, using the Light Cycler 480 System (Roche Applied Science, UK), is the method used to measure the viral copy number and detection of the virus DNA in the infected cells and tissues as well as measuring the viral gene expression profiles throughout the project work. The technique is utilized to amplify and quantify a target DNA based on the sequence-specific probes tagged with fluorescence probe upon hybridisation with its complementary DNA sequence in the presence of flanked primers. The probes and primer sequences for q RT-PCR used in this study are shown in table 4. The probes and primers were designed using Universal Probe Library (UPL) System Assay Design (<https://lifescience.roche.com/shop/products/universal-probelibrary-system-assay-design>). Probes were labelled with fluorescent reporter dye 5 carboxyfluorescein (FAM) at the 5' end and quencher N,N,N,N'-tetramethyl-6-carboxyrhodamine (TAMARA) at the 3' end. The technique was carried out utilizing the Light Cycler 480 Probes Master Kit (Roche Applied Science, UK) with the universal cycle profile. The 96-well plates were used for q RT-PCR with 20 µl added per reaction (well). For the test sample, each q RT-PCR mixture contained 1x light cycler probe master, 900 nM forward primer, 900 nM reverse primer, 100 nM probe, 2 µl (10-50) template DNA, made up to 20 µl with RNase free water. Each q RT-PCR reaction was carried out in duplicate. In addition, each q RT-

PCR trial comprises two no template controls (NTC), test samples, a control from non- infected cells along with a standard \log_{10} dilution series. The standard \log_{10} dilution series were used to produce standard curves. The efficiency of the standard curve was measured using the Light Cycler 480 (LC480) software. The PCR reaction efficiency, ideally, should be 100% meaning that the amount of product doubles each cycle ($E=2$) (Figure 5 & 6). The normalised values for the gene expression profile were measured using the advanced relative quantification method utilizing the Light Cycler 480 (LC480) analysis software. The genes selected for viral transcripts analysis (Table 4) are known with their involvement in latent and productive/lytic cycle in other herpesviruses. ORF73 encodes latency associated nuclear antigen (LANA), homologue to Epstein Barr virus nuclear antigen (EBVNA1) and KSAH ORF73 LANA protein involved in latent infection, ORF50 encodes RTA protein the transcriptional and replication activator responsible for the switch to lytic cycle, ORF25 encodes a major capsid protein highly expressed during viral replication, A4.5 similar to Bcl-2 family of apoptosis and virus cycle expression not known and A9.5 encodes a secreted glycoprotein that is similar to IL-4 and virus cycle expression not known.

Table 4 primers and probes used for target and reference genes throughout the study.

Gene symbol	Oligonucleotide sequence (5'-3')
ORF50 F	GCCACAGCCTCAATCTGAAT
ORF50 R	TTCTGGACGAACCTGGCTAT
ORF50 P	UPL23
ORF73 F	TGGGCCTTCTCCTTCAGAT
ORF73 R	AAGTGGACCAGGTTCTGTCTG
ORF73 P	UPL32
ORF25 F	TTCACCGTTATGCACAATAAGC
ORF25 R	CTTGTGCTTTGCCTGCACT
ORF25 P	UPL155
ORF A4.5 F	TTTGACCCGGGTAGTCAATC
ORF A4.5 R	GCTAGAATACATTCTGTGACCGTTAG
ORF A4.5 P	UPL92
ORF A9.5 F	CAACCAGTTTTGTTGTTATTCAATG
ORF A9.5 R	AAGAGAGTTAAAGTTAAATTTGGAGCA
ORF A9.5 P	UPL83
ORF63 F	GCTGTAATTGGCACTCTCAGG
ORF63 R	TCATGAGGCGGAAGTTGC
ORF63 P	UPL40
Rabbit SDHA1 F	ACCGTGAAGGGCTCTGAC
Rabbit SDHA1 R	TTTCTAGCTCGACCACAGAGG
Rabbit SDHA1 P	UPL158
Bovine RPS9 F	GCCTCGACCAAGAGCTGAAG
Bovine RPS9 R	GGGCAGCCTTTCGGATCT
Bovine RPS9 P	TGATCGGCGAGTATGGGCTCCG
Bovine G actin F	CACCTTCCAGCAGATGTGGA
Bovine G actin R	CTAGAAGCATTGCGGTGGAC
Bovine G actin P	AGCAAGCAGGAGTACG

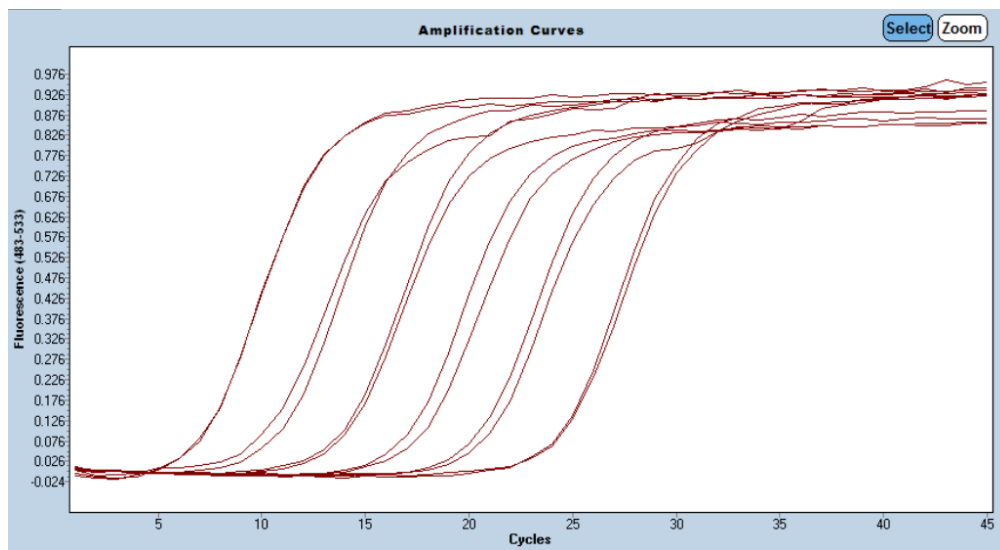


Figure 5 snapshot of q RT-PCR amplification curve.

The figure illustrates the amplification curves generated using Light Cycler 480 for determination of AIHV-1 DNA load from infected rabbit tissues utilizing ORF3 gene as a standard.

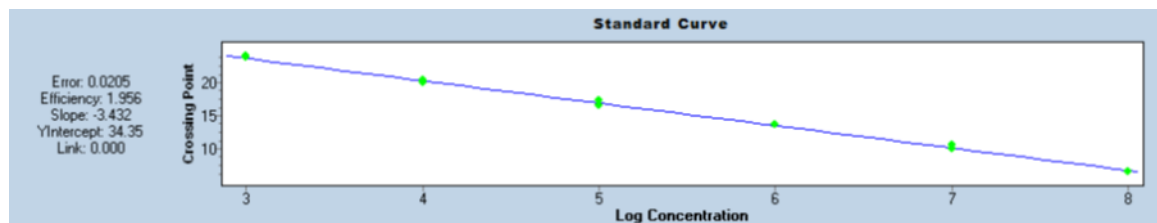


Figure 6 snapshot of q RT-PCR standard curve.

The figure shows the standard curve generated using Light Cycler for determination of AIHV-1 DNA load from infected rabbit tissues utilizing ORF3 gene as a standard and seven \log_{10} serial dilutions 10^{-3} to 10^{-8} and PCR efficiency of 1.95.

2.4.5 Quantification of DNA and RNA by spectrophotometer

DNA and RNA concentrations were assessed by a NanoDrop™ ND-8000 spectrophotometer (ThermoScientific, UK) according to the manufacturer's instructions using the software program NanoDrop ND-8000 version 2.2.0. To make the data as precise as possible, 1.5 µl blank was used for reading. After that, 1.5 µl of samples were loaded onto each lower measurement pedestal and read. The ratio of absorbance at 260 was used to measure the purity of nucleic acids. A ratio of ~1.8-2.0 showed pure nucleic acids and values outside this range were presumed to indicate the presence of proteins or phenols or other contaminants.

2.5 Flow cytometry

Flow cytometry was used to phenotype rabbit LGL samples (recognise the cell type and cell subset). Ten Eppendorf tubes labelled as non-stained, CD4 FITC, CD4 isotype control, CD8, CD11B (monocyte), B cell (CD19), Pan T (T cell), secondary antibody only FITC, secondary antibody only APC, and double staining (CD4&CD8) were used in this experiment. Labelling also includes rabbit LGL IDs (IYDY, IYJJ, LFLK, and LFKJ) for both 5-azacitidine-treated and non-treated LGL. After three weeks, RPMI (cat 61870-010 Gibco Life technologies) was used with 2% FCS supplement for cell labelling: The only direct conjugated antibodies used were the CD4 FITC and CD4 isotype control (primary antibodies/one step labelling) For indirect immunofluorescence, the secondary antibodies used were mouse IgG1 FITC (CD11B, B cell, Pan T, and secondary FITC only) and mouse IgG1 APC (CD8, CD4&CD8, and secondary APC only). Table 5 shows the antibodies and the dilution factors used in the experiment.

Table 5 Labelling steps

Antibody specificity	Primary antibody + dilution factor	Secondary antibody + dilution factor
CD4	mouse IgG2a anti-rabbit CD4 FITC (KEN-4, AbD Serotec)	NO
CD4 isotype control	mouse IgG2a CD4 isotype control-FITC (MCA929F, AbD Serotec)	NO
Non-stained	NO	NO
CD11b	Anti-rabbit CD11b (1:10) (MCA802GA, AbD Serotec)	Goat anti-mouse IgG1 FITC (1:20)
B cell	Anti-rabbit B cells (1:10)	Goat anti-mouse IgG1 FITC (1:20)
Pan T cell	Anti-rabbit Pan T cell (1:10) (RTH2A, 2BScientific)	Goat anti-mouse IgG1 FITC (1:20)
CD8	Anti-rabbit CD8 (1 :10) (MRB107A, 2BScientific)	Goat anti-mouse IgG1 APC (1:20) (A10530, Invitrogen, UK)
CD8&CD4	Anti-rabbit CD8 (1 :10) and mouse IgG2a anti-rabbit CD4 FITC (1:10)	Goat anti-mouse IgG1 APC (1:20)
APC	NO	anti-mouse IgG1 FITC (1:20)
FITC	NO	anti-mouse IgG1 FITC (1:20)

Ten tubes were labelled for each cell line and four cell lines (IYJJ, IYDY, LFLK, and LFKJ) were used in the experiment.

2.5.1 Direct Immunofluorescence labelling of cells

For this purpose, cells were spun at 2000 rpm for 5 minutes and pelleted then RPMI culture medium was added. Cells were counted to 5×10^5 cells/45 μ l and placed in Eppendorf tubes. Antibodies of 5 μ l mouse IgG2a anti-rabbit CD4 FITC (KEN-4, AbD Serotec) to CD4 and CD4 & CD8 tubes, and 5 μ l mouse IgG2a CD4 isotype control-FITC (MCA929F, AbD Serotec) were added to CD4 iso tube. 5 μ l of anti-rabbit CD8 (ISC29E, WS0768U-100, USA) (1:10) to CD8 and CD4 & CD8 tubes, 5 μ l of anti-rabbit CD11B (MCA802GA, AbD Serotec) (1:10) to CD11B tubes, 5 μ l of anti-rabbit Pan T cells (RTH2A, 2BScientific) (1:10) to Pan T tube, and 5 μ l of anti-rabbit B cells (MRB107A, 2BScientific) (1:10) to B cell tubes. Labelled Eppendorf tubes incubated in the dark in the fridge for 30 minutes.

2.5.2 Indirect Immunofluorescence labelling of cells

After that, cells were centrifuged at 2000 rpm for 2 minutes and washed twice with RPMI then 5 μ l (1:20 diluted) of goat anti-mouse IgG1 FITC (secondary Ab) was added to CD11b, B cell, and Pan T tubes, 5 μ l (1:20) of anti-mouse IgG1 APC (A10530, Invitrogen, UK) to CD8 and CD4 & CD8 tubes, 5 μ l (1:20) of anti-mouse IgG1 FITC secondary only tubes, 5 μ l (1:20) of anti-mouse IgG1 APC to APC secondary only tubes. Labelled Eppendorf tubes were again incubated in the dark in the fridge for 30 minutes. Cells were washed twice by spinning at 2000 rpm for 2 minutes leaving 100 μ l

supernatant. Cells were fixed with 2% PFA and finally suspended in 0.5 ml of PBS.

2.5.3 Flow cytometry analysis of labelled cells

The cells were centrifuged and rinsed then directed to FACScan™ flow cytometer system (Becton Dickinson, Bioscience, USA). The Cells population were gated out to appropriate forward scatter (FSC), side scatter (SSC), 280 and 400, respectively. Cell's samples were then acquired by CellQuest pro-software (BD Bioscience, USA). Finally, the fluorescence data analysis was performed by FACSDiva software (BD Bioscience, USA) and the quadrant sitting for labelled and unlabelled cells was based on antibody-isotype control fluorescence.

2.6 Animals

Ten three month old New Zealand white female rabbits were used (Purchased from Harlan UK). Animals were kept at the animal facility at Sutton Bonington, University of Nottingham. Animal experiments were under ASPA (UK) regulations with a project license held by David Haig at the University of Nottingham. Ethical review was obtained from the local SVMS ethics committee and the University of Nottingham AWERB committee. After infection (see section 2.6.1) animals were observed and temperature was recorded daily using a subcutaneous mini chip. Animals were

ethanized when high body temperature (40°C) developed for two consecutive days or more along with an accumulation of clinical signs typical of MCF that would progress the disease to a higher severity limit than moderate (limited by ASPA project license held by D Haig).

2.6.1 Inoculation

Wildebeest-associated MCF virus (AIHV-1) contained in mesenteric lymph node cells isolated from a rabbit previously infected with AIHV-1 virus C500 strain was used to infect the rabbits injected intravenously (IV, ear vein) with 2×10^6 cells in 1 ml PBS.

2.6.2 Experiment (1) design

Ten rabbits were infected with AIHV-1 C500 strain on day 0 of the experiment as described above. Six of the ten rabbits were treated with cyclosporine A (Cat# 239835, CALBIOCHEM, Germany) every other day starting at day 0 at dose of 0.25-0.5ml IV (depending on the weight of the rabbit) to give a dose of 20mg/kg body weight. The CsA was dissolved in 1XPBS D- α -Tocopherol 25mg/ml per animal in 1XPBS (Cat# 57668-25G, Sigma) containing 2% v/v ethanol in PBS. The remaining four rabbits were given vehicle (tocopherol- ethanol-PBS) only every other day intravenously.

2.6.3 Experiment (2) design

The second experiment was similar to the first one with the exception that the number of rabbit groups included an uninfected control group. Four were infected with the virus; four were infected and treated with cyclosporine A as before except that it was dissolved in PBS containing castor oil 25mg/ml per animal (Kolliphor® EL, cat# C5135-500G, Sigma) and two non-infected controls given vehicle only.

Experiment # 1	Inoculation	Treatment	Observations
10 rabbits	All animals infected with the virus from day 0 of the experiment IV	6 rabbits treated with CsA (20 mg/kg body weight) IV every other day	D-α-Tocopherol 25mg/ml per animal in 1XPBS containing 2% ethanol IV used as a vehicle
Experiment # 2			
16 rabbits	12 rabbits infected with the virus from day 0 of the experiment IV 4 rabbits were not infected used as a control	6 rabbits treated with CsA (20mg/kg body weight) IV every other day 6 rabbits no treatment	Castor oil 25mg/ml per animal IV used as a vehicle

2.6.4 Sample collection

Liver, kidney, lung, spleen, and appendix tissues about 1cm³ were collected (four pieces per tissue) and one piece each placed in Eppendorf tubes containing 500 µl RNA-later (Cat# AM7020,

ThermoFisher Scientific, UK), and placed immediately in -20 C° freezer until RNA extraction. A second piece of each tissue was placed in Eppendorf tubes without adding RNA-later and then placed in -20 C° freezer for subsequent DNA extraction. Mesenteric (MLN) and popliteal lymph nodes were placed in 60ml tubes containing 40ml sterile 1XPBS. The lymph nodes were processed immediately after collection (see section 2.2.1). Blood samples ~ 1800µl were placed in Eppendorf tubes and then placed in -20 C° freezer. The third piece of liver, kidney, lung spleen, and appendix were placed in 7ml bijoux tubes containing 5ml 4% paraformaldehyde (Cat# P/0840/53, Fisher Scientific) in PBS for 48 hours prior to paraffin embedding (see section 2.7.1) for *in situ* hybridisation work. Finally, the fourth piece of each tissue (liver, kidney, lung, spleen, and appendix) was placed in 60ml tubes containing 40ml 10% neutral-buffer-formalin (Cat# 361387P, VWR International) for 24-48 hours prior to paraffin embedding (see section 2.7.1) for H&E staining.

2.7 Histology

Histological approaches are used to investigate the structural organisation of tissue.

2.7.1 Paraffin embedding

Following fixation (see above), tissues were placed in an embedding cassette and dehydrated by processing with an increasing gradient of absolute ethanol in a tissue processor (Leica TP 1020, Leica microsystem. UK) as the following protocol:

- 70% (v/v) Ethanol, 1 hour.
- 80% (v/v) Ethanol, 1 hour.
- 95% (v/v) Ethanol, 1 hour.
- 100% (v/v) Ethanol, four changes, 30 min each.
- HistoClear, three changes, 1 hour.
- Paraffin wax (56-58 C°), two changes, 1 hour and half each.

Finally, the processed tissue samples were oriented and embedded into paraffin molds and kept on the cold plate for 30 minutes to set. Then the mold is removed and the excessive paraffin is trimmed off.

2.7.2 Tissue sectioning and staining

Sections, 6µm thickness, from kidney and appendix fixed in buffered formalin were cut, de waxed and then stained with haematoxylin and eosin stain (H&E) according to the standard histological approach (described below) to visualize the histological structure of the tissues. The slides of tissue sections were passed into HistoClear (two changes for 5 min each), dabbed to remove excess fluid, then rehydrated in a series of alcohol concentrations (100%, 95%, and 70%) for 2 minutes each and then rinsed in running water. Slides were immersed in a bath comprising haematoxylin (Cat# H9627,

Sigma-Aldrich) for 3 minutes and then washed in running tap water. After that, slides were placed in 1% acid alcohol (300ml ethanol+ 3ml HCl) for few seconds, and then washed in water.

Slides were immersed in Eosin (cat# 318906-500 ml, Sigma-Aldrich) for 5 minutes and then briefly washed in water. Eventually, slides were dehydrated by passing through different concentrations of ethanol (Cat# E10650DF/17, Fisher Chemicals) (95% and 100% alcohol), dabbed to remove excess, and then cleared in xylene for 5 minutes in a fume hood before being mounted with 1,3-diethyl-8-phenylxanthine (DPX) (Fluka analytical, Sigma Aldrich, UK). Sections were visualized using upright microscopy Leica DM 5000B epifluorescence imaging system.

For the third experiment, sample preparation and fixation was performed manually applying the same parameters with the exception that xylene (cat# x10200/17, Fisher Chemicals) was used as an alternative to histoclear. In addition, DEPC-treated water was used in 1XPBS to make up 4% paraformaldehyde.

2.8.1 RNA *in situ* hybridisation

In situ hybridisation is the technique by which gene transcripts (mRNA) can be located on tissue using a combination of molecular and histological approaches providing that the tissue components (RNA and morphological features) are maintained.

2.8.1.1 Preparation of riboprobes for virus gene transcripts

RNA probe synthesis is one of the steps towards achieving comprehensive *in situ* hybridisation procedure. The other two main steps include tissue fixation and sectioning and hybridisation of probes.

2.8.1.2 Primers design

The PCR primers used in preparing the riboprobes for AIHV-1 ORF 65 and ORF A9.5 were designed by professor James Stewart (ORF65) and Dr George Russell and colleagues (Russell et al., 2013). Table 6 shows the primers sequence and their amplicon size.

Table 6 shows AIHV-1 ORF65 and ORF A9.5 primer sequences and amplicon size

AIHV-1 gene	Oligonucleotides sequence	Amplicon size
ORF 65 Forward	GCACGCTAGGCCTAAACTTCC	730 bp
ORF 65 Reverse	GCCTTTGCCTAGTTTTCTCTGG	
ORF A9.5 Forward	TGGTTGTGAGAATGAAACACTTG	525 bp
ORF A9.5 Reverse	GCACAAACCGAGTTTGACAG	

2.8.1.3 Polymerase chain reaction (PCR) amplification

PCR was used to amplify the genes of interest according to the protocol described in the materials and methods, section (2.4.2) using Taq polymerase enzyme (NEB). The benefit of using Taq polymerase enzyme is to add a single deoxyadenosine A to the 3'

end of the PCR product. The PCR fragment of the gene of interest was then inserted into a linearized plasmid vector (TOPO-TA one shot cloning kit, Invitrogen) having single overhanging 3' deoxythymidine T residues. This will provide efficient ligation of the PCR insert with the plasmid DNA vector. Complementary DNA (cDNA) from rabbit's kidney infected with AIHV-1 C500 strain was used to amplify the gene of interest. The reason for using cDNA is to obtain coding sequence without any introns (non-coding sequence), hence avoiding any complication while synthesising the RNA probe. Figure 7 shows the amplicon size for both genes.

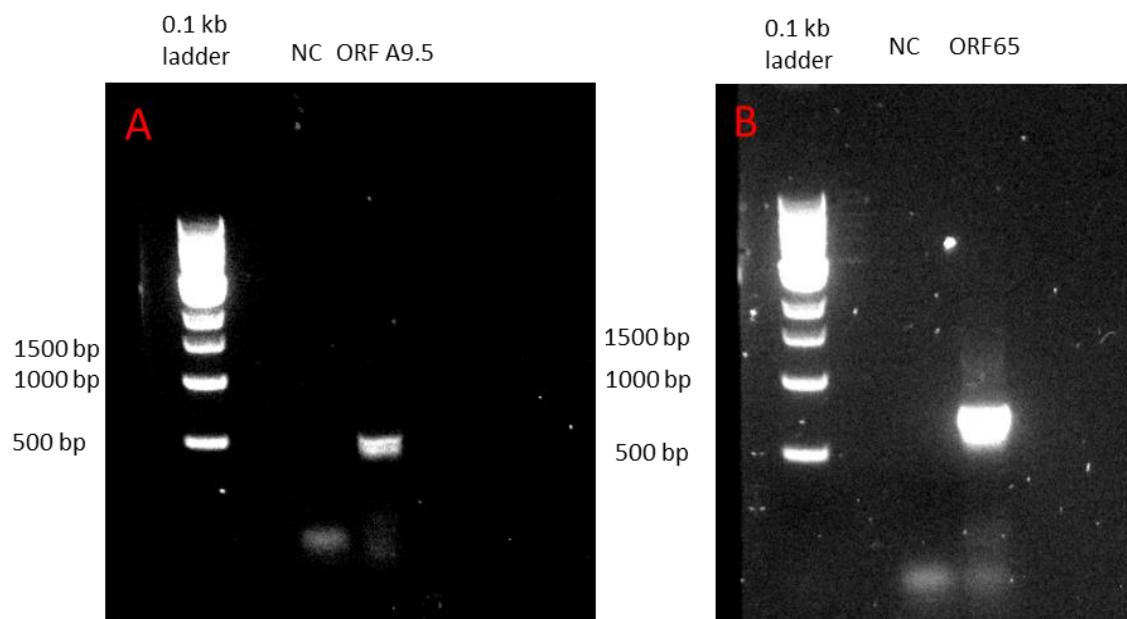


Figure 7 AIHV-1 PCR products for ORF A9.5 and ORF65 genes.

The figure illustrates the PCR products (cDNA) for two AIHV-1 genes used to generate RNA probes utilizing plasmid vector. Image (A) shows the product size (525 bp) of ORF A9.5 while image (B) shows the product size (730 bp) of ORF65. One kilo base pair ladder was used to analyse the genes product size. NC: negative control.

2.8.1.4 Gel extraction for ORF65 product

Gel extraction was performed on ORF65 PCR products as it did not give a clear single band using QIAquick Gel Extraction Kit (Cat# 28704, Qiagen). The protocol used was according to the manufacturer's instructions as the following. The DNA fragment was excised from the agarose gel with a clean, sharp scalpel, weighed in a colourless tube, and 3 volumes Buffer QG were added to 1 volume gel. The tube incubated at 50 °C for 10 min and 10 µl 3 M sodium acetate was added. One volume isopropanol was added to the sampled and mixed. The sample was applied to a QIAquick spin column in 2 ml collection tube and centrifuged for 1 min. The flow-through was discarded. A volume of 500 µl Buffer QG was added to the spin column and centrifuged for 1 min. The flow-through was discarded. A volume of 750 µl Buffer BE was added to QIAquick column and centrifuged for 1 min to wash the DNA. The flow-through was discarded. The QIAquick column was placed in a clean 1.5 ml micro-centrifuge tube. A volume of 30 µl Buffer EB (10 mM Tris-Cl, pH 8.5) was added to the centre of the QIAquick membrane, let stand for 1 min, and then centrifuged for 1 min to elute the DNA.

2.8.2 Plasmid cloning, transformation and bacterial culture

The PCR products for the genes of interest were then cloned into TOPO vector (PCR II TOPO, Invitrogen) utilizing TOPO-TA one shot cloning kit (Invitrogen) according to the following steps: Two μl of fresh PCR product mixed with 1 μl salt solution (1.2 M NaCl, 0.06 M MgCl₂) and 2 μl of RNase free water was added then 1 μl of plasmid (10 ng/ μl linearized plasmid, 50 glycerol, 50 mM Tris, 1mM DTT, 0,1% 100x triton, 100 $\mu\text{g}/\text{ml}$ BSA, phenol red) was added to make a final mixture of 6 μl cloning mix. The mixture was incubated for 5 minutes at room temperature. The mix then placed on ice.

Two μl of the TOPO cloning reaction was added to the chemically competent *E. coli* in a vial (one shot, Invitrogen), mixed gently and then incubated on ice for 30 minutes. The cells were then heat-shocked for 30 seconds at 42°C in water bath without shaking and quickly transferred on ice. A 250 μl of room temperature supplied SOC medium (Invitrogen) was added to the bacterial vial. The vial was capped tightly and placed horizontally (200 rpm) at 37°C for 1 hour in a shaker.

Upon incubation, 40 μl of the transformed cells were spread on agar plate with 50 $\mu\text{g}/\text{ml}$ kanamycin (Cat# 15160054, Thermo-fisher Scientific) and x gal (Cat# 15520-018, Thermo-fisher Scientific) for white or blue colony screening. The plates were incubated overnight at 37°C. The following day six white colonies were chosen and

cultured in 5 ml nutrient broth containing 50 µg/ml kanamycin and then incubated for 24 hours at 37°C in universal tubes in orbital shaker at 200 rpm.

2.8.2.1 Plasmid purification

2.8.2.1.1 Minimum isolation of plasmid DNA (Mini-prep)

The plasmid DNA was isolated using resource plasmid mini kit (cat # SBS27104, Source Bio Science, UK). One to five ml bacterial overnight culture was pelleted by centrifugation at 6000 g for 3 min at room temperature. Pelleted bacterial cells were re-suspended in 250 µl buffer 1 and then transferred to a micro-centrifuge tube. A volume of 250 µl Buffer 2 was added and mixed thoroughly by inverting the tube 4-6 times until the solution becomes clear. A volume of 350 µl Buffer 3 was added, mixed immediately and thoroughly by inverting the tube 4-6 times, and then centrifuged for 10 min at 17,900 g in table-top micro-centrifuge. The supernatant was applied to spin column in a 2ml collection tube, washed by adding 0.5ml Buffer B and centrifuged for 1 min. The flow-through was discarded. The spin column was washed by adding 0.75ml Buffer E and centrifuged for 1 min. The flow-through was discarded. The spin column was further centrifuged for 1 min to remove residual wash buffer. The spin column was placed in a clean 1.5 ml micro-centrifuge tube and 50 µl Elution buffer was added to the

centre of the spin column, let stand for 1 min, and then centrifuged for 1 min to elute the DNA.

2.8.2.1.2 Maximum isolation of plasmid DNA (maxi-prep)

The maximum isolation of plasmid DNA was performed using plasmid maxi kit (Cat# 12362, Qiagen). The 150 ml overnight nutrient broth culture was harvested by centrifuging at 6000 g for 15 min at 4 °C and the bacterial pellet was completely re-suspended in 10 ml Buffer P1. A volume of 10 ml Buffer P2 was added mixed thoroughly by inverting 4-6 times, and incubated at room temperature for 5 min. During the incubation, the QIAfilter Cartridge cap was screwed onto the outlet nozzle of the QIAfilter Cartridge in a falcon tube. A volume of 10 ml chilled Buffer P3 was added and mixed thoroughly by inverting 4-6 times. The lysate was loaded into the barrel of the QIAfilter Cartridge, incubated at room temperature for 10 min. After removing the cap from the QIAfilter Cartridge outlet nozzle, a plunger was gently inserted into the QIAfilter Cartridge to filter the cell lysate into the falcon tube. A volume of 2.5 ml Buffer ER was added to the filtered lysate, mixed by inverting the tube 10 times, and then incubated on ice for 30 min. A QIAGEN-tip 500 was equilibrated by applying 10 ml Buffer QBT and allowed the column to empty by gravity flow into a falcon tube. The filtered lysate placed on ice was applied to the QIAGEN-tip and allowed to enter the tip. The QIAGEN-tip was washed twice with 30 ml Buffer

QC. The DNA was eluted with 15 ml Buffer QN into a 30 ml endotoxin free tube, precipitated by adding 10.5 ml room-temperature isopropanol, mixed, and then centrifuged at 15,000 g for 30 min at 4 °C. The supernatant was carefully discarded and the DNA pellet was washed with 5 ml of endotoxin-free room-temperature 70% ethanol, and centrifuged at 15,000 g for 30 min at 4 °C. the supernatant was carefully decanted without disturbing the pellet. The DNA pellet was air-dried for 5-10 min and re-dissolved in a suitable volume (100 µl) of endotoxin-free Buffer TE.

2.8.2.1.3 DNA sequencing

The plasmid DNA containing the PCR product inserts of the genes of interest were sent for a sequence check to Source Bioscience (Rochdale, UK) utilizing universal primers (M13 reverse and M13 forward) to sequence sense and anti-sense DNA strands. The data obtained from the sequence analysis were compared with the genes of interest sequence available at

(<http://www.ncbi.nlm.nih.gov/nucore/10140926/>) using clustalW2 software programme.

2.8.2.1.4 Restriction digestion for plasmid DNA preparation

In order to prepare DNA template, plasmids were linearized using suitable restriction enzymes generating correct DNA cut. A volume of 8 µg of DNA was mixed with 8 µl restriction enzyme and 8 µl

restriction enzyme buffers (10X). The volume was then completed to 100 µl RNase free water and then incubated for 2 hours at 37°C. A volume of 2.5 µl of the digested DNA were run on 1% agarose gel as described in section (2.4.2.2) to compare the size of plasmid and gene of interest. The restriction enzymes used were Bam H I (Ref# 10798975001, version 12, Roche) to prepare anti-sense probe and Xho I (Ref# 10899194001, version 22, Roche) to prepare sense probe. Digested DNA was purified utilizing Phenol:Chloroform:Isomyl (25:24:1) (P 3803-100, Sigma) Chloroform:Isomyl alcohol (24:1) (Cat# C0549-1QT, Sigma) and ethanol and then suspended in 50 µl RNase free water and kept in -20°C freezer.

2.8.2.1.5 In vitro transcription of digoxigenin (dig)-labelled RNA probes

In order to produce digoxigenin-labelled RNA probes, the linearized DNA template was used for *in vitro* riboprobe synthesis utilizing Dig RNA labelling kit (Cat # 11175025910, Roche, USA) in line with the manufacturer's instructions. An amount of 1 µg of purified template DNA was added into Eppendorf tube and 2 µl of 10X NTP labelling mix, 2 µl of 10X transcription buffer, 1 µl of protector RNase inhibitor, 2 µl RNA polymerase SP6 to generate sense probe or 2 µl RNA polymerase T7 to produce anti-sense probe and then the volume was made up to 13 µl with RNase free water. The mix was centrifuged briefly and then incubated for 2 hours at 37°C. a

volume of 2 μ l DNase I were added and incubated for 15 minutes at 37°C to degrade the template DNA. The reaction was then stopped by adding 2 μ l of 0.2 M EDTA pH 8. A volume of 1 μ l of 1 mg/ml carrier yeast tRNA was added to the DNase digested probes, precipitated by ethanol and then re-suspended in 50 μ l RNase free water.

2.8.2.1.6 Dot blot analysis of generated probes

In order to check the excellence of the generated probes, serial dilutions of sense, antisense and T7 control were prepared in 10 μ g/ml yeast tRNA (cat # VYAM7119, Fisher Scientific, UK) and tested by dot blot hybridization. A volume of 5 μ l of each dilution was spotted on Amersham's nylon membrane (Amersham Pharmacia biotech, Hybond-N+, England) from 10^{-5} to 10^{-1} in a petri dish. Upon drying, the dish containing the membrane was placed in UV crosslinker (stratalinker) to fix the probes. The membrane was then placed on a bigger dish on a shaker and washed in 100 ml washing buffer (0.1 M maleic acid, 0.15 M NaCl pH 7.5, 0.3 % v/v Tween 20) for 2 minutes. The membrane was soaked in 100 ml blocking solution (Dig-wash and block, cat # 11585762001, version 10, Roche) (0.1 M maleic acid, 0.15 M NaCl, pH 7.5) on a shaker for 30 minutes. After that, the membrane was incubated with 20 ml labelled anti-DIG antibody solution (anti-Digoxigenin-AP FAb fragments, cat# 11093274910, Roche) diluted 1:5000 in blocking

solution) for 30 minutes. The membrane was then washed twice with 100 ml washing buffer for 15 minutes and equilibrated in detection buffer (0.1 M Tris-HCl, 0.1 M NaCl, pH 9.5) for 3 minutes. The colour substrate was prepared by dissolving one tablet Sigma fast BCIP/NBT (Cat# B5655-25TAB, Sigma) in 10 ml RNase free water. The dish was then placed in the dark until the dot blot colour develop. The reaction was then stopped by adding 50 ml TE buffer for 5 minutes.

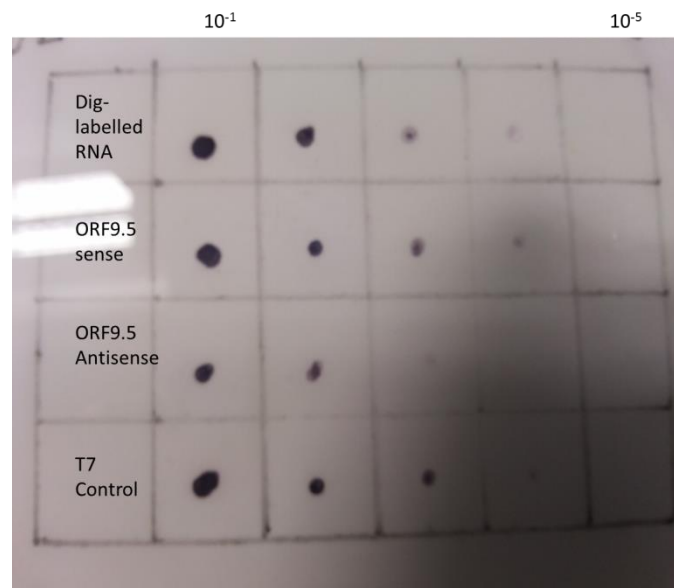


Figure 8 dot blot analysis of AIHV-1 ORF A9.5 RNA probe

The figure shows the \log_{10} dilutions of sense, antisense, dig-labelled RNA and T7 control which were spotted on Amersham's nylon membrane from 10^{-1} to 10^{-5} concentrations. The membrane was washed and blocked using dig-wash and block solutions to develop the dot blot colour.

2.8.3 Deparaffinisation, proteolysis, and acetylation of tissue sections

Deparaffinisation was performed by placing tissue sections in xylene (Cat# X/0200/17, Fisher Scientific) twice in staining dishes for 5 minutes. The sections were then rehydrated by dipping twice in 100% ethanol for 5 minutes and 96% and 70% once for 5 minutes. The slides were dipped in DEPC treated water (diethyl pyrocarbonate, cat# E174-25G, Amresco) in staining dish for 5 minutes. The slides were then transferred to coplin jar and washed with 1XPBS for 5 minutes.

To achieve proteolysis, slides were incubated in 0.2 M HCl at room temperature for 30 minutes. Slides were then incubated twice 2X sodium saline citrate with 5 mM EDTA at 50°C for 30 minutes, trailed by digestion in proteinase K solution (proteinase K, recombinant PCR grade, cat# 03115836001, Roche), with 1 M TRIS pH 8 and 0.1 M CaCl₂ made up to 60 ml DEPC treated water) for 15 minutes at 37°C. Fixation steps were performed in room temperature through incubation in 0.2% glycine-PBS for 5 minutes, followed by washing in 4% paraformaldehyde for 4 minutes and then washing in 1XPBS for 2 minutes and 15 minutes in 5mM MgCl₂ in 1XPBS.

Acetylation was done through incubation with 0.25% acetanhydrid (Cat# 45830-250ML-F, Sigma) with 0.1 M triethanolamine (Cat# 1.08379.0250, VWR International Ltd) pH 7.5, followed by washing

in 1XPBS twice for one minute and once for 15 minutes in room temperature.

2.8.4 Hybridisation of probes

Pre-hybridisation, hybridisation, and post hybridisation wash:

The slides were prepared for hybridisation by pre-warming in pre-hybridisation buffer (0.1 mg/ml salmon sperm DNA [Sigma] and 0.25 mg/ml yeast tRNA in a pre-hybridisation stock mix of 30% v/v 20X SSC, 45% v/v 100% deionised formamide [cat# 11FORMD002, MP Biomedicals, LLC], 10% v/v 50x Denhardt's solution [Invitrogen] with 14% DEPC-treated dH₂O) in coplin jar at 52°C for 1 hour.

To perform the hybridisation step, slides were transferred to metal tray and covered with 30-40 µl/ tissue section hybridisation buffer consisting of 250µg/ml tRNA, 10mg/ml salmon sperm DNA, 80 µl dextran sulfate, 2-6 µl RNA probe (1:100) dilution added to 700 µl hybridisation mix 100% deionised formamide, 20X of 0.5 M EDTA pH 8, 0.5 M piperazin-N,N'bis 2-ethanesulfate-acid-PIPES pH 7.0 (cat# P3768-25G, Sigma), 5 M NaCl, 50X Denhardt's solution, heparin 20,000 U (Cat# H 3393-25 KU, Sigma), and 10% Triton X-100. Slides were covered with hydrophobic surface of gel-bond film (Cat# LZ53734, Scientific Laboratory Supplies LTD, Uk), sealed with Fix-O-gum gel (Marabu, Tamm, Germany) and incubated at 52°C in a moist box overnight.

The following day gel bond was carefully removed and slides placed again in coplin jar for post hybridisation wash. Washes were performed twice in 6XSSC with 45% formamide (Cat# 1.09684.1000, VWR International LTD) at 42°C for 15 minutes, followed by two washes in 2XSSC for 5 minutes at room temperature and twice in 0.2XSSC at 50°C for 15 minutes.

2.8.5 Anti-DIG labelling for probe detection

Tissue sections were washed with buffer 1 (TRIS 100mM, NaCl 100mM, pH 7.5) for one minute at room temperature. Slides were then washed with blocking solution (sterile neutral sheep serum {NSS, cat# S2263-100ML, Signa}, 10% Triton X-100) for 30 minutes at room temperature. Slides were then placed on metal tray, carefully dried, and circled by water repellent pen (PAP-PEN). Antibody solution 400 µl/slide (30 µl AP-conjugated {Anti-DIG-AK-AP 1:200}, 42 µl NSS, 188 µl 10% Triton X-100, 6 ml buffer1) were added on top of the tissue sections for 2 hours at room temperature. Slides were then transferred to coplin jar and washed with buffer 1 twice for 15 minutes at room temperature. Tissue sections were further washed with buffer 3 (TRIS 100mM, NaCl 100mM, pH 9.5, MgCl₂+6H₂O) for two minutes at room temperature. Ultimately, slides were incubated in the dark with staining solution (three tablets of BCIP/NBT, 30 mg levamisole (Cleaveland et al. L9756-5G, Sigma), 60 ml buffer 3) for long time

up to 1 week. Slides were periodically inspected under light microscope for signal development (dark blue colour in cell cytoplasm). The reaction was stopped by incubating slides with buffer 4 (TRIS 10mM and EDTA 1mM, pH 8) in the dark for 10 minutes. Slides were kept in double distilled water for 5 minutes. Counter staining was done by dipping slides in haematoxylin (Ref# HHS32-1L, Sigma Aldrich) for 10 seconds. After that, slides were blueing in tap water for 5 minutes. Slides were then dried and covered with cover slip using 1, 3-diethyl-8-phenylxanthine (DPX) (Fluka analytical, Sigma Aldrich, UK) and then stored in the dark.

2.9 RNA quality measurement using Agilent Bio-analyser Nano 6000 kit

Agilent Nano chips (Agilent Technologies, Stevens Creek Blvd, USA) comprise a set of micro channels used to separate nucleic acid fragments based on base sizes as they are driven through it electrophoretically. RNase ZAP (Cat# AM9780, ThermoFisher Scientific) which removes RNases and reduce nuclease contamination in RNA purification laboratories and RNase free water were used to decontaminate the electrodes by washing for 1 minute and 10 seconds respectively. All the reagents and samples used in the technique were equilibrated at room temperature for 30 minutes. A volume of 550 μ l of Agilent 6000 Nano gel matrix (red colour tube in the kit) was placed in a spin filter and centrifuged for 10 minutes at 1500 g. A volume of 65 μ l filtered gel was aliquoted in RNase free 0.5ml micro-centrifuge tubes. For single use, the gel dye mix was prepared by adding 1 μ l of RNA 6000 Nano dye (blue colour) to 65 μ l aliquot of pre-prepared filtered gel. The tube was mixed thoroughly by vortex and then centrifuged for 10 minutes at room temperature at 13000 g. The gel dye mix was loaded into the RNA Nano chip by pipetting 9 μ l of the mix at the bottom of the wells marked  (Figure 9) after the chip was being placed on the chip priming station. The plunger was positioned at 1 ml position and the chip priming station was closed for 30 seconds. The plunger of the syringe was held down until it was held by the clip. After 30

seconds the plunger was released by a clip release mechanism. The chip priming station was opened and 9 μl of the gel dye mix was pipetted in the wells marked **G** (Figure 9). 5 μl of RNA 6000 Nano marker (green colour) was pipetted into the 12 wells and the wells marked **H** (Figure 9). The RNA samples and the ladder were heat denatured at 70°C for 2 minutes to minimise secondary structure. 1 μl of the ladder was pipetted to the wells marked **H** (Figure 9) and 1 μl of each sample into each of the 12 sample wells. The chip was horizontally placed in the adapter of the available vortex mixer and vortexed for 1 minute at 2000 rpm. The chip was inserted in the Agilent 2100 Bioanalyzer and read. Figure 9 shows the Agilent 6000 Nano chip shape and its various loading wells.

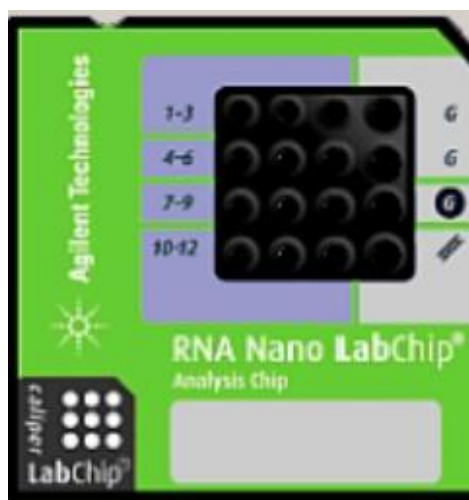


Figure 9 shows the Agilent 6000 Nano chip appearance and its different loading wells

2.10 RNA sequencing (RNA-Seq) methods

RNA-seq is also known as whole transcriptome shotgun sequencing (WTSS) and utilizes next-generation sequencing (NGS) to detect and quantify RNA molecule by way of DNA copies in a given biological sample (Morin et al., 2008, Wang et al., 2009). The use of this technique has enabled scientists to analyse cellular transcriptomes and simplified looking at alternative gene spliced transcripts, changes in gene expression, single nucleotide polymorphism (SNP), posttranscriptional modifications and the ability to look at RNA populations including mRNA, micro-RNA (miRNA), small RNA, total RNA, tRNA and ribosomal RNA (Ingolia et al., 2012, Maher et al., 2009). There are many approaches by which RNA sequencing can be achieved.

2.10.1 RNA poly (A) library

In this approach the polyadenylated (poly (A)) tail is targeted to guarantee that coding RNA is split from non-coding RNA. This can be done by using poly (T) magnetic beads (Wang et al., 2009). Because ribosomal RNA (rRNA) represent up to 80% of total RNA in a given cell resulting in dilution of mRNA species, tRNA is removed by either enzymatic degradation or hybridisation-based depletion approaches (Chen and Duan, 2011, Yi et al., 2011). Prior to cDNA synthesis, RNA samples are fragmented by either chemical hydrolysis or enzymatic digestion to approximately 200-250

nucleotide (nt) long (Mortazavi et al., 2008). After that, complementary DNA (cDNA) is synthesized by reverse transcriptase and oligonucleotides, used as adapters, are utilized to ligate to cDNA to assist amplification and allowing sequencing (Chu and Corey, 2012).

2.11 Illumina machine NextSeq500 sequencing

platform work flow

The work flow of the Illumina sequencing machine comprises four main steps; sample preparation, cluster generation, sequencing and data analysis. In the first step, the sample of interest (total RNA) is subjected to a series of stages to fragment the RNA molecule, converted into cDNA and then amplified to produce cDNA library. This library is then placed in an eight-lane flow cell in which the cDNA fragments are attached to oligonucleotide primers complementary through its adapters. The cDNA fragments then undergo a series of amplification by which clusters of double stranded DNA are produced. The flow cell is placed in the sequencing machine where each cluster is sequenced and at each cycle four-fluorescence labelled nucleotides are added and the emitted signals are recorded. The intensity of the fluorescence is translated into base-calls. The cycle numbers show the length of the reads whereas clusters numbers define the number of reads (Bullard et al., 2010).

2.12 Bioinformatics tools

The activities that can be covered by bioinformatics include sequence alignment, prediction of gene expression, mapping and analysing DNA and protein sequencing and aligning DNA. All of these activities can be achieved by various bioinformatics tools (Luscombe et al., 2001).

2.12.1 Blast like alignment tool (BLAT)

BLAT is a sequence alignment tool introduced by Jim Kent in 2002 to facilitate the assembly and annotation of the human genome. BLAT was ~500 times faster with performing mRNA/DNA alignment and ~50 times faster with protein/protein alignments than any other alignment tools. BLAT can be used for aligning multiple RNA sequences onto a DNA assembly to deduce their genomic matches, aligning of a protein or mRNA sequence from one species onto a sequence data base from another species and identification of gene family members of certain gene query. BLAT and BLAST have many things in common however they vary in some aspects. While BLAT scans the query sequence for matches, BLAST searches the data base for matches. BLAT is less sensitive than BLAST. BLAT involves query sequence in FASTA format, whereas BLAST requires the query in accession number and FASTA-formatted sequence. BLAT can be utilized as server-client programme or as stand-alone programme (Kent, 2002).

2.12.2 Scythe-a Bayesian adapter trimmer

Scythe utilizes a Bayesian method categorising contaminant substrings in sequence reads. The software has the ability to remove the 3' -end adapters which contain low quality bases. The process of a poor-quality trimmer is required before mapping, analysis and assemblies for the next generation sequencing run to pick out low quality bases. The mechanism of scythe is based on two probabilities i.e. the likelihood of identifying the matches in a given contaminant or not given contaminant. Assuming that the read is contaminated, the likelihood of seeing the specific number of matches and mismatches is reliant on how good the quality of the sequence is. In the later model, the likelihood of seeing the specific number of matches and mismatches is an accidental. Scythe does not function on 5'-end contaminant or any other contaminants (Lindgreen, 2012).

2.12.3 Sickle- a windowed adaptive trimming tool for FASTQ files using quality

The majority of contemporary sequencing technologies generate reads that have relapsing quality towards the 3'-end and some towards the 5'-end which in turn can affect mapping, assemblies, and data analysis. Sickle is a bioinformatics tool that utilizes sliding windows along with quality and length thresholds in order to define when quality is appropriately low to remove the 3'-end of reads and

also determine when the quality is adequately high to trim the 5'-end of the reads. Sickle also rejects reads based upon the length threshold. Sickle slides a window across quality values whose length is 0.1 times the length of the reads. Sickle backs up three sorts of quality standards i.e. Illumina, Solexa and Sanger. Sickle comprises two techniques to work with both paired-end reads and single-end reads sickle se and sickle pe (Joshi and Fass., 2011)

2.12.4 HISAT

The first step in RNA-Seq downstream data analysis is to align the reads against a reference genome. The use of pre-existing and vastly utilised alignment programmes such as TopHat2 and GSNAP is time consuming. In order to overcome this deficit, HISAT, a spliced aligner tool, was produced with indexing approach based on the Burrows-Wheeler transform and the FM index. The programme algorithms occupy two various sorts of indexes: a global FM index that denotes the whole genome and several small FM indexes that collectively cover the entire genome. Each index exemplifies $\sim 64,000$ bp and $\sim 48,000$ bp are required to cover the human genome. These small indexes (local indexes) are stored in small set of files and other optimisations are applied to reduce the memory requirements. This has allowed the human genome to be indexed in almost 4 GB of space. The advantage of using these small indexes in combination with numerous alignment approaches is in allowing

effective alignment of RNA-seq reads, especially, reads spanning multiple exons. HISAT is a fast, accurate and sensitive alignment programme for mapping RNA-seq reads (Kim et al., 2015).

2.12.5 Sequence alignment map (SAM) tool

The sequence alignment map is a TAB-delimited text format comprising a header section which is optional and an alignment section. The header line begins with '@' whereas alignment lines do not. Each alignment line contains 11 compulsory fields for important alignment information like mapping location and changeable figure for optional fields. SAM is a universal format for saving sequence nucleotide alignments and easy to work with. SAM's file size is compact and permits the file to be indexed by genomic location to professionally recover all reads aligning to a locus. SAM permits most of the processes on the alignment to function on a stream without loading the whole genome into a memory. SAM tools deliver different advantages for handling alignments in the SAM format comprising merging, sorting and generating alignments in pre-located format (Li et al., 2009).

2.12.6 String Tie assembler tool

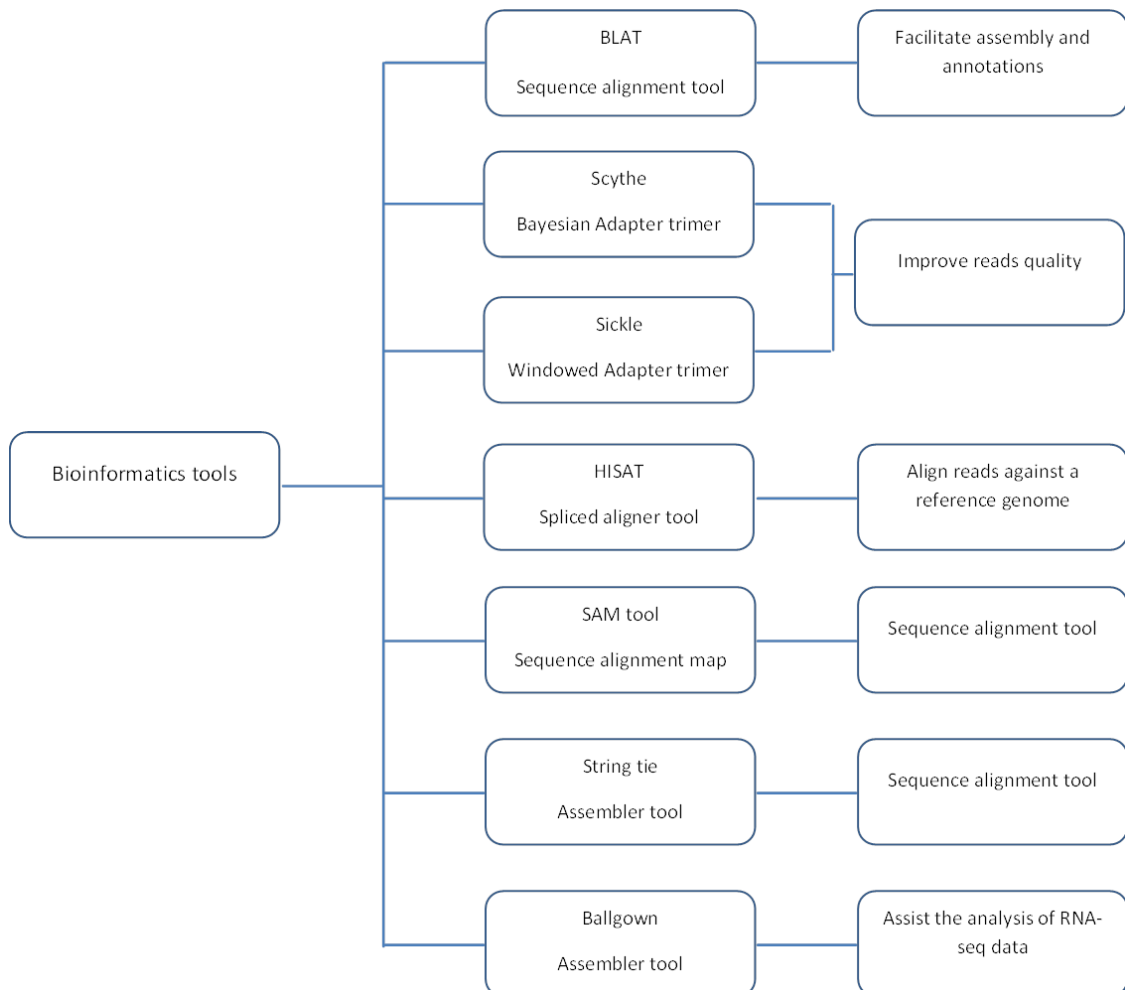
The approaches utilised to sequence the transcriptome such as RNA-seq generate more than 200 million short sequences. Each of these short reads is 100-150 bp. Due to the fact that various transcripts

have highly variable sequence coverage and alternative transcripts from the same locus can share exons, this has made assembling the short reads a hard task. String Tie is a computational approach enforcing a network flow algorithm initially designed in optimisation theory along with optional de novo assembly to assemble a complex data into transcripts. In comparison with other superior transcript assembly packages such as Cufflings, Isolasso, scripture and Traph, String tie generates comprehensive and precise reconstructions of genes and better evaluates the expression level. The software is faster on all data sets than other assembly softwares (Pertea et al., 2015).

2.12.7 Ballgown

Ballgown is a software package to assist the analysis of RNA-Seq data. It supplies assignments to organise, visualize and analyse the expression quantities for transcriptome assembly. There are a number of pre-processing stages required prior to the use of ballgown R package i.e. the RNA-Seq reads should be aligned to a reference genome, a transcriptome should be assembled and expression for the traits (transcript, intron and exon junctions) ought to be evaluated in ballgown readable format. There are two sample pipelines for pre-processing and they are pipeline one (tophat2 + stringtie) and pipeline two (tophat2 + cufflinks + table maker). Certain files should be produced by stringtie and

tablemaker for ballgown to load and some of these are e_data.ctab, i_data.ctab and t_data.ctab. Data is then loaded utilizing ballgown function. The soft contain six slots to access the assembly data: structure, expr, indexes, dirs, mergedDate, and meas. Ballgown delivers broad bundles of simple, fast statistical approaches such as limma and statstest for examining whether transcripts are differentially expressed between experimental conditions or across a continuous covariate (such as time) (Frazee et al., 2014).



2.13 Statistical analysis

Differential statistical analysis was performed by ball gown (Frazee et al., 2014) and the experiment replicate was in duplicate (N=2). The gene expression analysis was done with q PCR LightCycler 480 software and Microsoft Office Excel 2010 applying Pfaffl method (Pfaffl., 2004). LGL viral load was calculated using LightCycler 480 software the experiment replicate was done in duplicate (N=2) and two-way ANOVA used to analyse the data followed Sidak's multiple comparisons test.

Chapter 3

AIHV-1 infection of epithelial and endothelial cell lines

3.1 Abstract

Malignant catarrhal fever is characterised by accumulation of lymphocytes in non-lymphoid tissues, vasculitis and epithelial damage. The pathogenesis of MCF is not well understood. It could be due to the cytotoxic activity of infiltrated T cells or direct infection and destruction of tissues (particularly epithelium or endothelium) or a mixture of both. It is also not clear whether infection of these cell types establishes latent or productive virus life cycle or both. To address this, rabbit epithelium and bovine endothelium cell lines were used to attempt infection and measure virus life cycle gene transcripts. Bovine turbinate fibroblasts were included as a positive control for productive virus infection. The cells were infected with low pass AIHV-1 (fully virulent virus) and high pass AIHV-1 C500 strain (attenuated with gene deletions and translocations, Handley et al., 1995, Wright et al., 2003). Polymerase chain reaction and q PCR were used to detect the viral DNA and measure the viral gene transcript profiles in the infected cells. It was found that the virus infected the epithelial and endothelial cells (as measured by viral DNA). There was, however, no CPE and very low level gene expression such that it can only be concluded that there was no or limited productive infection in the infected epithelium and endothelium *in vitro* compared to a productive transcript

profile seen in the control BT Cells, or alternatively, that the cells were latently-infected. Importantly though, when the virus extracted from the BAE and SIRC cells was used to infect BT cells, a productive infection (with CPE) was recorded. This indicated that virus from the BAE and SIRC cells was infective and intact (expressed genes).

3.2 Introduction

Malignant catarrhal fever is characterized by infiltration of lymphocytes in non-lymphoid tissues, lymphoid hyperplasia vasculitis and epithelial and endothelial degeneration (Buxton et al., 1984, Jacoby et al., 1988, Liggitt and DeMartini, 1980a, Liggitt and DeMartini, 1980b, Simon et al., 2003). The severity of the lesions in particular in the epithelium of the oral cavity, gastrointestinal tract, urinary bladder, liver, biliary ducts, and kidneys as well as damage to the endothelium of arteries and veins is associated with an increase in T lymphocyte (mainly CD8⁺ T cells) infiltration a proportion of which are infected with virus in these tissues (Dewals et al., 2008, Dewals et al., 2011, Palmeira et al., 2013). Furthermore, this damage becomes more pronounced towards the end of the disease course (Liggitt and DeMartini, 1980a, Liggitt and DeMartini, 1980b). In addition, the paucity of viral transcripts supporting productive virus cycle as well as for the latent cycle (where this is expected possibly) in the tissues of animals infected with AIHV-1 has been reported (Dewals et al., 2008, Dewals et al., 2011) leading to the hypothesis that MCF is a disease of latency. However, there is evidence of productive virus cycle transcripts in infected cells and *ex vivo* LGLs as well as antibody responses to envelope and capsid proteins that would indicate productive virus infection. The mechanism of epithelium and endothelium damage is not proved. It could be due to the cytotoxic activity of the

accumulating infected T cells in the tissues or may be due to direct infection of these cells and destruction of them (cytopathic effect) or possibly a combination of both mechanisms. The aim of this study is to examine whether AIHV-1 (low culture passage, virulent C500 AIHV-1 or high pass attenuated virus) can infect epithelial and endothelial cells and cause cell damage, and also to investigate whether the virus is able to establish a productive/lytic infection or latent one in the infected cells. BT cells were used as controls where productive virus infection occurs.

3.3 Materials and methods

3.3.1 Virus

Low culture pass (virulent) AIHV-1 C500 strain and high pass attenuated C500 AIHV-1 were obtained from inoculated bovine turbinate fibroblasts (BT cells) and titrated as described in M&M chapter 2 (section 2.2.5). Titres obtained were $\sim 10^3$ TCID₅₀ per ml for low pass and $\sim 10^6$ TCID₅₀ per ml for high pass virus. The cells were infected with the virus (see virus dose below) when they become 80% confluent (confluency is the percentage of the cells covering the vessel). This is carried out by discarding the old media, washing the cells with 1x PBS and then inoculating the virus directly onto the cell surface with serum free media until the surface is covered.

3.3.2 Virus dose

Statens seruminstitut rabbit cornea (SIRC) epithelial cells, BT fibroblasts and bovine aortic endothelium (BAE) cells were cultured as described in Chapter 2 (section 2.2). The cells were infected with high pass AIHV-1 virus C500 strain at a dose of 5×10^4 TCID₅₀ per 50 μ l inoculum for SIRC and BAE and 5×10^3 TCID₅₀ per 5 μ l for BT cells. For low pass virus 2×10^3 TCID₅₀ per 2 ml inoculum was used to infect both SIRC and BAE cells and 1×10^3 TCID₅₀ per 1 ml inoculum for BT cells.

3.4 In vitro infection

3.4.1 Direct virus infection

Bovine turbinate fibroblast (BT) cells, SIRC, and BAE were cultured in two types of media IMDM or DMEM as described in chapter two (2.2). The cells were infected as described (3.3.1) with either low pass or high pass ALHV-1 virus C500 strain with the doses described above and DNA was extracted from the cells on 2, 5, and 10 days after infection. This was to determine the presence or absence of the virus as viral DNA detected by PCR. BT cells at 50% CPE were harvested as a productive virus control (around day 5 post infection).

In order to determine whether the BAE and SIRC cells infected as described above contained infective virus, the cells and supernatant were harvested 7 days after infection and cell sonicate (to release cell-associated virus) and the supernatant were then added to uninfected cultures of BAE, SIRC and BT cells, which were analysed at different time points afterwards for the presence of virus DNA. For the harvest of the indirect (or secondary) infected cells, medium was collected from centrifuged cells placed into falcon tubes on ice. The cell pellet was re-suspended in medium after being centrifuged at 300xg for 10 minutes. The supernatant was collected and added to the collected supernatant placed on ice. The cell pellets were re-suspended in medium, freeze/thawed once in liquid nitrogen, sonicated in water bath sonicator and then spun down at 300xg for

10 minutes. This supernatant was added to the already collected medium and supernatant to make up viral product from the cells which was used to infect healthy SIRC and BAE cells at 80% confluence in 75cm³. The flasks were placed in a 37 C° 5% CO₂ incubator for seven days. During this time cells were monitored for CPE development under the microscope. Finally, (day 7), cells were harvested and DNA and RNA extracted for further analysis of viral DNA and viral gene transcripts (as shown in Table 7) by PCR and Q RT PCR (as described in chapter 2 sections 2.3.1 and 2.3.2).

Table 7 Viral gene transcripts representing either productive or latent cycle or involved in the virus life cycle.

AIHV-1 genes (ORF)	Putative function/homology to productive or lytic cycle herpesvirus genes.
ORF50	Encodes RTA the transcriptional and replication activator responsible for the switch to lytic cycle.
ORF25	Major capsid protein expressed during lytic cycle.
ORF63	Encodes structural protein during lytic cycle.
ORF73	Encodes LANA protein involved in latent infection.
A4.5	Similar to Bcl-2 family of apoptosis. Virus cycle expression not known.
A9.5	Encodes a secreted glycoprotein that is similar to IL-4. Virus cycle expression not known.

3.5 Results

3.5.1 Infection of the epithelial and endothelial cell lines

Three cell lines, BAE bovine endothelium, SIRC rabbit epithelium, and control BT bovine fibroblasts were infected with low and high pass AIHV-1 C500 strains. Bovine turbinate (BT) fibroblast cells showed a cytopathic effect (CPE) when infected with either low or high pass AIHV-1 virus five to six days after inoculation, indicating that both virus preparations contained infective virus capable of replicating and generating a CPE as part of the productive/lytic virus life cycle (Figure 10).

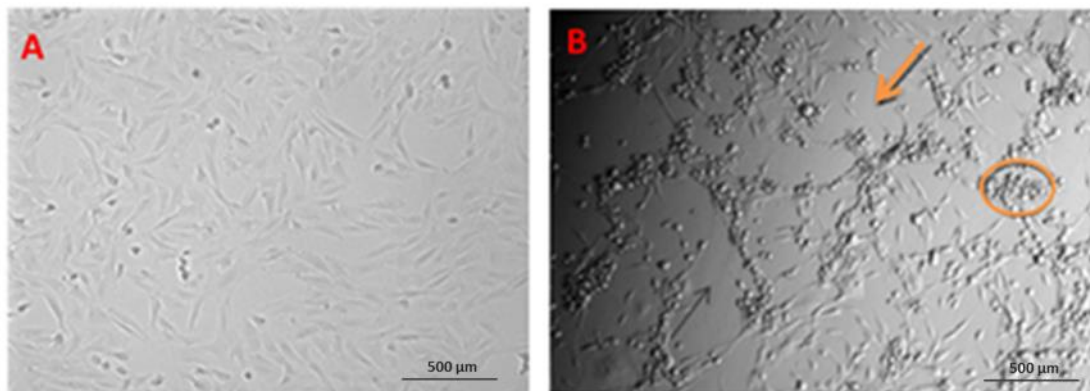


Figure 10 infection of bovine turbinate fibroblast (BT) cells
A: healthy BT cells used as a control, image B: infected BT cells with low pass AIHV-1 C500 strain. The arrow indicates the absence of monolayer and the circle shows the accumulation of dying or dead cells and debris. The pictures represent scale bar of 500 µm.

3.5.2 BAE endothelial cells

Infection of BAE cells directly or after secondary transfer of infected cell sonicates and supernatants to uninfected BAE cells did not show any signs of CPE and the cells remained intact up to ten days post

infection (Figure 11). Conversely, BT cells infected with cell sonicates and supernatant from directly infected BAE cells displayed CPE around day 5 post infection (Figure 12). This indicates that BAE cells were successfully infected and generated virus able to induce CPE in BT reporter cells.

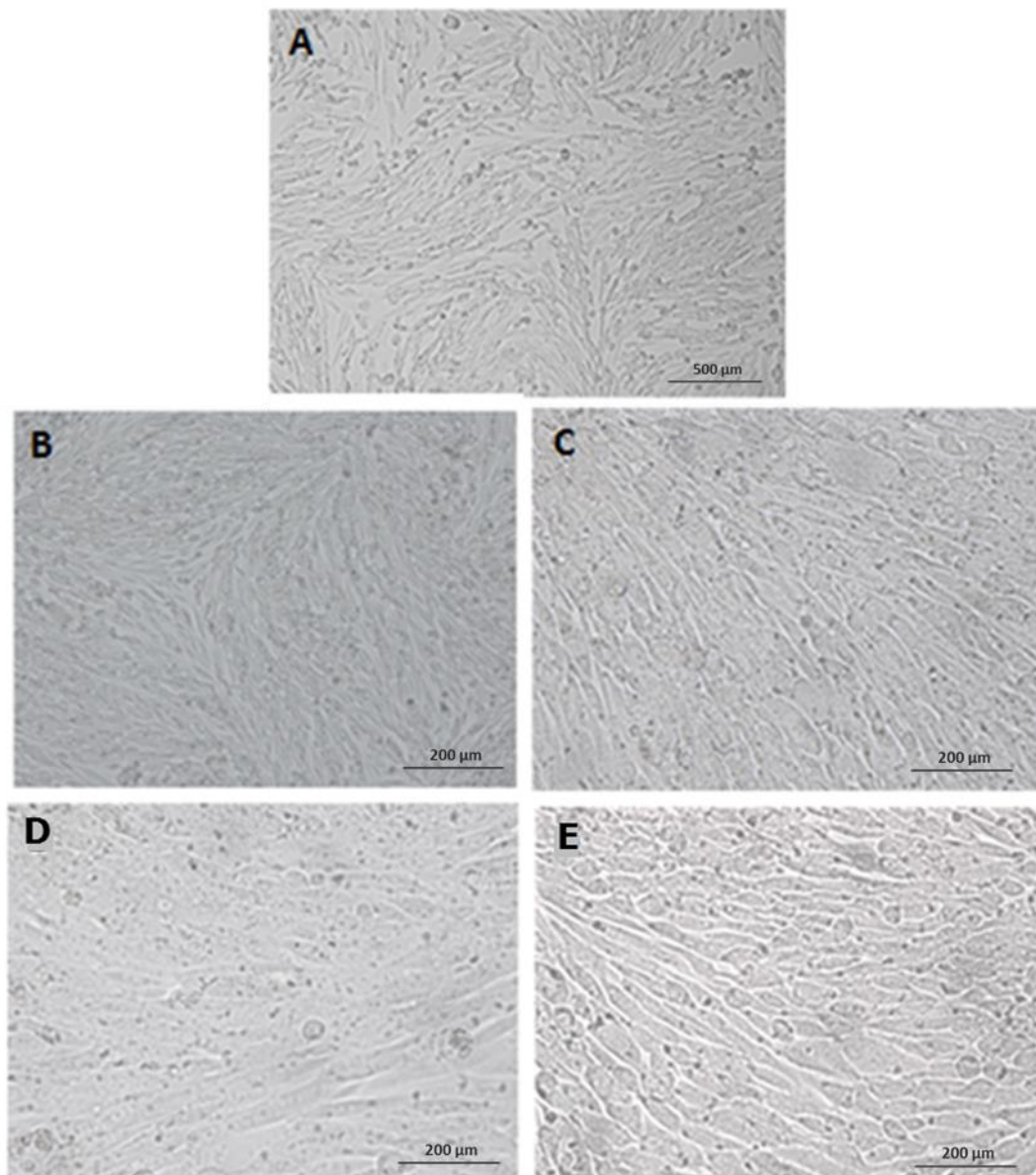


Figure 11 Infection of bovine aortic endothelial (BAE) cells
A: control uninfected BAE cells, B and C: BAE cells infected directly with low pass or high pass AIHV-1 C500 respectively (day 10 of culture), Serial infection, D and E: BAE infected with sonicate and supernatant material from directly-infected BAE

cells. No CPE seen in the cells up to ten days post infection but cells look unhealthy at this point. Picture A represents scale bar of 500 μm whereas pictures B, C, D and E represent scale bar of 200 μm .

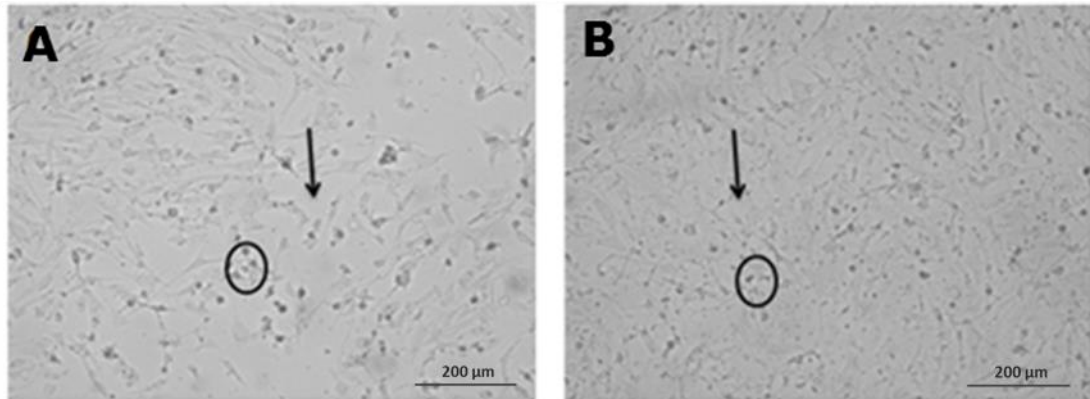


Figure 12 Infection of bovine turbinate BT cells with infected BAE
Serial infection, A and B: BT infected with directly-infected BAE and secondary BAE infected with cell sonicate and supernatant materials from directly infected cells, showing CPE of the BT cells. Arrows indicate absence of monolayers whereas circles indicate accumulation of cell debris. Pictures represent scale bar of 200 μm .

3.5.3 SIRC epithelial cells

There was no evidence of CPE in SIRC cells infected either directly or in a serial/ secondary infection using cell sonicates and supernatant, up to 10 days after infection (Figure 13). However, BT cells infected with cell sonicates and supernatant from directly-infected SIRC cells displayed CPE within a few days post inoculation (Figure 14), indicating that SIRC cells had supported infection and generated infective virus capable of inducing CPE in BT reporter cells.

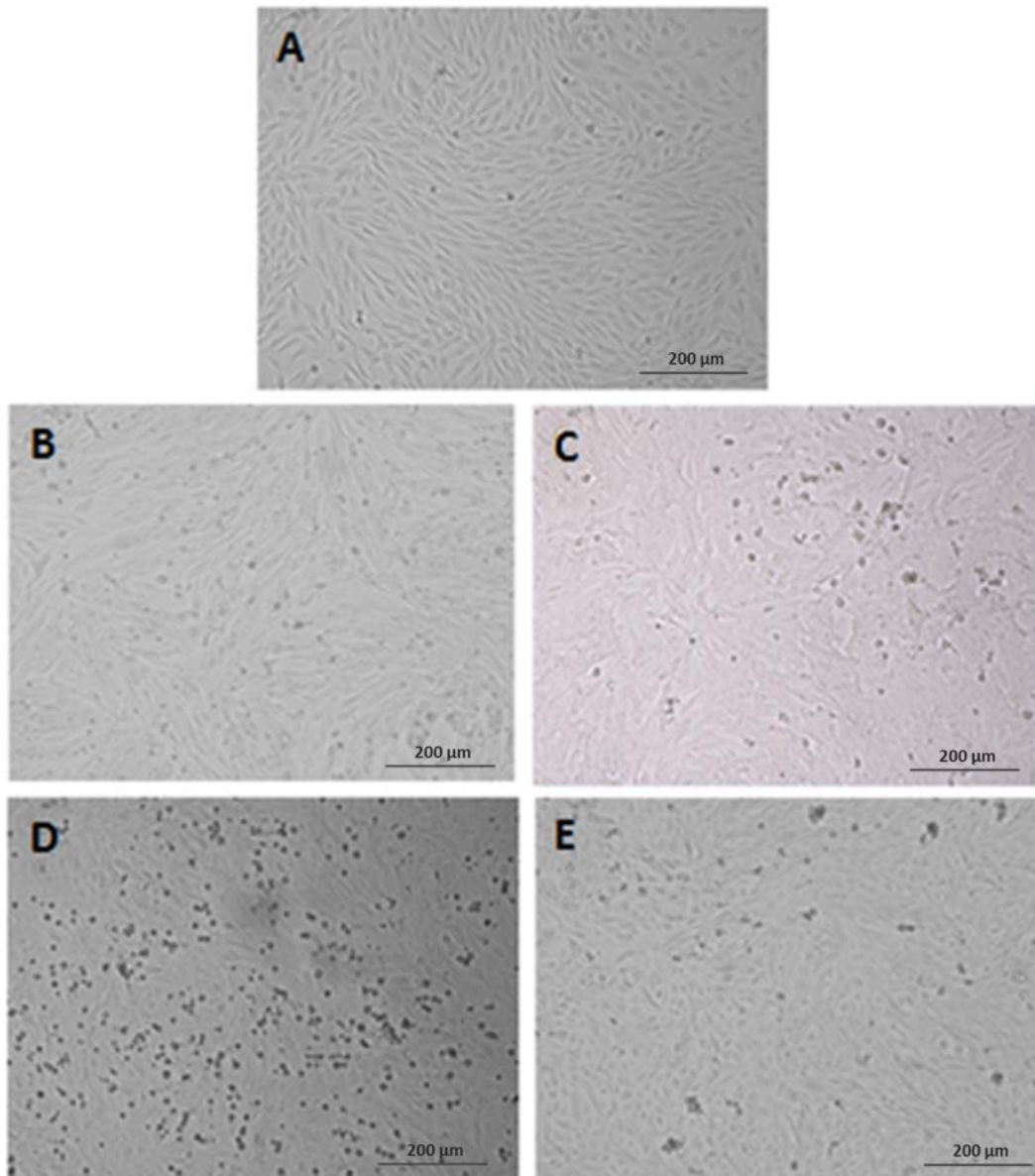


Figure 13 Infection of SIRC epithelial cells

A: SIRC uninfected control. B and C: SIRC cells infected directly with low or high culture pass AIHV-1 C500 strain respectively. D and E: Serial infection: SIRC cells infected with cell sonicates and supernatant derived from directly-infected SIRC cells. No CPE was seen in the cells up to ten days post infection but cells look unhealthy. Pictures represent scale bar of 200 μm .

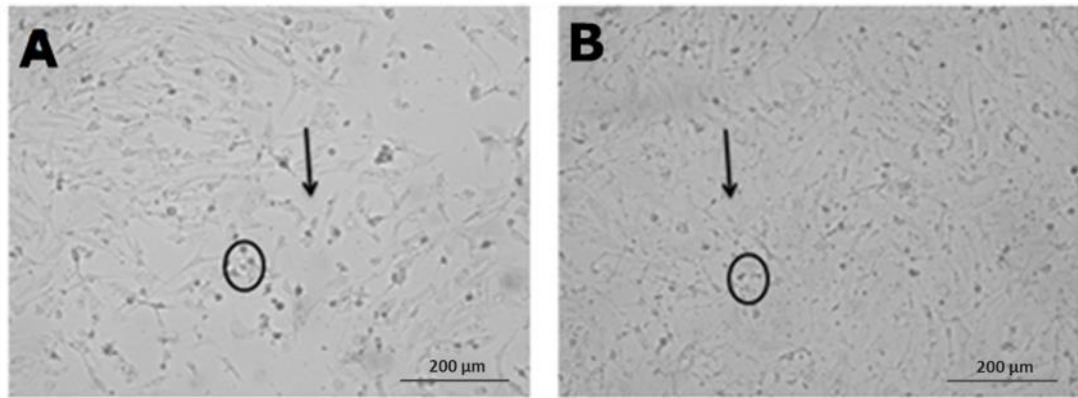


Figure 14 Infection of bovine turbinate BT cells with infected SIRC
 A and B, BT cells show CPE after infection with cell sonicates and supernatant derived from directly-infected SIRC and with SIRC infected with cell sonicate and supernatant materials from directly infected cells. Arrows indicate absence of monolayers and circles show accumulation of dying/dead cell and debris. Pictures represent scale bar of 200 µm.

3.5.4 Detection of viral DNA in the infected cells

Viral DNA was detected in SIRC, BAE and BT cells infected with either low pass AIHV-1 or high pass AIHV-1 at different time points (Figure 15 and 16) after infection. Viral DNA was not identified in non- infected cells (Figure 17).

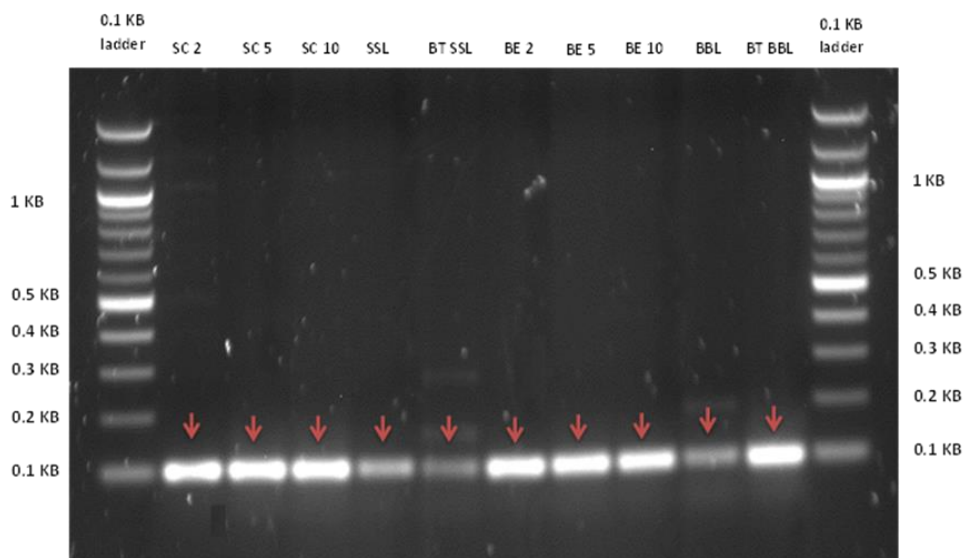


Figure 15 qPCR products for low-pass AIHV-1 ORF3 gene visualised on agarose gel.

SC2; DNA extracted from SIRC cells 2 days post infection with AIHV-1 low pass virus, SC5; DNA extracted from SIRC cells 5 days post infection with AIHV-1 low pass virus, SC10; DNA extracted from SIRC cells 10 days post infection with AIHV-1 low pass virus, SSL; Serial infection: DNA extracted from SIRC cells infected with whole cell sonicate plus supernatant collected from directly-infected SIRC cells infected (AIHV-1 low pass virus), BT SSL; serial infection: DNA extracted from BT cells infected with whole cell sonicate plus supernatant collected from directly-infected SIRC cells (AIHV-1 low pass virus), BE2; DNA extracted from BAE cells 2 days after infection with AIHV-1 low pass virus, BE5; DNA extracted from BAE cells 5 days after infection with AIHV-1 low pass virus, BE 10; DNA extracted from BAE cells 10 days after infection with AIHV-1 low pass virus, BBL; serial infection: DNA extracted from BAE cells infected with whole cell sonicate plus supernatant collected from directly-infected BAE cells (AIHV-1 low pass virus). BT BBL; DNA extracted from bovine turbinate cells infected with whole cell lysate collected from BAE cells infected with whole cell sonicate plus supernatant collected from directly-infected BAE cells (AIHV-1 low pass virus), 0.1KB ladder; 100 base pair ladder, red arrows; indicates PCR product.

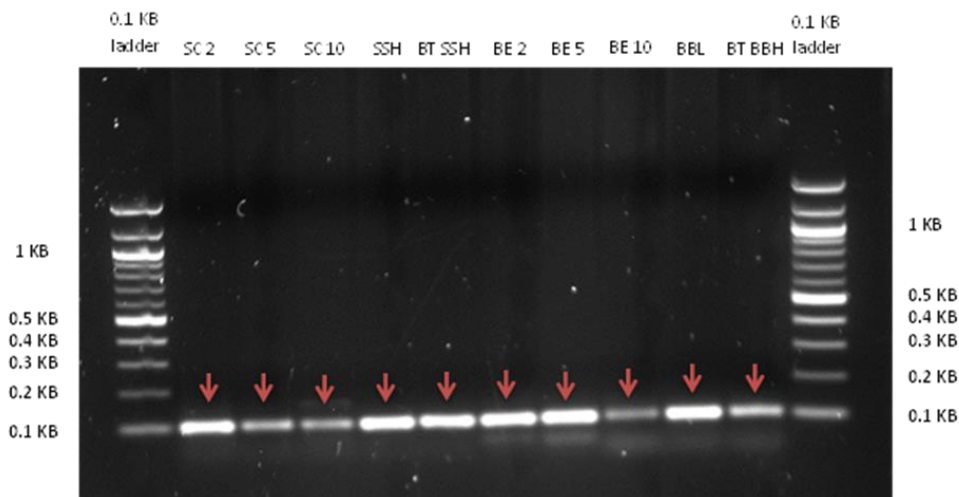


Figure 16 qPCR products for high-pass AIHV-1 ORF3 gene visualised on agarose gel

SC2; DNA extracted from SIRC cells 2 days post infection with AIHV-1 high pass virus, SC5; DNA extracted from SIRC cells 5 days post infection with AIHV-1 high pass virus, SC10; DNA extracted from SIRC cells 10 days post infection with AIHV-1 high pass virus, SSL; serial infection: DNA extracted from SIRC cells infected with whole cell sonicate plus supernatant collected from directly-infected SIRC cells (AIHV-1 high pass virus), BT SSL; serial infection: DNA extracted from BT cells infected with whole cell sonicate plus supernatant collected from directly-infected SIRC cells (AIHV-1 high pass virus), BE2; DNA extracted from BAE cells 2 days post infection with AIHV-1 high pass virus, BE5; DNA extracted from BAE cells 5 days post infection with AIHV-1 high pass virus, BE 10; DNA extracted from BAE cells 10 days post infection with AIHV-1 high pass virus, BBL; serial infection: DNA extracted from BAE cells infected with whole cell sonicate and supernatant collected from directly-infected BAE cells (AIHV-1 high pass virus), BT BBL; serial infection: DNA extracted from BT cells infected with whole cell sonicate and supernatant collected from directly-infected BAE cells (AIHV-1 high pass virus), 0.1KB ladder; 100 base pair ladder, red arrows; indicate the PCR products.

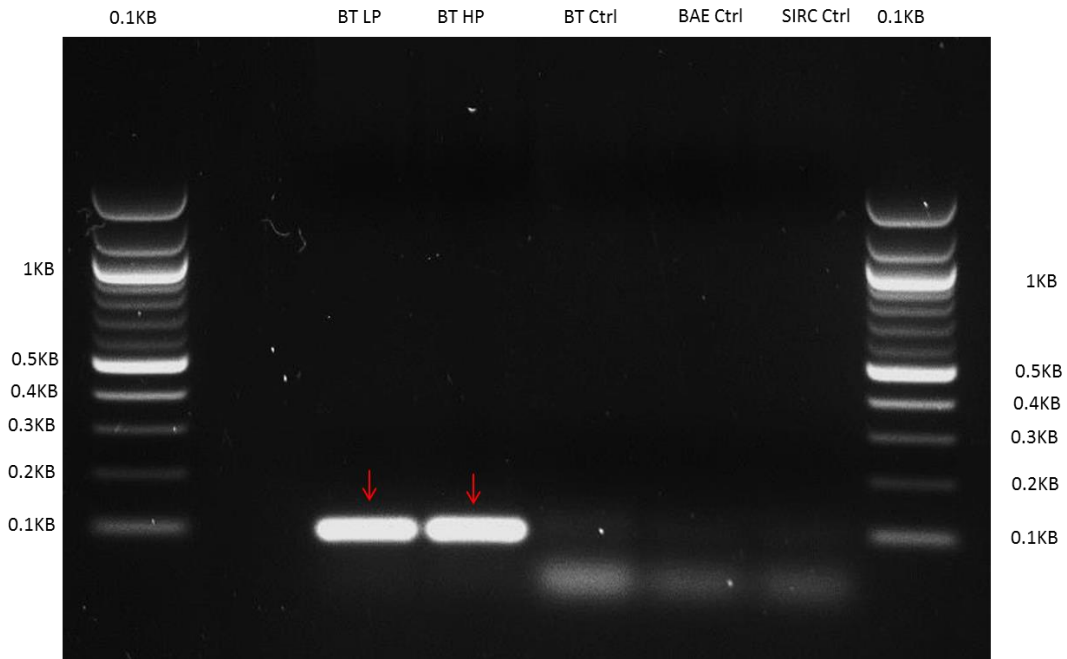


Figure 17 qPCR products for low and high pass AIHV-1 ORF3 gene visualised on agarose gel. Infected BT cells and controls uninfected BT, SIRC and BAE cells

BT LP; bovine turbinate cells infected with AIHV-1 low pass virus, BT HP; bovine turbinate cells infected with high pass virus, BT ctrl; non-infected bovine turbinate cells. BAE ctrl; non-infected bovine aortic endothelium cells, SIRC ctrl, non-infected statens seruminstitut rabbit cornea cells; 0.1 KB ladder; 100 base pair ladder, red arrows; indicate PCR products corresponding to ORF3 DNA.

3.5.5 Viral gene expression in the infected cells

The transcripts of six AIHV-1 genes (A4.5, ORF50, ORF25, ORF73, ORF63, and A9.5) were measured using qPCR. In BT cells infected with low pass virus, ORF50 and ORF25 genes were highly expressed compared to the others that were present at very low level (Figure 18A) indicating that these transcripts were associated with the productive/lytic cycle and as such they can be used as productive cycle positive control transcripts. The other transcripts were very poorly expressed (Figure 18A). There was no detectable expression of the transcripts in BT cells infected with serial/secondary infection

from BAE endothelium and SIRC epithelium cell sonicates and supernatant after infection with low pass virus (Figure 18A). On the other hand, in BT cells infected with high pass AIHV-1, we detected ORF50 transcript and the A4.5 gene transcript in all BT cells infected, although levels were variable between different cultures (hence the large error bars) (Figure 18B). In BT cells infected with cell sonicates and supernatant from directly-infected SIRC or BAE cells, variable but low levels of A4.5 and ORF 50 were also detected. There was no virus gene expression in non-infected BT cells (Figure 18 A and B).

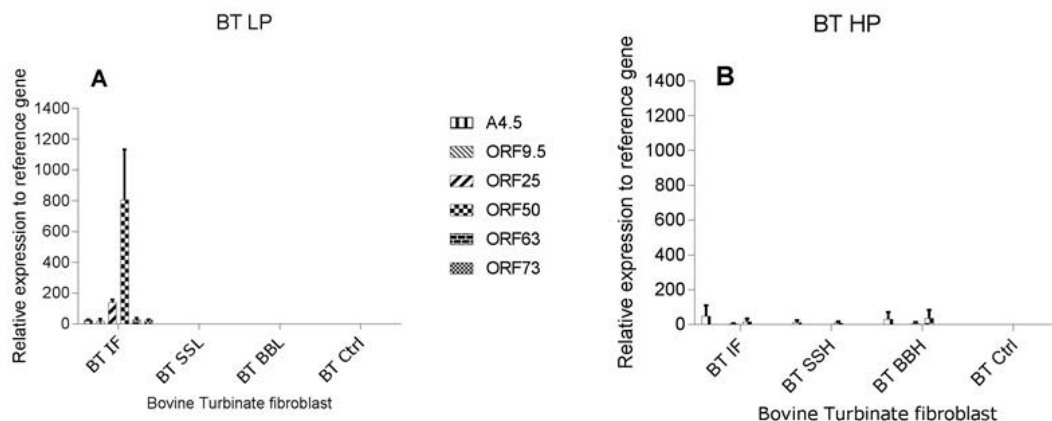


Figure 18 AIHV-1 transcripts in infected BT cells

Viral transcripts of six AIHV-1 C500 strain genes (A4.5, ORF9.5, ORF25, ORF50, ORF63, and ORF73) in BT cells infected with low and high pass virus. BT INF; BT cells infected directly with low culture pass virus (A) and high pass virus (B), BT SSL (A) and BT SSH (B); BT cells infected with whole cell sonicate and supernatant derived from SIRC cells directly-infected with low and high pass virus respectively, BT BBL and BT BBH; BT cells infected with whole cell sonicate and supernatant derived from directly-infected BAE cells (low culture pass (A) and high pass virus (B)), BT Ctrl; non-infected BT cells. Q RT PCR was used to measure the viral transcripts by normalizing the target genes with bovine ribosomal protein S 9 (RPS9) reference gene (chapter 2, section 2.4.4). The error bars indicate SD of duplicate samples from infected BT cells.

The viral gene transcript profile of the six virus genes revealed that they were expressed at very low levels in both endothelium (Figure 19) and epithelium (Figure 20) infected with either low culture passage AIHV-1 or high pass virus. There was no gene expression in endothelial and epithelial cells serially-infected with directly-infected endothelium and epithelium-derived virus. The use of different reference genes in the bovine cells (BT and BAE) make the gene expression comparison between the two cell lines difficult. This is because the expression rate varies between the two genes.

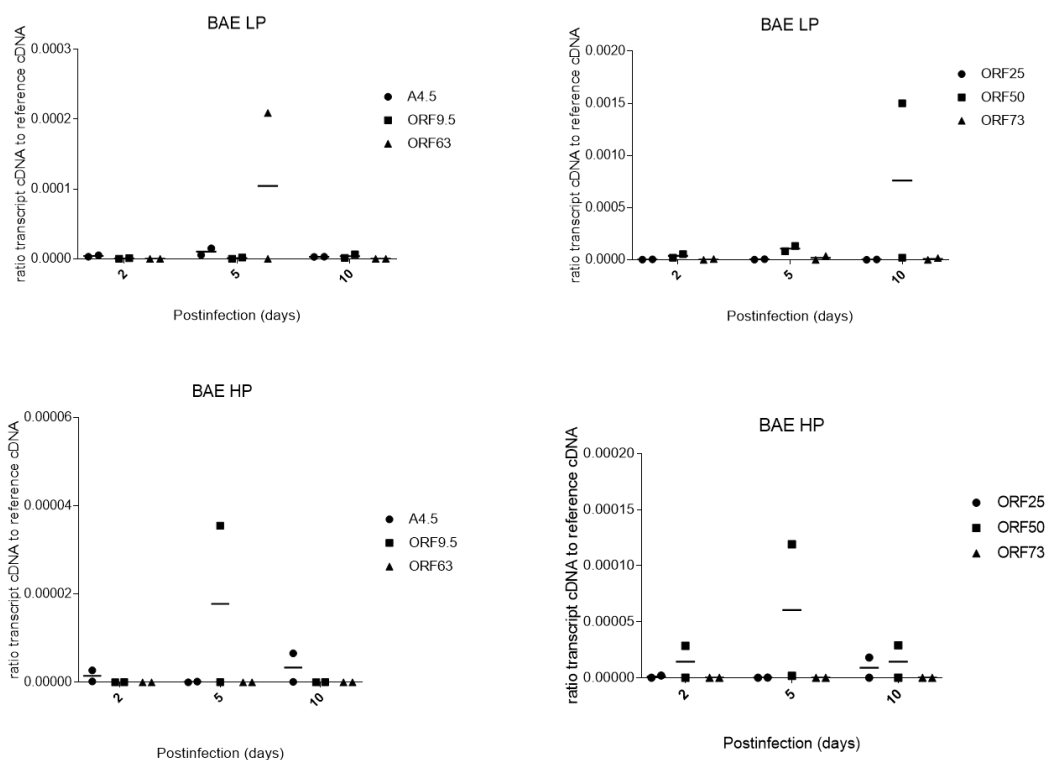


Figure 19 AIHV-1 transcripts in infected endothelial cells

Viral transcripts of six AIHV-1 C500 strain genes (ORF25, ORF50, ORF73, A4.5, ORF9.5, and ORF63) in bovine aortic endothelial (BAE) cells infected with low and high pass virus. BAE was infected directly on day 0 and transcripts were measured at different time point two, five, and ten days post infection for both

low and high pass virus. Error bar, represented by continuous black dashed line, represents the variation between samples. q PCR was used to measure the viral transcripts by normalizing the target genes with bovine G actin reference gene (chapter 2 section 2.4.4).

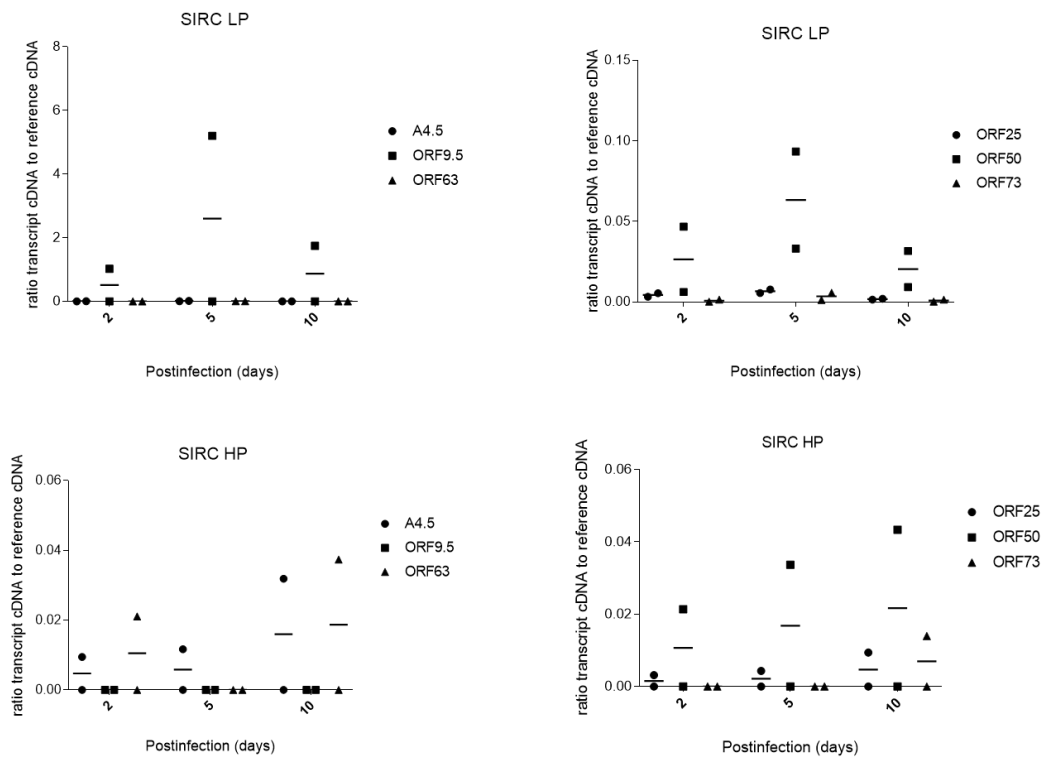


Figure 20 AIHV-1 transcripts in infected epithelial cells

Viral transcripts of six AIHV-1 C500 strain genes (ORF25, ORF50, ORF73, A4.5, ORF9.5, and ORF63) in stans seruminstitut rabbit cornea (SIRC) cells infected with low and high pass virus. SIRC was infected directly on day 0 and transcripts were measured at different time point two, five, and ten days post infection for both low and high pass virus. Error bar, represented by continuous black dashed line, represents the variation between samples. q PCR was used to measure the viral transcripts by normalizing the target genes with rabbit SDHA1 reference gene (chapter 2 section 2.4.4).

Table 8 Summary of results.

Virus	Cell type/ infection ¹	Viral DNA	CPE	Transcripts
Low pass	BT	+	+	ORF50; ORF25
AIHV-1	SIRC	+	-	Low level ORF50, A9.5
	BAE	+	-	V low level ORF50
	BT+SIRCV ²	+	+	-
	BT+BAEV ²	+	+	-
	SIRC+SIRCV ²	+	-	-
	BAE+BAEV ²	+	-	-
High pass	BT	+	+	Low level ORF50, A4.5
AIHV-1	SIRC	+	-	V low ORF50, A4.5, A9.5
	BAE	+	-	V low ORF50
	BT+SIRCV ²	+	+	V low ORF50, A4.5
	BT+BAEV ²	+	+	V low ORF50, A4.5
	SIRC+SIRCV ²	+	-	-
	BAE+BAEV ²	+	-	-

¹BT fibroblasts support productive virus infection; SIRC epithelial cells and BAE endothelial cells. ²Serial infection: uninfected cells were inoculated with cell sonicates and supernatant from directly-infected SIRC (SIRCV) or BAE (BAEV) after ~10 days in culture. Transcripts analysed: ORF50; ORF25; ORF63; ORF73; A4.5 and A9.5. Inoculated cells analysed on days 2, 5 and 10 after inoculation. CPE occurred around day 5 In BT cells. Viral DNA scored positive and transcripts listed only if present at all-time points after inoculation.

3.6 Discussion

In this series of experiments (summarised in table 8), rabbit epithelial corneal SIRC cells, bovine aortic endothelium (BAE) cells and bovine turbinate fibroblasts (BT) cells were infected with either low culture passage virus or high pass AIHV-1 C500 strain to determine whether the endothelial cells and /or the epithelial cells could be infected, and if so whether they could induce CPE in the cells or not. A selection of viral gene transcripts was analysed, representing either productive cycle (ORF50, ORF 25, ORF 63), latent cycle (ORF 73) or where their involvement in the virus life cycle was unknown (A4.5, A9.5).

The results indicate that low pass and high pass virus were able to infect SIRC and BAE cells although there was no CPE. This might indicate establishment of the latent cycle, and this was supported by the results of the gene transcription profiles that were of low abundance in these cells in spite of good evidence of viral DNA, indicating the presence of virus (Table 8 summary). The virus was intact and infective as, when directly-infected SIRC and BAE cell sonicates and culture supernatant were used to infect BT cells that support the productive life cycle, the BT cells were infected and showed CPE, evidence of virus replication and the productive life cycle. However, there was little or no viral gene transcription, possibly indicating a low level of gene expression.

To speculate, a consequence of the study could be that BAE and SIRC represent endothelium and epithelium *in vivo* but a lack of direct virus-induced CPE *in vitro* may reflect a similar lack of CPE *in vivo* and that the destruction of epithelium and endothelium is the result of infected T cell damage. The BAE and SIRC cells may be in a latent state (low gene expression and lack of CPE in spite of infective virus present in the cells). This requires further study.

The lack of knowledge of latency transcripts in particular in MCF is hampered by difficult access to the natural reservoir species for AIHV-1 – the wildebeest. This is where the latent and lytic cycles will have evolved and not in the disease-susceptible species where the virus is less likely to persist. Recent work from the Stewart laboratory may be challenging this view though, where evidence of subclinical infections is seen in cattle (unpublished results).

The high expression of ORF50 and ORF25 in BT cells infected with low pass virus indicates their involvement in productive cycle, which given what they code for is expected. Why ORF63 was not seen here is a mystery, but may reflect the low abundance of the viral transcripts and lack of sensitivity of the q PCR used. The low expression and absence of productive/lytic ORFs has also been reported in lymphoid and non-lymphoid tissues from animals infected with AIHV-1 C500 strain (Dewals et al., 2008, Palmeira et al., 2013).

In BT cells infected with high pass virus and epithelium and endothelium derived virus, there was an expression of ORF50 and ORF A4.5 but no expression of the other genes, indicating that A4.5 is probably a productive virus life cycle gene. The absence of the expression of the other genes is probably due to the deletion, translocation, and rearrangement that the high pass virus undergoes where ORF50 and ORFA6 were truncated and translocated (distal part of ORF50b, proximal of A6 and distal part of A10) (Wright et al., 2003). ORF A4.5 may be involved in preventing cell death, hence supporting cell survival and the establishment of either productive and/or latent infection. This is because the gene encodes a protein similar to Epstein-Barr virus EBV BALF1 and cellular B-cell lymphoma genes of the BCL-2 family that controls apoptosis (Hart et al., 2007b, Russell et al., 2009). The respiratory system including turbinate cells are the primary site of infection in OvHV-2 MCF-affected animals (Cunha et al., 2008, Myster et al., 2015) and this is likely to be the case with AIHV-1 MCF as well.

Recent work has shown that AIHV-1 establishes latency in infected tissues and cells (Dewals et al., 2008, Dewals et al., 2011, Palmeira et al., 2013) and that MCF is therefore a disease of latency. The epithelial and endothelial cell lines infected with the virus did not show any CPE. It was possible though that the virus may support latent infection in these cells. However, the undetectable levels of ORF73, a latency-associated transcript make it difficult to be clear

on this point. It would be interesting to establish sensitive detection methods for the transcripts and co-culture cells with uninfected activated T cells to see if this forces a latency programme in the cultured epithelial and endothelial cells. These cells may play, *in vivo*, a role in enforcing the virus to establish latency in order to avoid detection by the immune system (Blake, 2010). In addition, the longevity of infection may be required for the virus to support latency.

To conclude, Endothelial and epithelial cells were infected with AIHV-1 but there was no evidence of productive infection and although there was some indication that there may be a latent state (lack of CPE). The low level of gene transcripts makes a definitive conclusion currently difficult.

Chapter 4

**The effect of 5-azacitidine on
AIHV-1 viral gene expression
in large granular lymphocytes
(LGLs) and infected bovine
turbinate (BT) cells**

4.1 Abstract

Malignant catarrhal fever is fatal lymphoproliferative disease of even-toed ungulates. Although the tissue damage leading to animals' death is linked to lymphocytes accumulating within these tissues, the pathogenesis is still unknown. Culture of infected tissues cells can be achieved *ex vivo* to develop large granular lymphocytes (LGL) that represent the infected cells *in vivo*. These cells enrich for MCF virus-infected cells and are useful to study virus-host interactions. In this series of experiments, AIHV-1 virus genes, known for their involvement in productive/lytic and latent life cycles, were examined in LGLs in the presence and absence of 5-azacitidine, a drug used to drive latency programming from a productive cycle one (Thonur et al, 2006). In addition, bovine turbinate fibroblast (BT) cells were studied as they support the productive virus life cycle and virus genes expressed in these represent important ones in the productive virus life cycle. Flow cytometry was used to phenotype the LGL, which were predominantly CD8⁺ T cells. The results showed that LGL show gene expression representative of a mixture of productive/lytic and latent life cycle and the effect of 5-azacitidine on gene expression was irregular and inconsistent with respect to identifying key latency genes. Interestingly, 5-azacitidine had an impact on LGL phenotype where it increased the percentage of pan T cells in the treated LGLs group. There was also a slight increase in CD8⁺ cells in 5-aza

treated group in comparison to non-treated group. In the BT cells infected with the virus, productive/lytic associated genes ORF50, ORF25, and ORF A4.5 were highly expressed. The expression of these genes was reduced when BT cells were treated with 5-azacitidine but there was no elevation in ORF73 latency-associated transcript. Importantly, there was no CPE in the infected and treated cells.

4.2 Introduction

The mechanism by which the MCF related viruses (AIHV-1 and OvHV-2) induce disease is not yet well known (Li et al., 2014, Russell et al., 2009). Nonetheless, the pathogenesis of MCF is attributed *in vivo* to T cells accumulating in the tissues, many of which are infected with MCF virus (Dewals et al., 2011, Palmeira et al., 2013). Infected cells (LGL) can be developed in culture and are useful to study host-pathogen interactions (Reid et al., 1989, Reid et al., 1983). LGL are found to be capable of transmitting MCF when inoculated into naive rabbits (Reid et al., 1989). The viral genes profile, especially those responsible for productive/lytic and latent infection, from LGL derived from tissues of both reservoir and susceptible species, has been studied and found to be variable (Rosbottom et al., 2002). The ability to manipulate the productive/latent virus cycle, using drugs such as doxorubicin, which was found to stimulate productive virus cycle in lymphocytes infected with Epstein Barr virus (EBV) and 5-azacitidine, which had been found to drive latency in gamma herpes viruses (Szyf et al., 1985, Feng et al., 2004) has motivated researchers to study virus life cycle in OvHV-2 MCF-affected animals (Thonur et al., 2006). Here we study the effect of 5-azacitidine to drive the AIHV-1 latent virus cycle in rabbits LGL and in BT cells.

4.3 Materials and methods

4.3.1 Samples collection

Popliteal lymph nodes were obtained from rabbits infected with AIHV-1 C500 strain virus (see general materials and methods (2.6.4)). Samples were collected from rabbits IYDY, IYJJ, LFLK and LFKJ which were euthanized on day 17 of the experiment. The lymph node samples were placed in 1XPBS and processed immediately (see materials and methods section 2.2.1).

4.3.2 Tissue culture and infection

Large granular lymphocytes (LGL) were cultured and BT cells were cultured and infected as described in materials and methods chapter 2 sections (2.2.1 and 2.2). Quantitative PCR and PCR were performed as described in materials and methods, sections (2.4.4 and 2.4.2) to detect the virus and measure the viral DNA load.

4.3.3 Drug treatments

LGL derived from AIHV-1-infected rabbits were cultured as described in materials and methods chapter, section (2.2.1) and treated with 25µM 5-azacitidine (CALBICHEM, cat# 189825, Germany) over a period of three weeks with culture medium removal and drug replacement. This dose of drug was determined to be the highest concentration that did not affect the viability and growth of the LGLs or BT cells. Cultured LGL were exposed to the above mentioned

concentration for three days after which the drug was diluted by changing two thirds of the medium with fresh IL-2 IMDM medium every three days and adding fresh 5-azacitidine. Infected BT cells were treated with 5-azacitidine exactly in the same manner as the LGLs with the exception that the medium was completely discarded and replaced with fresh containing 5-azacitidine.

4.3.4 Flow cytometry

The protocol is as described in the materials and methods (chapter2, section 2.5.3).

4.4 Results

4.4.1 Viral DNA detection

Quantitative PCR was used to detect AIHV-1 DNA in LGL and BT cells. AIHV-1 ORF3 gene was utilised to perform the procedure. This is due to the fact that AIHV-1 ORF3 is validated for AIHV-1 DNA detection and quantitation (Traul et al., 2005). The results showed that AIHV-1 DNA was identified in all samples (Figures 21, 22 and 23) demonstrating that LGL were infected with the virus. The virus DNA was not identified in non-infected BT cells (Figure 23).

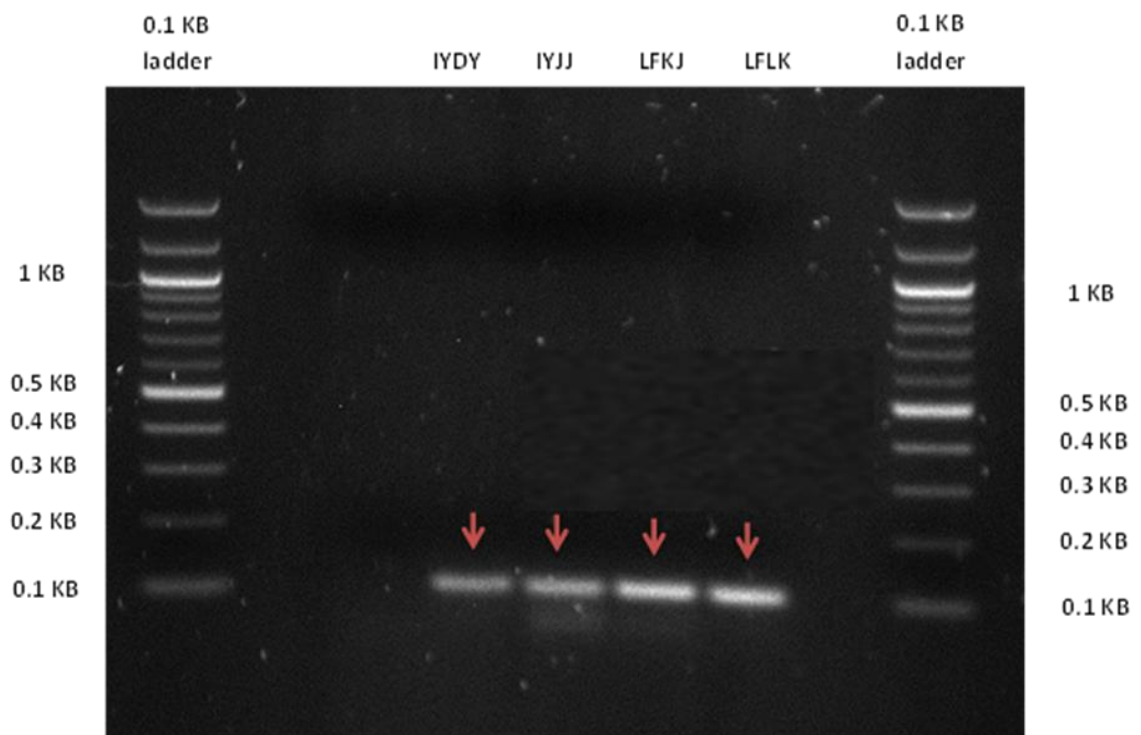


Figure 21 Q PCR and PCR products for AIHV-1 ORF3 gene
The figure shows qPCR and PCR products of AIHV-1 ORF3 in the rabbit LGL (110 bp) visualised on agarose gel. PCR product was estimated by comparison with the standard DNA (0.1 kb) ladder. AIHV-1 ORF3 was detected in LGL samples treated with 5-azacitidine drug. IYDY, IYJJ, LFKJ, and LFLK; different rabbit IDs from different cell lines, 0.1 KB ladder, 100 bp ladder, red arrows; indicate to the PCR product of the corresponding cell line.

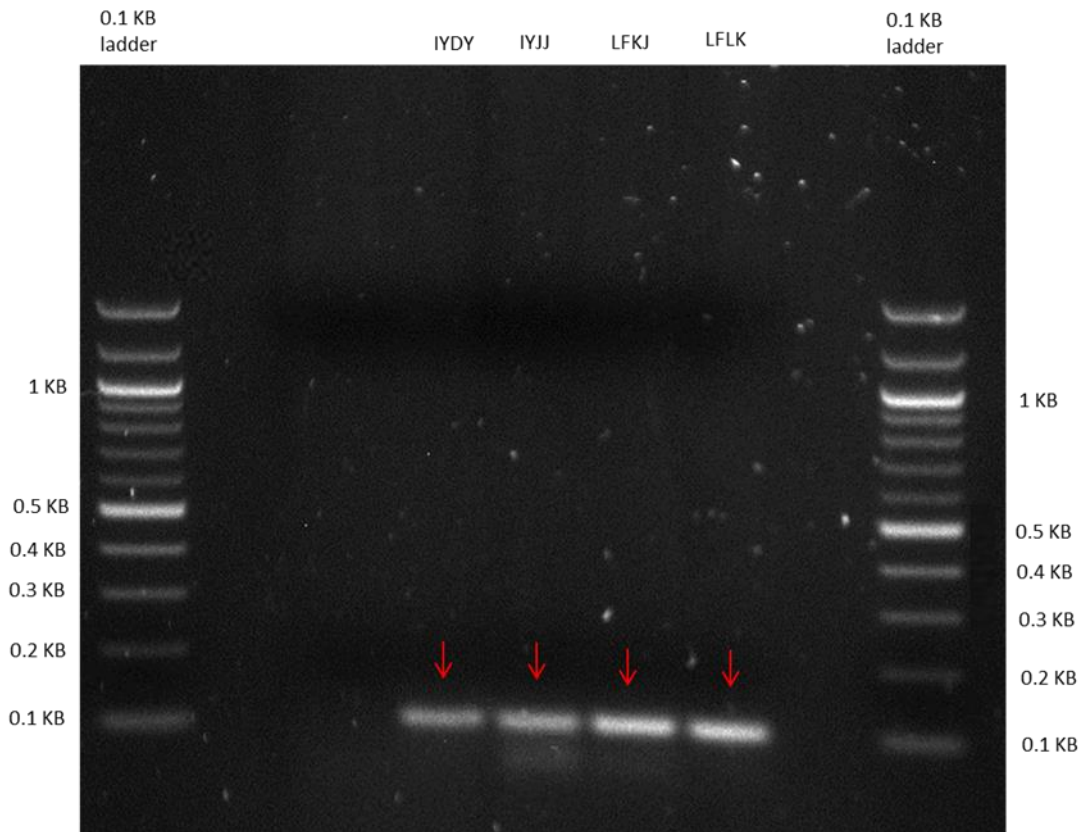


Figure 22 Q PCR and PCR products for AIHV-1 ORF3 gene

The figure shows qPCR and PCR products of AIHV-1 ORF3 in the rabbit LGL (110 bp) visualised on agarose gel. The size of the gene was estimated by comparison with the standard DNA (0.1 kb) ladder. AIHV-1 ORF3 was detected in non-treated LGL samples. IYDY, IYJJ, LFKJ, and LFLK; different rabbit IDs from different cell lines, 0.1 KB ladder, 100 bp ladder, red arrows; indicate to the PCR product of the corresponding cell line.

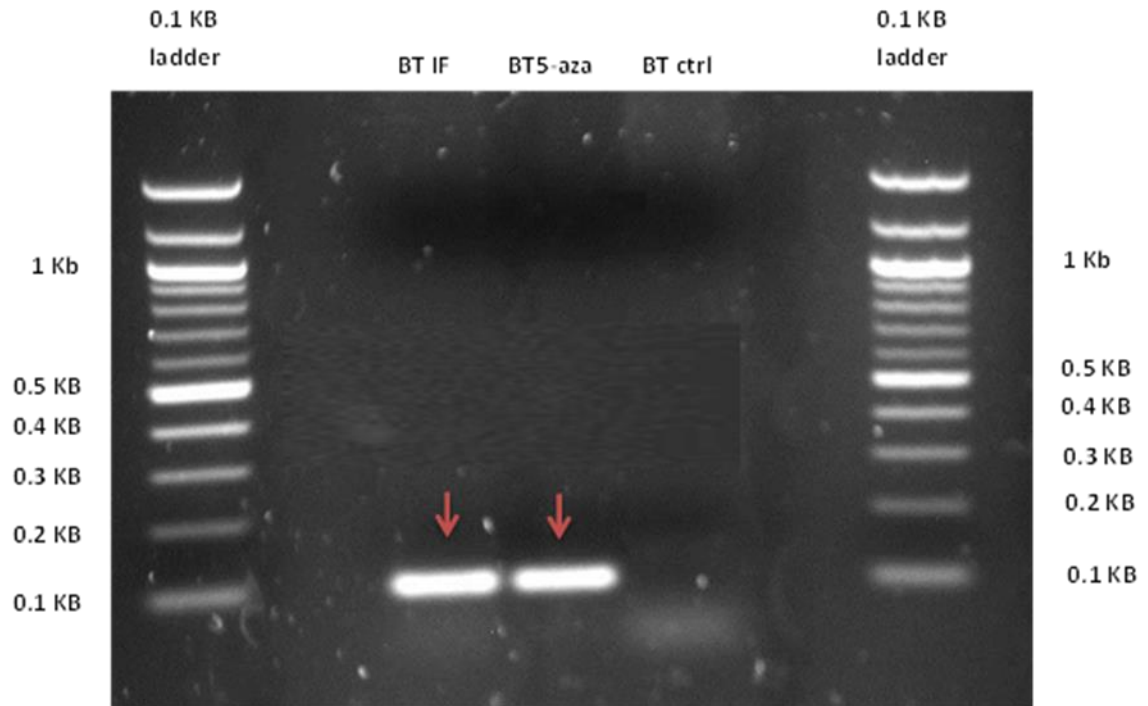


Figure 23 Q PCR and PCR products of AIHV-1 ORF A3 gene

The figure shows q PCR and PCR products of AIHV-1 ORF3 (110 bp) visualised on agarose gel. The size of the gene was estimated by comparison with the standard DNA (0.1 kb) ladder. AIHV-1 ORF3 was detected in BT cells samples (infected only and infected and treated with 5-azacitidine) whereas the viral DNA was not detected in uninfected BT control. BT IF; bovine turbinate cells infected with AIHV-1 virus, BT 5-aza; bovine turbinate cells infected with AIHV-1 virus and treated with 5-azacitidine drug, BT ctrl; bovine turbinate cells not infected with the virus and not treated with 5-azacitidine; 0.1 KB ladder; 100 base pair ladder; red arrows; indicate to the PCR products of the corresponding cells.

4.4.2 Viral DNA load in LGLs

To evaluate AIHV-1 copy number in LGL (treated and non-treated samples), q PCR assay was performed on LGL samples. The viral DNA copy number was estimated by normalising AIHV-1 ORF3 gene with 10^5 rabbit β globin reference gene as described in Dewals et al. (2008). The data obtained showed that the viral load is nearly

similar in both groups (Figure 24) with values between $1-1.6 \times 10^5$ AIHV-1 copy numbers per 10^5 rabbit β globin.

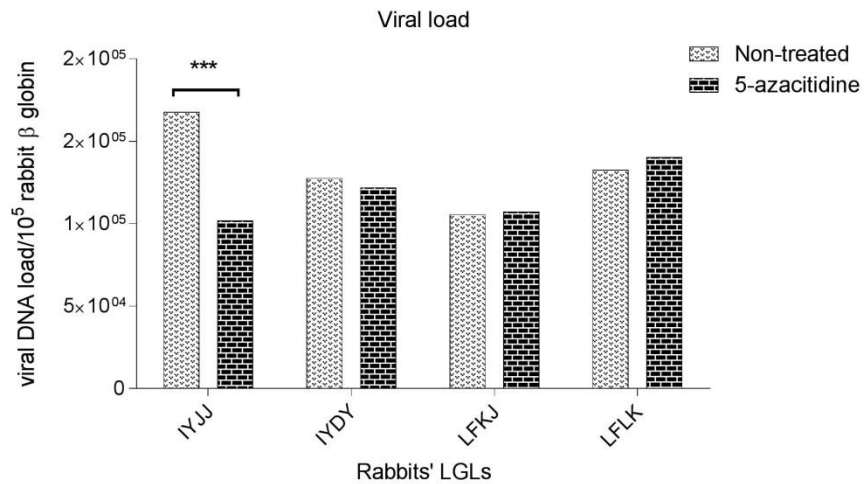


Figure 24 AIHV-1 DNA copy number in rabbits' large granular lymphocytes. The figure illustrates the viral load (as copy numbers per 105 beta globin DNA copies) in large granular lymphocytes (LGL) from rabbits infected with AIHV-1 C500 strain. Four lines (IYJJ, IYDY, LFKJ, and LFLK) were treated with 5-azacitidine drug or kept without treatment as a control. The viral load was estimated by normalizing the viral DNA copy number per 105 rabbit β globin reference gene using qPCR. The primers and probe (FAMAIHV-1) for AIHV-1 ORF3 were used inside the standard sequence and then analysed using Roche Light Cycler 480 system. Two-way ANOVA was performed to do the statistical analysis using Sidak's multiple comparisons test. The primers and probe (FAM) for rabbit β globin reference gene was utilized within the standard sequence.

4.4.3 The effect of 5-azacitidine on BT cells

There was an obvious cytopathic effect (CPE) in BT cells infected with the virus. However, the development of CPE was not seen in BT cells infected and treated with 5-azacitidine. Figure 25 shows the difference between infected BT cells in the presence and absence of 5-azacitidine.

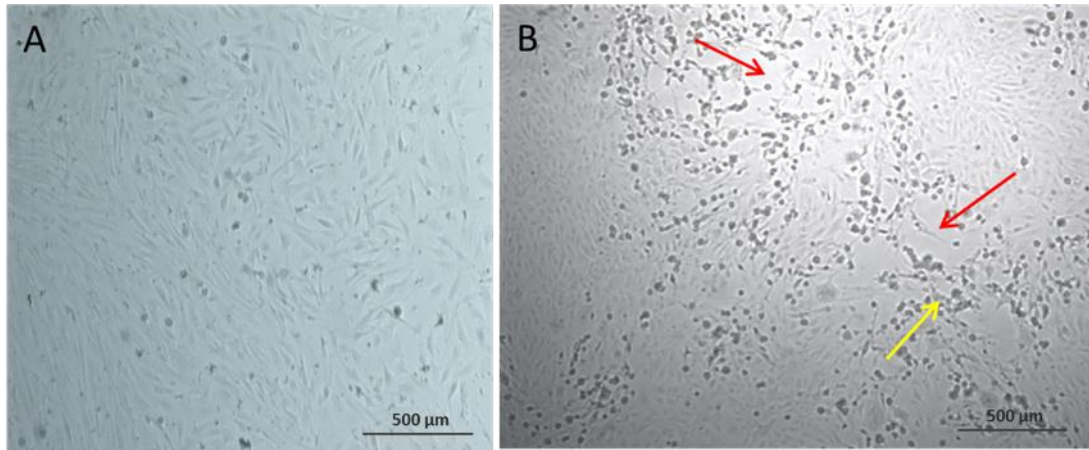


Figure 25 BT cells infected with AIHV-1 C500 strain and infected and treated with 5-azacitidine

The figure depicts BT cells infected with AIHV-1 and treatment of one of the samples with 5-azacitidine. Image (A) shows BT cells infected with the virus and treated with the drug the following day and the drug was changed every three days up to day 17 post infection. No CPE was seen after treatment. Image (B) BT infected with the virus without treatment and there was CPE detected from around day 5 post infection. The red arrows indicate the absence of monolayer and the yellow arrow show the accumulation of cell debris.

4.4.4 Measuring viral gene transcripts

In order to examine the viral gene profiles in LGL and BT cells, cDNA was synthesised from RNA for q PCR as described in chapter two, section (2.4.1). The results showed that all viral gene transcripts examined were expressed at very low level in two of the LGL lines (LFLK and LFKJ) and were not detected in the other two lines (IYDY

and IYJJ) (Figure 26). AIHV-1 ORF73 was expressed at a higher level in the 5-azacitidine treated group than non-treated in LFLK cell line. However, ORF50 expression is also identified. The expression of ORF 25, ORF63 and ORF A4.5 varied in each cell line in both groups.

In infected BT cells there was high expression of ORF50, ORF25, and ORF A4.5 in comparison with the other genes (Figure 27). In BT cells infected and treated with 5-azacitidine there was an obvious reduction in the genes supporting productive/lytic infection namely ORF50 and ORF25, but no increase in ORF73 transcripts (Figure 27) even though the cells did not show any CPE illustrating that the drug has had an effect on the expression of these genes. No virus gene expression was seen in non-infected and non-treated control BT cells (Figure 27).

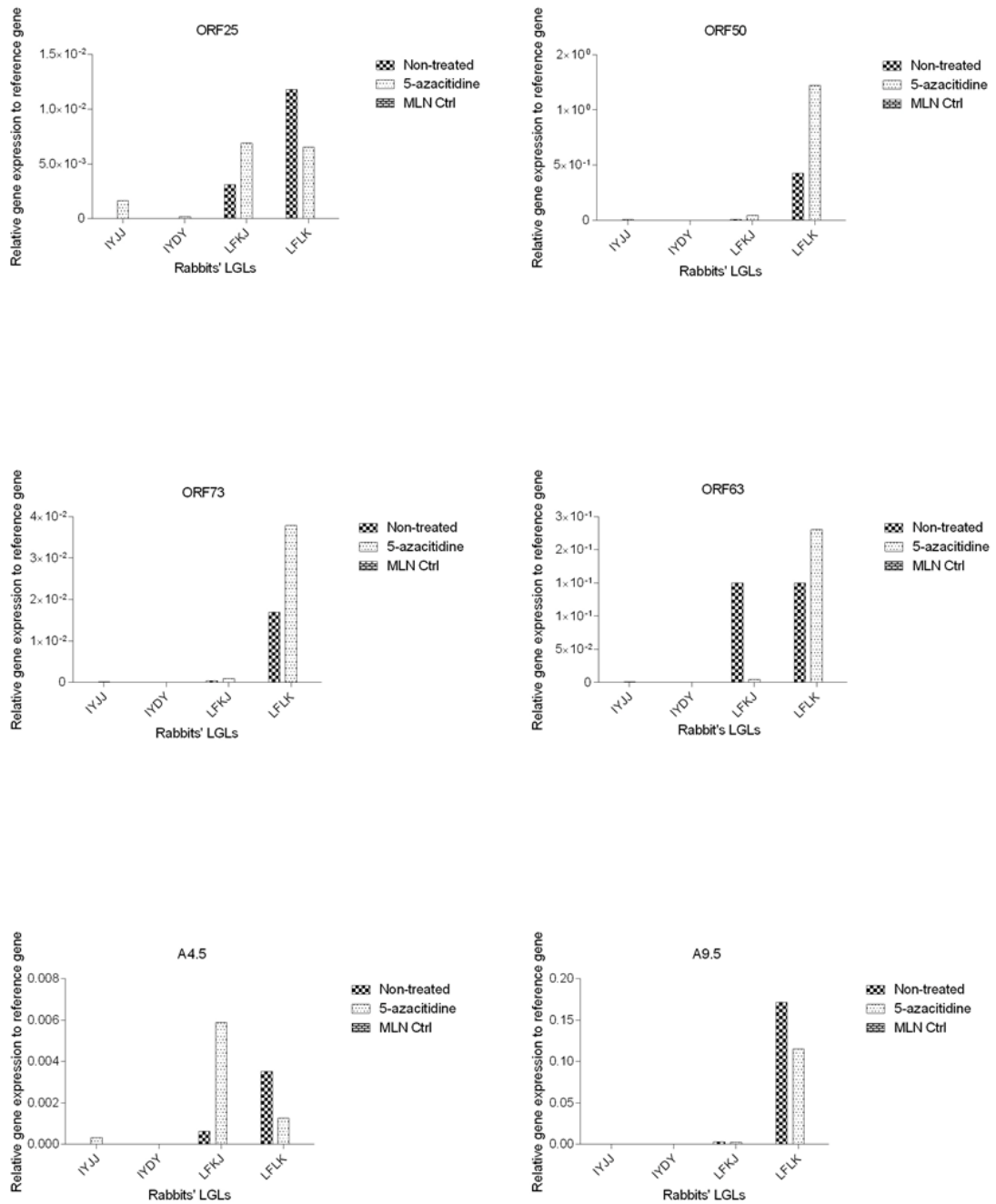


Figure 26 viral gene transcripts of AIHV-1 C500 in rabbit LGLs

The figure shows the viral gene profiles of AIHV-1 C500 strain genes (ORF25, ORF50, ORF73, ORF63, ORF A4.5, and ORF A9.5) in rabbit LGLs treated with 5-azacitidine or not-treated. Rabbit mesenteric lymph node cells from a non-infected rabbit were used as a negative control. Q PCR was used to measure the gene expression by normalizing the target genes with rabbit SDHA1 reference gene (chapter 2 section 2.4.4).

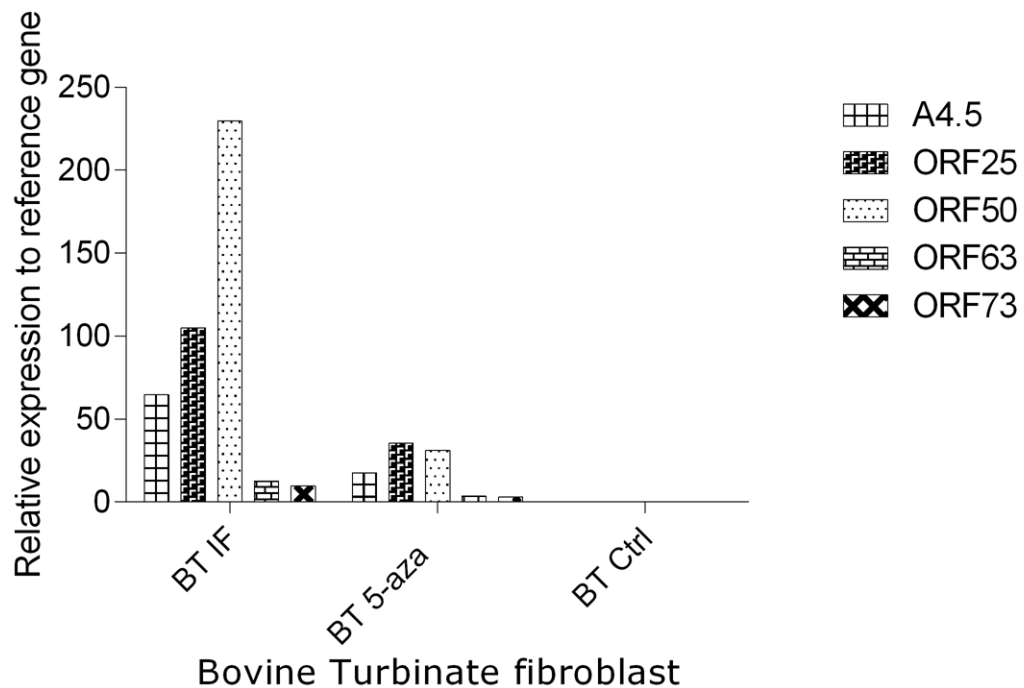


Figure 27 viral gene transcripts of AIHV-1 C500 strain in BT cells

The figure shows the viral gene transcripts of five AIHV-1 C500 genes (ORF A4.5, ORF25, ORF50, ORF63, and ORF73) in BT cells. QPCR was used to measure the gene expression by normalizing the target genes with bovine ribosomal protein S9 (RPS9) used as a reference gene (chapter 2, section 2.4.4). BT INF; infected BT without treatment, BT 5-aza; infected BT and treated with 5-azacitidine, BT Ctrl; non-infected and non-treated BT cells.

4.4.5 Flow cytometry analysis of LGL

Monoclonal antibodies directed against CD4, CD8, CD11b, B cell, and Pan T cells were used for flow cytometry analysis of the rabbit LGLs (material and methods (2.5.3)). The results revealed that the predominant cell type in the LGLs was CD8⁺ whereas CD4⁺ T cells were not detected. Figure 28 depicts the percentage of mononuclear cells in LGLs in the absence or presence of 5-azacitidine. In addition, the results showed that the percentage of Pan T cells is low in non-treated LGL but the percentage was high in 5-azacitidine treated

cells. The cell lines in both groups were devoid of both CD11b cells (expressed on leukocytes, particularly most monocyte/macrophage series cells) and CD19+ B cells. There was a bias towards CD8⁺ in the double staining samples used for all cell lines (Figure 29). Figure 29 shows the typical results in one cell line (IYDY) in both treated and non-treated groups.

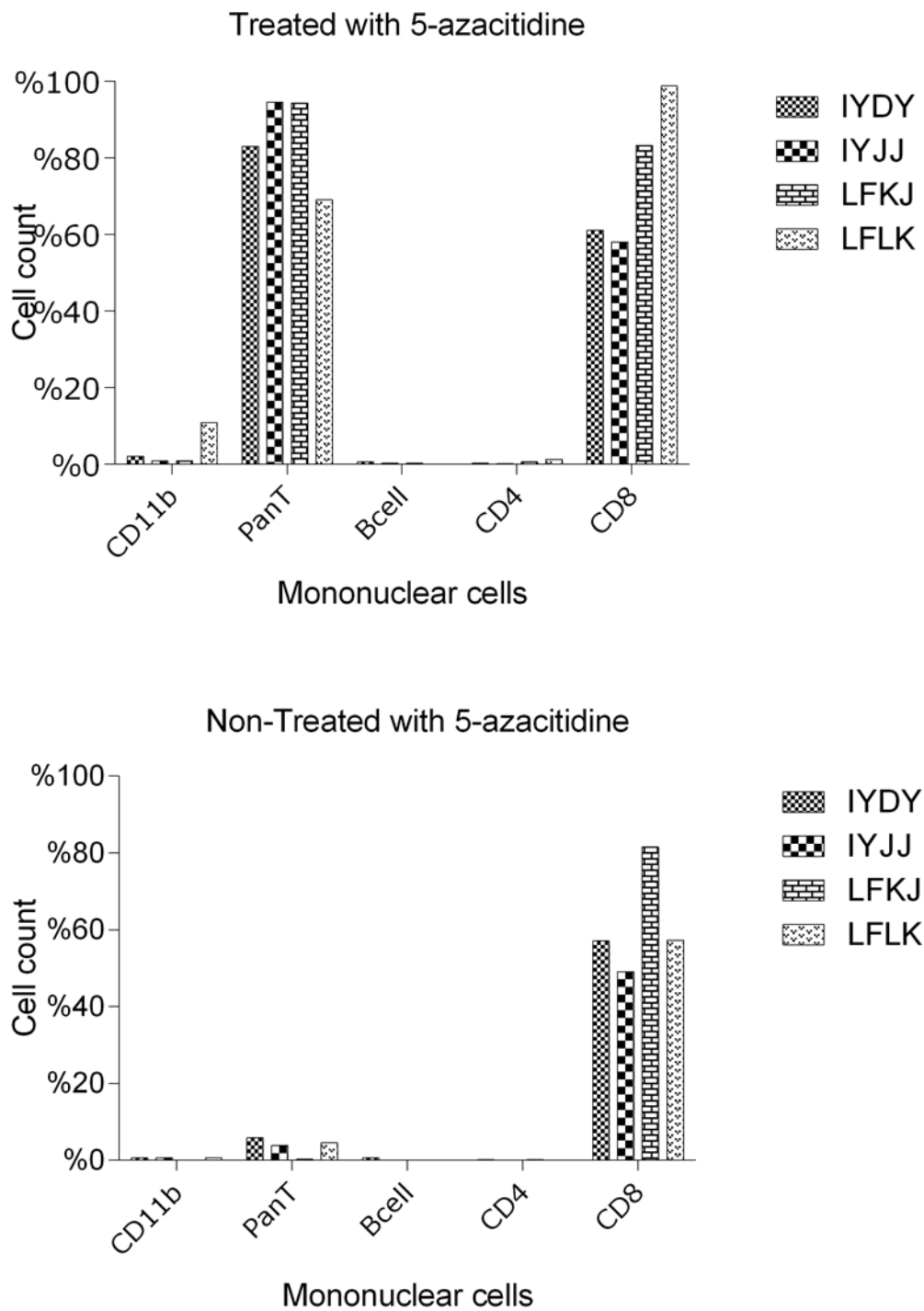


Figure 28 flow cytometry analysis of mononuclear cells in LGL non-treated and treated with 5-azacitidine

The figure illustrates the percentage of cell types within LGL upon analysis by flow cytometry. CD8 represents the majority of expressed T cell subset in both 5-azacitidine treated group and non-treated group whereas Pan T cell was high in 5-azacitidine treated group and low in non-treated group. CD4, CD11b and B cell were not detected in both groups.

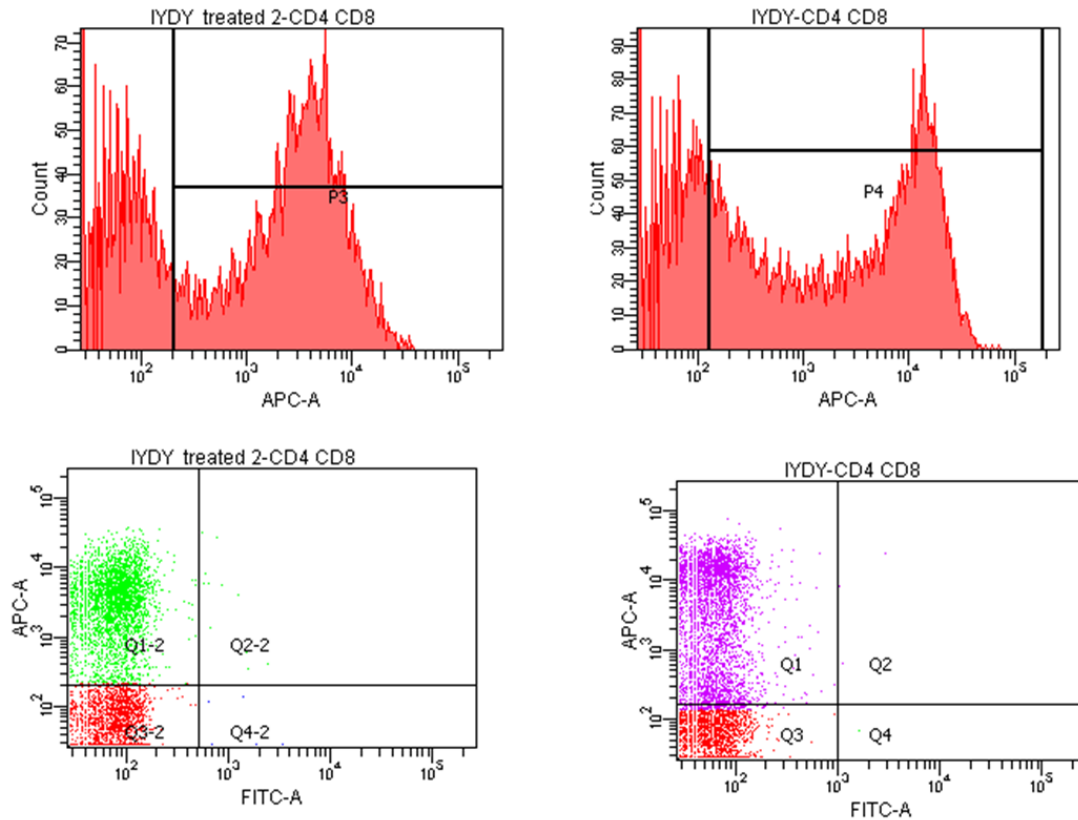


Figure 29 flow cytometry analysis of LGL double stained with two fluorescence antibodies in 5-azacitidine treated and non-treated IYDY cell lines

The figure shows the flow cytometry dot blot double staining of IYDY LGL lines with secondary antibody APC for CD8 and primary antibody conjugated with FITC CD4. High percentage of labelled cells lie in the quadrants 1-2 and 1 representing APC fluorescence for CD8 whereas no cells labelled with FITC for CD4 in quadrants 4-2 and 4 in both treated and non-treated IYDY cell lines. The figure also shows high percentage of CD8 when parameter of count used versus fluorescence in both groups. For the calculation of cell percentage, CD4 isotype control was used as a negative control for CD4 samples. Therefore, the figures of CD4 isotype control were subtracted from the values of CD4 for each sample. Due to the fact that the secondary antibodies have a role in the detection and do not bind directly to the cells; the figures for secondary APC and secondary FITC can be subtracted from the figures of each cell type to give percentage of cell count. For example, secondary FITC must be subtracted from CD11b, Pan T, B cell and FITC only. Secondary APC must be subtracted from CD8, double stained and APC only.

4.5 Discussion

In this study, Rabbit LGLs were shown to be infected as determined by viral DNA presence, but expressed only a low abundance of transcripts. In a few, a mixture of known productive cycle (ORF50, ORF25, ORF63) and latent cycle (ORF73) transcripts were detected,

but not in all the LGLs. ORF50 is the R transactivator (RTA) which plays a role in driving the productive viral programme from latency (Frame and Dalziel, 2008, Goodwin et al., 2001); ORF 25 encodes a major capsid protein that is expressed during lytic cycle indicating viral replication (Dewals et al., 2008); ORF 73 encoding the latency associated nuclear antigen (LANA) is important for driving latent infection (Dewals et al., 2011, Hu et al., 2002, Palmeira et al., 2013). ORF63 encodes a tegument protein which is involved in preventing apoptosis (Boyle and Monie, 2012). This indicates that ORF63 may serve a function within the lytic life cycle. ORF A4.5 (a bcl-2 anti-apoptosis orthologue) (Mills et al., 2003) and A9.5 (secreted cytokine orthologue) (Lankester et al., 2015a, Russell et al., 2013) were included in the study to see if they could be identified as either productive cycle or latent cycle expressed. ORF73, ORF50, ORF63 and ORF25 were expressed in two LGL lines, indicating possibly predominance of productive cycle, but with no indication of a latent cycle within some of the cells which remains a possibility. This is consistent with the observation made by Thonur et al., (2006) in cattle and rabbits using LGL infected with OvHV-2. There was also expression of ORF A4.5 in two of the rabbit lines (LFLK and LFKJ). Thonur et al. (2006) found similar results with Ov4.5 in LGL cell lines infected with OvHV-2 virus. ORF A9.5 was expressed in one of the lines (LFLK). However, the role of this gene in latent and productive/lytic life cycle remains unclear.

Upon treatment with 5-azacitidine, there was an increase in ORF73 expression in one cell line (LFLK) in comparison to the non-treated control. This is consistent with 5-azacitidine driving latency and was also seen in LGL infected with OvHV-2 virus and treated with 5-azacitidine (Thonur et al., 2006). It is worth mentioning that ORF73 can be 'leaky' with respect to expression in the different virus life cycles such that absence of ORF73 in productive infection is not necessarily absent (Thonur et al., 2006). The expression also of ORF50 indicates that the cells support both latent and lytic infection. The expression of the other genes: ORF25, ORF63 and ORF A9.5 were different in each cell line in 5-aza treated and non-treated groups. This may indicate that LGL support both productive/lytic and latent virus cycle. In addition, the viral gene expression may be irregular in these cells. ORF A4.5 was expressed to a much lower level in 5-aza treated LGLs than the untreated control cells, indicating a role in the productive virus life cycle. ORF A9.5 was not investigated because of the time limit and lab authorisation required to repeat the experiment.

5-azacitidine is a DNA hypo-methylating agent that functions by inhibiting DNA methyltransferase. It has also been found that 5-azacitidine has different effects on different virus gene expression patterns (Chang et al., 2014, Qiu et al., 2010). In herpes-virus saimiri, 5-azacitidine encourages productive cycle from latency (Mossman et al., 1989) while it appears that it changes the form of

EBV expression from type I latency to type III latency in lymphoma cell lines (Schaefer et al., 1997). It seems therefore that the effect of 5-azacitidine on gene expression is possibly virus and cell-type specific (Thonur et al., 2006). Thonur et al. (2006) also discovered differences in viral gene expression between cattle and rabbit LGLs samples. As defined by Gardella analysis (Gardella et al., 1984), bovine LGLs infected with OvHV-2 supports predominately latent infection (circular DNA) and only a weak band (smear) of linear DNA. OvHV-2 -infected rabbit LGLs showed productive infection (linear DNA) and only a small amount of circular DNA. Unfortunately, time ran out before Gardella gels could be performed on the samples in this study. However, the match between Gardella analysis and productive and latent gene expression was high (Thonur et al., 2006).

The high level of expression of ORF50, A4.5 and ORF25 in infected BT cells confirms the support of the virus productive/lytic cycle in these cells, which undergo a CPE and release infectious virions into the culture medium. However, when treated with 5-azacitidine, there was a lack of CPE and a sharp decline in the expression of these genes (ORF50, A4.5 and ORF25) consistent with a latency programme. This confirms the latency-inducing activity of 5-aza in this study with AIHV-1. ORF73 expression however was not increased, but this in itself may not be diagnostic of the latent state (i.e. an increase in expression rather than just expression).

MCF viruses (OvHV-2 and AIHV-1), initially, replicate in the respiratory system, in particular in the nasal turbinate (Li et al., 2008, Myster et al., 2015) where ORF25 is identified. Afterwards, the virus disseminates to the blood where, in the case of one set of studies with AIHV-1 infection, it establishes latency in lymphocytes (mainly CD8⁺ T cells) and ORF73 expression is detected (Dewals et al., 2008, Palmeira et al., 2013). ORF A4.5 may be involved in preventing cell death, hence supporting cell survival and the establishment of productive infection. This is because the gene encodes a protein similar to Epstein-Barr virus EBV BALF1 and cellular B-cell lymphoma genes of the BCL-2 family that controls apoptosis (Hart et al., 2007, Mills et al., 2003).

Flow cytometry analysis of the rabbit LGLs showed that the predominant cell type was CD8⁺ in both 5-azacitidine-treated and non-treated cells. The results are in line with the observations made in other studies that also found that the main cell type in LGL and infected tissues *in vivo* was CD8⁺ cells (Dewals et al., 2008, Dewals et al., 2011). The results showed that the LGL were devoid of CD4⁺ cells. Dewals et al. (2008) discovered that the rise in CD8⁺ cells is correlated with a reduction in CD4⁺ cells. The observation that T cells proliferating in MCF affected tissues outnumbered CD4⁺ cells was also highlighted by other researchers (Anderson et al., 2007). LGL are indiscriminately cytotoxic and have the morphology of T/natural killer (NK) cells (Swa et al., 2001).

However, in this study there was a surprising result. Very few LGL cells reacting with the Pan-T marker were detected in the LGLs not treated with 5-aza, whereas in the treated cells, the pan T marker was present on the majority of the cells. The actual antigenic target of the Pan-T antibody used is not known (Parameswaran et al., 2014). However, a recent study showed that MCF virus infection is associated with an effect on T cell phenotype of infected cells. The A2 gene (transcription regulator) had an effect on the regulation of LGL T cell phenotype where there was downregulation of $\gamma\delta$ TCR receptors and upregulation of $\alpha\beta$ TCR receptors in the absence of A2 gene (Parameswaran et al., 2014). This may explain the reduction in pan T cells in the non-treated group if A2 is involved in latency versus productive cycle gene expression affecting this phenotype. The effect of 5-azacitidine on human T cells in particular CD4 and CD8 has been reported. It was established that 5-azacitidine treatment of Human T cells reduced CD8⁺ T cells while CD4⁺ T cells increased (Stübig et al., 2014).

In conclusion, 5-azacitidine affected the latency programme as evidenced in BT cells, where it prevented CPE and inhibited markedly productive virus gene transcription. In LGLs the effect of 5-aza was less clear due to the low level of viral transcripts although in some lines there appeared to be a small effect. The drug clearly affected the LGLs as there was a marked increase in the pan T cell

marker on T cells compared to infected untreated controls. At this stage it is not clear what this means.

Chapter 5

**Cellular and viral gene
expression analysis (RNA-
Seq) in rabbit LGLs and BT
cells infected with AIHV-1 and
treated with 5-azacitidine**

5.1 Abstract

The goal of this study was to determine the molecular-biochemical pathways affected by treatment of AIHV-1 infected rabbit large granular lymphocytes (LGLs) and bovine turbinate (BT) cells infected with the virus, with 5-azacitidine (5-aza). The hypothesis is that 5-aza will suppress productive virus infection and aid identification of virus latency transcripts and the host transcriptome in latently-infected cells. In order to achieve this objective, RNA-Seq was performed on the cell RNA (as copy DNA) samples. The results showed differences in gene expression patterns between treated and untreated cells, both LGLs and BT cells. Pathways identified using David® and Ingenuity Pathway analysis software showed that cell death (apoptosis), T cell chemo-attraction, proliferation and immune response pathways affected in 5-aza-treated LGLs compared to non-treated ones. In addition, the analysis indicated that mRNA translation, gene expression, cell cycle, DNA replication and post transcriptional modification pathways were affected in 5-aza treated BT cells in comparison to non-treated BT cells. In conclusion the pathway analysis showed that there were variations between rabbit LGLs and cattle BT cells. While LGLs have pathways that aid T cell proliferation and accumulation and immune responsiveness in 5-aza-treated groups compared to untreated ones, BT cells contain pathways that support gene expression and mRNA translation in treated groups compared to untreated. In

addition, it is unclear whether rabbit LGLs support productive or latent virus cycle. RNA-Seq was not sensitive enough to pick up any other than a few viral transcripts.

5.2 Introduction

In the previous chapter, the issue of 5-azacytidine effect on the viral productive and latency programmes was studied. In this chapter, the global transcriptome of LGLs and BT cells was compared in treated versus untreated cells using RNAseq. Although Gamma herpes virus latency, generally, is not connected with disease development, latency in lymphocytes can produce malignant lymphocyte activation and proliferation dependent upon the viral species and the infected host (Barton et al., 2011, Ensser and Fleckenstein, 2005). Latency is regulated by the control of a viral gene expression programme in the infected cells enabling the virus to avoid the detection by the host immune system and persist in the infected cells. One of the approaches the virus adopts to induce latency is the control of the expression of transcriptomes including mRNA and non-coding RNAs such as micro-RNAs (miRNA) (Bartel, 2009, Kincaid and Sullivan, 2012, Pfeffer et al., 2004). The advent of sequence-based approaches such as deep sequencing, in particular RNA-Seq have opened opportunities to researchers to look at post transcriptional modification, mutations and gene expression alterations (Kumar et al., 2012, Wang et al., 2009, Wilhelm and Landry, 2009). Here, RNA-Seq technique is used to map host (and viral) gene transcripts in LGLs derived from rabbits infected with AIHV-1 virus and bovine turbinate (BT) cells infected with AIHV-1 virus to look for host pathways associated with latency and the lytic

cycle. LGLs represent the T cells naturally-infected *in vivo* and in the previous chapter, as with a previous study with OvHv-2 (Thonur et al., 2006) infected rabbit cells showed that the cells supported a mixture of latency and productive cycle genes, although in this study gene expression was low and the results not particularly clear cut. 5-aza could suppress the productive virus life cycle and reveal latency transcripts. Cattle BT cells support productive virus infection and they are a control for viral productive cycle transcripts. It was of interest to compare the host responses in 5-aza-treated and untreated cells for both species.

5.3 Materials and methods

5.3.1 Tissue and infection

Large granular lymphocytes (LGL) were obtained and cultured and BT cells were cultured and infected as described in materials and methods chapter 2 sections (2.2.1). Quantitative PCR was performed as described in materials and methods, sections (2.4.4) to measure the viral DNA load.

5.3.2 RNA extraction

Total (viral and cellular) RNA was extracted using RNeasy Plus Universal Mini Kit (cat # 73404, Qiagen) according to the manufacturer's instructions as described in materials and methods chapter, section (2.3.2).

5.3.3 RNA quality measurement using utilizing Agilent Bio-analyser Nano 6000 kit

The RNA quality measurement was as described in the materials and methods, section (2.9).

5.3.4 Complimentary (cDNA) DNA Library preparation and sequencing

This was done by Deepseq (University of Nottingham). Total RNA was measured using Qubit RNA BR assay kit (Life technologies, Q10210). 1µg of Total RNA was used for enrichment of mRNA using NEBNext Poly(A) mRNA Magnetic Isolation Module (NEB, E7490). Illumina stranded whole transcriptome sequencing libraries were prepared using NEBNext Ultra Directional RNA library prep kit for Illumina (NEB, E7420S). Library QC was performed using the bioanalyser HS kit (Agilent biotechnologies, 5067-4626). Libraries were quantified using qPCR (Kapa Biosystems, KK4824). Libraries were pooled at desired concentrations, denatured and loaded for sequencing according to the manufacturer's instructions. Sequencing was performed on the Illumina NextSeq500 sequencing platform to generate 2 x 75bp reads.

5.3.5 Sequence analysis, bioinformatics and statistics

This was done by Deepseq (University of Nottingham) with bioinformatics by ADAC (UoN). Ingenuity pathway analysis (IPA, www.ingenuity.com/products/pathway) was performed to look at relationships between the differentially-expressed gene lists (5-aza treated versus untreated for both cell types). The data from both species (cattle and rabbits) were interpreted utilizing the core analysis function included in IPA system in the context of biological

processes, pathways and networks. The up and down regulators were described as value parameters for the analysis. The significance of predicted bio-functions and canonical pathways was examined by the Fisher Exact test p-value (McKinney et al., 1989). Bio-functions were categorised in diseases and disorders, molecular and cellular functions. In a similar manner, canonical pathways were clustered in metabolic and signalling pathways. The bovine and rabbit (Cattle=Bos-taurus UMD3.1, rabbit=Oryctolagus-cuniculus 2.0 from ensemble genome version 82) as contained in BT cells and rabbit LGLs respectively were used to map transcript sequences. The viral genome annotation file was modified to include A9.5_ORF. BLAT (Kent, 2002) was used to identify the overlapping sequence regions. The viral genome sequence and their cosponsoring annotations were merged with the cow and rabbit files so that the viral genome sequence appeared to represent an additional contig within the host genome.

The reads were trimmed with scythe (Lindgreen, 2012) to remove residual adaptor contamination and with sickle (Joshi and Fass., 2011) to remove low quality bases. The trimmed Reads were aligned to the modified reference genomes using HISAT v2 (Kim et al., 2015). Technical replicates from different lanes were merged with SAM tools (Li et al., 2009). The merged alignments were assembled using string tie (Pertea et al., 2015) and differential expression analysis was performed using Ballgown (Frazee et al.,

2014). Scripts used in this analysis pipeline can be found in appendices in the soft copy version section (8.10).

5.4 Results

5.4.1 Viral DNA load in LGLs

To evaluate AIHV-1 copy number in LGL (5-azacitidine-treated and non-treated samples), q PCR assay was performed on LGL samples. The viral DNA copy number was estimated by normalising AIHV-1 ORF3 gene with 10^5 rabbit β globin reference gene copies as described in Dewals et al. (2008). The data obtained showed that the viral load is similar in both groups (Figure 30). This is the same as the figure shown in Chapter 2, as the same cells were used and analysed just prior to sending samples off for RNA-seq and doing the viral transcript studies in chapter 2. This is repeated here to provide context for this chapter.

5.4.2 RNA Integrity Number (RIN) measurement

The RNA integrity number is measured by a set of bio-analytical devices, which is a combination of microfluidic chips, voltage-induced size separation in gel filtered channels and laser-induced fluorescence detection and analysis of data using Agilent software tool (Schroeder et al., 2006). The RIN number ranges from 1 to 10. A RIN number of 1 show completely degraded RNA whereas a RIN number of 10 indicate totally intact RNA samples. Upon RNA extraction, the RNA integrity was estimated and samples with RIN

numbers 7 and more were used for further analysis. Figure 31 shows the RIN number in the some of the RNA samples sent for RNA-Seq analysis. Table 9 shows sample number, sample name, RNA concentrations and RNA integrity numbers (RIN) for samples sent for RNA-Seq analysis.

Table 9 sample number, sample name, RNA concentrations and RNA integrity numbers (RIN) for LGL and BT samples sent for RNA-Seq analysis.

Sample number	Sample name	Sample type	Concentration ng/ μ l	RIN #
1	LGLLK5aza	Total RNA	297	10
3	LGLKJ5aza	Total RNA	291	10
4	LGLLKcon	Total RNA	655	9.90
5	LGLKJcon	Total RNA	1217	9.90
6a	BTinfa	Total RNA	1788	8.40
6b	BTinfb	Total RNA	1341	8.40
7a	BT5AZa	Total RNA	1335	9.60
7b	BT5AZb	Total RNA	916	9.60

LGLLK5aza and LGLKJ5aza: large granular lymphocytes derived from rabbit IDs LFLK and LKKJ and treated with 5 azacitidine, LGLLK con and LGLKJ con: Large granular lymphocytes derived from rabbits IDs LFLK and LFKJ without treatment, BTinfa and b: Bovine turbinate infected only with AIHV-1 virus, BT5AZa and b: BT treated only with 5-azacitidine.

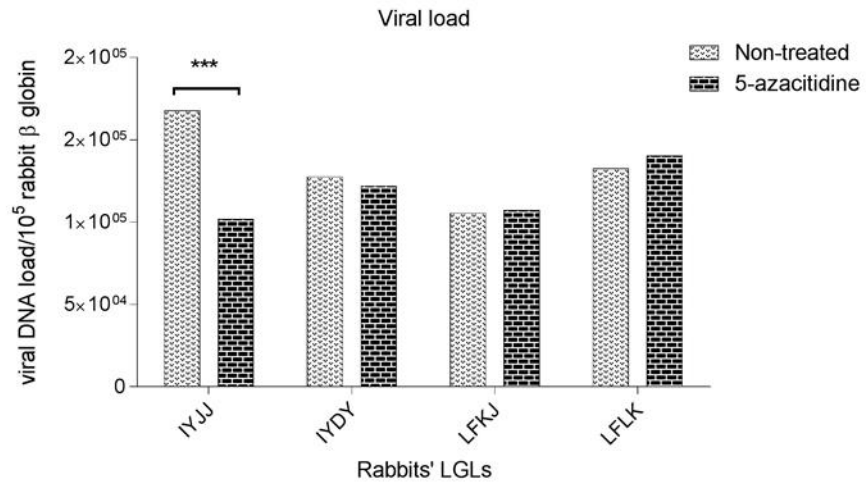


Figure 30 AIHV-1 DNA copy number in rabbit large granular lymphocytes

The figure illustrates the viral load (as DNA copy numbers per 10^5 beta globin DNA copies) in large granular lymphocytes (LGL) from rabbits infected with AIHV-1 C500 strain. Four lines (IYJJ, IYDY, LFKJ, and LFLK) were treated with 5-azacitidine drug or kept without treatment as a control. The viral load was estimated by normalizing the viral DNA copy number per 10^5 rabbit β globin reference gene using qPCR. The primers and probe (FAMAIHV-1) for AIHV-1 ORF3 were used inside the standard sequence and then analysed using Roche Light Cycler 480 system. Two-way ANOVA was performed to do the statistical analysis using Sidak's multiple comparisons test. The primers and probe (FAM) for rabbit β globin reference gene was utilized within the standard sequence.

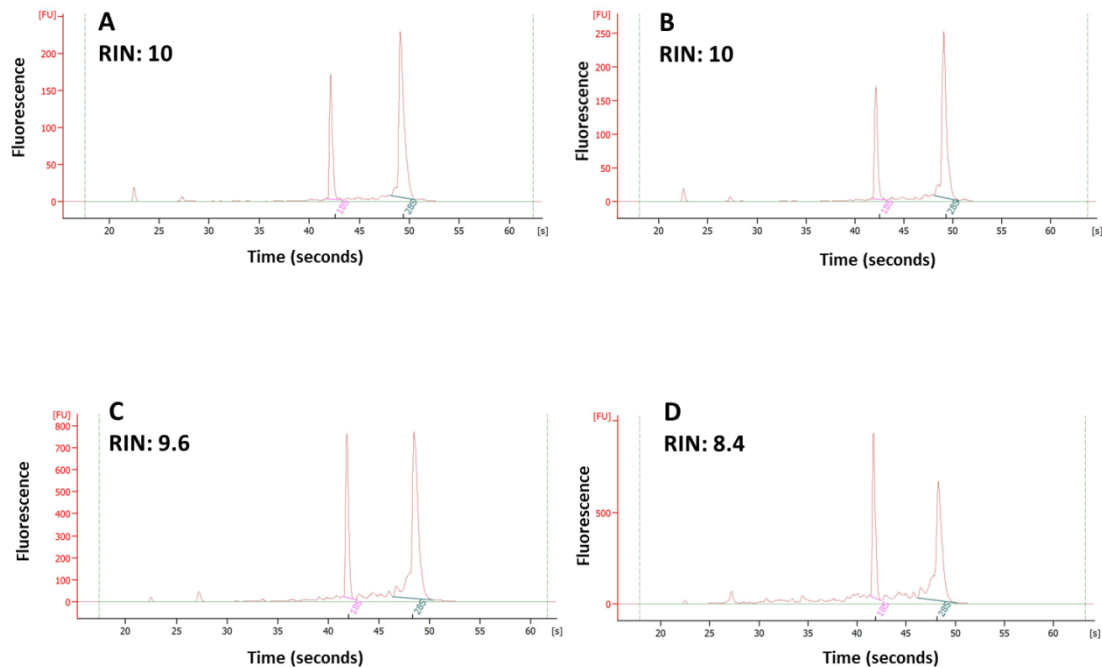


Figure 31 RNA Integrity Number.

Samples with different RIN numbers show various RNA qualities. A RIN of 1 shows a completely degraded RNA sample while a RIN of 10 demonstrates a fully intact RNA sample. The two peaks in the electropherogram represent the 18S and 28S areas of the ribosomal RNA (rRNA) molecule during the single RNA cleavage. The height of 28S peak reflects the status of the RNA degradation as it dissolves faster than 18S peak. The highest peaks for categories 9 and 10 and the lowest for 1-3. (A), RIN value for LGLLK5aza sample; (B), RIN value for LGLKJ5aza sample; (C), RIN value for BT5Aza sample; (D), RIN value for BTinfa sample.

5.4.3 Mapping results

The raw data containing reads with low sequencing score were filtered and aligned to adapter sequences. All filtered reads were mapped against the reference genome (AIHV-1, Bos-taurus 8 and Oryctolagus-cuniculus 2) in line with known gene exon coordinates using HISAT2 (Kim et al., 2015). The data revealed that the number of trimmed reads ranged from 85.86 million reads for sample (LGLLFLKctrl) to nearly 112 million reads for (LGLLFLK5-aza) (Figure 32). In addition, the number of mapped reads ranged from 23

million reads for (LGL LFLK ctrl) with sample to 35 million reads for sample (BTinfb) with percentage of 98% (Figure 33). Of those mapped reads, the correctly mapped reads ranged from 22 million counts to 35 million counts for the same samples respectively (Figure 32). The percentage of mapped reads ranged from 92.93% for sample (LGL LFLK ctrl) to 98.5% for ample (BT5Aza) and those for correctly mapped reads ranged from 89.8% to 96.8% for sample (LGL LFKJ5-aza) and (BT5Aza) respectively (Figure 33).

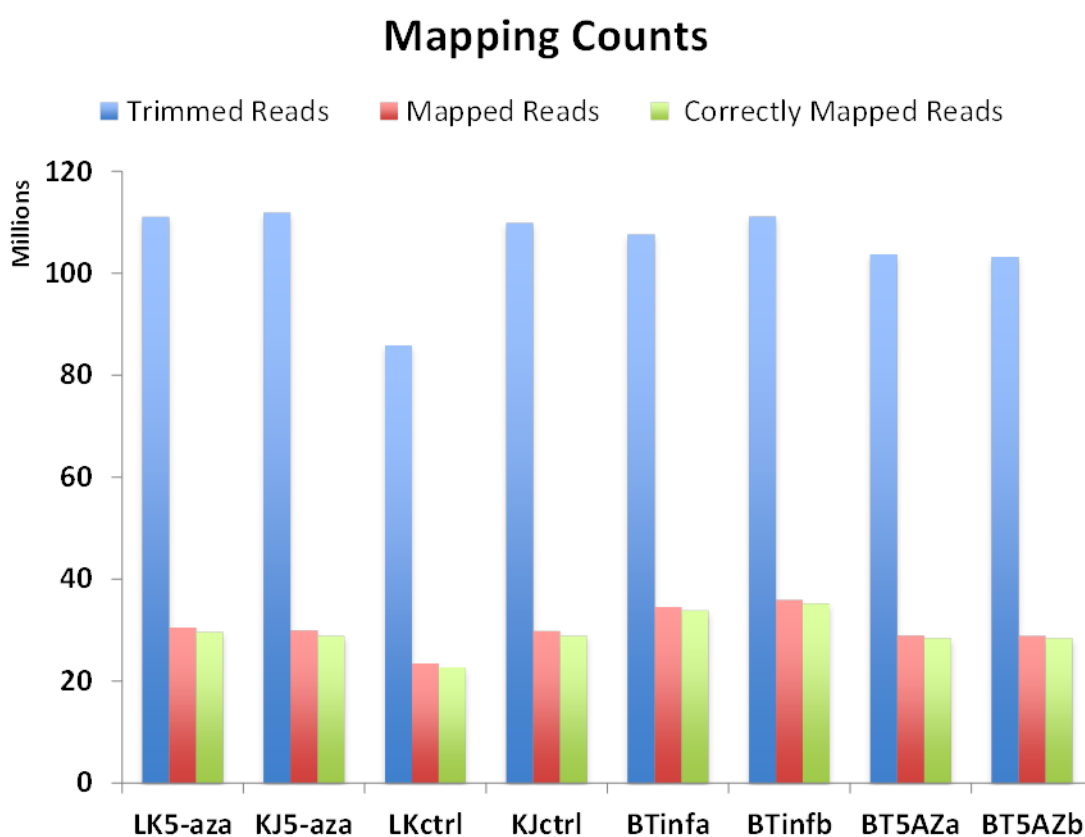


Figure 32 genome coverage for rabbits (*Oryctolagus cuniculus2*) and cattle (*Bos taurus 8*).

The figure shows the mapping count of trimmed reads, mapped reads and uniquely and correctly mapped reads for rabbit and cattle transcripts. The highest counts for trimmed reads were nearly 112 million reads and the lowest was 85 million reads. The highest counts for mapped reads were 35.9 million counts while the lowest was 28.9 million counts. The highest counts for uniquely and correctly

mapped reads were 35 million reads whereas the lowest was 22 million counts. Reads with low sequencing score and reads aligned to adapter sequences were filtered. These reads were mapped against the rabbit and cattle gene transcripts in the context of known gene exon coordinates by HISAT mapping tool. LK5-aza; LGLs LFLK treated with 5-azacitidine, KJ5-aza; LGLs LFKJ treated with 5-azacitidine, LKctrl; non-treated LGL LFLK, KJ ctrl; non-treated LGLs LFKJ, BTinfa; BT infected with AIHV-1 sample a, BTinfb; BT infected with AIHV-1 sample b, BT5Aza; BT infected with AIHV-1 virus and treated with 5-azacitidine sample a, BT5AZb; BT infected with AIHV-1 virus and treated with 5-azacitidine sample b.

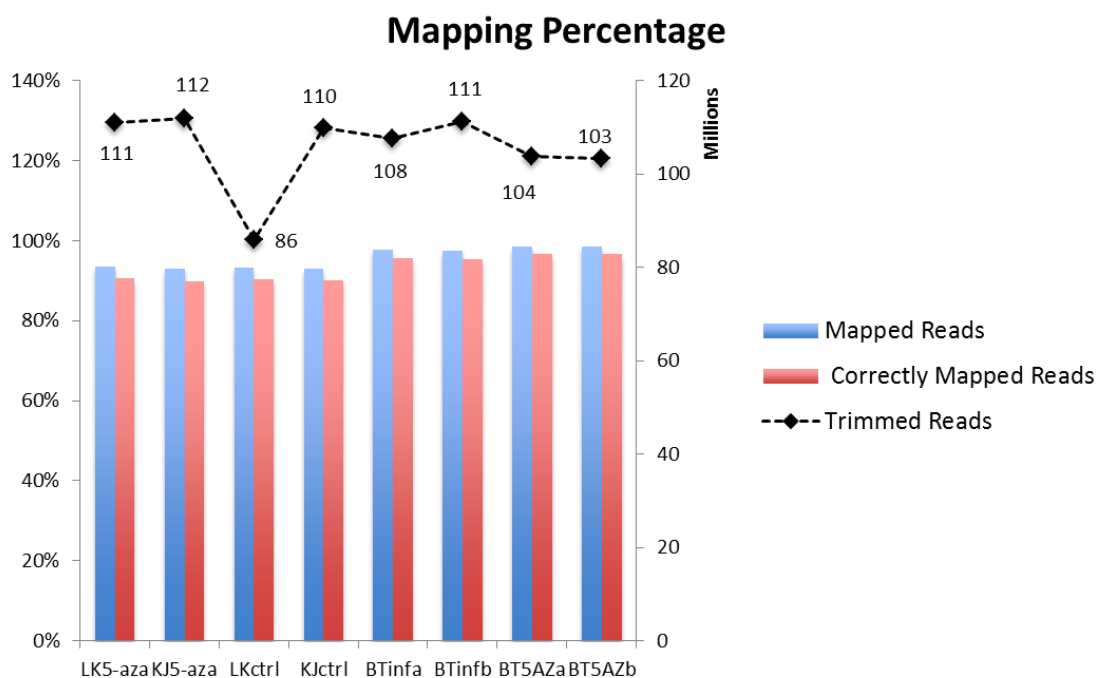


Figure 33 mapping percentage for rabbits (*Oryctolagus cuniculus*2) and cattle (*Bos taurus* 8) genomes.

The figure shows the mapping count of mapped reads and uniquely and correctly mapped reads for rabbit and cattle transcripts. The highest counts for trimmed reads were nearly 112 million reads and the lowest was 85 million reads. The highest percentage for mapped reads was 98.5 % while the lowest was 92.9 %. The highest percentage for uniquely and correctly mapped reads was 96.8 % whereas the lowest was 89.8 %. Reads with low sequencing score and reads aligned to adapter sequences were filtered. These reads were mapped against the rabbit and cattle reference transcripts in the context of known gene exon coordinates by HISAT mapping tool. LK5-aza; LGLs LFLK treated with 5-azacitidine, KJ5-aza; LGLs LFKJ treated with 5-azacitidine, LKctrl; non-treated LGL LFLK, KJ ctrl; non-treated LGLs LFKJ, BTinfa; BT infected with AIHV-1 sample a, BTinfb; BT infected with AIHV-1 sample b, BT5Aza; BT infected with AIHV-1 virus and treated with 5-azacitidine sample a, BT5AZb; BT infected with AIHV-1 virus

5.4.4 Differentially expressed host genes

The data obtained from RNA sequencing analysis were run in BioMart- ensemble www.ensembl.org/biomart to identify the transcript descriptions for both species. The excel look up function was used to annotate the differential transcript lists with the clusters identified by David analysis (see sections (8.6 and 8.8)). Five top clusters represented the most affected pathways based on their enrichment score (the highest values) and then the overlapped differentially-expressed genes were identified between the clusters for both species. Table 10 and 11 show the pathways most affected in both species and the differentially expressed host genes expressed in the presence of 5-azacitidine in comparison to infected control as well as the up-regulated and down regulated genes.

The data also revealed that the pathways that had the majority of genes that were down regulated in rabbits are nuclear lumen (cell structural components), lipid biosynthesis, DNA repair, apoptosis and cell cycle in the presence of 5-azacitidine in comparison to the infected control (Table 12-16). The data also showed that the principle affected pathways that had down-regulated genes overall in cattle (BT) cells are those involved in mitochondrion integrity, endosome (structural cell components), organelle lumen (structural cell components), lysosome (structural cell components), and purine and pyrimidine biosynthesis in the presence of 5-azacitidine in comparison to infected control (Table 17-21).

Some of the genes belong to the Bcl-2 family of apoptosis such as BCL2-Associated X Protein (BAX) and BCL2/Adenovirus E1B 19kDa Interacting Protein 2 (BNIP2), which were up-regulated in 5-aza-treated LGLs compared to untreated controls are considered as pro and anti-apoptotic genes respectively while BCL2/Adenovirus E1B 19kDa Interacting Protein 1 (BNIP1) and BCL2/Adenovirus E1B 19kDa Interacting Protein 3 (BNIP3), which were down regulated are thought to be cell death suppressor and cell death activator respectively. The upregulated genes known to inhibit apoptosis were Tumor Necrosis Factor Receptor Superfamily, Member 1B (TNFRSF1B) and X-Linked Inhibitor of Apoptosis, E3 Ubiquitin Protein Ligase (XIAP) (Table 12-16).

There were overlapped genes between the different pathways that are known to act as anti-apoptotic such as Mitogen-Activated Protein Kinase 7 (MAPK 7) and Pim-1 Proto-Oncogene, Serine/Threonine Kinase (PIM1) and genes acting as cell death activator like STE20-Like Kinase (SLK), Receptor (TNFRSF)-Interacting Serine-Threonine Kinase 1 (RIPK1) and Macrophage Erythroblast Attacher (MAEA) (Table 10). In addition, the overlapped genes involved in apoptosis with unknown function, either as pro or anti apoptotic, were Brain and Reproductive Organ-Expressed (TNFRSF1A Modulator) (BRE), Tubulin, Beta Class I (TUBB), Coagulation Factor II (Thrombin) Receptor-Like 3 (PAR4)

and Nuclear Receptor Subfamily 2, Group C, Member 2 (NR2C2) (Table 12-16).

The host differentially-expressed genes in BT cells that were down regulated in 5-aza treated BT cells compared to untreated controls included Polymerase (RNA) III (DNA Directed) Polypeptide F, 39 KDa (POLR3F), Proliferating Cell Nuclear Antigen (PCNA), GATA Binding Protein 2 (GATA2), Polyglutamine Binding Protein 1 (PQBP1), and Kruppel-Like Factor 4 (Gut) (KLF4) (Table 17-21). All of these genes are involved in transcription, translation, post-translational activity and DNA replication.

Table 10 conserved gene matrix of rabbit LGLs differentially expressed genes in the presence of 5-azacitidine in comparison to infected only control.

	Nuclear lumen	Lipid biosynthesis	DNA repair	Cell death and apoptosis	Cell cycle
Nuclear lumen	22	X	14 7	10 6	9 2
Lipid biosynthesis	X	2	1 0	X	X
DNA repair	14 7	1 1	9	11 8	6 3
Cell death and apoptosis	10 4	X	11 3	12	7 4
Cell cycle	9 7	X	6 3	7 3	10
					15

The table contains the most affected pathways in rabbits in the presence of 5-azacitidine in comparison to the infected control. The total of differentially expressed genes in 5-aza compared to untreated controls in each cluster

is in bold black font, the up regulated genes are in red font, the down regulated genes are in green font and no overlapping is represented by X. The total number of the genes in the same cluster is split to halves. The line was drawn to split the genes in each pathway to up-regulated and down regulated genes.

Table 11 conserved gene matrix of cattle's differentially expressed genes in the presence of 5-azacitidine in comparison to infected control.

	Mitochondrion	Endosome	Organelle lumen	Lysosome	Purine and pyrimidine biosynthesis
Mitochondrion	20 34	4 2	12 5	9 5	6 2
Endosome	4 2	8 6	X	7 4	X
Organelle lumen	12 7	X	18 27	X	2 1
Lysosome	9 4	7 3	X	5 4	1 1
Purine and pyrimidine biosynthesis	6 4	X	2 1	1 0	9 8

The table contains the most affected pathways in rabbits in the presence of 5-azacitidine in comparison to the infected control. The total of differentially expressed genes in 5-aza compared to untreated controls in each cluster is in bold black font, the up regulated genes are in red font, the down regulated genes are in green font and no overlapping is represented by X. The total number of the genes in the same cluster is split to halves. The line was drawn to split the genes in each pathway to up-regulated and down regulated ones.

Table 12 up-regulated and down regulated of rabbit gene transcripts involved in lipid bio-synthesis

Gene ID	Gene name/description	p-value	Log FC
Lipid biosynthesis			
ENSOCUG00000025649	TPI1 triosephosphate isomerase 1	0.003501	-2.1
ENSOCUG00000005722	CERS6 Cyramide synthase 6	0.007421	1.2
ENSOCUG00000015384	OXSM 3 Oxacyl-ACP-synthase, mitochondarial	0.018148	-1.2
ENSOCUG00000014801	Uncharacterised protein	0.035263	-3.5
ENSOCUG00000024832	Uncharacterised protein	0.02456	1.2
ENSOCUG00000003499	FADS 2 fatty acid desaturase 2	0.011453	-3.5
ENSOCUG00000022356	Uncharacterised protein	0.016451	-0.9
ENSOCUG00000004549	CYP51A1 cytochrome P450, family 51, subfamily A, polypeptide 1	0.040602	-0.8
ENSOCUG00000015843	MCAT Malonyl CO:CAP acyltransferase (mitochondorial)	0.040358	-1.2

The table shows the rabbits' genes name involved in the lipid bio-synthesis pathway along with their gene IDs. (-) values of log FC indicates gene down regulation where positive values indicate gene transcript up-regulation in 5-aza treated compared to untreated controls. P values are significant ≤ 0.04 .

Table 13 up-regulated and down regulated LGL transcripts involved in the nuclear lumen pathway

Gene ID	Gene name/description	p-value	Log FC
Nuclear lumen			
ENSOCUG00000011841	LIG1 ligase I, DNA, ATP-dependent	0.000739	-1.67635
ENSOCUG00000006346	PSKH1 protein serine kinase H1 [Source:HGNC Symbol;Acc:HGNC:9529]	0.001056	0.527987
ENSOCUG00000014274	MNAT1 MNAT CDK-activating kinase assembly factor 1	0.003235	0.0827
ENSOCUG00000015063	URI1 URI1, prefoldin-like chaperone	0.008231	0.54297
ENSOCUG00000029326	serine/arginine-rich splicing factor 10	0.010133	3.421816
ENSOCUG00000007138	EXOSC2 exosome component 2	0.01081	-0.1158
ENSOCUG00000003624	RFC3 replication factor C (activator 1) 3, 38kDa	0.015444	-0.24525
ENSOCUG00000010418	SAP30 Sin3A-associated protein, 30kDa	0.015697	-1.5082
ENSOCUG00000015154	MAPK7 mitogen-activated protein kinase 7	0.018904	0.796661

ENSOCUG00000005172	ZSCAN30 zinc finger and SCAN domain containing 30	0.019611	-0.59829
ENSOCUG00000017150	HNRNPH1 heterogeneous nuclear ribonucleoprotein H1 (H)	0.022724	0.573093
ENSOCUG00000009275	PPP1CC protein phosphatase 1, catalytic subunit, gamma isozyme	0.023446	-1.71405
ENSOCUG00000006975	NR2C2 nuclear receptor subfamily 2, group C, member 2	0.023524	-0.35353
ENSOCUG00000008735	MAK16 MAK16 homolog	0.034845	0.145717
ENSOCUG00000005398	CCNE2 cyclin E2	0.040346	-0.85486
ENSOCUG00000025072	Uncharacterized protein	0.041209	-0.08768
ENSOCUG00000005276	NF2 neurofibromin 2 (merlin)	0.04231	0.231713
ENSOCUG00000002802	FANCD2 Fanconi anemia, complementation group D2	0.042852	-0.59767
ENSOCUG00000027381	Uncharacterized protein	0.04345	-0.44872
ENSOCUG00000000322	PARN poly(A)-specific ribonuclease	0.043932	-0.19677
ENSOCUG00000007979	TBP TATA box binding protein	0.045047	0.407046
ENSOCUG00000024051	IDH3B isocitrate dehydrogenase 3 (NAD+) beta	0.045702	0.159479
ENSOCUG00000003848	TCOF1 Treacher Collins-Franceschetti syndrome 1	0.04798	0.278411
ENSOCUG00000014124	SENP5 SUMO1 /sentrin specific peptidase 5	0.048374	-0.53382

ENSOCUG00000002541	BNIP3 BCL2/adenovirus E1B 19kDa interacting protein 3	0.010643	-2.36666
ENSOCUG00000011703	PQBP1 polyglutamine binding protein 1	0.02809	1.548224
ENSOCUG00000004604	EME1 essential meiotic structure-specific endonuclease 1	0.009054	0.278554
ENSOCUG00000000408	Uncharacterized protein	0.018583	-1.83834
ENSOCUG00000003879	CTDP1 CTD (carboxy-terminal domain, RNA polymerase II, polypeptide A) phosphatase, subunit 1	0.013843	0.268011
ENSOCUG00000010012	AK4 adenylate kinase 4	0.01612	-3.43355
ENSOCUG00000006610	MAEA macrophage erythroblast attacher	0.02166	-0.85255
ENSOCUG00000012396	ZMYM3 zinc finger, MYM-type 3	0.049674	0.179336
ENSOCUG00000014778	MORF4L2 mortality factor 4 like 2	0.008387	0.524559
ENSOCUG00000021243	EXOSC4 exosome component 4	0.026038	-2.99464
ENSOCUG00000024309	SMAD7 SMAD family member 7	0.002216	0.707824
ENSOCUG00000016827	ETV6 ets variant 6	0.032107	-0.57071
ENSOCUG00000006642	XRCC5b X-ray repair complementing defective repair in Chinese hamster cells 5 (double-strand-break rejoining)	0.024364	0.140797

ENSOCUG00000014717	Uncharacterized protein	0.013059	2.937234
ENSOCUG00000010624	POLR3G polymerase (RNA) III (DNA directed) polypeptide G (32kD)	0.016503	0.121737
ENSOCUG00000017091	MBIP MAP3K12 binding inhibitory protein 1	0.028152	0.787543
ENSOCUG00000003587	ZMIZ1 zinc finger, MIZ-type containing 1	0.048565	0.274723
ENSOCUG00000008568	ANKRD28 ankyrin repeat domain 28	0.042355	-0.53151
ENSOCUG00000012218	MRPS26 mitochondrial ribosomal protein S26	0.01552	-0.14257
ENSOCUG00000004933	SUPV3L1 SUV3-like helicase	0.024445	-0.1046

The table shows the rabbits' genes name involved in the nuclear lumen pathway along with their gene IDs. (-) values of log FC indicates gene down regulation where positive values indicate gen up-regulation in 5-aza compared to untreated controls. P values are significant ≤ 0.04 .

Table 14 up-regulated and down regulated of LGL transcripts involved in the DNA repair pathway

Gene ID	Gene name/description	p-value	Log FC
DNA repair			
ENSOCUG00000022356	Uncharacterized protein	0.016451	-0.96062
ENSOCUT00000006644	XRCC5 X-ray repair complementing defective repair in Chinese hamster cells 5 (double-strand-break re-joining)	0.024364476	0.140797037
ENSOCUT00000021649	Uncharacterized protein	0.043449515	-
ENSOCUG00000011841	LIG1 ligase I, DNA, ATP-dependent	0.000739	-1.67635
ENSOCUG00000014274	MNAT1 MNAT CDK-activating kinase assembly factor 1	0.003235	0.0827
ENSOCUT00000002540	BNIP3 BCL2/adenovirus E1B 19kDa interacting protein 3	0.010643207	-2.36666053
ENSOCUG00000003624	RFC3 replication factor C (activator 1) 3, 38kDa	0.015444	-0.24525
ENSOCUG00000002802	FANCD2 Fanconi anemia, complementation group D2	0.042852	-0.59767
ENSOCUG00000004604	EME1 essential meiotic structure-specific endonuclease 1	0.009054	0.278554

ENSOCUG00000014778	MORF4L2 mortality factor 4 like 2	0.008387	0.524559
ENSOCUT00000010697	BRE Brain And Reproductive Organ-Expressed (TNFRSF1A Modulator)	0.040783077	0.323317894
ENSOCUG00000017091	MBIP MAP3K12 binding inhibitory protein 1	0.028152	0.787543
ENSOCUT00000005398	CCNE2 Cyclin E2	0.040346282	- 0.854855505
ENSOCUG00000012218	MRPS26 mitochondrial ribosomal protein S26	0.01552	-0.14257
ENSOCUT00000012453	EIF2AK3 Eukaryotic Translation Initiation Factor 2-Alpha Kinase 3	0.001836194	0.588992333
ENSOCUT00000009875	XIAP X-Linked Inhibitor Of Apoptosis, E3 Ubiquitin Protein Ligase	0.023859876	- 1.292221674
ENSOCUT00000003039	SLK STE20-Like Kinase	0.013003841	2.362971241
ENSOCUT00000011792	RIPK1 Receptor (TNFRSF)-Interacting Serine-Threonine Kinase 1	0.031130748	0.443478374
ENSOCUT00000014532	PARP4 Poly (ADP-Ribose) Polymerase Family, Member 4	0.047262905	0.218631005
ENSOCUT00000024642	BAX BCL2-Associated X Protein	0.03360173	1.01942528

The table shows the rabbits' genes name involved in the DNA repair pathway along with their gene IDs. (-) values of log FC indicates gene down regulation where positive values indicate gene up-regulation in 5-aza treated to untreated controls. P values are significant ≤ 0.04 .

Table 15 up-regulated and down regulated LGL transcripts involved in cellular death and apoptosis pathway

Gene ID	Gene name/ description	p-value	Log FC
Cell death and apoptosis			
ENSOCUG00000014274	MNAT1 MNAT CDK-activating kinase assembly factor 1	0.003235	0.0827
ENSOCUG00000027381	Uncharacterized protein	0.04345	-0.44872
ENSOCUG00000002541	BNIP3 BCL2/adenovirus E1B 19kDa interacting protein 3	0.010643	-2.36666
ENSOCUG00000006642	XRCC5 X-ray repair complementing defective repair in Chinese hamster cells 5 (double-strand-break re-joining)	0.024364	0.140797
ENSOCUG00000012451	EIF2AK3 eukaryotic translation initiation factor 2-alpha kinase 3	0.001836	0.588992
ENSOCUG00000009878	XIAP E3 ubiquitin-protein ligase XIAP	0.02386	-1.29222
ENSOCUG00000011791	RIPK1 receptor (TNFRSF)-interacting serine-threonine kinase 1	0.031131	0.443478
ENSOCUG00000006423	BAX BCL2-associated X protein	0.033602	1.019425
ENSOCUG00000014529	PARP4 poly (ADP-ribose) polymerase family, member 4	0.047263	0.218631
ENSOCUG00000003035	SLK STE20-like kinase	0.013004	2.362971

ENSOCUG00000010695	BRE brain and reproductive organ-expressed (TNFRSF1A modulator)	0.040783	0.323318
ENSOCUG00000015154	MAPK7 mitogen-activated protein kinase 7	0.018904	0.796661
ENSOCUG00000006975	NR2C2 nuclear receptor subfamily 2, group C, member 2	0.023524	-0.35353
ENSOCUG00000005276	NF2 neurofibromin 2 (merlin)	0.04231	0.231713
ENSOCUG00000007979	TBP TATA box binding protein	0.045047	0.407046
ENSOCUG00000006610	MAEA macrophage erythroblast attacher	0.02166	-0.85255
ENSOCUG00000014717	Uncharacterized protein	0.013059	2.937234
ENSOCUG00000001542	RIPK2 receptor-interacting serine-threonine kinase 2	0.001105	-0.59341
ENSOCUG00000000172	VAV3 vav 3 guanine nucleotide exchange factor	0.006063	1.138616
ENSOCUG00000007938	ALDH1A3 aldehyde dehydrogenase 1 family, member A3	0.010062	0.170754
ENSOCUG00000012028	PIM1 Pim-1 proto-oncogene, serine/threonine kinase	0.019968	0.398831
ENSOCUG00000004627	APH1B APH1B gamma secretase subunit	0.020786	0.424591
ENSOCUG00000015236	Uncharacterized protein	0.021786	-1.71366
ENSOCUG00000006277	BNIP2 BCL2/adenovirus E1B 19kDa interacting protein 2	0.034452	0.307168
ENSOCUG00000000040	BNIP1 BCL2/adenovirus E1B 19kDa interacting protein 1	0.025577	-3.16923

ENSOCUG00000014127	TNFRSF1B tumor necrosis factor receptor superfamily, member 1B	0.048762	-1.25577
ENSOCUG00000002187	TUBB tubulin, beta class I	0.038957	-0.37109
ENSOCUG00000006958	TMEM173 transmembrane protein 173	0.039155	0.522144
ENSOCUG00000028156	Uncharacterized protein	0.020263	-0.21927
ENSOCUG00000017921	BCAP31 B-cell receptor-associated protein 31	0.043509	-0.3856
ENSOCUG00000015961	PPP2CA Serine/threonine-protein phosphatase 2A catalytic subunit alpha isoform	0.007485	0.092106
ENSOCUG00000015961	PPP2CA Serine/threonine-protein phosphatase 2A catalytic subunit alpha isoform	0.007485	0.092106
ENSOCUG00000015413	PDCD10 programmed cell death 10	0.008327	0.106757
ENSOCUG00000026354	PGF placental growth factor	0.032233	0.349872

The table shows the rabbits' genes name involved in the cellular death and apoptosis pathway along with their gene IDs. (-) values of log FC indicates gene down regulation where positive values indicate gene up-regulation in 5-aza treated in comparison to untreated controls. P values are significant ≤ 0.04 .

Table 16 up-regulated and down regulated LGL transcripts involved in the cell cycle pathway

Gene ID	Gene name/ description	p-value	Log FC
Cell Cycle			
ENSOCUG00000014274	MNAT1 MNAT CDK-activating kinase assembly factor 1	0.003235	0.0827
ENSOCUG00000006423	BAX BCL2-associated X protein	0.033602	1.019425
ENSOCUG00000015154	MAPK7 mitogen-activated protein kinase 7	0.018904	0.796661
ENSOCUG00000006975	NR2C2 nuclear receptor subfamily 2, group C, member 2	0.023524	-0.35353
ENSOCUG00000006610	MAEA macrophage erythroblast attacher	0.02166	-0.85255
ENSOCUG00000012028	PIM1 Pim-1 proto-oncogene, serine/threonine kinase	0.019968	0.398831
ENSOCUG00000002187	TUBB tubulin, beta class I	0.038957	-0.37109
ENSOCUG00000011841	LIG1 ligase I, DNA, ATP-dependent	0.000739	-1.67635
ENSOCUG00000005398	CCNE2 cyclin E2	0.040346	-0.85486
ENSOCUG00000002802	FANCD2 Fanconi anemia, complementation group D2	0.042852	-0.59767
ENSOCUG00000004921	DCLRE1A DNA cross-link repair 1A	0.009148	0.087371

ENSOCUG00000009275	PPP1CC protein phosphatase 1, catalytic subunit, gamma isozyme	0.023446	-1.71405
ENSOCUG00000014124	SENP5 SUMO1/sentrin specific peptidase 5	0.048374	-0.53382
ENSOCUG00000007827	SASS6 SAS-6 centriolar assembly protein	0.00895	-0.42226
ENSOCUG00000011298	FAM83D family with sequence similarity 83, member D	0.018536	-1.03649
ENSOCUG00000009879	STAG2 cohesin subunit SA-2	0.021314	0.364604
ENSOCUG00000016706	KIF11 kinesin family member 11	0.027452	-0.19417
ENSOCUG00000006348	PSMB10 proteasome subunit beta 10	0.028911	0.5946833 23
ENSOCUG00000001418	PSMD14 proteasome 26S subunit, non-ATPase 14	0.029403	-0.62192
ENSOCUG00000001097	CGRRF1 cell growth regulator with ring finger domain 1	0.035752	-1.73356
ENSOCUG00000000791	RPL24 ribosomal protein L24	0.043664	-1.61249
ENSOCUG00000003623	ITGB1 integrin, beta 1	0.00548	4.106411
ENSOCUG00000014903	RGCC regulator of cell cycle	0.042739	0.620927
ENSOCUG00000010944	NEDD1 neural precursor cell expressed, developmentally down-regulated 1	0.033882	-1.16131

ENSOCUG00000005880	PDS5A PDS5 cohesin associated factor A	0.048663	0.879025
--------------------	---	----------	----------

The table shows the rabbits' genes name involved in the cell cycle pathway along with their gene IDs. (-) values of log FC indicates gene down regulation where positive values indicate gen up-regulation in 5-aza treated compared to untreated controls. P values are significant ≤ 0.04 .

Table 17 up-regulated and down regulated of cattle BT transcripts involved in the mitochondrion integrity pathway

Gene ID	Gene name/description	p-value	Log FC
Mitochondrion			
ENSBTAG00000006272	nth -like DNA glycosylase 1	0.017064	0.52413
ENSBTAG00000015294	COX10 heme A:farnesyltransferase cytochrome c oxidase assembly factor	0.016254	-0.62018
ENSBTAG00000045703	cytochrome c oxidase assembly homolog 15 (yeast)	0.018873	4.340498
ENSBTAG00000007332	Uncharacterized protein	0.029911	-7.33293
ENSBTAG00000005791	uroporphyrinogen III synthase	0.036102	-4.84748
ENSBTAG00000047462	Uncharacterized protein	0.045345	-2.40732
ENSBTAG00000046690	Uncharacterized protein	0.023888	1.060966
ENSBTAG00000011931	CD63 antigen	0.028907	-0.32749
ENSBTAG00000006065	proliferating cell nuclear antigen	0.004827	-2.10674
ENSBTAG00000015006	mitochondrial ribosomal protein L11	0.009037	-1.45233
ENSBTAG00000047906	mitochondrial ribosomal protein L36	0.015561	0.068833

ENSBTAG00000015567	translocase of inner mitochondrial membrane 44 homolog (yeast)	0.016698	-0.84677
ENSBTAG00000015833	DEAH (Asp-Glu-Ala-His) box helicase 30	0.016792	-8.03291
ENSBTAG00000001780	serine--tRNA ligase, mitochondrial precursor	0.019816	-1.32708
ENSBTAG00000001780	serine--tRNA ligase, mitochondrial precursor	0.029509	-1.15327
ENSBTAG00000009091	ribonuclease L (2',5'-oligoadenylate synthetase-dependent)	0.036661	1.759817
ENSBTAG00000001107	calcyclin binding protein	0.040685	0.183786
ENSBTAG00000006978	hydroxysteroid (17-beta) dehydrogenase 4	0.046434	0.519715
ENSBTAG00000009839	glutathione S-transferase kappa 1	0.049364	-0.69816
ENSBTAG00000015098	Rab9 effector protein with kelch motifs	0.008312	7.027562
ENSBTAG00000004019	premelanosome protein	0.020502	-1.15137
ENSBTAG00000008135	SRA stem-loop-interacting RNA-binding protein, mitochondrial	0.004899	-3.087
ENSBTAG00000011760	mitochondrial ribosomal protein L14	0.011364	-2.85854
ENSBTAG00000002474	MAD1 mitotic arrest deficient-like 1 (yeast)	0.012979	-1.7572
ENSBTAG00000011809	nudix (nucleoside diphosphate linked moiety X)-type motif 8	0.014434	4.202557
ENSBTAG00000020898	carbohydrate (chondroitin 4) sulfotransferase 12	0.014673	4.543596

ENSBTAG00000018770	hydroxysteroid dehydrogenase like 1	0.015835	2.683234
ENSBTAG00000014653	spinster homolog 1 (Drosophila)	0.016729	1.300334
ENSBTAG00000009682	LOC532995 protein; Uncharacterized protein	0.017564	-4.66056
ENSBTAG00000008730	sideroflexin 4	0.019208	0.333715
ENSBTAG00000008077	solute carrier family 37 (glucose-6-phosphate transporter), member 4	0.020471	-3.86726
ENSBTAG00000043959	platelet derived growth factor C	0.020528	-5.22392
ENSBTAG00000019854	ATP-binding cassette, sub-family E (OABP), member 1	0.021995	-1.79642
ENSBTAG00000021780	SCO1 cytochrome c oxidase assembly protein	0.02314	-0.33666
ENSBTAG00000003177	solute carrier family 25 (pyrimidine nucleotide carrier), member 33	0.023753	-0.50344
ENSBTAG00000001463	tankyrase, TRF1-interacting ankyrin-related ADP-ribose polymerase	0.024295	1.709409
ENSBTAG00000015255	ST6 (alpha-N-acetyl-neuraminy-2,3-beta-galactosyl-1,3)-N-acetylgalactosaminide alpha-2,6-sialyltransferase 2	0.031701	0.68046
ENSBTAG00000024781	39S ribosomal protein L17, mitochondrial	0.031911	-0.41802
ENSBTAG00000008629	mitochondrial fission regulator 1	0.036049	-0.20923
ENSBTAG00000004240	thymopoietin	0.037698	-4.9725

ENSBTAG00000006398	translocase of outer mitochondrial membrane 7 homolog (yeast)	0.037962	-5.25928
ENSBTAG00000000301	Glycerol kinase; Uncharacterized protein	0.038167	-0.30485
ENSBTAG00000001962	mitochondrial ribosomal protein S27	0.040067	-0.25581
ENSBTAG000000021790	apolipoprotein O-like	0.040527	-2.04374
ENSBTAG000000047836	NADH dehydrogenase [ubiquinone] 1 alpha subcomplex subunit 2	0.041881	2.67723
ENSBTAG000000008438	ADP-ribosylation factor interacting protein 1	0.042427	2.705246
ENSBTAG000000012107	solute carrier family 25 (mitochondrial iron transporter), member 28	0.042458	-4.15644
ENSBTAG000000005903	low density lipoprotein receptor-related protein 5	0.042508	3.191428
ENSBTAG000000012072	NADH dehydrogenase (ubiquinone) Fe-S protein 8, 23kDa	0.046031	-2.11016
ENSBTAG000000030566	GLE1 RNA export mediator	0.046476	-0.51529
ENSBTAG000000034827	platelet derived growth factor D	0.046738	6.932076
ENSBTAG000000006966	nurim (nuclear envelope membrane protein)	0.046957	-3.65053
ENSBTAG000000013282	NECAP endocytosis associated 2	0.048582	-0.20713
ENSBTAG000000046671	Wolfram syndrome 1 (wolframin)	0.049274	2.497423

The table shows cattle gene names involved in the mitochondrion pathway along with their gene IDs. (-) values of log FC indicates gene down regulation where positive values indicate gen up-regulation in 5-aza treated compared to untreated controls. P values are significant ≤ 0.04 .

Table 18 up-regulated and down regulated of cattle BT transcripts involved in endosomal pathways

Gene ID	Gene name/description	p-value	Log FC
endosome			
ENSBTAG00000046690	Uncharacterized protein	0.023888	1.060966
ENSBTAG00000011931	CD63 antigen	0.028907	-0.32749
ENSBTAG00000016094	solute carrier family 36 (proton/amino acid symporter), member 1	0.002693	-3.00111
ENSBTAG00000018202	cytochrome b561 family, member A3	0.013663	-3.80245
ENSBTAG00000039968	transmembrane protein 55A	0.023713	3.109691
ENSBTAG00000034689	zinc and ring finger 1, E3 ubiquitin protein ligase	0.036233	1.176685
ENSBTAG00000003745	WD repeat domain 48	0.037767	0.725065
ENSBTAG00000015098	Rab9 effector protein with kelch motifs	0.008312	7.027562
ENSBTAG00000004019	premelanosome protein	0.020502	-1.15137
ENSBTAG00000046467	protein tyrosine phosphatase type IVA, member 3	0.009776	-2.61277
ENSBTAG00000018915	WASH complex subunit FAM21	0.01622	3.690243

ENSBTAG00000025297	membrane magnesium transporter 1	0.018348	10.41085
ENSBTAG00000003565	tripartite motif containing 3	0.022235	4.037245
ENSBTAG00000021639	activity-regulated cytoskeleton-associated protein	0.040311	-0.17954

The table shows cattle's genes name involved in the endosome pathway along with their gene IDs. (-) values of log FC indicates gene down regulation where positive values indicate gen up-regulation in 5-aza-treated compared to untreated controls. P values are significant ≤ 0.04 .

Table 19 up-regulated and down regulated of cattle BT gene transcripts involved in the organelle lumen pathway

Gene ID	Gene name/description	p-value	Log FC
Organelle lumen			
ENSBTAG00000006272	nth-like DNA glycosylase 1	0.017064	0.52413
ENSBTAG00000008825	polymerase (RNA) III (DNA directed) polypeptide F, 39 kDa	0.038073	-1.69785
ENSBTAG00000006065	proliferating cell nuclear antigen	0.004827	-2.10674
ENSBTAG00000015006	mitochondrial ribosomal protein L11	0.009037	-1.45233
ENSBTAG00000047906	mitochondrial ribosomal protein L36	0.015561	0.068833
ENSBTAG00000015567	translocase of inner mitochondrial membrane 44 homolog (yeast)	0.016698	-0.84677
ENSBTAG00000015833	DEAH (Asp-Glu-Ala-His) box helicase 30	0.016792	-8.03291
ENSBTAG00000001780	serine--tRNA ligase, mitochondrial precursor	0.019816	-1.32708
ENSBTAG00000001780	serine--tRNA ligase, mitochondrial precursor	0.029509	-1.15327
ENSBTAG00000009091	ribonuclease L (2',5'-oligoadenylate synthetase-dependent)	0.036661	1.759817
ENSBTAG00000001107	calcyclin binding protein	0.040685	0.183786

ENSBTAG0000006978	hydroxysteroid (17-beta) dehydrogenase 4	0.046434	0.519715
ENSBTAG0000009839	glutathione S-transferase kappa 1	0.049364	-0.69816
ENSBTAG00000011360	pre-mRNA-splicing factor SYF1	0.00146	-1.66151
ENSBTAG0000003849	guanine nucleotide binding protein-like 2 (nucleolar)	0.005061	-3.48445
ENSBTAG00000016606	polycomb group ring finger 1	0.00592	7.051528
ENSBTAG00000019707	GATA binding protein 2	0.007854	-0.29559
ENSBTAG0000007323	cleavage and polyadenylation specific factor 6, 68kDa	0.008762	1.478988
ENSBTAG00000012777	serum response factor	0.008861	-1.61675
ENSBTAG0000009562	zinc finger protein 593	0.0127	-1.68797
ENSBTAG00000016332	inhibitor of growth family, member 3	0.015852	-2.50246
ENSBTAG00000012575	macrophage erythroblast attacher	0.016016	1.536743
ENSBTAG00000008190	sulfatase modifying factor 2	0.0175	-0.57121
ENSBTAG0000007480	cold inducible RNA binding protein	0.018909	8.773147
ENSBTAG00000038409	methyl-CpG binding domain protein 3	0.01934	-0.93366
ENSBTAG00000026585	transcription elongation factor B (SIII), polypeptide 3 (110kDa, elongin A)	0.019828	1.808792

ENSBTAG0000003697	TAR DNA binding protein	0.021319	-6.7882
ENSBTAG00000015946	retinoblastoma binding protein 5	0.021543	1.793306
ENSBTAG00000020490	NACC family member 2, BEN and BTB (POZ) domain containing	0.02163	-4.77528
ENSBTAG00000005076	synovial apoptosis inhibitor 1, synoviolin	0.025081	1.024949
ENSBTAG00000021192	glioma tumor suppressor candidate region gene 2	0.025745	0.595285
ENSBTAG00000006112	SprT-like N-terminal domain	0.027078	1.98873
ENSBTAG00000010384	cell division cycle 6	0.0276	-1.29413
ENSBTAG00000021845	striatin, calmodulin binding protein 3	0.028528	-1.55617
ENSBTAG00000016271	small nuclear ribonucleoprotein polypeptide F	0.029432	-1.43929
ENSBTAG00000003423	DEAD (Asp-Glu-Ala-Asp) box helicase 24	0.030951	-2.64543
ENSBTAG00000018498	polyglutamine binding protein 1	0.031957	-5.22647
ENSBTAG00000017582	checkpoint kinase 1	0.032011	4.752555
ENSBTAG00000008905	folliculogenesis specific bHLH transcription factor	0.03221	-0.81315
ENSBTAG00000012699	exosome component 1	0.034345	-1.84211
ENSBTAG00000008704	fidgetin	0.038805	-1.51006

ENSBTAG00000019846	alkB homolog 2, alpha-ketoglutarate-dependent dioxygenase	0.03964	11.41241
ENSBTAG00000017219	DEAD (Asp-Glu-Ala-Asp) box polypeptide 51	0.044658	3.336827
ENSBTAG00000020355	Kruppel-like factor 4 (gut)	0.045216	-9.77397
ENSBTAG00000003934	paraspeckle component 1	0.047011	5.469299

The table shows cattle's genes name involved in the organelle lumen pathway along with their gene IDs. (-) values of log FC indicates gene down regulation where positive values indicate gene up-regulation in 5-aza treated compared to untreated controls. P values are significant ≤ 0.04 .

Table 20 up-regulated and down regulated of cattle BT gene transcripts involved in lysosomal pathways

Gene ID	Gene name/description	p-value	Log FC
Lysosome			
ENSBTAG00000011960	glutamic-oxaloacetic transaminase 1, soluble	0.009702	0.410793
ENSBTAG00000046690	Uncharacterized protein	0.023888	1.060966
ENSBTAG00000011931	CD63 antigen	0.028907	-0.32749
ENSBTAG00000016094	solute carrier family 36	0.002693	-3.00111
ENSBTAG00000018202	cytochrome b561 family, member A3	0.013663	-3.80245
ENSBTAG00000039968	transmembrane protein 55A	0.023713	3.109691
ENSBTAG00000034689	zinc and ring finger 1, E3 ubiquitin protein ligase	0.036233	1.176685
ENSBTAG00000003745	WD repeat domain 48	0.037767	0.725065
ENSBTAG00000000484	hyaluronoglucosaminidase 2	0.042501	-0.97983

The table shows cattle's genes name involved in the lysosome pathway along with their gene IDs. (-) values of log FC indicates gene down regulation where positive values indicate gen up-regulation in 5-aza-treated compared to untreated controls. P values are significant ≤ 0.04 .

Table 21 up-regulated and down regulated of cattle BT gene transcripts involved in purine and pyrimidine biosynthesis pathways

Gene ID	Gene name/description	p-value	Log FC
Purine and pyrimidine biosynthèses			
ENSBTAG00000011960	glutamic-oxaloacetic transaminase 1, soluble	0.009702	0.410793
ENSBTAG00000006272	nth-like DNA glycosylase 1	0.017064	0.52413
ENSBTAG00000008825	polymerase (RNA) III (DNA directed) polypeptide F, 39 kDa	0.038073	-1.69785
ENSBTAG00000015294	COX10 heme A:farnesyltransferase cytochrome c oxidase assembly factor	0.016254	-0.62018
ENSBTAG00000045703	cytochrome c oxidase assembly homolog 15 (yeast)	0.018873	4.340498
ENSBTAG00000007332	Uncharacterized protein	0.029911	-7.33293
ENSBTAG00000005791	uroporphyrinogen III synthase	0.036102	-4.84748
ENSBTAG00000047462	Uncharacterized protein	0.045345	-2.40732
ENSBTAG00000015509	nicotinamide phosphoribosyltransferase	0.00014	6.215473
ENSBTAG00000019274	5-aminoimidazole-4-carboxamide ribonucleotide formyltransferase/IMP cyclohydrolase	0.006476	10.49776

ENSBTAG00000007758	phosphodiesterase 10A	0.011243	4.872506
ENSBTAG00000013776	inosine triphosphatase	0.013862	-0.93005
ENSBTAG00000003025	NME/NM23 nucleoside diphosphate kinase 6	0.032176	5.09935
ENSBTAG00000016552	NME/NM23 nucleoside diphosphate kinase 3	0.036335	14.84213
ENSBTAG00000004549	uracil phosphoribosyltransferase (FUR1) homolog	0.037439	-5.2164
ENSBTAG00000013825	branched chain amino-acid transaminase 1, cytosolic	0.044216	3.56528
ENSBTAG00000002689	NME/NM23 family member 7	0.048514	-0.52516

The table shows cattle's genes name involved in the purine and pyrimidine biosynthesis pathway along with their gene IDs. (-) values of log FC indicates gene down regulation where positive values indicate gene up-regulation in 5-aza-treated compared to untreated controls. P values are significant ≤ 0.04 .

5.4.5 Differentially-expressed virus genes detected by RNA-Seq

The sequence analysis revealed that one virus gene differentially expressed (ORF 8, down-regulated in 5-aza group compared to controls, figure 34) in the cattle samples whereas two virus genes (ORF 21 and ORF 7) were up-regulated in the rabbit samples in the presence of 5-azacitidine in comparison to infected control (Figure 34). Table 22 shows viral DNA load and viral gene transcripts in rabbit LGL and cattle BT cells in the presence and absence of 5-azacitidine as measured by PCR and qPCR.

Table 22 summary of viral gene transcripts and viral DNA load in rabbit LGL and cattle BT cells in the presence and absence of 5-azacitidine as measured by qPCR and PCR approaches.

Cell type/treatment	Viral DNA	Transcripts
Non-treated LGLs		
IYJJ	+	Undetectable level of all transcripts
IYDY	+	Undetectable level of all transcripts
LFKJ	+	Low level ORF25, ORF63, ORFA4.5 and undetectable level of ORF50, ORF73, ORF A.9.5
LFLK	+	Low level of all transcripts
5-aza treated LGLs		
IYJJ	+	Very low level of ORF25 and ORF A4.5
IYDY	+	Undetectable level of all transcripts
LFKJ	+	Low level ORF25, ORF A4.5 and undetectable level of ORF73, OR50, ORF63, ORF A9.5
LFLK	+	Low level of all transcripts
infected only BT cells	+	High level of ORF50, ORF25, ORF A4.5 and low level of ORF73, ORF63
5-aza treated and infected BT cells	+	Low level of ORF50, ORF25, ORF A4.5 and undetectable level of ORF73, ORF63

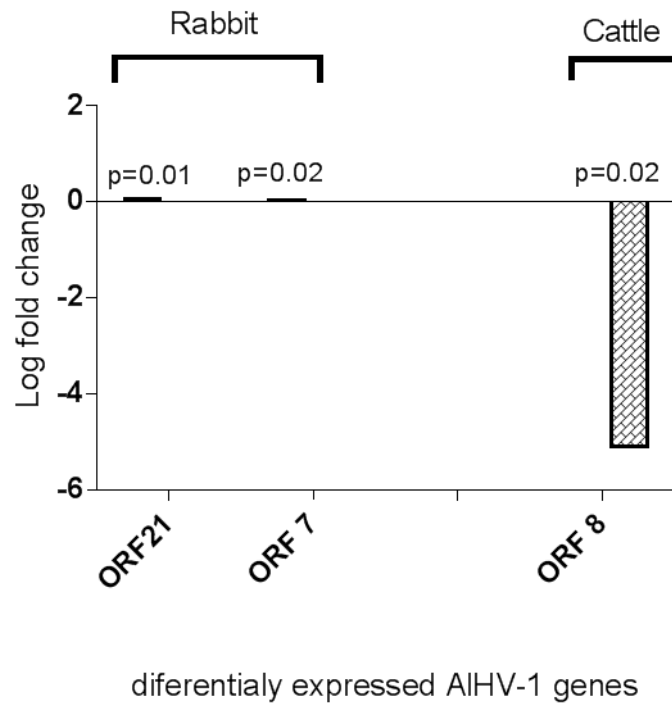


Figure 34 differentially expressed AIHV-1 virus in rabbits' LGLs and BT cells. The figure shows the differentially expressed genes (ORF 8) in bovine turbinate (BT) cells and ORF21 and ORF 7 in rabbits' LGLs in the presence of 5-azacitidine in comparison to infected control. The figure also shows that ORF 8 gene was down regulated (log FC) whereas ORF 7 and ORF 21 were up-regulated. The genes were significantly expressed with p value < 0.05.

5.4.6 David clustering

The human orthologue gene ID's lists for both rabbit and cattle were uploaded in David's software <http://david.ncifcrf.gov> in order to cluster the functionally annotated genes. The results showed that there were 93 and 100 clusters in rabbit and cattle species respectively (see the sections (8.2 and 8.3) in appendix). These were reduced to 15 and 11 clusters for both rabbit and cattle

respectively (see sections (8.7 and 8.9) in appendix) based upon the enrichment score by which the clusters trimmed. These clusters with enrichment score of ≥ 1 were kept for further analysis.

5.4.7 IPA results

Ingenuity pathway analysis (IPA) was performed on the data obtained from RNA sequencing analysis. For this it was necessary to generate one to one orthologues between our species (cattle and rabbit) and human using BioMart ensemble www.ensembl.org. The data obtained is placed in sections 8.6 and 8.7 in the appendix. The IPA system was used to investigate the differentially regulated pathways in the comparison between the treated (5-aza) and untreated cells (cattle or rabbit). The entire data sets were uploaded to the IPA software for global analysis. The top five significant canonical pathways affected in LGLs in the presence of 5-azacitidine in comparison to control LGLs were related to cell death and T cell activation (Table 23). The principal networks/pathways recognised contained those connected with: cell death and survival; cellular growth and proliferation; lymphoid tissue structure and development; lipid metabolism and the humoral immune response (Table 23). In general, genes within the pathways were down regulated in 5aza treated LGLs compared to untreated controls and the overall impact of this was possible induction of apoptosis and immune response genes. In addition, the top five significant canonical pathways affected in BT cells in the presence of 5-azacitidine in comparison to control BT cells were related to: mRNA translation and mitochondrion structure (Table 24). The most significant networks/pathways observed are those associated with

cell cycle, gene expression, DNA replication and cancer (Table 24). The balance of genes in the majority of affected pathways were down regulated in 5aza treated in BT cells compared to untreated controls and the overall affect was a decrease in transcription and translation.

Table 23 summary of ingenuity pathway analysis of rabbit LGLs in the presence of 5-azacitidine

Top Canonical Pathways		
	p-value	overlap
Ceramide Signalling	9.18E-05	8.8 % 7/80
Induction of Apoptosis by AIHV-1	1.40E-04	10.0 % 6/60
Death Receptor Signalling	2.21E-04	7.6 % 7/92
Tec Kinase Signalling	2.51E-04	5.7 % 9/157
NF-B Activation by Viruses	4.12E-04	8.2 % 6/73
Molecular and cellular functions		
	p-value	#Molecules
Cell Death and Survival	1.32E-02 - 9.08E-06	98
Cellular Function and Maintenance	1.32E-02 - 9.08E-06	49
Cellular Development	1.32E-02 - 1.34E-05	66
Cellular Growth and Proliferation	1.32E-02 - 1.34E-05	95
Lipid Metabolism	1.32E-02 - 3.65E-05	31
ID Associated Network Functions		Score
Antimicrobial Response, Cell Morphology, Cellular Assembly		51

and Organization	
Cancer, Organismal Injury and Abnormalities, Gastrointestinal Disease	41
Auditory and Vestibular System Development and Function, Cellular Development, Cellular Growth and Proliferation	35
Lymphoid Tissue Structure and Development, Organ Development, DNA Replication, Recombination, and Repair	33
Cell Death and Survival, Cancer, Organismal Injury and Abnormalities	30

IPA uses Fisher's Exact test to calculate p value

Table 24 summary of ingenuity pathway analysis of bovine turbinate (BT) cells in the presence of 5-azacitidine

Top Canonical Pathways		
	p-value	Overlap
Regulation of eIF4 and p70S6K Signaling	2.35E-04	6.8 % 10/146
EIF2 Signaling	1.43E-03	5.4 % 10/184
mTOR Signaling	1.61E-03	5.3 % 10/187
2-oxobutanoate Degradation I	2.89E-03	40.0 % 2/5
Oxidative Phosphorylation	2.89E-03	6.4 % 7/109

Molecular and Cellular Functions		
	p-value	#Molecules
Cellular Assembly and Organization	2.41E-02 - 2.67E-06	43
Gene Expression	1.73E-02 - 1.52E-04	62
RNA Damage and Repair	1.33E-02 - 1.52E-04	7
RNA Post-Transcriptional Modification	1.52E-04 - 1.52E-04	6
DNA Replication, Recombination, and Repair	2.24E-02 - 1.71E-04	35
ID Associated Network Functions		
		Score
Cancer, Organismal Injury and Abnormalities, Gastrointestinal Disease		53
Cancer, Organismal Injury and Abnormalities, Gastrointestinal Disease		41
Cell Cycle, DNA Replication, Recombination, and Repair, Gene Expression		36
Ophthalmic Disease, Organismal Injury and Abnormalities, Skeletal and Muscular Disorders		36
Cell Cycle, DNA Replication, Recombination, and Repair, Developmental Disorder		34

IPA uses Fisher's Exact test to calculate p value

5.5 Discussion

In this study the aim was to investigate the pathways affected by AIHV-1 in rabbit LGLs and cattle BT cells infected with AIHV-1 in the presence or absence of 5-azacitidine. The viral DNA copy number was used to identify the presence of AIHV-1 virus in LGLs samples. The RNA integrity number (RIN) results showed that all samples exhibited high quality RNA. This is important as the degradation of RNA can affect the gene expression level (Romero et al., 2014, Schroeder et al., 2006). The RNA sequencing analysis revealed that the mapping efficiency (the percentage of reads aligned to host genome or transcripts) was high (92% to 98%) indicating that high percentage of the RNA reads matched to rabbit and cattle transcripts (Benjamin et al., 2014, Mortazavi et al., 2008).

The pathway analysis indicated that cell death and T cell accumulation, proliferation and immune response pathways were augmented in 5-aza-treated LGLs in comparison to infected only control LGL suggesting that LGLs have selected genes involved in T cell activation, proliferation and apoptosis that are normally suppressed in infected untreated cells. This makes sense as the virus requires inhabiting the infected T cell without killing the cell or being removed by an activation process. From other published work (Swa et al., 2001) it is known that the infected LGLs do not exhibit significant apoptosis but do have a heightened activation state with respect to T cell cytotoxicity and constitutive activation of the T cell

receptor. Thus the RNA-Seq study is recording a net effect based on the genes differentially regulated by 5-aza, that may not affect other activation genes and pathways. This picture is also in agreement with observations made by other authors (Palmeira et al., 2013, Parameswaran et al., 2014, Russell et al., 2012) who found the similar pathways (in the *in vivo* study) from rabbit and cattle Lymph nodes infected with AIHV-1 and LGLs derived from rabbits infected with AIHV-1 virus. In addition, the results are in line with analysis of transcription profiles in lymph node tissues from OvHV-2 infected cattle (Meier-Trummer et al., 2009). As mentioned above the results showed that a number of genes involved in the various pathways were either up or down regulated in the presence of 5-aza in comparison to infected control, allowing a clue to overall function only when the activity of the particular genes is known. Among those genes were Bcl-2 family members, which can be either anti-apoptotic or pro-apoptotic (Czabotar et al., 2014, Tsujimoto, 1998). In this study, the overall effect of these changes was a net pro-apoptotic state in 5-aza-treated cells, but with no time course aspect to the analysis, it is difficult to see if there are any time related changes. However, the analysis was done when the LGLs were in a steady state of growth in IL-2 with a stable phenotype. The dysregulation of this gene family could also be under the effect of AIHV-1 ORF A4.5 or ORF A9 which has similarities to the Bcl-2 family (Hart et al., 2007, Mills et al., 2003). However, their role

whether they act as anti-apoptotic or cell death activator is yet unknown. The presence of the viral bcl-2 orthologues indicates that these are required in the virus life cycle. Importantly, the study only identifies changes associated with 5-aza treatment as both the control and treated cells were infected. Regarding the objective to this study it was hoped that the changes would represent those seen as part of a latent state induced by 5-aza. The impact of 5-azacitidine on the expression of OvHV-2 Ov4.5, the homologue of AIHV-1 A4.5, has been recorded where it increased in expression in cattle LGLs but not rabbit LGLs (Thonur et al., 2006). It is an advantage to the virus to escape the recognition by the immune system in order to survive and replicate within cells. Latency is the approach by which the virus can avoid the immune evasion by the expression of ORF73 LANA protein (Coscoy, 2007). 5-azacitidine is a nucleoside analogue which inhibits the methyltransferase enzyme and hence altering gene expression (Haaf, 1995, Jones, 1985). It was found that the drug can establish latency in LGLs from OvHV-2 infected rabbits (Thonur et al., 2006) but failed to control latency III in primary lymphoma cells infected with recombinant Epstein-Barr virus (Anastasiadou et al., 2005). Two genes (XIAP and TNFRSF1B) which are known as inhibitors of apoptosis (Morizane et al., 2005, Schall et al., 1990) were down regulated in the presence of 5-azacitidine indicating that the virus may affect these genes in order to alter cell survival. It was demonstrated that KSHV ORF73 LANA

was involved in tumour necrosis factor regulatory network which affects in the survival of latently infected cells (Si and Robertson, 2006, Uppal et al., 2014).

LGLs are known to be predominantly productive cycle programmed or latently programmed or have a mixture of both productive and latent virus cycles (Rosbottom et al., 2002, Thunor et al., 2006). The analysis demonstrated that many host genes involved in the various pathways; in particular cell death and cell cycle, acting as both cell death inhibitors and activators, were either up or down regulated in the presence of 5-aza compared to non-treated controls. In addition, two viral genes (ORF7 and ORF21), where their role in the life cycle and the pathogenesis of MCF is unknown, were up-regulated in the presence of 5-aza-treated group in comparison to non-treated controls. Moreover, the viral gene profiles from the previous chapter indicated that the expression of ORF73 and ORF50 supporting latent and productive virus cycle were very low (Table 22). Taking these observations together, one could extrapolate that it is not obvious that the cells support either productive or latent virus cycle or both.

The pathway analysis in treated BT cells versus infected controls is likely to identify productive cycle versus latency cycle changes better than in LGLs as the effect of 5-aza on infected BT cells was more profound (induction of a latency phenotype with respect to lack of CPE and reduction of productive cycle gene transcripts).

Overall, genes involved in mitochondrion integrity, mRNA translation, regulator of gene expression, cell cycle and DNA replication, post transcriptional modification and genes known to be associated with neoplasia were down regulated in 5-aza treated infected BT cells compared to untreated BT cells. These effects are compatible with the fact that the virus replicates in these cells and establishes a productive/lytic infection and may reveal the latency programme in the transcriptome of the cells treated with 5-aza. The results also showed that ORF8 gene was differentially expressed, being down regulated in the presence of 5-azacitidine in BT cells compared to non-treated control indicating that the virus may affect the expression of this gene. ORF8 is a glycoprotein required for viral entry to the host cell (Dry et al., 2016) and is also expressed during productive infection (Palmeira et al., 2013). This is therefore predicted as BT cells support productive virus infection (Dry et al., 2008, Dry et al., 2016, Parameswaran et al., 2014). However, upon treatment with 5-azacitidine, ORF 73 was not highly expressed (Table 22) even though BT cells did not show any CPE. The explanation of this is that the expression of ORF73 may not, in isolation, be diagnostic of the latent state (i.e. an increase in expression rather than expression per se). 5-azacitidine is a hypomethylation agent (Christman, 2002) which may have not completely removed ORF50 gene in BT cells meaning that ORF50 may have repressed the expression of ORF 73 gene. Recombinant

murine Gama herpesvirus (MHV-68) was engineered to overexpress RTA, transcriptional and replication activator encoded by ORF50 of Gama herpesviruses, was found to inhibit the expression of ORF73 gene and induce lytic virus cycle (Hair et al., 2007). The approach one could think of to address the expression of ORF73 in BT cells therefore is to completely remove ORF 50, the productive gene, by knockout gene technique.

The work study revealed that there were differences between the gene expression profiles between 5-aza treated and non-treated cells and also between rabbit LGLs and cattle BT cells, which reflects the different types of cell under study.

Chapter 6

The effect of Cyclosporine-A on T cell recruitment, viral gene expression and disease pathogenesis in infected rabbits

6.1 Abstract

The mechanism by which MCF viruses (AIHV-1 and OvHV-2) cause the disease is not fully understood. The tissue damage seen in the affected tissues is attributed to the accumulation of T lymphocytes. However, it is not well established whether the damage is due to the direct effect of infiltrated T lymphocytes (infected or bystander non-infected) or due to the effect of small number of infected non T cells or both. Cyclosporine A drug, in rabbits infected with OvHV-2 prevented lymphocyte accumulation but not overt MCF (Buxton et al., 1984). This is a key observation and the basis of the aims of this thesis. Rabbits were infected with AIHV-1 and treated with cyclosporine A. Unfortunately; the rabbits reacted badly to the CsA and infection such that they had to be euthanized before full onset of MCF. However, these animals showed some pathological changes and these data were analysed. In a subsequent trial to examine the pathogenesis of MCF in rabbits infected only with AIHV-1, results were again inadequate due to the early termination of the experiment as the animals reacted unexpectedly to infection. The viral transcript profile analysis revealed that the productive/lytic genes were expressed at low level in the infected only group indicating the virus may replicate at this stage of the disease.

6.2 Introduction

There has been a controversy for long time over the mechanism by which MCF viruses (AIHV-1 and OvHV-2) cause the disease (Buxton et al., 1984, Dewals et al., 2011, Palmeira et al., 2013, Schock et al., 1998). The core of this debate has been over the issue whether the tissue damage is due to dysregulated immune response or direct viral impact, and whether the disease is one of viral latency or not (Palmeira et al., 2013). Rabbits are a good model for MCF because they exhibit clinical signs and pathological changes similar to those seen in susceptible species (Anderson et al., 2007, Cunha et al., 2013). Treating rabbits infected with OvHV-2 with cyclosporine A, an immunosuppressive drug, eliminated the lymphocytes infiltrating the infected tissues but did not prevent disease development (Buxton et al., 1984). There is a scarcity of the virus in the infected tissues (Bridgen et al., 1992, Thonur et al., 2006) making analysis difficult. The phenotype and cytokine profile of the lymphoblastoid cells infiltrating the infected tissues represent unregulated cytotoxic cells (Schock et al., 1998, Swa et al., 2001). Nonetheless, growing evidence demonstrates that lymphocytes accumulating in MCF-affected tissues are infected with the virus and the virus establishes latency in them (Palmeira et al., 2013, Simon et al., 2003). Furthermore, the cells are cytotoxic and secrete cytokines and proteins that are responsible for the tissue damage seen (Dewals et al., 2008, Dewals et al., 2011, Palmeira et al., 2013). I aim to treat

AIHV-1 infected rabbits with CsA to examine the role of T lymphocytes in the pathogenesis of AIHV-1 MCF and to study the gene expression using known productive/lytic and latent viral transcripts in rabbits during MCF disease course. Cyclosporine acts by inhibiting calcineurin which is responsible for triggering a significant signal transduction pathway of T cell activation. The outcome of this action is a reduction in T cell maturation (Matsuda and Koyasu, 2000, Mott et al., 2004). We hoped to see whether ablation of T cells would alter the course of MCF and whether there was an associated change or not in gene transcription profiles. For this, q PCR and *in situ* hybridisation techniques will be used.

6.3 Materials and methods

6.3.1 Animals

See the materials and methods chapter section (2.6).

6.3.2 Inoculum

As described in the materials and methods chapter section (2.6.1).

6.3.3 Experimental design

As described in the materials and methods chapter sections (2.6.2) and (2.6.3).

6.3.6 Molecular techniques

The molecular approaches as described in materials and methods chapter. Quantitative R-T PCR was used to measure both viral load and gene expression in the infected tissues as described in materials and methods sections (2.4.3) and (2.4.4).

6.3.4 Samples collection

As described in the materials and methods chapter section (2.6.4).

6.3.5 Histology

See the materials and methods chapter section (2.7).

6.3.7 *In situ* Hybridization

The *in situ* hybridisation method used as described in materials and methods sections (2.8.1) to (2.8.5).

6.4 Results

6.4.1 Experiment (1) results

10 rabbits split into two groups of 6 to get CsA and infection and 4 to get infection only with vehicle IV rather than CsA (See table 25). Two rabbits were culled from CsA treated group (IYTU and IYDI) without collecting samples from them as they died suddenly (see below). Tissue samples were collected from the remaining animals in both CsA treated group (4 animals, day 12) and infected only group (4 animals, day 17).

6.4.1.1 Clinical signs

None of the rabbits injected with cyclosporine A and infected with ALHV-1 developed clinical signs until around day 10 of the experiment two rabbits died from the CsA treated group (IYTU and IYDI) after exhibiting fever, weight loss, and conjunctivitis (Table 25). They then died suddenly overnight. In the control group (infected with the virus along with vehicle), one of the rabbits developed a diarrhoea with high temperature that reached 41.2C° on day 17 of the experiment. Nearly all of the rabbits in this group exhibited high temperature, in-appetence, lethargy and conjunctivitis just prior to euthanasia. No other clinical findings were recorded on the rabbits up to the seventeenth day of the experiment when all rabbits were euthanized.

Table 25 shows the design of two rabbit's experiments infected and treated with cyclosporine A as long as pathological changes

Exp # (1)	Clinical signs/euthanasia	Pathological changes
4 rabbits infected + CsA	Started on day 10 (2 animals). Animals developed fever, conjunctivitis, apathy, weight loss. Remainder euthanized due to severe reaction to CsA on day 12.	Small numbers white foci on the kidney, intestines, liver and spleen. Lung haemorrhage in both IYBM and IYKA.
4 rabbits infected only	On day 15 animals developed fever, conjunctivitis, apathy and weight loss and were euthanized on day 17 of the experiment.	Multiple white foci on the kidney, liver, lung, enlarged lymph nodes and enlarged spleen. Some micro-haemorrhage in the intestines and lung.
Exp #(2)	Clinical signs/euthanasia	Pathological changes
4 rabbits infected + CsA	Adverse reaction to CsA seen days 9-10. Fever, apathy, and rapid demise. Animals euthanized on day 10	Slight lung haemorrhage, slight lymph nodes enlargement and small numbers of white foci on the liver and kidney.
4 rabbits infected not treated.	Day 9 animals exhibited fever and weight loss. Animals euthanized on day 10 of the experiment.	Enlarged spleen, white foci on the liver, haemorrhage in the intestines and lung.
2 rabbits, uninfected controls	No clinical signs seen. Animals euthanized on day 10.	No pathological changes seen.

6.4.1.2 Gross appearance of MCF lesions

In the cyclosporine A treated group there were some small white foci on the kidney, liver, intestines and spleen along with haemorrhage in the lung of the rabbit IYBM as well as haemorrhagic lung and red eyes in the rabbit IYKA (Table 25). In the infected control group, the lesions were diverse affecting many body systems and more pronounced in three rabbits (LFKJ, LFLK, and IYDY) ranging from multiple white foci on the kidneys, liver, and lung, enlarged lymph nodes (in particular popliteal lymph nodes) and slight enlargement in mesenteric lymph nodes (MLN), congested intestines, enlarged and dark spleen, and dark and enlarged urinary bladder (Table 25).

6.4.1.3 Viral DNA load measurement

Viral DNA load was identified in both blood and lymph nodes of three animals from each group (Figure 35). In the tissues (Liver, kidney, lung, spleen and appendix), the viral load was detected in the infected control group confirming infection. The viral copy number was below the detection level in the cyclosporine A treated group in these tissues (Figure 36).

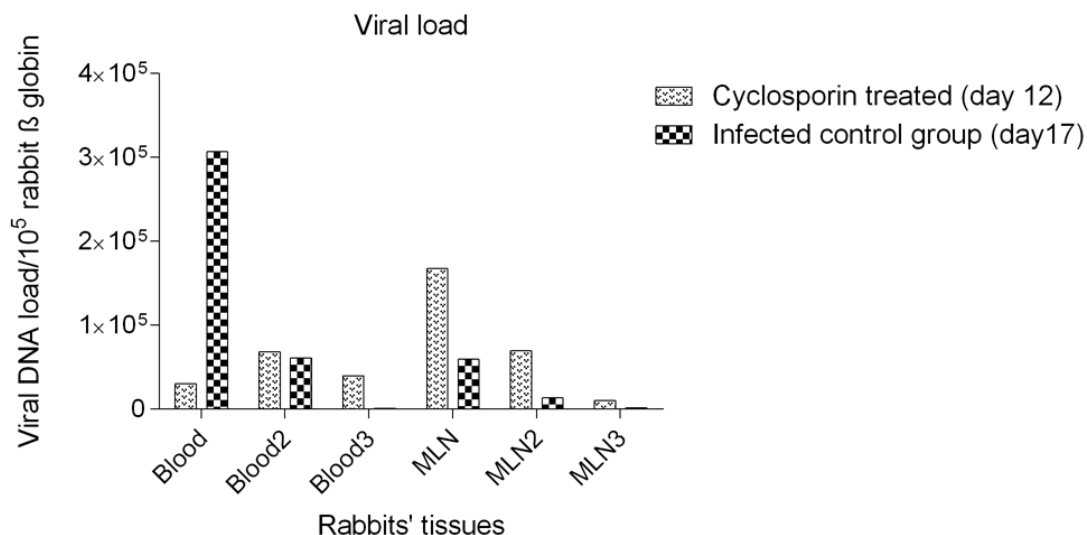


Figure 35 viral DNA load in lymph nodes and blood from rabbits tissues infected and treated with cyclosporine and infected only control animals. The figure shows viral DNA load in the blood and lymph nodes from rabbits infected with AIHV-1. Samples were collected on day 12 and 17 of the experiment. The viral load was estimated by normalizing the viral DNA per 10⁵ rabbit β globin using q PCR.

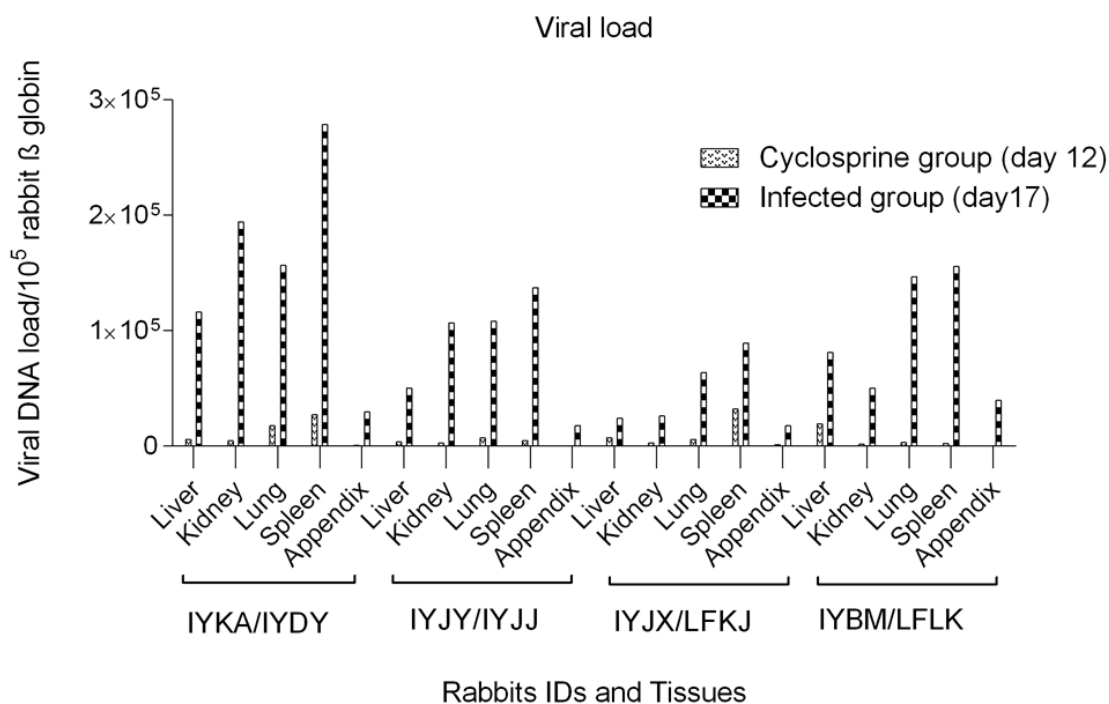


Figure 36 viral DNA load in rabbits' tissues infected and treated with cyclosporine A and infected only controls.

The figure demonstrates viral DNA load in rabbit tissues infected with AIHV-1 virus. Samples were collected on day 12 and 17 of the experiment. The viral load was estimated by normalizing the viral DNA copy number to 10^5 rabbit β globin gene copies using q PCR.

6.4.1.4 Histological analysis of AIHV-1 in rabbits

The major histological findings in regard to MCF lesions in rabbits in both groups (infected control and infected plus cyclosporine A treated) are summarised in Table 26. The non-lymphoid tissues in the control group (Liver, kidney, and lung) illustrated marked lymphocyte infiltration (accumulation of lymphoid cells) especially around the blood vessels, which showed evidence of vasculitis. In addition, there has been marked hyperplasia in the lymphoid follicles in the lymphoid tissues (appendix and spleen). In the cyclosporine A treated group there was not any change in either lymphoid or non-lymphoid tissues.

Table 26 cyclosporine A experiment: AIHV-1 MCF histology on lymphoid and non-lymphoid tissues.

Exp (1)	Exp (2)	Lymphoid Tissues				Non-lymphoid Tissues					
		Hyperplasia/Necrosis ¹				Lymphoid cell accumulation ²					
animal	animal	Appendix		spleen		Kidney		Liver		lung	
Infected only	Infected only										
LFKJ	JYDR	+/0	0/0	+/0	0/0	++	0	++	+	++	0
LFLK	JYBU	+/0	0/0	+/0	0/0	++	0	+	+	++	0
IYJJ	JYFC	+/0	0/0	+/0	0/0	++	0	++	+	++	0
IYDY	JYJE	+/0	0/0	+/0	0/0	++	0	+	-	++	0
CsA+infection	CsA+infection										
IYKA	JYIS	-/-	-/-	-/-	-/-	0	0	0	0	0	0
IYBM	JXXS	-/-	-/-	-/-	-/-	0	0	0	0	0	0
IYJY	JXTS	-/-	-/-	-/-	-/-	0	0	0	0	0	0

IYJX	JXJJ	-/-	-/-	-/-	-/-	0	0	0	0	0	0
IYTU (Culled)											
IYDI (Culled)											
Uninfected control	Uninfected control										
C1	JXXL	0	0	0	0	0	0	0	0	0	0
C2	JXXR	0	0	0	0	0	0	0	0	0	0

Lymphoid tissues: + = change present, 0 = change not present (hyperplasia = increased lymphoid cell accumulation /proliferation compared to the controls).

²Non- lymphoid tissues: Interstitial and perivascular lymphoid cell accumulations. ++ = marked accumulation, + = moderate accumulation, 0 = no accumulation. There was evidence of vasculitis (vascular endothelium thickening) in the infected control animal tissues. The rabbits were not marked in the table are those which were thrown away without samples being collected.

Kidney: there was perivascular lymphocyte infiltration in the cortex in the kidneys of the control group while in the cyclosporine A (CsA) treated group there was not any evidence of infiltration around the blood vessels (Figure 37).

Liver: in the infected control group there was an obvious perivascular lymphoid accumulation in the periportal area whereas there was no infiltration in the cyclosporine A treated group (Figure 38).

Lung: no lymphocyte accumulation seen in the lungs from the cyclosporine A group, however, there was a clear lymphocyte infiltration in the peri-bronchial region as well as disperse infiltration throughout the parenchyma (Figure 39).

Kidney

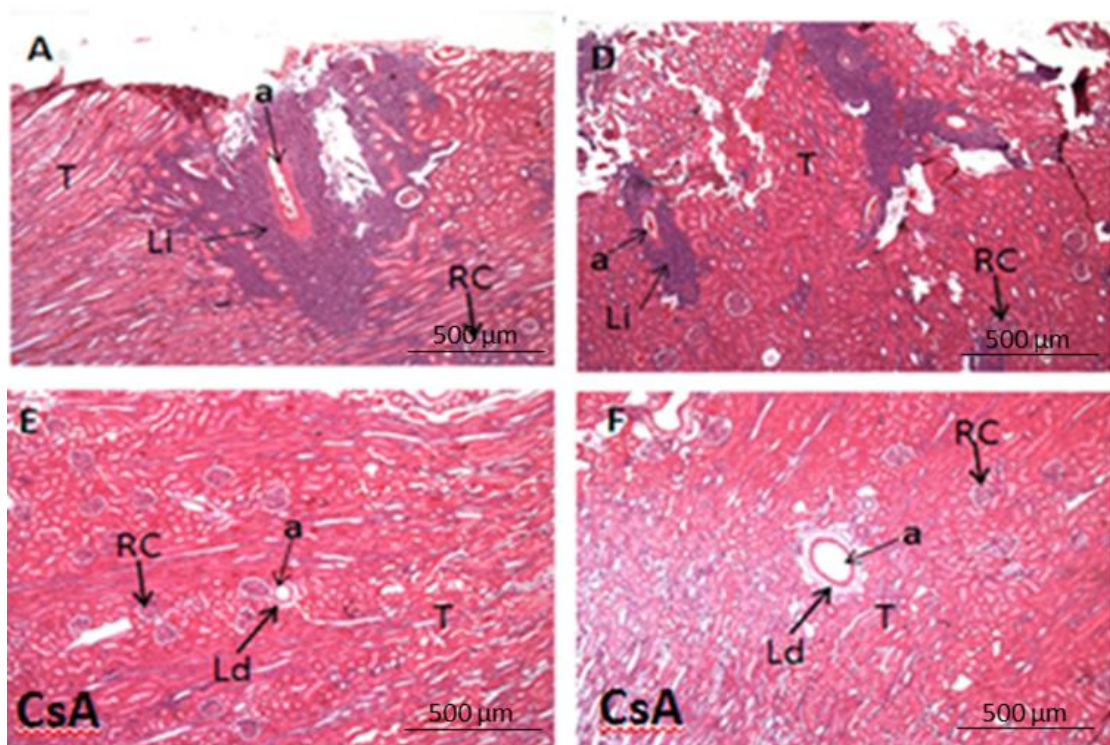


Figure 37 haematoxylin and eosin stain of rabbits' kidney

The images show the formalin fixed, haematoxylin and eosin stained histological sections of rabbits' kidney (A, D, E, and F). Slides A and D show typical histological lesions of MCF after infection with AIHV-1 C500 strain. The most obvious appearance in these slides is the infiltration of lymphocytes around the blood vessels in the cortex area. Slides (E and F) are from the rabbits infected with AIHV-1 C500 strain and treated with cyclosporine A. There is an absence of lymphocyte infiltration. (a) Blood vessel, (Li) lymphocyte infiltration, (Ld) No evidence of lymphocyte accumulation, (RC) renal corpuscle, (T) uriniferous tubules. Pictures represent scale bar of 500 μm .

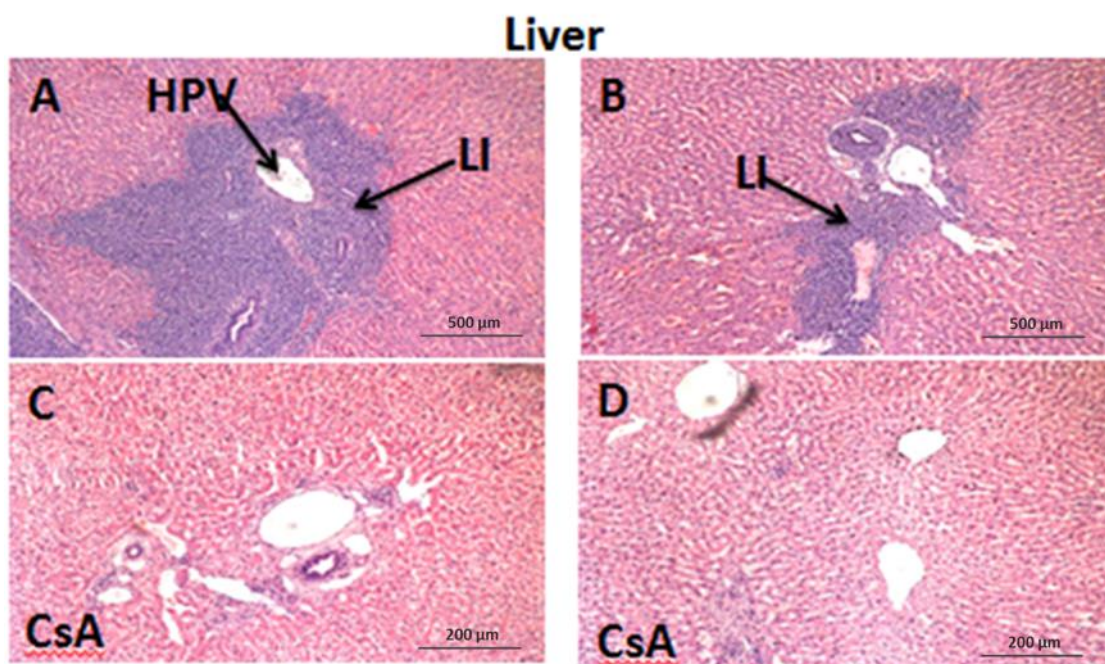


Figure 38 haematoxylin and eosin stain of rabbit's liver

The images depict the Formalin fixed, haematoxylin and eosin stained histological sections of rabbits' liver (A, B, C, D). There is obvious lymphoid infiltration around the blood vessels in the periportal area in the infected tissues only with AIHV-1 C500 strain virus (slide A and B) whereas no infiltration in the tissues infected with the same virus and treated with cyclosporine A drug (slides C and D). CsA: cyclosporine A treated group, LI: lymphoid infiltration, HPV: hepatic portal vein. Pictures A and B represent scale bar of 500 μm whereas pictures C and D represent 200 μm .

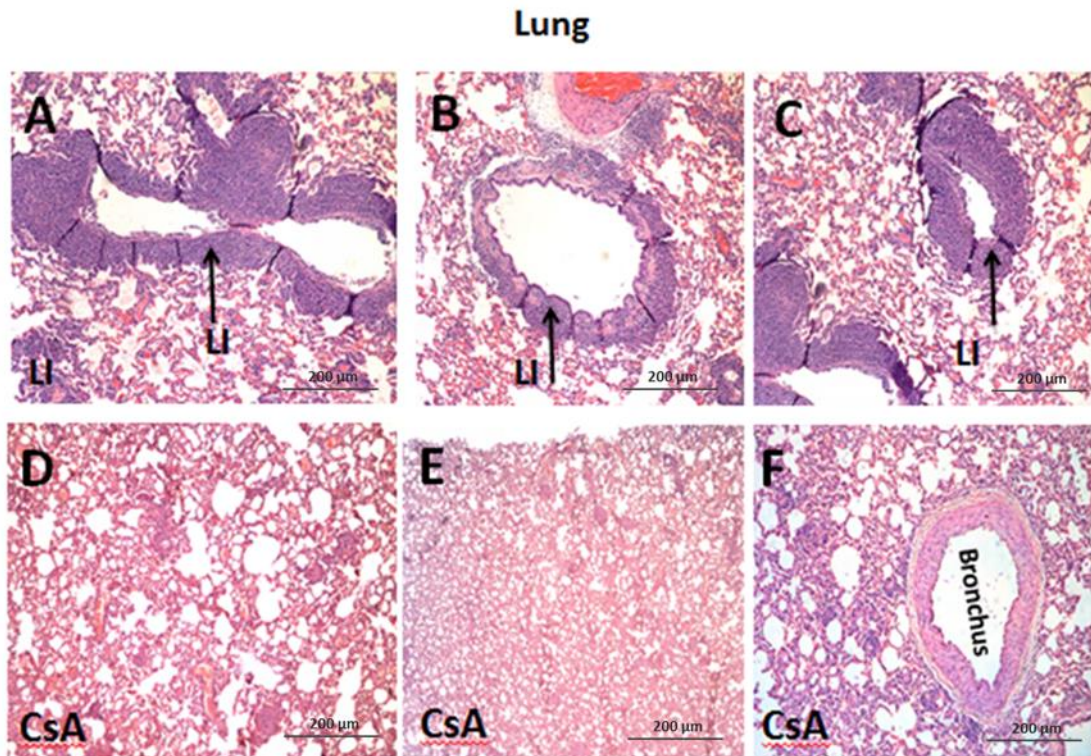


Figure 39 haematoxylin and eosin stain of rabbit's lung

The images depict the Formalin fixed, haematoxylin and eosin stained histological sections of rabbits' lung (A, B, C, D, E, F). There is obvious evidence of peribronchial lymphoid infiltration as well as dispersed lymphocyte infiltration throughout the parenchyma slides (A, B, C) in the tissues infected only with AIHV-1 C500 strain virus. No lymphocyte infiltration in the tissues infected with AIHV-1 C500 strain virus and treated with cyclosporine A drug slides (D, E, F). LI: lymphocyte infiltration. Pictures represent scale bar of 200 µm.

Appendix: there was an obvious expansion of the lymphatic nodules, absence of the inter-follicular space, haemorrhage in the blood vessels, and loss of the tissue architecture in the infected control group. No apparent changes in the cyclosporine A treated group (Figure 40).

Spleen: there were no remarkable changes in the tissues from the cyclosporine A treated group. However, there was hyperplasia in the

white bulb nodules, intensive scattered lymphocyte infiltration, and loss of architecture in the infected control group (Figure 41).

Appendix

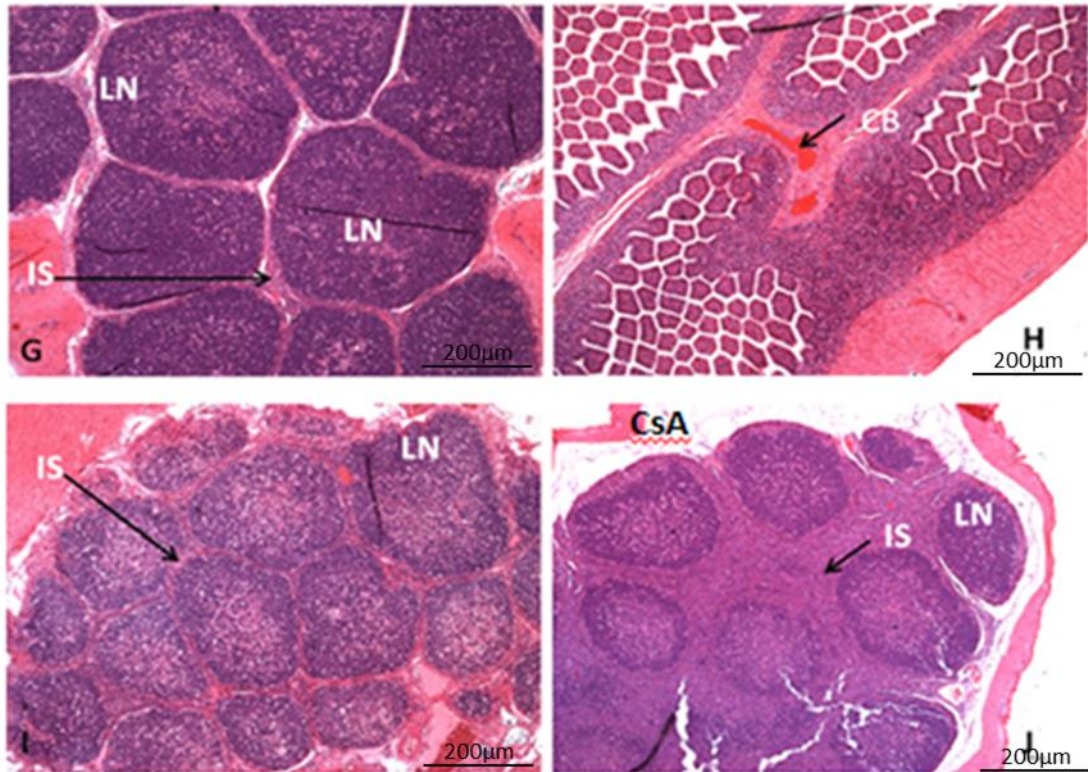


Figure 40 haematoxylin and eosin stain of rabbit's appendix
The images show the formalin fixed, haematoxylin and eosin stained histological sections of rabbit's appendix (G, H, I, and J). Slides G, H, and I are from rabbits infected with AIHV-1 virus without treatment with CsA. Slides illustrate expansion of follicles, relative absence of inter-follicular space, loss of tissue architecture as well as congested blood vessels. Slide J is from CsA treated group where the appearance is more normal. LN, lymphatic nodule; IS, inter-follicular space; CB, congested blood vessel. Pictures represent scale bar of 200 µm.

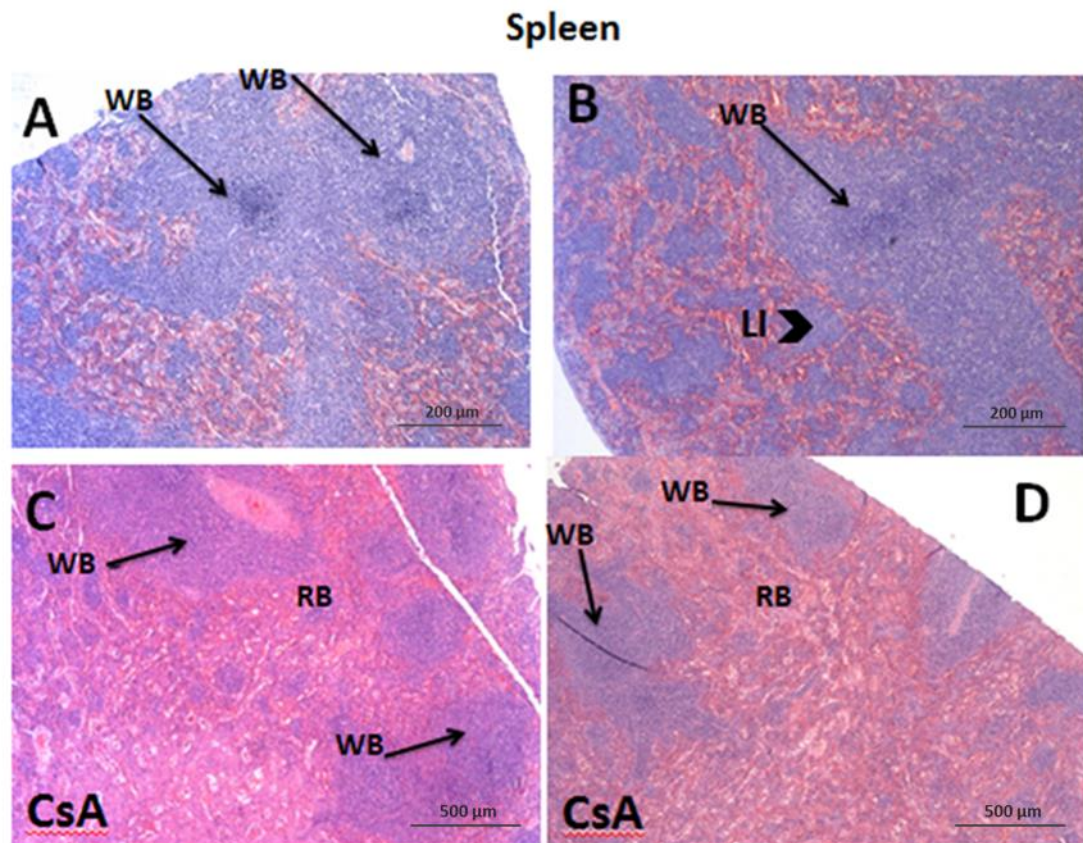


Figure 41 haematoxylin and eosin stain of rabbit's spleen

The images show the Formalin fixed, haematoxylin and eosin stained histological sections of rabbit's spleen (A, B, C, D). There was apparent hyperplasia in the white bulb (black arrow) as well as intensive dispersing of lymphoid cells throughout the tissue (arrow head) in the tissue infected only with AIHV-1 C500 strain virus slide (A and B). No clear and remarkable changes in the cyclosporine A treated group (C and D). CsA: cyclosporine A treated group, WB: white bulb, RB: red bulb, LI: lymphocyte infiltration. Pictures A and B represent scale bar of 200 µm whereas pictures C and D represent scale bar of 500 µm.

6.4.1.5 Gene expression

Gene expression in the infected tissues was measured by normalising viral target genes with rabbit SDHA1 reference gene using q PCR. The results showed that the gene expression of viral target genes was higher in infected controls than cyclosporine A treated group. Also, the pattern of expression was similar in nearly

all genes tested with highest values in spleen, lung, and kidney. ORF A4.5 recorded the highest gene expression in tissues of infected animals and in the spleen of the cyclosporine A treated group. The expression of ORF25, ORF50, and ORF63 was similar in the tissues of infected animals. The expression of ORF73 was lower than the other genes whereas ORF A9.5 was the lowest. Figure 42 shows the gene expression of 6 viral genes putatively responsible for productive/lytic and latent virus infection in rabbit tissues.

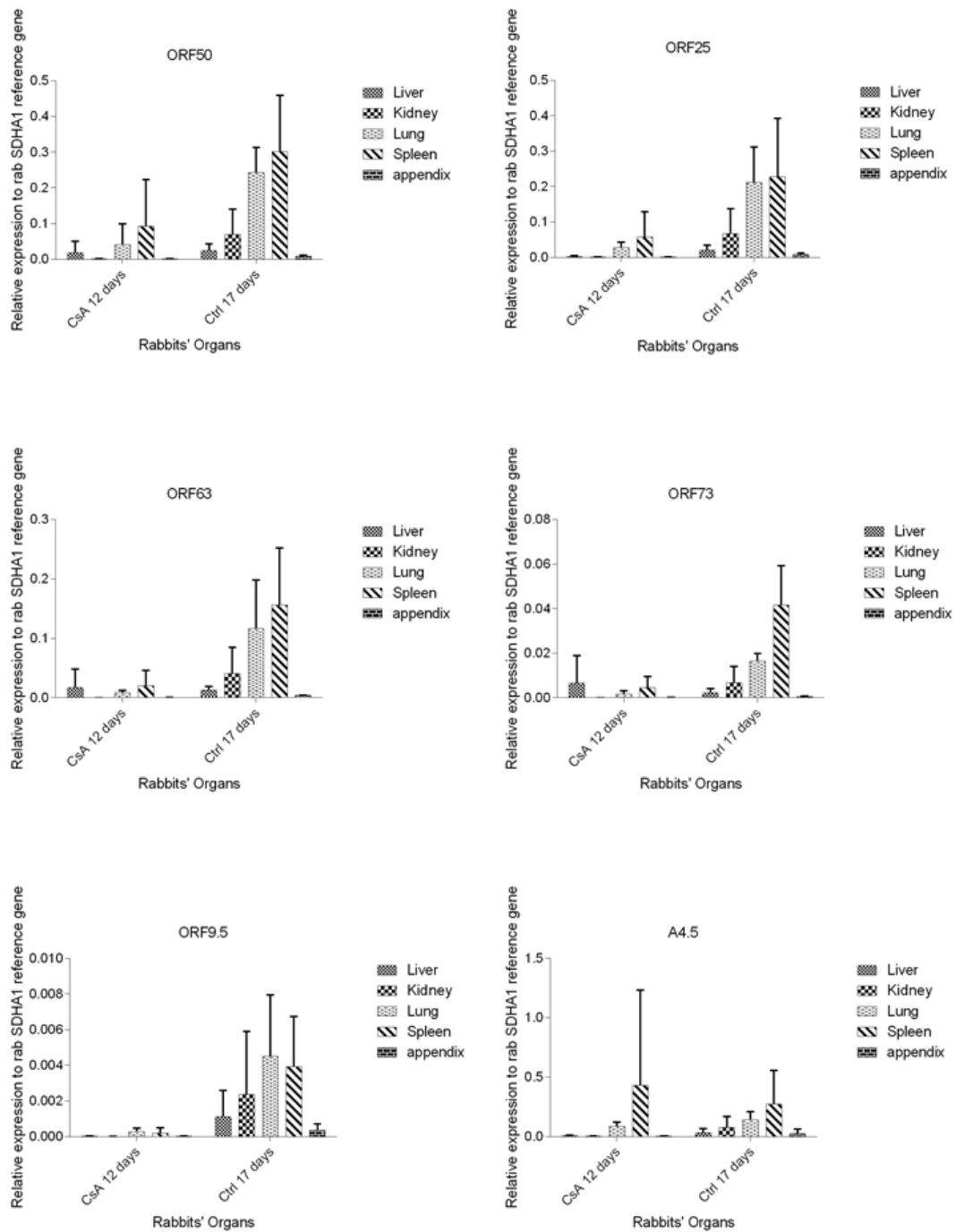


Figure 42 viral transcripts of six AIHV-1 genes in rabbits' tissues

The figure shows viral gene expression of six AIHV-1 genes (ORF50, ORF25, ORF63, ORF73, ORF9.5, and A4.5) in five rabbits' tissues (liver, kidney, lung, spleen, and appendix) from infected only and infected and treated with cyclosporine A groups euthanized on day 12 (CsA group) and 17 of the experiment. The transcripts were measured using qPCR and normalised with rabbit SDHA1 reference gene. CsA 12 day; cyclosporine A treated group euthanized on day 12 of the experiment, Ctrl 17 days; infected control group euthanized on day 17 of the experiment.

6.4.1.6 *In situ* Hybridisation

No results were obtained from the *in situ* hybridisation work despite the fact that synthesis of RNA probe for ORF65 and ORF A9.5 genes was unsuccessful.

6.4.2 Experiment (2) results

The clinical signs associated with MCF in the infected cyclosporine A treated group were fever, apathy, and rapid demise. At this time two CsA-treated rabbits showed a rapid decline with fever, respiratory distress and apathy, and were euthanized for humane reasons. In the infected control group number of animals developed fever, weight loss, enlarged spleen, white foci on the liver and haemorrhage in the intestines and lung. In the negative control group there were no clinical signs and pathological changes seen. All animals were euthanized on day 10.

In terms of the histological changes, the only changes were seen in the liver from infected group in form of small perivascular lymphocyte infiltration in the periportal area whereas there was no lymphoid infiltration in infected cyclosporine A treated group animals or the uninfected control group (Figure 43)

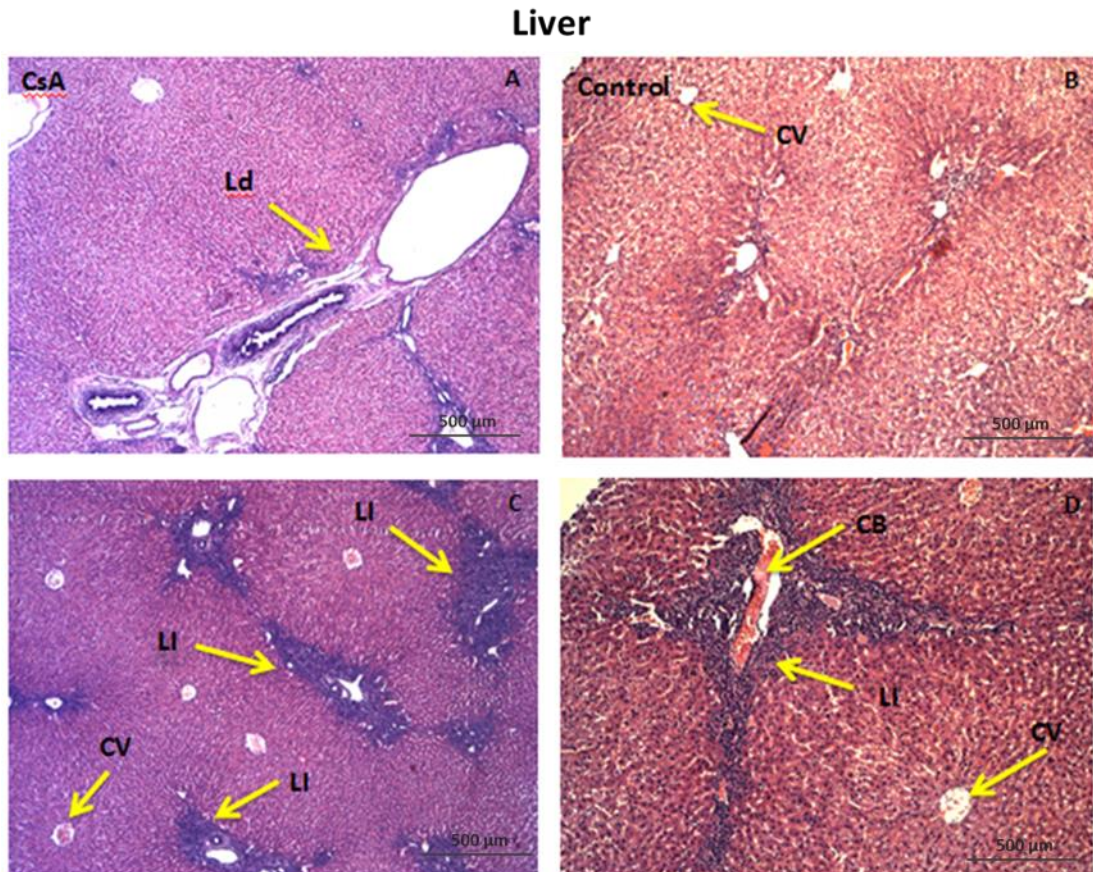


Figure 43 haematoxylin and eosin stain in rabbit's liver (1)

The figure illustrates formalin fixed, haematoxylin and eosin stained liver (A, B, C, D). There is obvious lymphoid infiltration around the blood vessels in the periportal area in the infected only group tissues (slides C and D) whereas no infiltration was seen in the tissues of the infected and CsA-treated animals (slide A) or the uninfected control (slide B). CsA: cyclosporine A treated group, LI: lymphoid infiltration, CV: central vein, CB: congested blood vessel, LD: infiltration disappearance. Pictures represent scale bar of 500 µm.

The viral DNA load data revealed that this was under detectable level in most animals' tissues except some liver and kidney samples from the CsA+infection group, the viral load was more than 3×10^6 in one of the kidneys (rabbit JXTS). There was no change recorded in the uninfected control group (Figure 44).

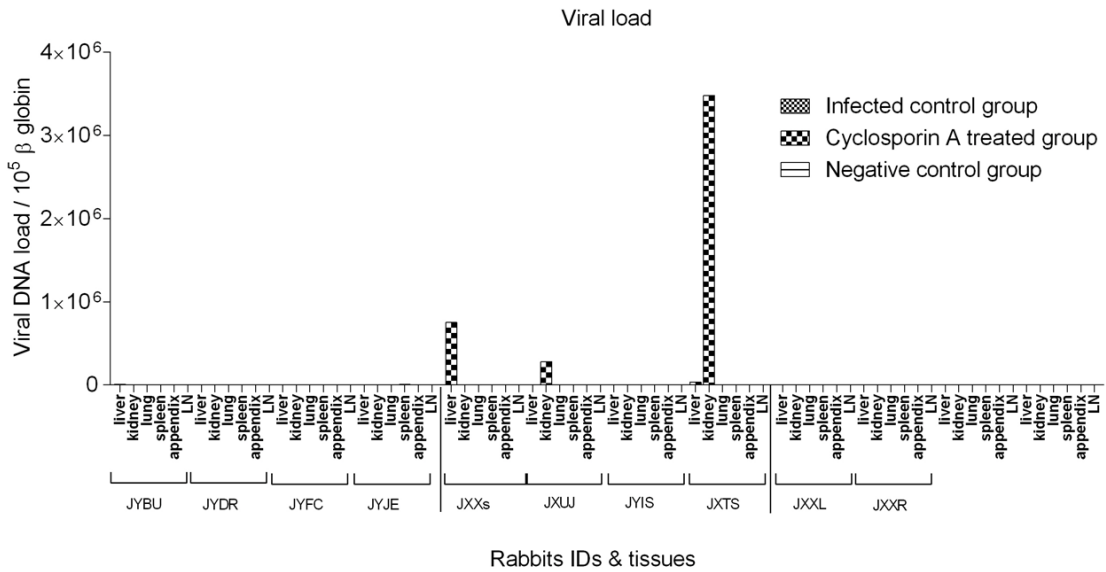


Figure 44 viral DNA load in tissues in infected only and infected and treated with cyclosporine A group animals (1)

The figure demonstrates the viral DNA load in infected tissues and from samples collected on day 10 of the experiment. Infected control group; rabbits infected only with the virus, Cyclosporine A treated group; rabbits infected with the virus and treated with cyclosporine A uninfected control group; non-infected and non-treated rabbits. The viral DNA load was calculated by normalizing the viral DNA per 105 rabbit β globin gene copy number using quantitative PCR.

No results were obtained from the gene expression experiment in any sample.

6.5 Discussion

Two *in vivo* experiments were carried out in order to investigate the role of CsA on MCF induction, and whether it would prevent T cell accumulation as shown previously (Buxton et al., 1984). The clinical signs and pathological changes observed in both experiments were typical for MCF in the control infected groups and consistent with other observations (Anderson et al., 2007, Dewals et al., 2008, Jacoby et al., 1988). There was a severe reaction to CsA in some animals necessitating the euthanasia of the entire group in each case. Thus, throughout this series of experiments the CsA-treated animal tissues examined represented an early stage of MCF and the infection only controls were not time matched to this in experiment 1.

Consequently, in terms of the histological findings, typical MCF-associated changes were seen in the infected only groups in all the tissues collected which is in agreement with previous observations (Anderson et al., 2007, Buxton et al., 1984, Palmeira et al., 2013). In the cyclosporine A treated group, however, the lymphocytes did not accumulate around the blood vessels. This is also in agreement with results recorded by Buxton et al. (1984) with OvHV-2 infection, but this is an early time in infection before control infection only animals got MCF and this most likely explains the result.

Similarly, possibly due to early euthanasia, it was noticed that the viral DNA load in the tissues of the control infection group was

considerably higher than the cyclosporine A treated group and in general although in some of the cyclosporine A animals viral DNA load was high in blood and MLN. However, detectable levels of MCF viral DNA (AIHV-1 and OvHV-2) can be identified as early as five days in the tissues and blood of infected animals (Cunha et al., 2012, Dewals et al., 2008, Taus et al., 2005).

All studied viral genes were expressed at low level in both groups and were higher in infected control groups than cyclosporine A treated group. Again this is due to the early death of the animals before MCF fully developed. The gene expression patterns were typical of AIHV-1 MCF with ORF73 (encoding latency associated nuclear antigen (LANA)) expressed at a lower level than most of the others. ORF A9.5 which encodes a secreted glycoprotein that is similar to IL-4 (Lankester et al., 2015, Russell et al., 2013) was expressed at very low level in the infected group. The role of this gene in the virus life cycle is still unknown.

It was hoped to perform *in situ* hybridisation to localise viral genes to tissues and cells *in vivo*. Much time was spent developing the technique. Although synthesis of RNA probes was achieved, there were no convincing results obtained from the *in situ* analysis of infected tissues. Time was not available to troubleshoot the technique further. *In situ* hybridisation is a powerful technique which is used to detect cellular location of certain genes representing latent or lytic cycle (Jin and Lloyd, 1997, Malarkey and

Maronpot, 1996, Nouri-Aria, 2008). This means that the viral mRNA copy numbers may have been below the *in situ* hybridisation threshold (Simon et al., 2003). The approach necessitates the presence of around 10-20 mRNA copy numbers in a single cell to make the signal detectable (Jin and Lloyd, 1997).

The second CsA experiment was terminated on the tenth day due to an adverse reaction to CsA once again in spite of changing the vehicle used to dissolve the drug. Consequently, there were no results obtained as MCF did not develop. We surmise that in both experiments the CsA may have not been fully dissolved and formed micro-precipitates causing vascular obstruction/damage. Buxton et al. (1984) injected rabbits with cyclosporine A intramuscularly which may delay the drug diffusion, hence its effect on the animals' tissues and the disease course. However, I applied intravenous route where the drug absorption time is fast.

Chapter 7

General discussion

7.1 General discussion

Although the pathological changes of MCF such as vasculitis, lymphocyte infiltration and tissue necrosis are well characterised, the pathogenesis of the disease is still not completely understood (Parameswaran et al., 2014, Russell et al., 2012). The tissue damage seen in MCF-affected tissues, especially epithelium and endothelium could be due to the infiltration and activity of cytotoxic T cells (either containing the virus or dysregulated non-infected cells) or virus infection of epithelium and endothelium or a mixture of both.

The main hypothesis of this project work was that malignant catarrhal fever is initiated by aberrant virus gene expression in infected T cells, epithelium and endothelium. Whether the disease was predominantly one of latency (as has been suggested (Palmeira et al., 2013, Dewals et al., 2008)) or productive virus infection still remains controversial. The first aim was to determine whether epithelium and endothelium can be infected *in vitro* using q PCR and, if so whether a latent or productive viral cycle is established. Rabbit epithelial (SRIC) cells, Bovine aortic endothelial (BAE) cells and bovine turbinate fibroblast (BT) cells (productive virus control) were infected with both low pass (virulent) and high (attenuated) AIHV-1. It was clear that both cell-types can be infected with either form of AIHV-1 as shown by the presence of viral DNA and the ability to transfer infection to uninfected fresh cells where, in BT

cells, a productive infection was detected. If these cells represent epithelial cells and endothelial cells *in vivo* then it is possible that these cell types can contain virus. Interestingly, a lack of CPE in the SIRC and BAE cells indicated a lack of productive viral life cycle, raising the possibility that the cells are latently infected. The viral gene transcription analysis of these cells did not confirm a latency pattern, but levels of transcripts were very low and there was no gene transcription pattern typically seen in productively-infected BT cells. The ability of virus isolated from the SIRC and BAE cells to induce a productive infection in BT cells (as measured by a CPE) strongly suggests the virus was latent in the SIRC and BAE cells. It is also possible that the low viral transcripts were due to the fact that the virus could not enter or penetrate the cells. Consequently, the effect in the serial infection may have been the result of transfer of virus direct from the supernatant or that was attached to the surface of the first cells, and not virus that had "infected" the first cells.

The question remains why ORF73 gene (the LANA equivalent latency-associated transcript) was not expressed in epithelium and endothelium in the *in vitro* model if the latent state was established. One explanation is that viral DNA load in the cells is present but transcript abundance is below detectable level. Another, explanation more speculative and less likely is that there might be biological factors in the *in vivo* system not available in the *in vitro* paradigm to

make the virus express ORF73 gene and hence establish true latency. One of these is a lack of immune cells in the *in vitro* system which may be important to establish latency to escape the detection by the immune system (Blake, 2010). Finally, an important point when studying latency in MCF, is that this will have evolved in the host reservoir species (wildebeest for AIHV-1) and not the disease-susceptible species, where the virus cannot transmit between animals (at least that we know of). Consequently, the virus life cycles may be altered or corrupted in some way in the MCF susceptible species cells, a possibility explored by Thonur et al., in studying cycles in LGLs from reservoir (sheep) and MCF susceptible animals in OvHV-2 MCF. A study of wildebeest cells infected with AIHV-1 was beyond the scope of this project.

So, what is in BT vs SIRC and BAE that causes the productive virus cycle to switch on. The RNA-Seq analysis of infected BT cells and LGLs with and without 5-aza did not reveal any obvious answer to this, at least from the host transcriptome analyses. There was not enough resource to do transcriptome analyses on infected SIRC or BAE cells versus infected BT cells to address this directly.

Large granular lymphocytes (LGLs), with T/natural killer cells morphology that are infected with AIHV-1 (Schock et al., 1998, Swa et al., 2001), were obtained from the infected rabbits and were treated with 5-azacitidine, a drug used to drive latency in gamma herpes viruses (Schaefer et al., 1997, Thonur et al., 2006). Bovine

turbinate fibroblast (BT) cells were infected with AIHV-1 and infected and treated with 5-azacitidine as productive cycle virus controls. The notion was to see if 5-aza could inhibit the productive cycle and establish a latent state and allow identification of latency-associated transcripts for AIHV-1. All infected cells treated or not were shown to have viral DNA using q PCR and PCR analysis indicating that the cells were infected with the virus. The most noticeable effect was in the infected BT cells where 5-aza treatment inhibited a CPE and this was associated with a marked reduction in gene transcripts associated with the productive viral life cycle (ORF50 and ORF25 and ORF A4.5 and low level expression of ORF 73 the latency-associated transcript). This confirms that 5-aza drives a latency-like state in AIHV-1-infected cells as it does with OvHV-2 infected cells (Thonur et al., 2006). The results for LGLs were less clear. 5-aza treatment caused a dramatic effect on the pan T antigen (uncharacterised to date) recognised by a monoclonal antibody, but although there was some evidence of changes in viral productive and latent gene expression this was at low level, near detection limits and not consistent between the LGL lines. It is known that the A2 gene of AIHV-1 is a leucine zipper transcriptional regulator that has multiple functions on gene regulation in rabbits infected with an A2 gene knock-out virus or wild-type /gene reinsertion controls (Parameswaran et al., 2014). One of these effects is to alter the T cell receptor phenotype, downregulating alpha-beta TCR and

augmenting the gamma-delta TCR. It is known that there is a gd T cell subset that expresses CD8 (the predominant T cell marker detectable on the LGLs), found particularly at mucosal sites (Nelson et al., 2010, Wilson et al., 2002, Davis et al., 1996).

Unfortunately, there is no gd T cell-specific antibody for the rabbit to test this theory out. Furthermore, the gd T cells lack the CD3 molecule that is a pan T cell marker (Owens et al., 2015).

Although the effect seen in this study is due to 5-aza treatment, it may be that this or the associated drive to a latent state may have stimulated this phenotypic change in the T cells and that A2 may be active in this way during latency. All of this speculation is open to further research. In contrast possibly, the impact of 5-azacitidine on (uninfected) human T cells especially CD4 and CD8 T cells has been documented. It was established that 5-azacitidine treatment of human T cells decreased CD8⁺ T cells whereas CD4⁺ T cells were augmented (Stübig et al., 2014). CD8⁺ T cells were the prevalent cell type after flow cytometry analysis of rabbit LGLs in both 5-azacitidine and non-treated groups. The results are compatible with the observations made by other researchers who found that CD8⁺ T cells were the main cell type in LGLs and infected tissues *in vivo* (Dewals et al., 2008, Dewals et al., 2011). Also, there was a lack of CD4⁺ T cells in both groups. Anderson et al. (2007) also observed the reduction in CD4⁺ T cells in MCF affected tissues. The target cell

in the T cell lineage for virus infection in MCF is unknown (Parameswaran et al., 2014).

The global transcriptome analysis by RNAseq on the 5-aza-treated and control infected LGLs and BT cells did not reveal an answer to the above speculation. However, the genes differentially expressed in 5-aza-treated versus untreated infected BT cells showed a pattern consistent with changes in mRNA translation, mitochondrion integrity, regulation of gene expression, cell cycle control, DNA replication, post transcriptional modification and in genes associated with neoplasia (see gene lists and pathway analyses in chapter 5). This is consistent with the fact that these changes are fully active in the untreated BT controls indicating productive/lytic virus cycle.

In LGLs, the effect of 5-aza treatment was less clear on viral gene transcripts and the host transcriptome when compared to untreated cells. Viral transcript profiles showed that there was low expression of ORF50, ORF25, ORF63 and ORF73 in LGLs in two cell lines (LFLK and LFKJ) and no evidence of expression in two others. This could be because the level of viral transcripts is low to start with, which is the most likely explanation, or that a latency state was in these cells. A Gardella gel analysis of viral genome configuration was not performed due to a lack of time left in the study. This would reveal whether the LGLs had closed circular DNA (latent configuration, tight band on the gel) or linear DNA (lytic cycle configuration, smear on the gel). In the Thonur et al., (2006) analysis of rabbit LGLs

infected with OvHV-2, a mixed latent and lytic configuration was seen. After 5-azacitidine treatment there was a rise in ORF73 expression in one cell line (LFLK) compared to the infected control but ORF50 was also detected. This is consistent with 5-azacitidine driving latency via increased ORF73 expression and was also seen in LGL infected with OvHV-2 virus and treated with 5-azacitidine (Thonur et al., 2006). It is worth mentioning that ORF73 can be 'leaky' with respect to expression in the different virus life cycles such that complete absence of ORF73 in productive infection is not usually recorded (Thonur et al., 2006). The expression of ORF50 confirms that the cells support at least productive infection and its transcript may be abundant. There was an increase in ORF A4.5 in one cell line due to 5-azacitidine. Thonur et al. (2006) found an increase in OvHV-2 Ov4.5 in cattle LGLs but not rabbit LGLs treated with 5-aza. The reason for the difference in this study is not known, but may be due to some difference between AIHV-1 and OvHv-2. The expression of ORF73 may not, in isolation, be diagnostic of the latent state (i.e. an increase in expression rather than expression per se). 5-azacitidine is a hypo-methylation agent (Christman, 2002) which may have not completely removed ORF50 gene in BT cells meaning that ORF50 may have blocked the expression of ORF 73 gene. The suppression of ORF73 gene and the induction of lytic virus cycle had been observed when ORF50 overexpressed using an

engineered recombinant murine Gama herpesvirus (MHV-68) (Hair et al., 2007).

The pathway analysis showed that cell death and T cell accumulation, proliferation and immune response pathways were increased in 5-azacitidine treated LGLs compared to infected-only control LGL indicating that LGLs have genes associated in immunological, cell death and proliferation processes. The pathways present in the untreated LGLs are similar to those in lymphoid tissues from MCF-affected cattle or rabbits (Palmeira et al., 2013, Paramiswaran et al., 2014, Russell et al., 2012). This indicates that the LGLs are an accurate representation of the host changes *in vivo*. The result also shows that 5-aza affects the above pathways (increased in treated versus untreated LGLs). This may be as a consequence of inducing a latent viral state, but there could also be some productive cycle activity as well as the results on this were not clear. It will be of interest in future work to determine if this is as a consequence of forcing the latent state for the virus and that these changes are at least in part stimulated by the latent gene expression programme or a lack of productive cycle gene expression. These pathways do not fit with classical latency, where inducing cell death in particular is not a good strategy for the virus. But, the viral gene expression may not be typical (i.e. is aberrant) in MCF-susceptible species. This all requires further research.

Importantly, although the pathway analysis identified several pathways affected by 5-aza-treated LGLs compared to untreated cells, the contribution of up and down regulated genes within these pathways can only really be assessed for a net overall effect if the precise functions of the genes are known in the context of the LGLs. For the apoptosis (cell death) pathway, this is possible as the function of many of the genes is known and conserved in animals. For example, there are both cell death inhibitors (BNIP1 and BNIP2) and activators (BAX and BNIP3) that were differentially expressed in the presence of 5-aza compared to non-treated controls. The overall effect is a tendency towards increased cell death in the 5-aza-treated LGLs compared to control cells.

In the final set of experiments, it was hoped that the Buxton et al., 1984 study on the effect of CsA on OvHV-2-infected rabbits could be repeated for AIHV-1-infected ones. This is because the CsA prevented the accumulation of T cells in the tissues, but did not prevent MCF. This key paper was the main reason for the hypothesis and objectives of this thesis, namely that if the accumulating T cells (that we now know are infected with virus) are not present to cause epithelial and endothelial damage /tissue damage in MCF, what other possible mechanisms can cause disease? That is why we looked at infecting epithelial cells and endothelial cells in chapter 1.

Unfortunately, the rabbits reacted badly to IV CsA and had to be euthanized early in the development of MCF (around 10-12 days over two experiments). Changing the formulation for CsA delivery did not help (experiment 2). In the Buxton paper, the formulation was given intramuscularly, which may have avoided the problems experienced in this study. Nonetheless, the pathological changes and clinical signs seen in infected only rabbits represented early stages of MCF. These observations are compatible with results observed by other authors (Anderson et al., 2007, Jacoby et al., 1988, Liggitt and DeMartini, 1980a, Liggitt and DeMartini, 1980b).

There was not any accumulation of lymphocytes in the tissues of the cyclosporine A treated group in the non-lymphoid tissues. This was probably due to the early demise of the animals. However, and interestingly, in the control infected animals in experiment two (euthanased on day 10 after infection and therefore at a similar time to the CsA-treated animals) lymphoid accumulations were seen, mainly around blood vessels (e.g figure 43). So some effect on lymphocyte accumulation by the CsA treatment is implied. Also interestingly, in the CsA-teredated animals but not the infected controls, high levels of viral DNA were seen in kidney and liver samples in some animals. These could be sites of virus replication at this time in the presence of CsA.

The viral transcript profiles in the experiments revealed that the level of gene expression was low but higher in the infected control

group than cyclosporine A treated group. This may have been due to the early finish of the experiment and also due to the variable viral copy number between the two groups as it was higher in the infected control than the cyclosporine A group. In addition, the results showed that the pattern of expression in the infected only animals was similar. Most of the genes especially those supporting productive/lytic virus cycles were expressed in the lung and spleen of the infected animals as seen in experiment 1 (Figure 42). The expression of ORF50, ORF25, ORF63 and ORF A4.5 and the low expression of ORF73 gene indicating that the virus may replicate and not tend to establish latency at this stage of the disease.

The other main objective of this series of experiments was to use *in situ* hybridisation to localise putative productive virus cycle or latency cycle gene transcripts to particular cells in various tissues. This was to determine whether MCF was associated with predominantly latent viral gene expression or a productive cycle one, comparing animals with and without T cell accumulation (CsA-treatment).

Unfortunately, no results were obtained as time ran out to perform a comprehensive study. ORF 65 (productive cycle gene) and ORF A9.5 (secreted IL-4 orthologue) riboprobes were made and the technique developed and validated (with help from Dashty Amin and James Stewart in Liverpool). First attempts to detect the transcripts in the tissues of the infected animals were unsuccessful. *In situ*

hybridisation is a powerful approach which is utilized to localize certain genes signifying latent or lytic cycle along with the detection of cellular cytokine mRNA during viral infection (Anderson et al., 2008, Anderson et al., 2001, Bridgen et al., 1992). It was documented that for potential detection of certain transcripts the approach requires the existence of approximately 10-20 mRNA copy numbers in a single cell to make the signal measurable (Jin and Lloyd, 1997). This may explain the inability to detect the transcripts in the affected tissues as viral mRNA copy numbers may have been below the *in situ* hybridisation threshold (Simon et al., 2003).

7.1.1 Conclusion and recommendations

The results of the *in vitro* epithelial and endothelial cell cultures indicate that the cells can be infected and establish a latent state, indicating that this is also possible *in vivo*, which should be looked at when studying MCF pathogenesis. The identification of proven latency transcripts by using 5-aza treatment on BTs and LGLs was unsuccessful, and more viral genes should be measured or other means as stimulating latency explored. The effect of 5-aza/ possible latency-associated expression the pan T antigen in LGLs is interesting and deserves further research. The transcriptome analyses in the infected and treated BTs and LGLs revealed several changes that may help future work to focus in on latency and productive infections *in vivo*. Moreover, the use of Gardella gel

analysis would have been useful in analysing the DNA configuration and hence the virus life cycle. The development of the *in situ* hybridisation work using productive virus cycle and latency gene riboprobes should proceed and the technique is partially developed here.

The conclusion from this study using q PCR is that MCF in rabbits involves virus expressing both productive and putative latency transcripts. This raises some doubts that MCF is a disease of latency. Gene expression may be 'aberrant' but more work is required.

Two papers are in preparation from this work. The first is on the *in vitro* analyses of more BT samples and LGLs with 5-aza, and also the use of phosphonoacetic acid as a treatment to induce latency. This has worked more efficiently on BT cells and LGLs than 5-aza treatment and was used by Abbie Jones, a student in D Haig lab. The second will be on the *in vitro* infection of endothelial and epithelial cells after some further analyses and increased sensitivity and extended range gene transcription analyses by q PCR. A work to address the role of ORF A9, a second bcl-2-like gene in AIHV-1 (along with A4.5) in the pathogenesis of MCF is ongoing by a graduate student.

7.1.2 Project summary

The research work was carried out to investigate the virus life cycle and the pathogenesis of malignant catarrhal fever (MCF). Rabbits, which are good model for MCF, were infected with alcelphine herpesvirus 1 (ALHV-1) and treated with cyclosporine A to suppress the accumulation of lymphocytes in the infected tissues. Large granular lymphocytes (LGLs) with the morphology of T/natural killer cells derived from the infected only rabbits were treated with 5-azacitidine in order to drive the latency programme in them. RNA-Seq was performed on the cells RNA (as copy DNA) samples to identify virus latency transcripts and the host transcriptome in latently-infected cells. Epithelial (SIRC) and endothelial (BAE) cells were infected with the virus *in vitro* to identify whether the cells can be infected and if so what kind of infection can be established (latent or productive/lytic). The results obtained can be summarised as following:

- The *in vitro* epithelium and endothelium cell culture showed that the cells can be latently infected with the virus and this may be possible *in vivo*.
- The identification of latency transcripts on LGLs and BT cells using 5-azacitidine was unsuccessful.
- The flow cytometry analysis of LGLs showed that CD8⁺ T cells was the predominant cell subset in both 5-aza treated and

non-treated LGLs and the percentage of Pan-T cells were higher 5-aza treated LGLs.

- The pathway analysis of LGLs and BT cells showed that there were variations between rabbit LGLs and cattle BT cells. LGLs have pathways supporting T cell proliferation and accumulation and immune responsiveness in 5-aza-treated groups compared to untreated ones, BT cells contain pathways that aid gene expression and mRNA translation in treated groups compared to untreated.
- The viral genes profile from the infected rabbits euthanized at early stage of the disease showed a mixture of both latent and productive virus cycle.
- Unfortunately, no results obtained from the *in situ* hybridisation work.

Appendices

8.1 SOLUTIONS

Use distilled water to make up solutions, then autoclave solution. When using distilled water within the protocol, use autoclaved distilled water.

8.1.1 DEPC water

(ddH₂O, diethylepyrocarbonate-treated)

1 ml DEPC (Fluka, 32490) add 1000 ml ddH₂O

Dissolve overnight on magnetic stirrer. Autoclave at 0.4 atm, 120°C, 20 min. Care: This solution is regarded as carcinogenic!

8.1.2 ddH₂O

Autoclave ddH₂O without DEPC (like all other solutions) at 0.4 atm, 120°C, 20 min.

8.1.3 TrisHCl

(MW 121.14): 1 M, pH 8.0

12.11g Tris(hydroxymethyl)aminomethane (Fluka, 93352) in 100 ml ddH₂O

Adjust pH with concentrated HCl.

8.1.4 CaCl₂

(MW 147.02) for proteinase K: 0.1 M

1.47 g CaCl₂ (Merck, 102382) in 100 ml ddH₂O

8.1.5 MgCl₂-hexahydrate

(MW 203.3) for PBS: 5mM MgCl₂

1 M: 20.33 g MgCl₂-hexahydrate (Merck, 105833) in 100 ml ddH₂O

8.1.6 NaCl

(MW 58,44; Merck, 1.06400.5000)

For hybridisation salts: 5 M = 29.22 g/100 ml ddH₂O

For RNase treatment: 3 M = 87.66 g/500 ml ddH₂O

8.1.7 0.2 M HCl (Sterilize prior to use; not 2 N HCl)

50 ml 2 N HCl (Merck, 1.09970. Titrisol®)

450 ml ddH₂O

8.1.8 PIPES

(Piperazin-N,N'-bis(2-ethanesulfate-acid)), pH 7,0 (MW 346.3;

Sigma, P3768)

For hybridisation salts: 0.5 M = 1.7315 g/10 ml ddH₂O (sterile preparation!)

8.1.9 10x PBS

(Phosphate buffered saline), 1x PBS:

Dilute some 10 x PBS 1:10 to 1x PBS (in ddH₂O without DEPC) and adjust the pH to 7.4 with 1M HCl or 1M NaCl.

8.1.10 Buffer 1, pH 7,5

Tris (MW 121,14) 12.11 g Tris (final concentration 100 mM)

NaCl (MW 58,44) 8.77 g NaCl (final concentration 100 mM)

add 1000 ml ddH₂O (without DEPC).

Adjust pH with concentrated HCl.

8.1.11 Buffer 3, pH 9.5

Prepare fresh! To 150ml ddH₂O without DEPC add;

Tris (MW 121,14) 2.422 g (3.633g) Tris (final concentration
100 mM)

NaCl (MW 58,44) 1.168 g (1.752g) NaCl (final concentration
100 mM)

Adjust pH to 9.5, then add

MgCl₂ + 6H₂O (MW 203,3) 2.034 g (3.051g) MgCl₂ (final
concentration 50 mM)

Make volume to 200 ml (300ml) with ddH₂O (without DEPC).

8.1.12 Buffer 4, pH 8.0

Tris (MW 121,14) 1.21 g Tris (final concentration 10 mM)

EDTA (MW 372,3) 0.37 g EDTA (final
concentration 1 mM; Serva, 11280.01)

add 1000 ml ddH₂O (without DEPC). Adjust pH with 2 N HCl.

8.1.13 1x PBS + 5 mM MgCl₂

10x PBS 10 ml

1 M MgCl₂ 0.5 ml

add 100 ml ddH₂O (without DEPC)

8.1.14 2x SSC + 5 mM EDTA-Na₂

20x SSC 50 ml

0.5 M EDTA-Na₂ 5 ml

add 500 ml ddH₂O (without DEPC)

8.1.15 0.2% Glycine in 1x PBS

1 g glycine

500 ml 1x PBS (adjust pH before!)

8.1.16 4% paraformaldehyde (PFA)

For 250 ml:

Dissolve 10 g paraformaldehyde in approx. 200 ml 1x PBS at approx. 60°C (on magnetic stirrer; do not increase the temperature above 70°C, as the solution will precipitate!); adjust pH to 7.35 – 7.4. Fill with 1x PBS to 250 ml. Solution can be stored for up to one month. N.B.: poisonous fumes so do this in hood. Takes about 2 hours.

8.1.20 50x TAE Electrophoresis Buffer

Tris free base 242 g

Disodium EDTA 18.61 g

Glacial Acetic Acid 57.1 ml

DDI H₂O to 1 l

Add the Tris free base and EDTA to approximately 700 ml DDI H₂O and stir until the Tris and EDTA are dissolved. Add the acetic acid and adjust the volume to 1 liter.

8.1.21 1x TAE Electrophoresis Buffer

The 1x TAE solution is 40mM Tris, 20mM Acetate and 1mM EDTA and typically has a pH around 8.6

(do not adjust).

Or add 480 ml DDI H₂O to 20 ml 50x TAE solution.

Hybridisation mix (HB-Mix):

100% formamide, deion. 16 ml

20x hybridisation salts 8 ml

50x Denhardts solution 3.2 ml

Heparin 400 µl (Heparin (20,000 U), diluted in 1 ml ddH₂O)

10% Triton X-100 320 µl

27.84 ml = 40 aliquots a 696 µl; store at -20°C.

8.1.22 ssDNA

Dissolve ssDNA (Deoxyribonucleic acid (DNA) Sodium Salt Type XIV from Salmon sperm; Sigma, D6898, 250 mg) in **buffer 4**, pH 8.0 to a final concentration of 10 mg/ml.

8.1.23 Proteinase K solution:

Is supplied by company (diluted in 10 mM TrisHCl, pH 7.5 (15.6 mg/ml); Roche Diagnostics, 1413783).

8.1.24 Dextransulfate solution

250mg dextransulfate + 400µl ddH₂O with DEPC; pipette into Eppendorf tube, mix well and dissolve by placing eppendorf in boiling waterbath; **takes time!**

8.1.25 RNA stock solution

10 mg RNA (Sigma, R 7250)

1 ml ddH₂O (DEPC-treated)

Need 1.3ml per run (for steps V and VI); keep on ice

8.1.26 Dye solution

Nitrobluetetrazoliumchloride (NBT):

Sigma, Order No. N 6639

1 g NBT add 13.3 ml 70% dimethylformamide (DMF: = 30 ml Aqua ddH₂O + 70 ml DMF) = Stock solution with 75 mg/ml final concentration

5-bromo-4-chloro-3-indolyephosphate (X-phosphate, BCIP)

Sigma, Order.No. B6777

500 mg X-Phosphate add 10 ml 100% dimethylformamide (syock solution)

The solutions are prepared in their original container. N.B.: toxic.



DAVID Bioinformatics Resources 6.7
National Institute of Allergy and Infectious Diseases (NIAID), NIH

2/29/2016 DAVID Database for Annotation, Visualization and Integrated Discovery (Laboratory of Immunopathogenesis and Bioinformatics (LB), National Inst...

Functional Annotation Clustering

Current Gene List: List_2

Current Background: Homo sapiens

288 DAVID IDs

Options Classification Stringency Medium ▾

Re-run using options Create Sublist

[Help and Manual](#)

93 Cluster(s)

Annotation Cluster	Enrichment Score	Count	P-Value	Benjamini
Annotation Cluster1	2.18	38	1.5E-3	3.3E-1
GOTERM_CC_FAT	nuclear lumen	44	1.7E-3	2.0E-1
GOTERM_CC_FAT	intracellular organelle lumen	44	2.7E-3	2.1E-1
GOTERM_CC_FAT	organelle lumen	44	3.8E-3	2.3E-1
GOTERM_CC_FAT	membrane-enclosed lumen	21	5.5E-2	6.4E-1
GOTERM_CC_FAT	nucleoplasm	17	7.6E-2	6.9E-1
GOTERM_CC_FAT	nucleolus	8	2.3E-1	9.6E-1
Annotation Cluster2	1.89	6	3.4E-4	2.6E-2
SP_PRL_KEYWORDS	Fatty acid biosynthesis	8	4.9E-4	2.9E-2
SP_PRL_KEYWORDS	lipid synthesis	6	7.2E-3	4.7E-1
GOTERM_BP_FAT	fatty acid biosynthetic process	7	3.2E-2	7.9E-1
GOTERM_BP_FAT	organic acid biosynthetic process	7	3.2E-2	7.9E-1
GOTERM_BP_FAT	carboxylic acid biosynthetic process	6	1.9E-1	9.5E-1
GOTERM_BP_FAT	fatty acid metabolic process	8	2.3E-1	9.6E-1
GOTERM_BP_FAT	lipid biosynthetic process	8	2.3E-1	9.6E-1
Annotation Cluster3	1.88	19	7.8E-4	6.7E-1
GOTERM_BP_FAT	DNA metabolic process	15	1.8E-3	4.0E-1
GOTERM_BP_FAT	response to DNA damage stimulus	12	4.4E-3	4.3E-1
GOTERM_BP_FAT	DNA repair	18	6.2E-3	4.7E-1
SP_PRL_KEYWORDS	cellular response to stress	8	2.0E-2	2.7E-1
SP_PRL_KEYWORDS	dna repair	8	2.7E-2	3.2E-1
SP_PRL_KEYWORDS	dna damage	3	9.7E-2	6.0E-1
SP_PRL_KEYWORDS	dna recombination	3	4.8E-1	9.9E-1
GOTERM_BP_FAT	DNA metabolic process	19	7.8E-4	6.7E-1
GOTERM_BP_FAT	response to DNA damage stimulus	12	4.4E-3	4.3E-1
GOTERM_BP_FAT	DNA repair	18	6.2E-3	4.7E-1
SP_PRL_KEYWORDS	cellular response to stress	8	2.0E-2	2.7E-1
SP_PRL_KEYWORDS	dna repair	8	2.7E-2	3.2E-1
SP_PRL_KEYWORDS	dna damage	3	9.7E-2	6.0E-1
SP_PRL_KEYWORDS	dna recombination	3	4.8E-1	9.9E-1
Annotation Cluster4	1.84	25	8.2E-4	3.1E-2
GOTERM_BP_FAT	mitochondrion	28	9.6E-3	3.1E-1
GOTERM_BP_FAT	mitochondrion	12	7.3E-2	1.0E0
UP_SFCO_FEATURE	transit peptide:mitochondrion	12	7.8E-2	5.3E-1
SP_PRL_KEYWORDS	transit peptide	Count	P-Value	Benjamini
Annotation Cluster5	1.82	8	6.1E-3	1.4E-1
SP_PRL_KEYWORDS	maturation	8	6.9E-3	6.2E-1
GOTERM_MF_FAT	metal ion-binding site:Manganese	3	8.0E-2	1.0E0
UP_SFCO_FEATURE	metal ion-binding site:Manganese	3	8.0E-2	1.0E0
Annotation Cluster6	1.82	16	3.8E-4	2.3E-2
SP_PRL_KEYWORDS	apoptosis	21	1.1E-3	5.9E-1
GOTERM_BP_FAT	apoptotic cell death	23	1.5E-3	5.1E-1
GOTERM_BP_FAT	cell death	23	1.7E-3	4.4E-1
GOTERM_BP_FAT	death	20	2.3E-3	3.7E-1
GOTERM_BP_FAT	apoptosis	20	3.9E-2	7.9E-1
GOTERM_BP_FAT	resolution of apoptosis	20	4.3E-2	7.9E-1
GOTERM_BP_FAT	resolution of apoptotic cell death	20	4.4E-2	7.7E-1
GOTERM_BP_FAT	resolution of cell death	11	4.6E-2	7.7E-1
GOTERM_BP_FAT	apoptotic resolution of apoptosis	11	4.9E-2	7.9E-1
GOTERM_BP_FAT	apoptotic resolution of apoptotic cell death	11	5.1E-2	7.7E-1
GOTERM_BP_FAT	apoptotic resolution of cell death	6	2.1E-1	9.6E-1
GOTERM_BP_FAT	anti-apoptosis	6	2.1E-1	9.6E-1

8.2 Rabbit DAVID cluster

https://david.ncicf.gov/terms.jsp?anno=52,9,79,85,25,32,39,1,3,47,45,63,76¤tList=1

2/29/2016 DAVID: Database for Annotation, Visualization, and Integrated Discovery (Laboratory of Immunopathogenesis and Bioinformatics (LB): National Inst...						
<input type="checkbox"/>	GOTERM_BP_FAT	RT		8	5.0E-1	9.9E-1
Annotation Cluster 7						
<input type="checkbox"/>	GOTERM_CC_FAT	RT		26	7.2E-3	3.2E-1
<input type="checkbox"/>	GOTERM_CC_FAT	RT		11	9.2E-3	3.4E-1
<input type="checkbox"/>	GOTERM_CC_FAT	RT		11	1.3E-2	3.6E-1
<input type="checkbox"/>	GOTERM_CC_FAT	RT		20	3.4E-2	5.7E-1
<input type="checkbox"/>	GOTERM_CC_FAT	RT		11	4.4E-2	6.0E-1
<input type="checkbox"/>	GOTERM_CC_FAT	RT		24	8.3E-2	6.9E-1
Annotation Cluster 8						
<input type="checkbox"/>	SP_PIR_KEYWORDS	RT		18	3.4E-4	3.4E-2
<input type="checkbox"/>	GOTERM_BP_FAT	RT		23	3.9E-3	4.6E-1
<input type="checkbox"/>	SP_PIR_KEYWORDS	RT		11	4.6E-3	1.2E-1
<input type="checkbox"/>	GOTERM_BP_FAT	RT		12	5.8E-3	4.7E-1
<input type="checkbox"/>	GOTERM_BP_FAT	RT		13	1.2E-2	5.4E-1
<input type="checkbox"/>	GOTERM_BP_FAT	RT		16	2.7E-2	7.6E-1
<input type="checkbox"/>	GOTERM_BP_FAT	RT		12	5.3E-2	7.7E-1
<input type="checkbox"/>	GOTERM_BP_FAT	RT		8	5.7E-2	7.7E-1
<input type="checkbox"/>	GOTERM_BP_FAT	RT		8	6.2E-2	7.9E-1
<input type="checkbox"/>	SP_PIR_KEYWORDS	RT		6	1.2E-1	6.3E-1
<input type="checkbox"/>	GOTERM_BP_FAT	RT		7	1.2E-1	9.1E-1
<input type="checkbox"/>	GOTERM_BP_FAT	RT		7	1.2E-1	9.1E-1
<input type="checkbox"/>	GOTERM_BP_FAT	RT		9	1.3E-1	9.2E-1
Annotation Cluster 9						
<input type="checkbox"/>	GOTERM_BP_FAT	RT		4	5.0E-3	4.4E-1
<input type="checkbox"/>	GOTERM_BP_FAT	RT		5	8.7E-3	5.0E-1
<input type="checkbox"/>	GOTERM_BP_FAT	RT		3	3.4E-2	7.6E-1
<input type="checkbox"/>	GOTERM_BP_FAT	RT		4	4.5E-2	7.7E-1
<input type="checkbox"/>	GOTERM_BP_FAT	RT		3	6.0E-2	7.8E-1
<input type="checkbox"/>	GOTERM_BP_FAT	RT		3	6.0E-2	7.8E-1
<input type="checkbox"/>	GOTERM_BP_FAT	RT		4	6.4E-2	7.9E-1
Annotation Cluster 10						
<input type="checkbox"/>	GOTERM_MF_FAT	RT		3	1.2E-2	6.5E-1
<input type="checkbox"/>	GOTERM_MF_FAT	RT		3	1.5E-2	6.4E-1
<input type="checkbox"/>	GOTERM_MF_FAT	RT		3	1.5E-2	6.4E-1
<input type="checkbox"/>	SP_PIR_KEYWORDS	RT		3	1.5E-2	6.4E-1
<input type="checkbox"/>	SP_PIR_KEYWORDS	RT		6	1.8E-2	2.7E-1
<input type="checkbox"/>	KEGG_PATHWAY	RT		5	2.0E-2	9.1E-1
<input type="checkbox"/>	SP_PIR_KEYWORDS	RT		4	2.3E-2	3.0E-1
<input type="checkbox"/>	GOTERM_MF_FAT	RT		7	2.7E-2	7.6E-1
<input type="checkbox"/>	GOTERM_MF_FAT	RT		3	3.3E-2	7.6E-1
<input type="checkbox"/>	GOTERM_MF_FAT	RT		4	4.1E-2	7.7E-1
<input type="checkbox"/>	GOTERM_MF_FAT	RT		3	6.1E-2	8.1E-1
<input type="checkbox"/>	GOTERM_MF_FAT	RT		3	2.5E-1	9.4E-1
Annotation Cluster 11						
<input type="checkbox"/>	SMART	RT		Count	P_Value Benjamini	
<input type="checkbox"/>	INTERPRO	RT		5	2.1E-2	9.3E-1
<input type="checkbox"/>	UP_SFO_FEATURE	RT		5	2.8E-2	9.9E-1
<input type="checkbox"/>	Annotation Cluster 12	RT		4	5.9E-2	1.0E0
Annotation Cluster 12						
<input type="checkbox"/>	GOTERM_BP_FAT	RT		28	1.9E-3	3.6E-1
<input type="checkbox"/>	GOTERM_BP_FAT	RT		28	1.9E-3	3.6E-1
<input type="checkbox"/>	GOTERM_MF_FAT	RT		15	3.8E-3	8.0E-1
<input type="checkbox"/>	SP_PIR_KEYWORDS	RT		9	8.2E-3	1.7E-1
<input type="checkbox"/>	SP_PIR_KEYWORDS	RT		13	8.5E-3	1.7E-1
<input type="checkbox"/>	SP_PIR_KEYWORDS	RT		19	9.7E-3	1.8E-1
<input type="checkbox"/>	GOTERM_BP_FAT	RT		22	1.1E-2	5.4E-1
<input type="checkbox"/>	GOTERM_MF_FAT	RT		46	1.1E-2	6.9E-1
<input type="checkbox"/>	INTERPRO	RT		12	1.5E-2	1.0E0
<input type="checkbox"/>	INTERPRO	RT		12	1.6E-2	9.9E-1

2/29/2016 DAVID: Database for Annotation, Visualization, and Integrated Discovery (Laboratory of Immunopathogenesis and Biinformatics (LB): National Inst...						
<input type="checkbox"/>	GOTERM_MF_FAT	protein kinase activity	RT	16	2.9E-2	7.5E-1
<input type="checkbox"/>	SP_PIR_KEYWORDS	nucleotide-binding	RT	34	3.7E-2	3.8E-1
<input type="checkbox"/>	UP_SEQ_FEATURE	binding site:ATP	RT	14	4.8E-2	1.0E0
<input type="checkbox"/>	GOTERM_BP_FAT	protein amino acid ribosylation	RT	17	5.0E-2	7.7E-1
<input type="checkbox"/>	UP_SEQ_FEATURE	active site:Proton acceptor	RT	16	5.1E-2	1.0E0
<input type="checkbox"/>	GOTERM_MF_FAT	purine nucleotide binding	RT	37	5.5E-2	8.4E-1
<input type="checkbox"/>	SMART	S_TKc	RT	8	5.8E-2	9.8E-1
<input type="checkbox"/>	UP_SEQ_FEATURE	nucleotide phosphate-binding region:ATP	RT	21	5.9E-2	1.0E0
<input type="checkbox"/>	SP_PIR_KEYWORDS	zinc-binding	RT	27	5.9E-2	5.0E-1
<input type="checkbox"/>	SP_PIR_KEYWORDS	transferase	RT	28	6.2E-2	4.9E-1
<input type="checkbox"/>	GOTERM_MF_FAT	purine ribonucleotide binding	RT	35	7.1E-2	8.4E-1
<input type="checkbox"/>	GOTERM_MF_FAT	ribonucleotide binding	RT	35	7.1E-2	8.4E-1
<input type="checkbox"/>	UP_SEQ_FEATURE	domain:Protein kinase	RT	12	7.5E-2	1.0E0
<input type="checkbox"/>	INTERPRO	Serine/threonine protein kinase	RT	8	8.4E-2	1.0E0
<input type="checkbox"/>	INTERPRO	Protein kinase, core	RT	12	8.8E-2	1.0E0
<input type="checkbox"/>	INTERPRO	Protein kinase, ATP binding site	RT	11	1.3E-1	1.0E0
<input type="checkbox"/>	GOTERM_MF_FAT	adenyl nucleotide binding	RT	29	1.4E-1	9.2E-1
<input type="checkbox"/>	GOTERM_MF_FAT	ATP binding	RT	29	1.6E-1	9.3E-1
<input type="checkbox"/>	GOTERM_MF_FAT	nucleoside binding	RT	27	1.6E-1	9.2E-1
<input type="checkbox"/>	GOTERM_MF_FAT	adenyl ribonucleotide binding	RT	29	1.7E-1	9.1E-1
<input type="checkbox"/>	SP_PIR_KEYWORDS	serine/threonine-specific protein kinase	RT	3	2.1E-1	7.7E-1
<input type="checkbox"/>	KEGG_PATHWAY	MAPK signaling pathway	RT	3	9.6E-1	1.0E0
Annotation Cluster13				Count	P_Value	Benjamini
<input type="checkbox"/>	GOTERM_BP_FAT	RNA catabolic process	RT	5	1.7E-2	6.6E-1
<input type="checkbox"/>	GOTERM_BP_FAT	mRNA catabolic process	RT	4	2.8E-2	7.6E-1
<input type="checkbox"/>	SP_PIR_KEYWORDS	nonsense-mediated mRNA decay	RT	3	6.0E-2	4.9E-1
<input type="checkbox"/>	GOTERM_BP_FAT	nuclear-transcribed mRNA catabolic process, nonsense-mediated decay	RT	3	7.7E-2	8.3E-1
<input type="checkbox"/>	GOTERM_BP_FAT	nuclear-transcribed mRNA catabolic process	RT	3	1.0E-1	8.8E-1
Annotation Cluster14				Count	P_Value	Benjamini
<input type="checkbox"/>	GOTERM_BP_FAT	regulation of kinase activity	RT	12	2.2E-2	7.1E-1
<input type="checkbox"/>	GOTERM_BP_FAT	regulation of ribosylation	RT	14	2.7E-2	7.7E-1
<input type="checkbox"/>	GOTERM_BP_FAT	regulation of transferase activity	RT	12	2.8E-2	7.5E-1
<input type="checkbox"/>	GOTERM_BP_FAT	regulation of ribonucleic acid metabolic process	RT	14	3.6E-2	7.7E-1
<input type="checkbox"/>	GOTERM_BP_FAT	regulation of ribonucleic acid metabolic process	RT	14	3.6E-2	7.7E-1
<input type="checkbox"/>	GOTERM_BP_FAT	regulation of protein kinase activity	RT	11	4.0E-2	7.7E-1
<input type="checkbox"/>	GOTERM_BP_FAT	positive regulation of catalytic activity	RT	14	5.7E-2	7.8E-1
<input type="checkbox"/>	GOTERM_BP_FAT	positive regulation of molecular function	RT	15	6.6E-2	8.0E-1
<input type="checkbox"/>	GOTERM_BP_FAT	positive regulation of kinase activity	RT	6	2.8E-1	9.7E-1
<input type="checkbox"/>	GOTERM_BP_FAT	positive regulation of transferase activity	RT	6	3.1E-1	9.7E-1
<input type="checkbox"/>	GOTERM_BP_FAT	positive regulation of protein kinase activity	RT	5	4.4E-1	9.9E-1
Annotation Cluster15				Count	P_Value	Benjamini
<input type="checkbox"/>	GOTERM_BP_FAT	regulation of apoptosis	RT	20	3.9E-2	7.8E-1
<input type="checkbox"/>	GOTERM_BP_FAT	regulation of programmed cell death	RT	20	4.3E-2	7.8E-1
<input type="checkbox"/>	GOTERM_BP_FAT	regulation of cell death	RT	20	4.4E-2	7.7E-1
<input type="checkbox"/>	GOTERM_BP_FAT	induction of apoptosis	RT	9	1.2E-1	9.1E-1
<input type="checkbox"/>	GOTERM_BP_FAT	induction of programmed cell death	RT	9	1.2E-1	9.1E-1
<input type="checkbox"/>	GOTERM_BP_FAT	positive regulation of apoptosis	RT	11	1.2E-1	9.2E-1
<input type="checkbox"/>	GOTERM_BP_FAT	positive regulation of programmed cell death	RT	11	1.3E-1	9.2E-1
<input type="checkbox"/>	GOTERM_BP_FAT	induction of apoptosis by extracellular stimulus	RT	11	1.3E-1	9.2E-1
<input type="checkbox"/>	GOTERM_BP_FAT	positive regulation of cell death	RT	4	2.5E-1	9.6E-1
Annotation Cluster16				Count	P_Value	Benjamini
<input type="checkbox"/>	INTERPRO	Nucleotide-binding, alpha-beta fold	RT	8	3.6E-2	9.9E-1
<input type="checkbox"/>	SMART	RNA	RT	7	6.3E-2	9.3E-1
<input type="checkbox"/>	INTERPRO	RNA recognition motif, RNPc_1	RT	7	8.8E-2	1.0E0
<input type="checkbox"/>	UP_SEQ_FEATURE	domain:RRM 3	RT	3	1.6E-1	1.0E0
<input type="checkbox"/>	UP_SEQ_FEATURE	domain:RRM 2	RT	4	1.8E-1	1.0E0

2/29/2016	DAVID: Database for Annotation, Visualization, and Integrated Discovery (Laboratory of Immunopathogenesis and Biostatistics (LBI); National Inst...						
<input type="checkbox"/>	UP_S6Q_FEATURE	domain:rrm 1	RT		4	1.8E-1	1.0E0
<input type="checkbox"/>	SP_PIR_KEYWORDS	<u>methylation</u>	RT		6	2.6E-1	8.2E-1
		Enrichment Score: 0.83	G		Count	P-Value	Benjamini
<input type="checkbox"/>	KEGG_PATHWAY	<u>Glycolysis / Gluconeogenesis</u>	RT		5	2.3E-2	7.6E-1
<input type="checkbox"/>	GOTERM_BP_FAT	<u>hexose metabolic process</u>	RT		8	2.8E-2	7.4E-1
<input type="checkbox"/>	SP_PIR_KEYWORDS	<u>gluconeogenesis</u>	RT		3	2.9E-2	3.3E-1
<input type="checkbox"/>	GOTERM_BP_FAT	<u>monosaccharide metabolic process</u>	RT		8	5.5E-2	7.8E-1
<input type="checkbox"/>	GOTERM_BP_FAT	<u>gluconeogenesis</u>	RT		3	5.6E-2	7.8E-1
<input type="checkbox"/>	GOTERM_BP_FAT	<u>hexose biosynthetic process</u>	RT		3	8.1E-2	8.5E-1
<input type="checkbox"/>	GOTERM_BP_FAT	<u>glucose metabolic process</u>	RT		6	8.6E-2	8.5E-1
<input type="checkbox"/>	GOTERM_BP_FAT	<u>cellular carbohydrate biosynthetic process</u>	RT		4	8.9E-2	8.6E-1
<input type="checkbox"/>	GOTERM_BP_FAT	<u>monosaccharide biosynthetic process</u>	RT		3	1.1E-1	9.0E-1
<input type="checkbox"/>	SP_PIR_KEYWORDS	<u>glycolysis</u>	RT		3	1.3E-1	6.5E-1
<input type="checkbox"/>	GOTERM_BP_FAT	<u>pyruvate metabolic process</u>	RT		3	1.3E-1	9.2E-1
<input type="checkbox"/>	GOTERM_BP_FAT	<u>alcohol biosynthetic process</u>	RT		3	1.5E-1	9.3E-1
<input type="checkbox"/>	GOTERM_BP_FAT	<u>glycolysis</u>	RT		3	1.6E-1	9.4E-1
<input type="checkbox"/>	GOTERM_BP_FAT	<u>glucose catabolic process</u>	RT		3	2.2E-1	9.6E-1
<input type="checkbox"/>	GOTERM_BP_FAT	<u>carbohydrate biosynthetic process</u>	RT		4	2.3E-1	9.6E-1
<input type="checkbox"/>	GOTERM_BP_FAT	<u>carbohydrate catabolic process</u>	RT		4	2.3E-1	9.5E-1
<input type="checkbox"/>	GOTERM_BP_FAT	<u>hexose catabolic process</u>	RT		3	2.8E-1	9.7E-1
<input type="checkbox"/>	GOTERM_BP_FAT	<u>monosaccharide catabolic process</u>	RT		3	3.0E-1	9.7E-1
<input type="checkbox"/>	GOTERM_BP_FAT	<u>alcohol catabolic process</u>	RT		3	3.5E-1	9.8E-1
<input type="checkbox"/>	GOTERM_BP_FAT	<u>cellular carbohydrate catabolic process</u>	RT		3	3.7E-1	9.8E-1
		Enrichment Score: 0.82	G		Count	P-Value	Benjamini
<input type="checkbox"/>	GOTERM_BP_FAT	<u>cellular macromolecule catabolic process</u>	RT		22	3.7E-3	4.8E-1
<input type="checkbox"/>	GOTERM_BP_FAT	<u>macromolecule catabolic process</u>	RT		23	4.2E-3	4.5E-1
<input type="checkbox"/>	SP_PIR_KEYWORDS	<u>ATP catabolism pathway</u>	RT		11	1.9E-1	7.4E-1
<input type="checkbox"/>	GOTERM_BP_FAT	<u>proteolysis involved in cellular protein catabolic process</u>	RT		13	2.1E-1	9.6E-1
<input type="checkbox"/>	GOTERM_BP_FAT	<u>cellular protein catabolic process</u>	RT		13	2.1E-1	9.5E-1
<input type="checkbox"/>	GOTERM_BP_FAT	<u>protein catabolic process</u>	RT		13	2.4E-1	9.6E-1
<input type="checkbox"/>	GOTERM_BP_FAT	<u>modification-dependent macromolecule catabolic process</u>	RT		12	2.6E-1	9.6E-1
<input type="checkbox"/>	GOTERM_BP_FAT	<u>modification-dependent protein catabolic process</u>	RT		12	2.6E-1	9.6E-1
<input type="checkbox"/>	GOTERM_BP_FAT	<u>ubiquitin-dependent protein catabolic process</u>	RT		5	5.1E-1	9.9E-1
<input type="checkbox"/>	GOTERM_BP_FAT	<u>proteolysis</u>	RT		17	5.5E-1	1.0E0
		Enrichment Score: 0.89	G		Count	P-Value	Benjamini
<input type="checkbox"/>	GOTERM_MF_FAT	<u>GTPase activity</u>	RT		8	3.3E-2	7.2E-1
<input type="checkbox"/>	GOTERM_MF_FAT	<u>GTP binding</u>	RT		10	8.9E-2	8.7E-1
<input type="checkbox"/>	GOTERM_BP_FAT	<u>small GTPase mediated signal transduction</u>	RT		9	9.2E-2	8.7E-1
<input type="checkbox"/>	SP_PIR_KEYWORDS	<u>gtp-binding</u>	RT		9	9.8E-2	5.9E-1
<input type="checkbox"/>	GOTERM_MF_FAT	<u>guanine ribonucleotide binding</u>	RT		10	1.0E-1	8.9E-1
<input type="checkbox"/>	GOTERM_MF_FAT	<u>guanyl nucleotide binding</u>	RT		10	1.0E-1	8.8E-1
<input type="checkbox"/>	UP_S6Q_FEATURE	<u>nucleotide phosphate-binding region:GTP</u>	RT		7	2.5E-1	1.0E0
<input type="checkbox"/>	INTERPRO	<u>Bas GTPase</u>	RT		4	3.1E-1	1.0E0
<input type="checkbox"/>	INTERPRO	<u>Small GTP-binding protein</u>	RT		4	4.4E-1	1.0E0
		Enrichment Score: 0.84	G		Count	P-Value	Benjamini
<input type="checkbox"/>	GOTERM_CC_FAT	<u>extrinsic to ribosome membrane</u>	RT		4	4.2E-2	6.2E-1
<input type="checkbox"/>	GOTERM_CC_FAT	<u>heterotrimeric G-protein complex</u>	RT		3	7.4E-2	7.0E-1
<input type="checkbox"/>	SP_PIR_KEYWORDS	<u>transducer</u>	RT		6	1.0E0	1.0E0
		Enrichment Score: 0.82	G		Count	P-Value	Benjamini
<input type="checkbox"/>	GOTERM_MF_FAT	<u>ribonucleoprotein ribonuclease activity</u>	RT		6	9.1E-2	8.6E-1
<input type="checkbox"/>	SP_PIR_KEYWORDS	<u>protein serine/threonine ribonuclease activity</u>	RT		5	1.1E-1	6.2E-1
<input type="checkbox"/>	GOTERM_MF_FAT	<u>protein kinase activity</u>	RT		3	1.4E-1	9.2E-1
<input type="checkbox"/>	GOTERM_BP_FAT	<u>protein serine/threonine phosphorylation</u>	RT		5	1.5E-1	9.3E-1
<input type="checkbox"/>	GOTERM_MF_FAT	<u>ribonuclease activity</u>	RT		7	1.5E-1	9.3E-1
<input type="checkbox"/>	GOTERM_BP_FAT	<u>dephosphorylation</u>	RT		5	2.1E-1	9.6E-1
<input type="checkbox"/>	SP_PIR_KEYWORDS	<u>absorbent monooxygen hydrolase</u>	RT		3	2.6E-1	8.2E-1
		Enrichment Score: 0.82	G		Count	P-Value	Benjamini

<https://david.ncfcr.gov/terms.jsp?rand=52.9,79.85,25.32,39,1,3,4,7,45,63,78¤tList=1>

2/29/2016 DAVID: Database for Annotation, Visualization, and Integrated Discovery (Laboratory of Immunopathogenesis and Bioinformatics (LB): National Inst...

<input type="checkbox"/>	INTERPRO	Nucleotide-binding, alpha-beta motif	RT	<input type="checkbox"/>	8	3.6E-2	9.9E-1
<input type="checkbox"/>	GOTERM_MF_FAT	RNA binding	RT	<input type="checkbox"/>	17	5.5E-2	8.2E-1
<input type="checkbox"/>	GOTERM_BP_FAT	mRNA metabolic process	RT	<input type="checkbox"/>	11	5.8E-2	7.7E-1
<input type="checkbox"/>	SMART	RBM	RT	<input type="checkbox"/>	7	6.3E-2	9.3E-1
<input type="checkbox"/>	INTERPRO	RNA recombinase motif, RNP1	RT	<input type="checkbox"/>	7	8.8E-2	1.0E0
<input type="checkbox"/>	GOTERM_BP_FAT	RNA splicing	RT	<input type="checkbox"/>	8	1.5E-1	9.3E-1
<input type="checkbox"/>	SP_PIR_KEYWORDS	mRNA binding	RT	<input type="checkbox"/>	12	1.5E-1	6.9E-1
<input type="checkbox"/>	SP_PIR_KEYWORDS	mRNA processing	RT	<input type="checkbox"/>	7	1.7E-1	7.2E-1
<input type="checkbox"/>	GOTERM_BP_FAT	RNA-colicin, via transcription activation with nuclear adenine base nucleoside	RT	<input type="checkbox"/>	5	2.1E-1	9.6E-1
<input type="checkbox"/>	GOTERM_BP_FAT	RNA-colicin, via transcription activation	RT	<input type="checkbox"/>	5	2.1E-1	9.6E-1
<input type="checkbox"/>	GOTERM_BP_FAT	nuclear mRNA splicing, via spliceosome	RT	<input type="checkbox"/>	5	2.1E-1	9.6E-1
<input type="checkbox"/>	GOTERM_BP_FAT	RNA processing	RT	<input type="checkbox"/>	12	2.2E-1	9.5E-1
<input type="checkbox"/>	GOTERM_BP_FAT	mRNA processing	RT	<input type="checkbox"/>	8	2.2E-1	9.6E-1
<input type="checkbox"/>	SP_PIR_KEYWORDS	mRNA splicing	RT	<input type="checkbox"/>	5	3.5E-1	8.8E-1
<input type="checkbox"/>	KEGG_PATHWAY	Spliceosome	RT	<input type="checkbox"/>	4	4.1E-1	9.5E-1
<input type="checkbox"/>	UP_SEQ_FEATURE	domain, RRM	RT	<input type="checkbox"/>	3	5.1E-1	1.0E0
<input type="checkbox"/>	Annotation Cluster23			<input type="checkbox"/>	Count	P_Value	Benjamini
<input type="checkbox"/>	KEGG_PATHWAY	Small cell lung cancer	RT	<input type="checkbox"/>	5	6.7E-2	9.4E-1
<input type="checkbox"/>	BIOCARTA	Role of Mitochondria in Apoptotic Signaling	RT	<input type="checkbox"/>	3	7.1E-2	8.9E-1
<input type="checkbox"/>	KEGG_PATHWAY	Apoptosis	RT	<input type="checkbox"/>	5	7.4E-2	9.0E-1
<input type="checkbox"/>	KEGG_PATHWAY	Colorectal cancer	RT	<input type="checkbox"/>	3	4.6E-1	9.5E-1
<input type="checkbox"/>	KEGG_PATHWAY	Pathways in cancer	RT	<input type="checkbox"/>	7	5.6E-1	9.7E-1
<input type="checkbox"/>	Annotation Cluster24			<input type="checkbox"/>	Count	P_Value	Benjamini
<input type="checkbox"/>	GOTERM_BP_FAT	regulation of binding	RT	<input type="checkbox"/>	6	8.6E-2	8.5E-1
<input type="checkbox"/>	GOTERM_BP_FAT	regulation of transcription factor activity	RT	<input type="checkbox"/>	4	2.1E-1	9.6E-1
<input type="checkbox"/>	GOTERM_BP_FAT	regulation of DNA binding	RT	<input type="checkbox"/>	4	2.8E-1	9.7E-1
<input type="checkbox"/>	Annotation Cluster25			<input type="checkbox"/>	Count	P_Value	Benjamini
<input type="checkbox"/>	SP_PIR_KEYWORDS	arc-domain transport	RT	<input type="checkbox"/>	7	1.2E-3	3.5E-2
<input type="checkbox"/>	SP_PIR_KEYWORDS	actinin transport	RT	<input type="checkbox"/>	9	3.9E-1	9.0E-1
<input type="checkbox"/>	GOTERM_BP_FAT	actinin transport	RT	<input type="checkbox"/>	11	7.4E-1	1.0E0
<input type="checkbox"/>	GOTERM_BP_FAT	establishment of actinin localization	RT	<input type="checkbox"/>	11	7.5E-1	1.0E0
<input type="checkbox"/>	GOTERM_BP_FAT	actinin localization	RT	<input type="checkbox"/>	12	8.0E-1	1.0E0
<input type="checkbox"/>	Annotation Cluster26			<input type="checkbox"/>	Count	P_Value	Benjamini
<input type="checkbox"/>	GOTERM_CC_FAT	scaffold	RT	<input type="checkbox"/>	7	2.7E-2	5.2E-1
<input type="checkbox"/>	GOTERM_CC_FAT	centriole	RT	<input type="checkbox"/>	3	8.3E-2	7.0E-1
<input type="checkbox"/>	GOTERM_CC_FAT	microtubule cytoskeleton	RT	<input type="checkbox"/>	14	8.5E-2	6.8E-1
<input type="checkbox"/>	SP_PIR_KEYWORDS	Cytoskeleton	RT	<input type="checkbox"/>	13	2.0E-1	7.5E-1
<input type="checkbox"/>	GOTERM_CC_FAT	microtubule organizing center	RT	<input type="checkbox"/>	7	2.0E-1	9.0E-1
<input type="checkbox"/>	GOTERM_CC_FAT	microtubule-organizing center part	RT	<input type="checkbox"/>	3	2.2E-1	8.9E-1
<input type="checkbox"/>	GOTERM_CC_FAT	centrosome	RT	<input type="checkbox"/>	6	2.7E-1	9.0E-1
<input type="checkbox"/>	GOTERM_CC_FAT	centrosome	RT	<input type="checkbox"/>	14	7.2E-1	9.9E-1
<input type="checkbox"/>	GOTERM_CC_FAT	Cytoskeleton	RT	<input type="checkbox"/>	18	8.7E-1	1.0E0
<input type="checkbox"/>	Annotation Cluster27			<input type="checkbox"/>	Count	P_Value	Benjamini
<input type="checkbox"/>	GOTERM_BP_FAT	negative regulation of cellular actinin	RT	<input type="checkbox"/>	9	6.5E-3	4.6E-1
<input type="checkbox"/>	GOTERM_BP_FAT	metabolic process	RT	<input type="checkbox"/>	9	8.2E-3	4.9E-1
<input type="checkbox"/>	GOTERM_BP_FAT	negative regulation of actinin, amino acid	RT	<input type="checkbox"/>	4	1.3E-2	5.6E-1
<input type="checkbox"/>	GOTERM_BP_FAT	allosteric regulation	RT	<input type="checkbox"/>	4	3.1E-2	7.7E-1
<input type="checkbox"/>	GOTERM_BP_FAT	negative regulation of ribosylation	RT	<input type="checkbox"/>	4	3.1E-2	7.7E-1
<input type="checkbox"/>	GOTERM_BP_FAT	negative regulation of actinin modification	RT	<input type="checkbox"/>	6	3.6E-2	7.6E-1
<input type="checkbox"/>	GOTERM_BP_FAT	metabolic process	RT	<input type="checkbox"/>	4	3.7E-2	7.6E-1
<input type="checkbox"/>	GOTERM_BP_FAT	negative regulation of ribosylate metabolic process	RT	<input type="checkbox"/>	4	3.7E-2	7.6E-1
<input type="checkbox"/>	GOTERM_BP_FAT	regulation of cell adhesion	RT	<input type="checkbox"/>	5	1.6E-1	9.4E-1
<input type="checkbox"/>	GOTERM_BP_FAT	negative regulation of catalytic activity	RT	<input type="checkbox"/>	7	2.5E-1	9.6E-1
<input type="checkbox"/>	GOTERM_BP_FAT	negative regulation of molecular function	RT	<input type="checkbox"/>	8	2.5E-1	9.6E-1
<input type="checkbox"/>	GOTERM_BP_FAT	negative regulation of fibroblast growth factor activity	RT	<input type="checkbox"/>	3	2.7E-1	9.7E-1
<input type="checkbox"/>	GOTERM_BP_FAT	negative regulation of lipase activity	RT	<input type="checkbox"/>	3	2.7E-1	9.7E-1

https://david.ncicf.gov/terms/sp?annot=52,9,7,9,85,25,32,39,1,3,47,45,63,78¤tList=1

2292016	DAVID: Database for Annotation, Visualization, and Integrated Discovery (Laboratory of Immunopathogenesis and Bioinformatics (LB): National Inst...					
<input type="checkbox"/>	regulation of arginine amino acid absorption	RT		5	2.7E-1	9.6E-1
<input type="checkbox"/>	regulation of arginine modification process	RT		7	3.0E-1	9.7E-1
<input type="checkbox"/>	regulation of cellular arginine metabolic process	RT		10	3.1E-1	9.7E-1
<input type="checkbox"/>	negative regulation of arginine ubiquitination	RT		3	3.1E-1	9.7E-1
<input type="checkbox"/>	regulation of fibroblast growth factor signaling	RT		3	3.4E-1	9.7E-1
<input type="checkbox"/>	regulation of lipase activity	RT		3	3.5E-1	9.8E-1
<input type="checkbox"/>	positive regulation of arginine ubiquitination	RT		3	3.7E-1	9.8E-1
<input type="checkbox"/>	negative regulation of arginine kinase activity	RT		3	3.9E-1	9.8E-1
<input type="checkbox"/>	negative regulation of kinase activity	RT		3	4.0E-1	9.8E-1
<input type="checkbox"/>	regulation of protein ubiquitination	RT		3	4.3E-1	9.9E-1
<input type="checkbox"/>	positive regulation of arginine modification process	RT		3	4.5E-1	9.9E-1
<input type="checkbox"/>	negative regulation of signal transduction	RT		3	7.8E-1	1.0E0
<input type="checkbox"/>	positive regulation of cellular protein metabolic process	RT		3	8.6E-1	1.0E0
<input type="checkbox"/>	positive regulation of arginine metabolic process	RT		3	8.8E-1	1.0E0
<input type="checkbox"/>	negative regulation of cell communication	RT		3	8.9E-1	1.0E0
<input type="checkbox"/>	Enrichment Score: 0.72	G		3	9.0E-1	1.0E0
<input type="checkbox"/>	ribonucleoprotein	RT		10	1.9E-2	2.7E-1
<input type="checkbox"/>	ribonucleoprotein complex	RT		14	5.7E-2	6.3E-1
<input type="checkbox"/>	ribosomal protein	RT		6	1.3E-1	6.5E-1
<input type="checkbox"/>	translational elongation	RT		4	2.0E-1	9.6E-1
<input type="checkbox"/>	ribosome	RT		6	2.4E-1	8.9E-1
<input type="checkbox"/>	translation	RT		8	2.5E-1	9.6E-1
<input type="checkbox"/>	structural constituent of ribosome	RT		4	4.4E-1	1.0E0
<input type="checkbox"/>	ribosome	RT		3	4.8E-1	9.5E-1
<input type="checkbox"/>	structural molecule activity	RT		7	9.0E-1	1.0E0
<input type="checkbox"/>	Enrichment Score: 0.62	G		17	7.6E-2	6.9E-1
<input type="checkbox"/>	antileish	RT		46	2.2E-1	8.8E-1
<input type="checkbox"/>	intracellular non-membrane-bounded organelle	RT		46	2.2E-1	8.8E-1
<input type="checkbox"/>	non-membrane-bounded organelle	RT		46	2.2E-1	8.8E-1
<input type="checkbox"/>	schistosome	RT		18	8.7E-1	1.0E0
<input type="checkbox"/>	Enrichment Score: 0.61	G		3	8.6E-2	8.5E-1
<input type="checkbox"/>	limbic system development	RT		3	2.6E-1	9.6E-1
<input type="checkbox"/>	telencephalon development	RT		3	2.6E-1	9.6E-1
<input type="checkbox"/>	forebrain development	RT		3	6.8E-1	1.0E0
<input type="checkbox"/>	Enrichment Score: 0.6	G		13	2.1E-1	9.0E-1
<input type="checkbox"/>	mitochondrial out	RT		6	2.8E-1	9.0E-1
<input type="checkbox"/>	mitochondrial matrix	RT		6	2.8E-1	9.0E-1
<input type="checkbox"/>	mitochondrial lumen	RT		6	2.8E-1	9.0E-1
<input type="checkbox"/>	Enrichment Score: 0.59	G		10	1.5E-1	9.3E-1
<input type="checkbox"/>	gamete development	RT		11	1.7E-1	9.4E-1
<input type="checkbox"/>	sexual reproduction	RT		11	2.1E-1	9.6E-1
<input type="checkbox"/>	reproductive process in a multicellular organism	RT		11	2.1E-1	9.6E-1
<input type="checkbox"/>	multicellular organism reproduction	RT		11	2.1E-1	9.6E-1
<input type="checkbox"/>	male gamete development	RT		6	5.1E-1	9.9E-1
<input type="checkbox"/>	spermatogenesis	RT		6	5.1E-1	9.9E-1
<input type="checkbox"/>	Enrichment Score: 0.58	G		5	2.0E-2	9.1E-1
<input type="checkbox"/>	RNA degradation	RT		6	1.4E-1	9.3E-1
<input type="checkbox"/>	ribonucleoprotein complex biogenesis	RT		3	2.1E-1	7.7E-1
<input type="checkbox"/>	RNA processing	RT		4	2.9E-1	9.7E-1
<input type="checkbox"/>	RNA transcription	RT		3	4.1E-1	9.9E-1
<input type="checkbox"/>	RNA metabolic process	RT		3	4.3E-1	9.9E-1
<input type="checkbox"/>	tRNA processing	RT		3	7.8E-1	1.0E0
<input type="checkbox"/>	mRNA metabolic process	RT		3	8.7E-1	1.0E0
<input type="checkbox"/>	Enrichment Score: 0.54	G		5	1.5E-1	9.3E-1
<input type="checkbox"/>	KEGG_PATHWAY	RT		5	2.0E-2	9.1E-1
<input type="checkbox"/>	GOTERM_BP_FAT	RT		6	1.4E-1	9.3E-1
<input type="checkbox"/>	SP_PIR_KEYWORDS	RT		3	2.1E-1	7.7E-1
<input type="checkbox"/>	GOTERM_BP_FAT	RT		4	2.9E-1	9.7E-1
<input type="checkbox"/>	GOTERM_BP_FAT	RT		3	4.1E-1	9.9E-1
<input type="checkbox"/>	GOTERM_BP_FAT	RT		3	4.3E-1	9.9E-1
<input type="checkbox"/>	GOTERM_BP_FAT	RT		3	7.8E-1	1.0E0
<input type="checkbox"/>	GOTERM_BP_FAT	RT		3	8.7E-1	1.0E0
<input type="checkbox"/>	Enrichment Score: 0.54	G		5	1.5E-1	9.3E-1
<input type="checkbox"/>	Enrichment Score: 0.54	G		5	1.5E-1	9.3E-1

<https://david.ncifcrf.gov/terms2.htm>|sp?annot=52,79,85,25,32,39,1,3,47,45,63,78¤tList=1

6/14

2/29/2016 DAVID: Database for Annotation, Visualization, and Integrated Discovery (Laboratory of Immunopathogenesis and Bioinformatics (LIB): National Inst...

<input type="checkbox"/>	GOTERM_BP_FAT	protein kinase cascade	RT	■	9	2.1E-1	9.6E-1
<input type="checkbox"/>	GOTERM_BP_FAT	MAPKK cascade	RT	■	5	3.1E-1	9.7E-1
<input type="checkbox"/>	GOTERM_BP_FAT	regulation of MAP kinase activity	RT	■	4	3.7E-1	9.8E-1
Annotation Cluster 35							
<input type="checkbox"/>	GOTERM_BP_FAT	kidney development	RT	■	4	1.8E-1	9.5E-1
<input type="checkbox"/>	GOTERM_BP_FAT	urogenital system development	RT	■	4	2.4E-1	9.5E-1
<input type="checkbox"/>	GOTERM_BP_FAT	tissue morphogenesis	RT	■	5	3.0E-1	9.7E-1
<input type="checkbox"/>	GOTERM_MF_FAT	protein homodimerization activity	RT	■	6	5.3E-1	1.0E0
Annotation Cluster 36							
<input type="checkbox"/>	GOTERM_CC_FAT	mitochondrial outer membrane	RT	■	4	1.6E-1	8.9E-1
<input type="checkbox"/>	GOTERM_CC_FAT	outer membrane	RT	■	4	2.2E-1	8.9E-1
<input type="checkbox"/>	GOTERM_CC_FAT	outer membrane	RT	■	4	2.3E-1	8.9E-1
<input type="checkbox"/>	GOTERM_CC_FAT	mitochondrial envelope	RT	■	8	4.7E-1	9.6E-1
<input type="checkbox"/>	GOTERM_CC_FAT	mitochondrial membrane	RT	■	7	5.7E-1	9.7E-1
Annotation Cluster 37							
<input type="checkbox"/>	GOTERM_CC_FAT	Potassium channel, voltage-dependent, Kv, inactivated	RT	■	4	4.0E-2	9.9E-1
<input type="checkbox"/>	GOTERM_CC_FAT	potassium channel complex	RT	■	5	4.4E-2	5.8E-1
<input type="checkbox"/>	GOTERM_CC_FAT	voltage-gated potassium channel complex	RT	■	5	4.4E-2	5.8E-1
<input type="checkbox"/>	GOTERM_MF_FAT	voltage-gated potassium channel activity	RT	■	5	5.6E-2	8.0E-1
<input type="checkbox"/>	GOTERM_MF_FAT	potassium channel activity	RT	■	5	1.3E-1	9.1E-1
<input type="checkbox"/>	UP_SEQ_FEATURE	domain, BTB	RT	■	5	1.5E-1	1.0E0
<input type="checkbox"/>	GOTERM_CC_FAT	cation channel complex	RT	■	5	1.5E-1	8.3E-1
<input type="checkbox"/>	GOTERM_MF_FAT	voltage-gated cation channel activity	RT	■	5	1.6E-1	9.2E-1
<input type="checkbox"/>	SMART	BTB	RT	■	5	2.2E-1	1.0E0
<input type="checkbox"/>	GOTERM_BP_FAT	BTB/POZ-like	RT	■	5	2.3E-1	9.6E-1
<input type="checkbox"/>	INTERPRO	BTB/POZ-like	RT	■	5	2.6E-1	1.0E0
<input type="checkbox"/>	GOTERM_MF_FAT	voltage-gated channel activity	RT	■	5	3.1E-1	9.8E-1
<input type="checkbox"/>	GOTERM_MF_FAT	ion channel complex	RT	■	5	3.9E-1	9.4E-1
<input type="checkbox"/>	GOTERM_CC_FAT	BTB/POZ fold	RT	■	4	4.9E-1	1.0E0
<input type="checkbox"/>	INTERPRO	metal ion transmembrane transporter activity	RT	■	6	5.1E-1	1.0E0
<input type="checkbox"/>	GOTERM_MF_FAT	zinc ion transmembrane transporter activity	RT	■	6	5.4E-1	1.0E0
<input type="checkbox"/>	GOTERM_MF_FAT	cation channel activity	RT	■	5	5.6E-1	1.0E0
<input type="checkbox"/>	GOTERM_MF_FAT	gated channel activity	RT	■	5	6.6E-1	1.0E0
<input type="checkbox"/>	GOTERM_MF_FAT	ion channel activity	RT	■	6	6.6E-1	1.0E0
<input type="checkbox"/>	GOTERM_MF_FAT	substrate specific channel activity	RT	■	6	6.8E-1	1.0E0
<input type="checkbox"/>	GOTERM_MF_FAT	channel activity	RT	■	6	7.1E-1	1.0E0
<input type="checkbox"/>	GOTERM_MF_FAT	passive transmembrane transporter activity	RT	■	6	7.1E-1	1.0E0
<input type="checkbox"/>	GOTERM_BP_FAT	cation transport	RT	■	8	7.5E-1	1.0E0
<input type="checkbox"/>	GOTERM_BP_FAT	ion transport	RT	■	10	8.4E-1	1.0E0
<input type="checkbox"/>	GOTERM_BP_FAT	metal ion transport	RT	■	6	8.4E-1	1.0E0
<input type="checkbox"/>	SP_PRR_KEYWORDS	ionic channel	RT	■	3	9.4E-1	1.0E0
Annotation Cluster 38							
<input type="checkbox"/>	SP_PRR_KEYWORDS	metalloprotein	RT	■	5	1.0E-1	5.8E-1
<input type="checkbox"/>	SP_PRR_KEYWORDS	iron	RT	■	7	2.2E-1	7.7E-1
<input type="checkbox"/>	SP_PRR_KEYWORDS	chromoprotein	RT	■	3	2.2E-1	7.7E-1
<input type="checkbox"/>	GOTERM_MF_FAT	iron ion binding	RT	■	7	2.8E-1	9.8E-1
<input type="checkbox"/>	SP_PRR_KEYWORDS	heme	RT	■	3	5.1E-1	9.5E-1
<input type="checkbox"/>	GOTERM_MF_FAT	heme binding	RT	■	3	5.2E-1	1.0E0
<input type="checkbox"/>	GOTERM_MF_FAT	tetracycline binding	RT	■	3	5.6E-1	1.0E0
Annotation Cluster 39							
<input type="checkbox"/>	GOTERM_MF_FAT	protein heterodimerization activity	RT	■	7	8.0E-2	8.6E-1
<input type="checkbox"/>	GOTERM_BP_FAT	cell activation	RT	■	8	1.5E-1	9.3E-1
<input type="checkbox"/>	GOTERM_BP_FAT	lymphocyte activation	RT	■	6	1.9E-1	9.5E-1
<input type="checkbox"/>	GOTERM_BP_FAT	T cell activation	RT	■	4	3.0E-1	9.7E-1
<input type="checkbox"/>	GOTERM_BP_FAT	lymphocyte activation	RT	■	6	3.1E-1	9.7E-1
<input type="checkbox"/>	GOTERM_BP_FAT	B cell activation	RT	■	3	3.2E-1	9.7E-1

https://david.ncifcrf.gov/term.jsp?format=52,9,7,9,65,25,32,39,1,3,4,7,4,5,63,76¤tList=1

2/29/2016 DAVID: Database for Annotation, Visualization, and Integrated Discovery (Laboratory of Immunopathogenesis and Biostatistics (UB), National Inst...

<input type="checkbox"/>	SMART	zinc finger-type	RI	<input type="checkbox"/>	0	1.0E-1	1.0E0
<input type="checkbox"/>	SMART	RIHG	RI	<input type="checkbox"/>	6	3.6E-1	1.0E0
<input type="checkbox"/>	INTERPRO	Zinc finger_RING-type conserved site	RI	<input type="checkbox"/>	6	3.9E-1	1.0E0
<input type="checkbox"/>	INTERPRO	Zinc finger_RING-type	RI	<input type="checkbox"/>	6	4.3E-1	1.0E0
<input type="checkbox"/>	INTERPRO	Zinc finger_CH1C1_RING-type	RI	<input type="checkbox"/>	4	6.5E-1	1.0E0
Annotation Cluster#6							
<input type="checkbox"/>	GOTERM_MF_FAT	DNA-dependent ATPase activity	RI	<input checked="" type="checkbox"/>	3	2.0E-1	9.4E-1
<input type="checkbox"/>	SMART	AAA	RI	<input type="checkbox"/>	4	3.0E-1	1.0E0
<input type="checkbox"/>	SMART	AAA_0044-type_core	RI	<input type="checkbox"/>	4	3.5E-1	1.0E0
<input type="checkbox"/>	INTERPRO	ATPase activity_coupled	RI	<input type="checkbox"/>	5	5.5E-1	1.0E0
<input type="checkbox"/>	GOTERM_MF_FAT	ATPase activity	RI	<input type="checkbox"/>	5	7.1E-1	1.0E0
Annotation Cluster#7							
<input type="checkbox"/>	GOTERM_BP_FAT	hemostasis	RI	<input checked="" type="checkbox"/>	4	2.3E-1	9.6E-1
<input type="checkbox"/>	GOTERM_BP_FAT	regulation of body fluid levels	RI	<input type="checkbox"/>	4	3.7E-1	9.9E-1
<input type="checkbox"/>	GOTERM_BP_FAT	blood coagulation	RI	<input type="checkbox"/>	3	4.6E-1	9.9E-1
<input type="checkbox"/>	GOTERM_BP_FAT	coagulation	RI	<input type="checkbox"/>	3	4.6E-1	9.9E-1
<input type="checkbox"/>	GOTERM_BP_FAT	wound healing	RI	<input type="checkbox"/>	4	5.6E-1	1.0E0
Annotation Cluster#8							
<input type="checkbox"/>	GOTERM_BP_FAT	positive regulation of leukostasis	RI	<input checked="" type="checkbox"/>	4	1.9E-1	9.5E-1
<input type="checkbox"/>	GOTERM_BP_FAT	regulation of leukostasis	RI	<input type="checkbox"/>	4	2.3E-1	9.6E-1
<input type="checkbox"/>	GOTERM_BP_FAT	regulation of leukostasis	RI	<input type="checkbox"/>	6	3.4E-1	9.7E-1
<input type="checkbox"/>	GOTERM_BP_FAT	positive regulation of protein kinase cascade	RI	<input type="checkbox"/>	4	4.7E-1	9.9E-1
<input type="checkbox"/>	GOTERM_BP_FAT	positive regulation of signal transduction	RI	<input type="checkbox"/>	4	8.3E-1	1.0E0
<input type="checkbox"/>	GOTERM_BP_FAT	positive regulation of cell communication	RI	<input type="checkbox"/>	4	8.9E-1	1.0E0
Annotation Cluster#9							
<input type="checkbox"/>	GOTERM_BP_FAT	blood vessel morphogenesis	RI	<input checked="" type="checkbox"/>	8	4.4E-2	7.9E-1
<input type="checkbox"/>	GOTERM_BP_FAT	response to woun	RI	<input type="checkbox"/>	4	6.7E-2	7.9E-1
<input type="checkbox"/>	GOTERM_BP_FAT	blood vessel development	RI	<input type="checkbox"/>	8	8.2E-2	8.5E-1
<input type="checkbox"/>	GOTERM_BP_FAT	vasculature development	RI	<input type="checkbox"/>	8	9.1E-2	8.6E-1
<input type="checkbox"/>	GOTERM_BP_FAT	angiogenesis	RI	<input type="checkbox"/>	5	1.9E-1	9.5E-1
<input type="checkbox"/>	GOTERM_BP_FAT	regulation of cell migration	RI	<input type="checkbox"/>	5	2.6E-1	9.6E-1
<input type="checkbox"/>	GOTERM_BP_FAT	positive regulation of hydrolase activity	RI	<input type="checkbox"/>	5	2.9E-1	9.7E-1
<input type="checkbox"/>	GOTERM_BP_FAT	regulation of locomotion	RI	<input type="checkbox"/>	5	3.4E-1	9.7E-1
<input type="checkbox"/>	GOTERM_BP_FAT	regulation of cell motion	RI	<input type="checkbox"/>	5	3.4E-1	9.7E-1
<input type="checkbox"/>	GOTERM_CC_FAT	extrinsic-to-membrane	RI	<input type="checkbox"/>	10	3.6E-1	9.4E-1
<input type="checkbox"/>	GOTERM_BP_FAT	regulation of hydrolase activity	RI	<input type="checkbox"/>	6	5.9E-1	1.0E0
<input type="checkbox"/>	GOTERM_BP_FAT	ion homeostasis	RI	<input type="checkbox"/>	7	6.0E-1	1.0E0
<input type="checkbox"/>	GOTERM_BP_FAT	regulation of membrane potential	RI	<input type="checkbox"/>	4	6.1E-1	1.0E0
<input type="checkbox"/>	GOTERM_BP_FAT	ion homeostasis	RI	<input type="checkbox"/>	4	6.1E-1	1.0E0
<input type="checkbox"/>	GOTERM_BP_FAT	regulation of membrane potential	RI	<input type="checkbox"/>	3	6.1E-1	1.0E0
<input type="checkbox"/>	GOTERM_BP_FAT	cellular homeostasis	RI	<input type="checkbox"/>	5	6.4E-1	1.0E0
<input type="checkbox"/>	GOTERM_BP_FAT	calcium homeostasis	RI	<input type="checkbox"/>	5	6.4E-1	1.0E0
<input type="checkbox"/>	GOTERM_BP_FAT	di- th-valent inorganic calcium homeostasis	RI	<input type="checkbox"/>	4	7.1E-1	1.0E0
<input type="checkbox"/>	GOTERM_BP_FAT	cellular calcium ion homeostasis	RI	<input type="checkbox"/>	3	7.7E-1	1.0E0
<input type="checkbox"/>	GOTERM_BP_FAT	cellular calcium ion homeostasis	RI	<input type="checkbox"/>	3	7.9E-1	1.0E0
<input type="checkbox"/>	GOTERM_BP_FAT	chemical homeostasis	RI	<input type="checkbox"/>	7	8.0E-1	1.0E0
<input type="checkbox"/>	GOTERM_BP_FAT	cellular metal ion homeostasis	RI	<input type="checkbox"/>	3	8.1E-1	1.0E0
<input type="checkbox"/>	GOTERM_BP_FAT	hemostatic process	RI	<input type="checkbox"/>	10	8.2E-1	1.0E0
<input type="checkbox"/>	GOTERM_BP_FAT	cellular ion homeostasis	RI	<input type="checkbox"/>	5	8.3E-1	1.0E0
<input type="checkbox"/>	GOTERM_BP_FAT	cellular chemical homeostasis	RI	<input type="checkbox"/>	5	8.4E-1	1.0E0
<input type="checkbox"/>	GOTERM_BP_FAT	cellular di- th-valent inorganic calcium homeostasis	RI	<input type="checkbox"/>	3	8.7E-1	1.0E0
<input type="checkbox"/>	GOTERM_BP_FAT	cellular di- th-valent inorganic calcium homeostasis	RI	<input type="checkbox"/>	3	8.9E-1	1.0E0
<input type="checkbox"/>	GOTERM_BP_FAT	negative regulation of gene expression	RI	<input type="checkbox"/>	6	9.0E-1	1.0E0
<input type="checkbox"/>	GOTERM_BP_FAT	cellular calcium homeostasis	RI	<input type="checkbox"/>	3	9.0E-1	1.0E0
<input type="checkbox"/>	GOTERM_BP_FAT	cellular calcium homeostasis	RI	<input type="checkbox"/>	5	9.3E-1	1.0E0
Annotation Cluster#0							
<input type="checkbox"/>	GOTERM_CC_FAT	DNA-directed RNA polymerase II, holoenzyme	RI	<input checked="" type="checkbox"/>	4	1.3E-1	8.0E-1
<input type="checkbox"/>	GOTERM_BP_FAT	transcription inhibition	RI	<input type="checkbox"/>	3	3.6E-1	9.8E-1
<input type="checkbox"/>	GOTERM_CC_FAT	transcription factor complex	RI	<input type="checkbox"/>	4	6.4E-1	9.9E-1
<input type="checkbox"/>	GOTERM_BP_FAT	transcription, DNA-dependent	RI	<input type="checkbox"/>	4	8.3E-1	1.0E0

https://david.ncifcrf.gov/terms.jsp?amq=52.9,79.85,25,32,39,1,3,47,45,63,76¤tList=1

2/29/2016 DAVID: Database for Annotation, Visualization, and Integrated Discovery (Laboratory of Immunopathogenesis and Biomedicines (LB): National Inst...							
<input type="checkbox"/>	GOTERM_BP_FAT	<u>RNA biosynthetic process</u>	RT	■	4	8.3E-1	1.0E0
Annotation Cluster 91		Enrichment Score: 0.33	G	■	Count	P-Value	Benjamini
<input type="checkbox"/>	GOTERM_BP_FAT	<u>response to lipopolysaccharide</u>	RT	■	3	3.3E-1	9.7E-1
<input type="checkbox"/>	GOTERM_BP_FAT	<u>response to molecule of bacterial origin</u>	RT	■	3	3.8E-1	9.8E-1
<input type="checkbox"/>	GOTERM_BP_FAT	<u>response to bacterium</u>	RT	■	3	8.0E-1	1.0E0
Annotation Cluster 92		Enrichment Score: 0.33	G	■	Count	P-Value	Benjamini
<input type="checkbox"/>	SMART	<u>ANK</u>	RT	■	5	3.9E-1	1.0E0
<input type="checkbox"/>	UP_SEQ_FEATURE	repeat:ANK 1	RT	■	5	4.2E-1	1.0E0
<input type="checkbox"/>	UP_SEQ_FEATURE	repeat:ANK 2	RT	■	5	4.2E-1	1.0E0
<input type="checkbox"/>	SP_PIR_KEYWORDS	<u>ank repeat</u>	RT	■	5	4.4E-1	9.3E-1
<input type="checkbox"/>	INTERPRO	<u>ANKRD1</u>	RT	■	4	4.6E-1	1.0E0
<input type="checkbox"/>	UP_SEQ_FEATURE	repeat:ANK 3	RT	■	4	5.3E-1	1.0E0
<input type="checkbox"/>	UP_SEQ_FEATURE	repeat:ANK 4	RT	■	3	6.6E-1	1.0E0
Annotation Cluster 93		Enrichment Score: 0.32	G	■	Count	P-Value	Benjamini
<input type="checkbox"/>	GOTERM_BP_FAT	<u>cardiac muscle tissue development</u>	RT	■	3	2.2E-1	9.6E-1
<input type="checkbox"/>	GOTERM_BP_FAT	<u>heart development</u>	RT	■	5	4.2E-1	9.9E-1
<input type="checkbox"/>	GOTERM_BP_FAT	<u>striated muscle tissue development</u>	RT	■	3	5.5E-1	1.0E0
<input type="checkbox"/>	GOTERM_BP_FAT	<u>muscle tissue development</u>	RT	■	3	5.7E-1	1.0E0
<input type="checkbox"/>	GOTERM_BP_FAT	<u>muscle organ development</u>	RT	■	3	8.4E-1	1.0E0
Annotation Cluster 94		Enrichment Score: 0.32	G	■	Count	P-Value	Benjamini
<input type="checkbox"/>	GOTERM_CC_FAT	<u>cell fraction</u>	RT	■	19	4.1E-1	9.4E-1
<input type="checkbox"/>	GOTERM_CC_FAT	<u>membrane fraction</u>	RT	■	14	4.9E-1	9.6E-1
<input type="checkbox"/>	GOTERM_CC_FAT	<u>insoluble fraction</u>	RT	■	14	5.4E-1	9.7E-1
Annotation Cluster 95		Enrichment Score: 0.31	G	■	Count	P-Value	Benjamini
<input type="checkbox"/>	GOTERM_CC_FAT	<u>membrane-bounded vesicle</u>	RT	■	11	3.9E-1	9.4E-1
<input type="checkbox"/>	GOTERM_CC_FAT	<u>vesicle</u>	RT	■	12	4.7E-1	9.6E-1
<input type="checkbox"/>	GOTERM_CC_FAT	<u>cytosolic membrane-bounded vesicle</u>	RT	■	10	4.8E-1	9.6E-1
<input type="checkbox"/>	GOTERM_CC_FAT	<u>cytosolic vesicle</u>	RT	■	10	6.7E-1	9.9E-1
Annotation Cluster 96		Enrichment Score: 0.27	G	■	Count	P-Value	Benjamini
<input type="checkbox"/>	INTERPRO	<u>Tetradicocoonlike-like helical</u>	RT	■	4	4.0E-1	1.0E0
<input type="checkbox"/>	INTERPRO	<u>Tetradicocoonlike-TPR_1</u>	RT	■	3	4.3E-1	1.0E0
<input type="checkbox"/>	SMART	<u>TPR</u>	RT	■	3	4.6E-1	1.0E0
<input type="checkbox"/>	INTERPRO	<u>Tetradicocoonlike repeat</u>	RT	■	3	5.1E-1	1.0E0
<input type="checkbox"/>	INTERPRO	<u>Tetradicocoonlike region</u>	RT	■	3	5.3E-1	1.0E0
<input type="checkbox"/>	UP_SEQ_FEATURE	repeat:TPR 3	RT	■	3	5.9E-1	1.0E0
<input type="checkbox"/>	UP_SEQ_FEATURE	repeat:TPR 2	RT	■	3	6.4E-1	1.0E0
<input type="checkbox"/>	UP_SEQ_FEATURE	repeat:TPR 1	RT	■	3	6.4E-1	1.0E0
<input type="checkbox"/>	SP_PIR_KEYWORDS	<u>TPR repeat</u>	RT	■	3	6.7E-1	9.8E-1
Annotation Cluster 97		Enrichment Score: 0.27	G	■	Count	P-Value	Benjamini
<input type="checkbox"/>	KEGG_PATHWAY	<u>Chemokine signaling pathway</u>	RT	■	5	4.5E-1	9.5E-1
<input type="checkbox"/>	KEGG_PATHWAY	<u>Cc chemrta B-mediated antibiogenesis</u>	RT	■	3	5.2E-1	9.6E-1
<input type="checkbox"/>	KEGG_PATHWAY	<u>Bacteriara homodomain-type</u>	RT	■	5	6.4E-1	1.0E0
Annotation Cluster 98		Enrichment Score: 0.27	G	■	Count	P-Value	Benjamini
<input type="checkbox"/>	GOTERM_BP_FAT	<u>response to ionizing radiation</u>	RT	■	3	2.3E-1	9.5E-1
<input type="checkbox"/>	GOTERM_BP_FAT	<u>response to radiation</u>	RT	■	3	8.1E-1	1.0E0
<input type="checkbox"/>	GOTERM_BP_FAT	<u>response to abiotic stimulus</u>	RT	■	5	8.2E-1	1.0E0
Annotation Cluster 99		Enrichment Score: 0.25	G	■	Count	P-Value	Benjamini
<input type="checkbox"/>	GOTERM_CC_FAT	<u>cell membrane</u>	RT	■	5	3.3E-1	9.2E-1
<input type="checkbox"/>	GOTERM_CC_FAT	<u>cell membrane part</u>	RT	■	5	6.7E-1	9.9E-1
<input type="checkbox"/>	GOTERM_CC_FAT	<u>cell membrane</u>	RT	■	12	8.0E-1	1.0E0
Annotation Cluster 90		Enrichment Score: 0.24	G	■	Count	P-Value	Benjamini
<input type="checkbox"/>	UP_SEQ_FEATURE	repeat:LR 3	RT	■	6	4.2E-1	1.0E0
<input type="checkbox"/>	UP_SEQ_FEATURE	repeat:LR 1	RT	■	6	4.8E-1	1.0E0
<input type="checkbox"/>	SP_PIR_KEYWORDS	<u>leucine-rich repeat</u>	RT	■	6	4.8E-1	9.4E-1
<input type="checkbox"/>	UP_SEQ_FEATURE	repeat:LR 2	RT	■	6	4.9E-1	1.0E0
<input type="checkbox"/>	UP_SEQ_FEATURE	repeat:LR 10	RT	■	3	5.0E-1	1.0E0
<input type="checkbox"/>	SMART	<u>LR_TYF</u>	RT	■	3	5.2E-1	1.0E0
<input type="checkbox"/>	INTERPRO	<u>leucine-rich repeat, typical subtype</u>	RT	■	3	5.7E-1	1.0E0
<input type="checkbox"/>	UP_SEQ_FEATURE	Leucine-rich repeat	RT	■	3	5.8E-1	1.0E0
<input type="checkbox"/>	INTERPRO	Leucine-rich repeat	RT	■	4	6.0E-1	1.0E0

<https://david.ncifcrf.gov/terms.jsp?term=jsp?rank=52.977985.25.32.39.13.47.45.63768&cururl=1>

2292016 DAVID: Database for Annotation, Visualization, and Integrated Discovery (Laboratory of Immunopathogenesis and Biinformatics (LB): National Inst...

Gene	Category	Enrichment Score	Count	P-Value Benjamini
UP_SEQ_FEATURE	domain:PM	0.14	4	6.6E-1 1.0E0
SMART	RT		4	7.2E-1 1.0E0
INTERPRO	Pickstick homolog	0.15	4	7.7E-1 1.0E0
SP_PIR_KEYWORDS	Enrichment Score: 0.15	G	Count	P-Value Benjamini
GOTERM_CC_FAT	ultrason	RT	3	4.5E-1 9.3E-1
GOTERM_CC_FAT	ultrason	RT	3	8.9E-1 1.0E0
GOTERM_CC_FAT	vesicular fraction	RT	3	9.0E-1 1.0E0
Annotation Cluster74	Enrichment Score: 0.15	G	Count	P-Value Benjamini
GOTERM_BP_FAT	regulation of cell growth	RT	4	5.8E-1 1.0E0
GOTERM_BP_FAT	regulation of cell size	RT	4	6.1E-1 1.0E0
GOTERM_BP_FAT	regulation of cellular component size	RT	4	7.9E-1 1.0E0
GOTERM_BP_FAT	regulation of growth	RT	4	9.0E-1 1.0E0
Annotation Cluster75	Enrichment Score: 0.15	G	Count	P-Value Benjamini
GOTERM_MF_FAT	transcription corepressor activity	RT	3	6.2E-1 1.0E0
GOTERM_MF_FAT	transcription cofactor activity	RT	6	6.0E-1 1.0E0
Annotation Cluster76	Enrichment Score: 0.14	G	Count	P-Value Benjamini
GOTERM_MF_FAT	GTPase activator activity	RT	4	6.2E-1 1.0E0
GOTERM_MF_FAT	GTPase regulator activity	RT	6	7.0E-1 1.0E0
GOTERM_MF_FAT	mitochondrial ribonuclease regulator activity	RT	6	7.1E-1 1.0E0
GOTERM_MF_FAT	small GTPase regulator activity	RT	4	7.6E-1 1.0E0
GOTERM_MF_FAT	anyone activator activity	RT	4	8.7E-1 1.0E0
Annotation Cluster77	Enrichment Score: 0.14	G	Count	P-Value Benjamini
GOTERM_BP_FAT	cytoskeleton organization	RT	8	5.0E-1 9.9E-1
GOTERM_BP_FAT	actin cytoskeleton organization	RT	3	8.6E-1 1.0E0
GOTERM_BP_FAT	actin filament-based process	RT	3	8.9E-1 1.0E0
Annotation Cluster78	Enrichment Score: 0.13	G	Count	P-Value Benjamini
GOTERM_MF_FAT	transcription cofactor activity	RT	6	6.0E-1 1.0E0
GOTERM_MF_FAT	transcription corepressor activity	RT	3	8.2E-1 1.0E0
GOTERM_MF_FAT	transcription activator activity	RT	5	8.5E-1 1.0E0
Annotation Cluster79	Enrichment Score: 0.12	G	Count	P-Value Benjamini
GOTERM_CC_FAT	oligosaccharyl transferase activity	RT	34	6.1E-1 9.8E-1
GOTERM_CC_FAT	integral to plasma membrane	RT	16	8.3E-1 1.0E0
GOTERM_CC_FAT	ATPase to plasma membrane	RT	16	8.6E-1 1.0E0
Annotation Cluster80	Enrichment Score: 0.11	G	Count	P-Value Benjamini
SP_PIR_KEYWORDS	metal binding	RT	44	4.7E-1 9.4E-1
GOTERM_MF_FAT	transition metal ion binding	RT	39	6.8E-1 1.0E0
SP_PIR_KEYWORDS	Zinc finger	RT	23	7.3E-1 9.8E-1
GOTERM_MF_FAT	Zinc	RT	29	7.5E-1 9.9E-1
GOTERM_MF_FAT	cellular binding	RT	54	8.9E-1 1.0E0
GOTERM_MF_FAT	metal ion binding	RT	53	9.0E-1 1.0E0
GOTERM_MF_FAT	ion binding	RT	54	9.1E-1 1.0E0
GOTERM_MF_FAT	Zinc ion binding	RT	26	9.6E-1 1.0E0
Annotation Cluster81	Enrichment Score: 0.1	G	Count	P-Value Benjamini
GOTERM_BP_FAT	positive regulation of transcription from RNA polymerase II promoter	RT	6	6.7E-1 1.0E0
GOTERM_BP_FAT	regulation of transcription from RNA polymerase II promoter	RT	11	6.8E-1 1.0E0
GOTERM_BP_FAT	positive regulation of nucleoside, nucleotide, and nucleic acid metabolic process	RT	9	7.4E-1 1.0E0
GOTERM_BP_FAT	positive regulation of transcription	RT	8	7.7E-1 1.0E0
GOTERM_BP_FAT	positive regulation of metabolic process	RT	12	7.7E-1 1.0E0
GOTERM_BP_FAT	positive regulation of alcohol compound metabolic process	RT	9	7.7E-1 1.0E0
GOTERM_BP_FAT	positive regulation of gene expression dependent	RT	8	7.9E-1 1.0E0
GOTERM_BP_FAT	positive regulation of transcription, DNA dependent	RT	6	8.6E-1 1.0E0
GOTERM_BP_FAT	positive regulation of RNA metabolic process	RT	6	8.6E-1 1.0E0
GOTERM_BP_FAT	positive regulation of macromolecule biosynthetic process	RT	8	8.8E-1 1.0E0
GOTERM_BP_FAT	positive regulation of cellular biosynthetic process	RT	8	9.1E-1 1.0E0

<https://david.ncifcrf.gov/terms.jsp?rand=52.979.85.25.32.38.1.3.47.45.63.788.currentList=1>

2/29/2016 DAVID: Database for Annotation, Visualization, and Integrated Discovery (Laboratory of Immunopathogenesis and Bioinformatics (LBI): National Inst...

<input type="checkbox"/>	UP_SEQ_FEATURE	zinc finger region: C2H2-type 4	RT		6	9.2E-1	1.0E0
<input type="checkbox"/>	UP_SEQ_FEATURE	zinc finger region: C2H2-type 2	RT		6	9.4E-1	1.0E0
<input type="checkbox"/>	UP_SEQ_FEATURE	zinc finger region: C2H2-type 3	RT		6	9.5E-1	1.0E0
<input type="checkbox"/>	INTERPRO	Zinc Finger, C2H2-type/Interzone, NLA-binding	RT		5	9.8E-1	1.0E0
<input type="checkbox"/>	UP_SEQ_FEATURE	zinc finger region: C2H2-type 5	RT		4	9.8E-1	1.0E0
<input type="checkbox"/>	SMART	ZnF_C2H2	RT		6	9.8E-1	1.0E0
<input type="checkbox"/>	UP_SEQ_FEATURE	zinc finger region: C2H2-type 7	RT		3	9.9E-1	1.0E0
<input type="checkbox"/>	INTERPRO	Zinc Finger, C2H2-type	RT		6	9.9E-1	1.0E0
<input type="checkbox"/>	INTERPRO	Zinc Finger, C2H2-like	RT		6	9.9E-1	1.0E0
<input type="checkbox"/>	UP_SEQ_FEATURE	zinc finger region: C2H2-type 6	RT		3	9.9E-1	1.0E0
		Enrichment Score: 0.01	G		Count	P-Value	Benjamini
<input type="checkbox"/>	SP_PIR_KEYWORDS	cell adhesion	RT		4	9.4E-1	1.0E0
<input type="checkbox"/>	GOTERM_BP_FAT	cell adhesion	RT		6	9.8E-1	1.0E0
<input type="checkbox"/>	GOTERM_BP_FAT	biological adhesion	RT		6	9.8E-1	1.0E0
		Enrichment Score: 0	G		Count	P-Value	Benjamini
<input type="checkbox"/>	Annotation Character91	Immunoglobulin-like fold	RT		4	9.9E-1	1.0E0
<input type="checkbox"/>	SP_PIR_KEYWORDS	Immunoglobulin domain	RT		3	9.9E-1	1.0E0
<input type="checkbox"/>	INTERPRO	Immunoglobulin-like	RT		3	9.9E-1	1.0E0
		Enrichment Score: 0	G		Count	P-Value	Benjamini
<input type="checkbox"/>	SP_PIR_KEYWORDS	Immunoglobulin-like fold	RT		6	1.0E0	1.0E0
<input type="checkbox"/>	GOTERM_BP_FAT	G-protein-coupled receptor domain	RT		8	1.0E0	1.0E0
<input type="checkbox"/>	INTERPRO	G-protein-coupled receptor domain	RT		3	1.0E0	1.0E0
<input type="checkbox"/>	INTERPRO	GPCR, rhodopsin-like superfamily	RT		3	1.0E0	1.0E0
<input type="checkbox"/>	INTERPRO	7TM GPCR, rhodopsin-like	RT		3	1.0E0	1.0E0
<input type="checkbox"/>	PIR_SUPERFAMILY	PIR57800006:rhodopsin-like G protein-coupled receptors	RT		3	1.0E0	1.0E0
<input type="checkbox"/>	SP_PIR_KEYWORDS	a-arrestin-coupled receptor	RT		3	1.0E0	1.0E0
		Enrichment Score: 0	G		Count	P-Value	Benjamini
<input type="checkbox"/>	Annotation Character93	extracellular region part	RT		5	1.0E0	1.0E0
<input type="checkbox"/>	SP_PIR_KEYWORDS	Sarcosyl	RT		10	1.0E0	1.0E0
<input type="checkbox"/>	SP_PIR_KEYWORDS	disulfide bond	RT		20	1.0E0	1.0E0
<input type="checkbox"/>	UP_SEQ_FEATURE	glycosylation site: N-linked (GlcNAc...)	RT		33	1.0E0	1.0E0
<input type="checkbox"/>	SP_PIR_KEYWORDS	signal peptide	RT		23	1.0E0	1.0E0
<input type="checkbox"/>	UP_SEQ_FEATURE	oligocystin	RT		23	1.0E0	1.0E0
<input type="checkbox"/>	SP_PIR_KEYWORDS	extracellular matrix	RT		34	1.0E0	1.0E0
<input type="checkbox"/>	GOTERM_CC_FAT	disulfide bond	RT		12	1.0E0	1.0E0
<input type="checkbox"/>	UP_SEQ_FEATURE		RT		15	1.0E0	1.0E0

217 terms were not clustered.

Please cite [Nature Protocols 2009, 4\(1\):44](#) & [Genome Biology 2003, 4\(9\):23](#) within any publication that makes use of any methods inspired by DAVID.



[Term of Service](#) | [Contact Us](#) | [Site Map](#)



DAVID Bioinformatics Resources 6.7
National Institute of Allergy and Infectious Diseases (NIAID), NIH

2292016 DAVID : Database for Annotation, Visualization, and Integrated Discovery (Laboratory of Immunopathogenesis and Bioinformatics (LBj), National Ins...

Functional Annotation Clustering

Current Gene List: List_1

Current Background: Homo sapiens

323 DAVID IDs

Options Classification Stringency Medium
 Re-run using options Create Sublist

[Help and Manual](#)

100 Cluster(s)

Annotation Cluster 1	Enrichment Score: 2.27	Count	P-Value	Benjamini
<input type="checkbox"/> GOTERM_GG_FAT	mitochondrion	33	3.6E-4	5.0E-2
<input type="checkbox"/> SP_PR_KEWOROS	mitochondrion	28	4.6E-4	3.6E-2
<input type="checkbox"/> GOTERM_GG_FAT	cytosolic envelope	22	7.2E-4	6.6E-2
<input type="checkbox"/> GOTERM_GG_FAT	cytosol	22	7.5E-4	5.2E-2
<input type="checkbox"/> GOTERM_GG_FAT	cytosolic membrane	30	3.5E-3	1.8E-1
<input type="checkbox"/> GOTERM_GG_FAT	mitochondrial membrane	15	3.6E-3	1.6E-1
<input type="checkbox"/> GOTERM_GG_FAT	mitochondrial part	19	5.7E-3	1.5E-1
<input type="checkbox"/> GOTERM_GG_FAT	cytosolic lumen	13	5.7E-3	1.4E-1
<input type="checkbox"/> GOTERM_GG_FAT	mitochondrial inner membrane	12	8.9E-3	1.9E-1
<input type="checkbox"/> GOTERM_GG_FAT	transit peptide/mitochondrion	13	8.0E-2	1.0E0
<input type="checkbox"/> SP_SEQ_FEATURE	transit peptide	13	8.6E-2	7.5E-1
<input type="checkbox"/> SP_PR_KEWOROS	mitochondrion inner membrane	6	2.0E-1	8.4E-1
Annotation Cluster 2	Enrichment Score: 2.09	Count	P-Value	Benjamini
<input type="checkbox"/> SP_PR_KEWOROS	cytosol	12	6.0E-4	3.7E-2
<input type="checkbox"/> GOTERM_GG_FAT	cytosol	11	2.7E-2	3.6E-1
<input type="checkbox"/> SP_PR_KEWOROS	lysosome	7	3.4E-2	5.1E-1
Annotation Cluster 3	Enrichment Score: 2	Count	P-Value	Benjamini
<input type="checkbox"/> GOTERM_GG_FAT	mitochondrial membrane	43	3.7E-3	1.4E-1
<input type="checkbox"/> GOTERM_GG_FAT	membrane-anchored lumen	44	4.7E-3	1.5E-1
<input type="checkbox"/> GOTERM_GG_FAT	cytosolic lumen	43	5.6E-3	1.6E-1
<input type="checkbox"/> GOTERM_GG_FAT	nuclear lumen	35	1.0E-2	1.9E-1
<input type="checkbox"/> GOTERM_GG_FAT	nucleolus	20	9.7E-2	6.5E-1
Annotation Cluster 4	Enrichment Score: 1.88	Count	P-Value	Benjamini
<input type="checkbox"/> GOTERM_GG_FAT	ltdc_vccycle	9	1.8E-2	2.9E-1
<input type="checkbox"/> GOTERM_GG_FAT	lysosome	9	1.8E-2	2.9E-1
<input type="checkbox"/> SP_PR_KEWOROS	lysosome	7	3.4E-2	5.1E-1
<input type="checkbox"/> GOTERM_GG_FAT	lysosome	9	4.5E-2	5.2E-1
Annotation Cluster 5	Enrichment Score: 1.37	Count	P-Value	Benjamini
<input type="checkbox"/> SP_PR_KEWOROS	nucleolar metabolic	5	2.6E-4	2.7E-2
<input type="checkbox"/> GOTERM_BP_FAT	nucleolar metabolic	4	1.7E-3	9.1E-1
<input type="checkbox"/> GOTERM_BP_FAT	KEGG_PATHWAY	7	3.0E-3	2.9E-1
<input type="checkbox"/> GOTERM_BP_FAT	nucleolar metabolic	5	3.5E-3	9.2E-1
<input type="checkbox"/> GOTERM_BP_FAT	active site:Pro-sphingosidine intermediate	3	3.8E-3	9.7E-1
<input type="checkbox"/> SMART	NDK	3	6.1E-3	5.1E-1
<input type="checkbox"/> INTERPRO	Nucleoside diphosphate kinase_coxe	3	6.9E-3	9.7E-1
<input type="checkbox"/> GOTERM_MF_FAT	nucleoside diphosphate kinase activity	3	8.9E-3	7.1E-1
<input type="checkbox"/> GOTERM_BP_FAT	cytosolic metabolic process	4	9.2E-3	9.7E-1
<input type="checkbox"/> GOTERM_BP_FAT	ltdc_metallic_process	3	1.0E-2	9.5E-1
<input type="checkbox"/> GOTERM_BP_FAT	GTP biosynthetic process	3	1.0E-2	9.5E-1
<input type="checkbox"/> GOTERM_BP_FAT	ltdc_biosynthetic_process	3	1.0E-2	9.5E-1
<input type="checkbox"/> GOTERM_BP_FAT	CTP metabolic process	3	1.3E-2	9.5E-1
<input type="checkbox"/> GOTERM_BP_FAT	cytosolic ribonucleoside triphosphate biosynthetic process	3	1.3E-2	9.5E-1
<input type="checkbox"/> GOTERM_BP_FAT	nucleoside metabolic process	3	1.3E-2	9.5E-1

[Download File](#)

8.3 Cattle DAVID clusters

https://david.ncifcrf.gov/htm2/htm1sp?rand=52.9179.05.25.32.39.1.3.47.45.63.78&currList=0

22/9/2016	DAVID : Database for Annotation, Visualization, and Integrated Discovery (Laboratory of Immunopathogenesis and Biinformatics (UB): National Inst...						
<input type="checkbox"/>	GOTERM_BP_FAT	<u>CTP biosynthetic process</u>	RT	■	3	1.3E-2	9.5E-1
<input type="checkbox"/>	GOTERM_BP_FAT	<u>oxymandipine nucleoside triphosphate biosynthetic process</u>	RT	■	3	1.8E-2	9.5E-1
<input type="checkbox"/>	GOTERM_BP_FAT	<u>GTP metabolic process</u>	RT	■	3	1.8E-2	9.5E-1
<input type="checkbox"/>	KEGG_PATHWAY	<u>Purine metabolism</u>	RT	■	7	2.8E-2	7.9E-1
<input type="checkbox"/>	GOTERM_BP_FAT	<u>oxymandipine ribonucleoside biosynthetic process</u>	RT	■	3	2.8E-2	9.8E-1
<input type="checkbox"/>	GOTERM_BP_FAT	<u>oxymandipine ribonucleoside metabolic process</u>	RT	■	3	3.1E-2	9.6E-1
<input type="checkbox"/>	GOTERM_BP_FAT	<u>oxymandipine ribonucleoside metabolic process</u>	RT	■	3	3.5E-2	9.5E-1
<input type="checkbox"/>	GOTERM_BP_FAT	<u>oxymandipine nucleoside biosynthetic process</u>	RT	■	3	5.6E-2	9.7E-1
<input type="checkbox"/>	GOTERM_BP_FAT	<u>nitroben compound biosynthetic process</u>	RT	■	11	6.0E-2	9.7E-1
<input type="checkbox"/>	GOTERM_BP_FAT	<u>ribosyltransferase activity, ribonucleoside</u>	RT	■	3	1.0E-1	9.0E-1
<input type="checkbox"/>	GOTERM_BP_FAT	<u>nucleoside metabolic process</u>	RT	■	4	1.0E-1	9.8E-1
<input type="checkbox"/>	GOTERM_BP_FAT	<u>oxirine ribonucleoside biosynthetic process</u>	RT	■	5	1.5E-1	9.8E-1
<input type="checkbox"/>	GOTERM_BP_FAT	<u>nucleosides, nucleoside, nucleotide kinase activity</u>	RT	■	3	1.5E-1	9.3E-1
<input type="checkbox"/>	GOTERM_BP_FAT	<u>ribonucleoside biosynthetic process</u>	RT	■	5	1.7E-1	9.8E-1
<input type="checkbox"/>	GOTERM_BP_FAT	<u>ribonucleoside metabolic process</u>	RT	■	3	1.9E-1	9.9E-1
<input type="checkbox"/>	GOTERM_BP_FAT	<u>nucleoside triphosphate metabolic process</u>	RT	■	5	2.0E-1	9.9E-1
<input type="checkbox"/>	GOTERM_BP_FAT	<u>oxirine ribonucleoside metabolic process</u>	RT	■	5	2.2E-1	9.9E-1
<input type="checkbox"/>	GOTERM_BP_FAT	<u>nucleoside biosynthetic process</u>	RT	■	6	2.3E-1	9.9E-1
<input type="checkbox"/>	GOTERM_BP_FAT	<u>oxirine ribonucleoside triphosphate biosynthetic process</u>	RT	■	4	2.5E-1	9.9E-1
<input type="checkbox"/>	GOTERM_BP_FAT	<u>nucleosides, nucleoside and nucleotide biosynthetic process</u>	RT	■	6	2.5E-1	9.9E-1
<input type="checkbox"/>	GOTERM_BP_FAT	<u>nucleoside triphosphate biosynthetic process</u>	RT	■	4	2.5E-1	9.8E-1
<input type="checkbox"/>	GOTERM_BP_FAT	<u>oxirine nucleoside triphosphate biosynthetic process</u>	RT	■	4	2.5E-1	9.8E-1
<input type="checkbox"/>	GOTERM_BP_FAT	<u>oxirine nucleoside metabolic process</u>	RT	■	5	4.1E-1	9.9E-1
<input type="checkbox"/>	GOTERM_BP_FAT	<u>respiratory chain complex IV assembly</u>	RT	■	3	8.0E-3	9.8E-1
<input type="checkbox"/>	GOTERM_BP_FAT	<u>cellular protein complex assembly</u>	RT	■	7	6.6E-2	9.7E-1
<input type="checkbox"/>	GOTERM_BP_FAT	<u>generation of precursor metabolites and energy</u>	RT	■	8	3.1E-1	9.9E-1
	Annotation Cluster 6				Count	P-Value	Benjamini
<input type="checkbox"/>	GOTERM_BP_FAT	<u>transferrin metal ion binding</u>	RT	■	5	4.1E-1	9.9E-1
<input type="checkbox"/>	GOTERM_BP_FAT	<u>metal binding</u>	RT	■	62	6.2E-3	7.3E-1
<input type="checkbox"/>	SP_PIR_KEYWORDS	<u>zinc-chloride</u>	RT	■	65	8.3E-3	2.8E-1
<input type="checkbox"/>	SP_PIR_KEYWORDS	<u>zinc</u>	RT	■	40	1.8E-2	4.1E-1
<input type="checkbox"/>	GOTERM_BP_FAT	<u>zinc ion binding</u>	RT	■	43	1.3E-1	7.7E-1
<input type="checkbox"/>	GOTERM_BP_FAT	<u>metal ion binding</u>	RT	■	45	1.4E-1	9.3E-1
<input type="checkbox"/>	GOTERM_BP_FAT	<u>cation binding</u>	RT	■	76	1.4E-1	9.2E-1
<input type="checkbox"/>	GOTERM_BP_FAT	<u>ion binding</u>	RT	■	76	1.6E-1	9.4E-1
	Annotation Cluster 7				Count	P-Value	Benjamini
<input type="checkbox"/>	GOTERM_BP_FAT	<u>adenyl nucleotide binding</u>	RT	■	76	2.0E-1	9.5E-1
<input type="checkbox"/>	GOTERM_BP_FAT	<u>oxirine nucleoside binding</u>	RT	■	37	2.2E-2	8.4E-1
<input type="checkbox"/>	GOTERM_BP_FAT	<u>adenyl ribonucleotide binding</u>	RT	■	37	2.6E-2	8.5E-1
<input type="checkbox"/>	GOTERM_BP_FAT	<u>nucleoside binding</u>	RT	■	35	2.7E-2	8.1E-1
<input type="checkbox"/>	UP_SEQ_FEATURE	<u>binding site/ATP</u>	RT	■	37	2.9E-2	7.9E-1
<input type="checkbox"/>	GOTERM_BP_FAT	<u>ATP binding</u>	RT	■	16	3.2E-2	1.0E0
<input type="checkbox"/>	SP_PIR_KEYWORDS	<u>atp-binding</u>	RT	■	34	3.6E-2	8.2E-1
<input type="checkbox"/>	GOTERM_BP_FAT	<u>nucleotide binding</u>	RT	■	31	3.8E-2	5.3E-1
<input type="checkbox"/>	GOTERM_BP_FAT	<u>nucleoside phosphate-binding region/ATP</u>	RT	■	47	5.2E-2	8.7E-1
<input type="checkbox"/>	GOTERM_BP_FAT	<u>oxirine nucleotide binding</u>	RT	■	23	6.5E-2	1.0E0
<input type="checkbox"/>	GOTERM_BP_FAT		RT	■	40	7.9E-2	9.2E-1

<https://david.ncfcr.gov/terms.jsp?and=-52.9.79.85.25.32.39.1.3.47.46.63.78¤t=15>

2292016 DAVID: Database for Annotation, Visualization, and Integrated Discovery (Laboratory of Immunopathogenesis and Bioinformatics (LB): National Inst...

Annotation Cluster#	Enrichment Score	Count	P_Value	Benjamini
Annotation Cluster#16	0.94	6	2.4E-1	8.7E-1
SP_PRR_KEYWORDS	G			
Annotation Cluster#16	0.84	3	7.1E-2	9.1E-1
GOTERM_MF_FAT	G			
SP_PRR_KEYWORDS	G			
Annotation Cluster#17	0.82	3	2.9E-1	9.7E-1
GOTERM_MF_FAT	G			
Annotation Cluster#18	0.82	19	3.0E-3	1.3E-1
SP_PRR_KEYWORDS	G			
Annotation Cluster#19	0.82	27	2.1E-2	9.5E-1
GOTERM_BP_FAT	G			
Annotation Cluster#20	0.82	16	1.5E-1	7.9E-1
GOTERM_BP_FAT	G			
Annotation Cluster#21	0.83	6	4.7E-2	5.1E-1
GOTERM_BP_FAT	G			
Annotation Cluster#16	0.84	6	2.4E-1	8.7E-1
endothelinase activity, production 5-	G			
phosphonucleotides	G			
endonuclease activity	G			
Endonuclease	G			
nuclease	G			
endonuclease activity, active with either	G			
5'- or deoxyribonucleic acids and	G			
production 5'-phosphonucleotides	G			
nuclease activity	G			
endonuclease activity	G			
endonuclease activity	G			
RNA binding	G			
RNA recombination motif, RNP-1	G			
Nucleotide-binding, alpha-beta dalt	G			
domain:RPM	G			
domain:RPM 2	G			
domain:RPM 1	G			
Zinc finger, RING-type, conserved site	G			
RING	G			
Zinc finger, C2HC2 RING-type	G			
zinc finger region:RING-type	G			
Enrichment Score	G			
phosphorus metabolic process	G			
phospholipid metabolic process	G			
binding sterolATP	G			
ATP binding	G			
ATP-binding	G			
nucleotide phosphate-binding	G			
Serine/threonine-arginin kin	G			
phosphorylation	G			
Serine/threonine-arginin kin	G			
domain:Protein kinase	G			
Protein kinase, core	G			
kinase	G			
serine/threonine-arginin kin	G			
protein kinase activity	G			
Protein kinase, ATP binding site	G			
S_TKc	G			
Acute myeloid leukemia	G			
Serine/threonine-arginin kinase	G			
protein serine/threonine kinase activity	G			
protein amino acid phosphorylation	G			
active site:Protein acceptor	G			
Chaperonin signaling pathway	G			
Intracellular signaling cascade	G			
Enrichment Score: 0.82	G			
ncRNA metabolic process	G			
ncRNA processing	G			
RNA processing	G			
RNA metabolic process	G			
Iron processing	G			
Enrichment Score: 0.83	G			
mitochondrial ATP synthesis coupled	G			
mitochondrial membrane dalt	G			
acetylcholinesterase	G			

<http://www.uniprot.org/keywords/?query=serine/threonine-protein%20kinase>

2292016	DAVID : Database for Annotation, Visualization, and Integrated Discovery (Laboratory of Immunopathogenesis and Bioinformatics (UB): National Inst...						
<input type="checkbox"/>	GOTERM_BP_FAT	ATP synthesis coupled electron transport	RT		4	7.5E-2	9.9E-1
<input type="checkbox"/>	GOTERM_BP_FAT	oxidative phosphorylation	RT		5	9.3E-2	9.9E-1
<input type="checkbox"/>	GOTERM_BP_FAT	respiratory electron transport chain	RT		4	1.0E-1	9.9E-1
<input type="checkbox"/>	KEGG_PATHWAY	Oxidative phosphorylation	RT		5	1.3E-1	9.3E-1
<input type="checkbox"/>	GOTERM_BP_FAT	electron transport chain	RT		5	1.4E-1	9.9E-1
<input type="checkbox"/>	GOTERM_BP_FAT	energy derivation by oxidation of organic compounds	RT		4	2.4E-1	9.9E-1
<input type="checkbox"/>	GOTERM_BP_FAT	mitochondrial respiratory chain	RT		5	2.5E-1	9.9E-1
<input type="checkbox"/>	GOTERM_BP_FAT	generation of precursor metabolites and energy	RT		3	2.6E-1	9.0E-1
<input type="checkbox"/>	GOTERM_CC_FAT	respiratory chain	RT		8	3.1E-1	9.9E-1
<input type="checkbox"/>	GOTERM_CC_FAT	electron transport	RT		3	3.3E-1	9.2E-1
<input type="checkbox"/>	SP_PIR_KEYWORDS		RT		3	4.8E-1	9.5E-1
<input type="checkbox"/>	GOTERM_BP_FAT	In vitro embryonic development	RT		8	3.5E-2	9.5E-1
<input type="checkbox"/>	GOTERM_BP_FAT	chloride embryonic development	RT		9	2.3E-1	9.9E-1
<input type="checkbox"/>	GOTERM_BP_FAT	embryonic development, end in birth or sex description	RT		9	2.3E-1	9.9E-1
<input type="checkbox"/>	GOTERM_BP_FAT	embryonic organ development	RT		5	3.6E-1	9.9E-1
<input type="checkbox"/>	Annotation Cluster22		RT		Count	P_Value	Benjamini
<input type="checkbox"/>	GOTERM_BP_FAT	regulation of apoptosis	RT		20	1.1E-1	9.9E-1
<input type="checkbox"/>	GOTERM_BP_FAT	regulation of programmed cell death	RT		20	1.2E-1	9.9E-1
<input type="checkbox"/>	GOTERM_BP_FAT	regulation of cell death	RT		20	1.2E-1	9.9E-1
<input type="checkbox"/>	GOTERM_BP_FAT	negative regulation of apoptosis	RT		10	1.7E-1	9.9E-1
<input type="checkbox"/>	GOTERM_BP_FAT	negative regulation of programmed cell death	RT		10	1.8E-1	9.9E-1
<input type="checkbox"/>	GOTERM_BP_FAT	anti-apoptosis	RT		6	2.9E-1	9.9E-1
<input type="checkbox"/>	Annotation Cluster24		RT		Count	P_Value	Benjamini
<input type="checkbox"/>	GOTERM_BP_FAT	oxidative phosphorylation	RT		5	9.3E-2	9.9E-1
<input type="checkbox"/>	KEGG_PATHWAY	Oxidative phosphorylation	RT		5	1.3E-1	9.3E-1
<input type="checkbox"/>	GOTERM_MF_FAT	Hydrogen ion transmembrane transport	RT		4	1.8E-1	9.4E-1
<input type="checkbox"/>	GOTERM_MF_FAT	ATPase activity	RT		5	2.3E-1	9.6E-1
<input type="checkbox"/>	GOTERM_MF_FAT	hydrolytic cation transmembrane transporter activity	RT		4	2.4E-1	9.6E-1
<input type="checkbox"/>	Annotation Cluster25		RT		Count	P_Value	Benjamini
<input type="checkbox"/>	GOTERM_CC_FAT	non-membrane-bounded organelle	RT		50	8.4E-2	6.2E-1
<input type="checkbox"/>	GOTERM_CC_FAT	intracellular non-membrane-bounded organelle	RT		50	8.4E-2	6.2E-1
<input type="checkbox"/>	GOTERM_CC_FAT	Cytoskeleton	RT		21	6.8E-1	9.9E-1
<input type="checkbox"/>	Annotation Cluster26		RT		Count	P_Value	Benjamini
<input type="checkbox"/>	GOTERM_BP_FAT	mitotic cell cycle	RT		13	3.0E-2	9.9E-1
<input type="checkbox"/>	GOTERM_BP_FAT	cell cycle	RT		22	3.2E-2	9.6E-1
<input type="checkbox"/>	GOTERM_BP_FAT	Interphase of mitotic cell cycle	RT		6	3.5E-2	9.6E-1
<input type="checkbox"/>	GOTERM_BP_FAT	Interphase	RT		6	3.9E-2	9.5E-1
<input type="checkbox"/>	GOTERM_BP_FAT	cell cycle phase	RT		12	1.1E-1	9.9E-1
<input type="checkbox"/>	GOTERM_BP_FAT	Cell cycle	RT		5	1.2E-1	9.7E-1
<input type="checkbox"/>	GOTERM_BP_FAT	cell cycle arrest	RT		15	1.2E-1	9.9E-1
<input type="checkbox"/>	GOTERM_BP_FAT	regulation of cell cycle	RT		10	1.3E-1	9.7E-1
<input type="checkbox"/>	GOTERM_BP_FAT	organellar fusion	RT		4	2.1E-1	9.9E-1
<input type="checkbox"/>	GOTERM_BP_FAT	cell cycle checkpoint	RT		4	2.1E-1	9.9E-1
<input type="checkbox"/>	GOTERM_BP_FAT	G1/S transition of mitotic cell cycle	RT		3	2.6E-1	9.9E-1
<input type="checkbox"/>	GOTERM_BP_FAT	mitosis	RT		6	3.4E-1	9.9E-1
<input type="checkbox"/>	GOTERM_BP_FAT	nuclear division	RT		8	3.5E-1	9.9E-1
<input type="checkbox"/>	GOTERM_BP_FAT	M phase	RT		6	3.4E-1	9.9E-1
<input type="checkbox"/>	GOTERM_BP_FAT	M phase of mitotic cell cycle	RT		4	4.1E-1	9.4E-1
<input type="checkbox"/>	GOTERM_BP_FAT	spindle	RT		7	4.1E-1	9.9E-1
<input type="checkbox"/>	GOTERM_BP_FAT	cell division	RT		6	4.2E-1	9.4E-1
<input type="checkbox"/>	SP_PIR_KEYWORDS	regulation of mitotic cell cycle	RT		4	5.0E-1	1.0E0
<input type="checkbox"/>	SP_PIR_KEYWORDS	mitosis	RT		4	5.7E-1	9.9E-1
<input type="checkbox"/>	Annotation Cluster27		RT		Count	P_Value	Benjamini

22/20/16 DAVID: Database for Annotation, Visualization and Integrated Discovery (Laboratory of Immunopathogenesis and Bioformatics (UB): National Inst...							
<input type="checkbox"/>	SP_PIR_KEYWORDS	actin transport	RT		13	9.6E-2	7.4E-1
<input type="checkbox"/>	GOTERM_BP_FAT	cellular protein localization	RT		12	1.1E-1	9.9E-1
<input type="checkbox"/>	GOTERM_BP_FAT	cellular microtubule localization	RT		12	1.1E-1	9.9E-1
<input type="checkbox"/>	GOTERM_BP_FAT	actin transport	RT		19	1.2E-1	9.9E-1
<input type="checkbox"/>	GOTERM_BP_FAT	intracellular actin transport	RT		11	1.2E-1	9.9E-1
<input type="checkbox"/>	GOTERM_BP_FAT	stabilishment of actin localization	RT		19	1.3E-1	9.7E-1
<input type="checkbox"/>	GOTERM_BP_FAT	actin localization	RT		20	2.1E-1	9.9E-1
<input type="checkbox"/>	GOTERM_BP_FAT	actin localization in cytosol	RT		5	2.5E-1	9.9E-1
<input type="checkbox"/>	GOTERM_BP_FAT	actin transport	RT		6	3.2E-1	9.9E-1
<input type="checkbox"/>	GOTERM_BP_FAT	intracellular transport	RT		14	3.7E-1	9.9E-1
<input type="checkbox"/>	GOTERM_BP_FAT	actin import	RT		3	6.7E-1	1.0E0
<input type="checkbox"/>	Annotation Cluster/28						
<input type="checkbox"/>	INTERPRO	Protein Kinase, C-terminal	G		Count	P_Value	Benjamini
<input type="checkbox"/>	SMART	S_LTK_X	RT		3	1.4E-1	1.0E0
<input type="checkbox"/>	SMART	S_LTK	RT		3	2.1E-1	9.7E-1
<input type="checkbox"/>	INTERPRO	AGC-Kinase, C-terminal domain;AGC-Kinase C-terminal	RT		7	2.1E-1	9.5E-1
<input type="checkbox"/>	UP_SEQ_FEATURE	Serine/threonine actin kinase	RT		3	2.2E-1	1.0E0
<input type="checkbox"/>	INTERPRO		RT		3	2.2E-1	1.0E0
<input type="checkbox"/>	Annotation Cluster/29						
<input type="checkbox"/>	GOTERM_CC_FAT	microtubule cytoskeleton	G		Count	P_Value	Benjamini
<input type="checkbox"/>	GOTERM_CC_FAT	microtubule organization center;act	RT		15	5.0E-2	5.2E-1
<input type="checkbox"/>	GOTERM_CC_FAT	centrosome	RT		4	5.7E-2	5.2E-1
<input type="checkbox"/>	GOTERM_CC_FAT	microtubule organization center	RT		8	6.3E-2	5.4E-1
<input type="checkbox"/>	GOTERM_BP_FAT	microtubule-based process	RT		8	1.0E-1	6.4E-1
<input type="checkbox"/>	GOTERM_BP_FAT	microtubule cytoskeleton organization	RT		8	1.6E-1	9.9E-1
<input type="checkbox"/>	SP_PIR_KEYWORDS	Cytoskeleton	RT		5	2.6E-1	9.9E-1
<input type="checkbox"/>	GOTERM_BP_FAT	M.tubse	RT		13	3.3E-1	9.3E-1
<input type="checkbox"/>	GOTERM_BP_FAT	cell division	RT		8	3.5E-1	9.9E-1
<input type="checkbox"/>	GOTERM_CC_FAT	cytoskeletal part	RT		7	4.1E-1	9.9E-1
<input type="checkbox"/>	GOTERM_BP_FAT	cytoskeleton organization	RT		16	5.3E-1	9.7E-1
<input type="checkbox"/>	GOTERM_BP_FAT	Cytoskeleton	RT		8	6.5E-1	1.0E0
<input type="checkbox"/>	Annotation Cluster/30						
<input type="checkbox"/>	SP_PIR_KEYWORDS	Apoptosis	G		Count	P_Value	Benjamini
<input type="checkbox"/>	GOTERM_BP_FAT	cell death	RT		10	1.6E-1	8.2E-1
<input type="checkbox"/>	GOTERM_BP_FAT	death	RT		17	1.9E-1	9.9E-1
<input type="checkbox"/>	GOTERM_BP_FAT	apoptosis	RT		17	2.0E-1	9.9E-1
<input type="checkbox"/>	GOTERM_BP_FAT	programmed cell death	RT		14	2.6E-1	9.9E-1
<input type="checkbox"/>	Annotation Cluster/31						
<input type="checkbox"/>	GOTERM_CC_FAT	chromosomal part	G		Count	P_Value	Benjamini
<input type="checkbox"/>	GOTERM_CC_FAT	chromosome	RT		11	8.2E-2	6.2E-1
<input type="checkbox"/>	GOTERM_CC_FAT	chromatin	RT		11	1.8E-1	8.2E-1
<input type="checkbox"/>	SP_PIR_KEYWORDS	chromosomal protein	RT		5	3.9E-1	9.3E-1
<input type="checkbox"/>	GOTERM_BP_FAT		RT		4	4.1E-1	9.4E-1
<input type="checkbox"/>	Annotation Cluster/32						
<input type="checkbox"/>	GOTERM_BP_FAT	cellular microtubule complex subunit organization	G		Count	P_Value	Benjamini
<input type="checkbox"/>	GOTERM_BP_FAT	cellular protein complex assembly	RT		12	5.0E-2	9.6E-1
<input type="checkbox"/>	GOTERM_BP_FAT	cellular microtubule complex assembly	RT		7	6.6E-2	9.7E-1
<input type="checkbox"/>	GOTERM_BP_FAT	microtubule complex subunit organization	RT		10	1.1E-1	9.9E-1
<input type="checkbox"/>	GOTERM_BP_FAT	microtubule complex assembly	RT		14	4.7E-1	1.0E0
<input type="checkbox"/>	GOTERM_BP_FAT	actin complex assembly	RT		12	6.2E-1	1.0E0
<input type="checkbox"/>	GOTERM_BP_FAT	actin complex assembly	RT		9	6.6E-1	1.0E0
<input type="checkbox"/>	GOTERM_BP_FAT	actin complex biogenesis	RT		9	6.6E-1	1.0E0
<input type="checkbox"/>	Annotation Cluster/33						
<input type="checkbox"/>	SP_PIR_KEYWORDS	Chaperone	G		Count	P_Value	Benjamini
<input type="checkbox"/>	GOTERM_MF_FAT	heat shock protein binding	RT		6	1.1E-1	7.6E-1
<input type="checkbox"/>	GOTERM_BP_FAT	protein folding	RT		3	3.4E-1	9.9E-1
<input type="checkbox"/>	GOTERM_BP_FAT		RT		5	3.8E-1	9.9E-1
<input type="checkbox"/>	Annotation Cluster/34						
<input type="checkbox"/>	GOTERM_BP_FAT	mRNA metabolic process	G		Count	P_Value	Benjamini
<input type="checkbox"/>	GOTERM_BP_FAT	mRNA processing	RT		8	1.1E-1	9.9E-1
<input type="checkbox"/>	GOTERM_BP_FAT	ribonucleoside complex biogenesis	RT		7	1.1E-1	9.9E-1
<input type="checkbox"/>	GOTERM_BP_FAT		RT		6	2.1E-1	9.9E-1
<input type="checkbox"/>	GOTERM_BP_FAT		RT		4	3.4E-1	9.9E-1

<https://david.ncifcr.gov/terms.jsp?and=62.9.79.85.25.32.38.1.3.47.45.63.76¤tlist=0>

22/9/2016 DAVID: Database for Annotation, Visualization, and Integrated Discovery (Laboratory of Immunopathogenesis and Bioinformatics (LB)). National Inst...

Annotation Cluster	Enrichment Score	Count	P-Value	Benjamini
Annotation Cluster 35				
<input type="checkbox"/> GOTERM_BP_FAT	rRNA processing	4	2.0E-1	2.7E-1
<input type="checkbox"/> GOTERM_BP_FAT	rRNA metabolic process	3	4.8E-1	1.0E0
<input type="checkbox"/> GOTERM_BP_FAT	Enrichment Score: 0.8	3	5.0E-1	1.0E0
<input type="checkbox"/> GOTERM_CC_FAT	nuclear envelope	3	1.0E-1	6.5E-1
<input type="checkbox"/> GOTERM_CC_FAT	nuclear pore	7	1.0E-1	6.5E-1
<input type="checkbox"/> GOTERM_CC_FAT	pore complex	3	3.5E-1	9.2E-1
<input type="checkbox"/> GOTERM_BP_FAT	Enrichment Score: 0.69	3	4.4E-1	9.5E-1
Annotation Cluster 36				
<input type="checkbox"/> GOTERM_BP_FAT	regulation of apoptosis	20	1.1E-1	9.8E-1
<input type="checkbox"/> GOTERM_BP_FAT	regulation of programmed cell death	20	1.2E-1	9.8E-1
<input type="checkbox"/> GOTERM_BP_FAT	regulation of cell death	20	1.2E-1	9.8E-1
<input type="checkbox"/> GOTERM_BP_FAT	induction of apoptosis	8	3.3E-1	9.9E-1
<input type="checkbox"/> GOTERM_BP_FAT	induction of programmed cell death	8	3.3E-1	9.9E-1
<input type="checkbox"/> GOTERM_BP_FAT	positive regulation of apoptosis	10	3.5E-1	9.9E-1
<input type="checkbox"/> GOTERM_BP_FAT	positive regulation of programmed cell death	10	3.5E-1	9.9E-1
<input type="checkbox"/> GOTERM_BP_FAT	positive regulation of cell death	10	3.5E-1	9.9E-1
<input type="checkbox"/> GOTERM_BP_FAT	induction of apoptosis by extracellular stimulus	3	5.9E-1	1.0E0
<input type="checkbox"/> GOTERM_BP_FAT	Enrichment Score: 0.69	Count	P-Value	Benjamini
<input type="checkbox"/> GOTERM_BP_FAT	endocytosis	7	1.9E-1	9.9E-1
<input type="checkbox"/> GOTERM_BP_FAT	membrane invagination	7	1.9E-1	9.9E-1
<input type="checkbox"/> GOTERM_BP_FAT	endocytosis	4	2.0E-1	8.5E-1
<input type="checkbox"/> GOTERM_BP_FAT	vesicle-mediated transport	13	3.1E-1	9.9E-1
<input type="checkbox"/> GOTERM_BP_FAT	membrane organization	8	5.0E-1	1.0E0
<input type="checkbox"/> GOTERM_BP_FAT	Enrichment Score: 0.64	Count	P-Value	Benjamini
<input type="checkbox"/> GOTERM_BP_FAT	Zinc Finger	17	1.6E-1	9.8E-1
<input type="checkbox"/> GOTERM_BP_FAT	zinc finger region:CH2-type 9	10	1.6E-1	1.0E0
<input type="checkbox"/> GOTERM_BP_FAT	PIR_SUPERFAMILY	5	1.7E-1	1.0E0
<input type="checkbox"/> GOTERM_BP_FAT	zinc finger region:CH2-type 1	13	1.7E-1	1.0E0
<input type="checkbox"/> GOTERM_BP_FAT	zinc finger region:CH2-type 2	14	1.9E-1	1.0E0
<input type="checkbox"/> GOTERM_BP_FAT	Zinc Finger, CH2-type/interase DNA binding	14	2.0E-1	1.0E0
<input type="checkbox"/> GOTERM_BP_FAT	zinc finger region:CH2-type 3	14	2.1E-1	1.0E0
<input type="checkbox"/> GOTERM_BP_FAT	Zinc Finger, CH2-like	17	2.2E-1	1.0E0
<input type="checkbox"/> GOTERM_BP_FAT	zinc finger region:CH2-type 8	10	2.4E-1	1.0E0
<input type="checkbox"/> GOTERM_BP_FAT	Zinc Finger, CH2-type	16	2.8E-1	1.0E0
<input type="checkbox"/> GOTERM_BP_FAT	zinc finger region:CH2-type 7	10	3.1E-1	1.0E0
<input type="checkbox"/> GOTERM_BP_FAT	zinc finger region:CH2-type 4	12	3.4E-1	1.0E0
<input type="checkbox"/> GOTERM_BP_FAT	zinc finger region:CH2-type 11	7	3.4E-1	1.0E0
<input type="checkbox"/> GOTERM_BP_FAT	zinc finger region:CH2-type 5	11	3.7E-1	1.0E0
<input type="checkbox"/> GOTERM_BP_FAT	zinc finger region:CH2-type 12	6	3.9E-1	1.0E0
<input type="checkbox"/> GOTERM_BP_FAT	zinc finger region:CH2-type 6	10	4.0E-1	1.0E0
<input type="checkbox"/> GOTERM_BP_FAT	domain:KRAB	7	4.5E-1	1.0E0
<input type="checkbox"/> GOTERM_BP_FAT	zinc finger region:CH2-type 10	7	4.6E-1	1.0E0
<input type="checkbox"/> GOTERM_BP_FAT	KRAB	7	4.6E-1	1.0E0
<input type="checkbox"/> GOTERM_BP_FAT	Kruenzel-associated box	7	4.6E-1	1.0E0
<input type="checkbox"/> GOTERM_BP_FAT	zinc finger region:CH2-type 13	4	6.4E-1	1.0E0
<input type="checkbox"/> GOTERM_BP_FAT	Enrichment Score: 0.63	Count	P-Value	Benjamini
<input type="checkbox"/> GOTERM_BP_FAT	Wnt signaling pathway	5	1.9E-1	9.5E-1
<input type="checkbox"/> GOTERM_BP_FAT	Wnt signaling pathway	4	3.1E-1	9.2E-1
<input type="checkbox"/> GOTERM_BP_FAT	Wnt receptor signaling pathway	4	4.1E-1	9.9E-1
<input type="checkbox"/> GOTERM_BP_FAT	Enrichment Score: 0.63	Count	P-Value	Benjamini
<input type="checkbox"/> GOTERM_BP_FAT	response to anionic stimulus	3	1.5E-1	9.8E-1
<input type="checkbox"/> GOTERM_BP_FAT	response to cytokine stimulus	3	3.0E-1	9.9E-1
<input type="checkbox"/> GOTERM_BP_FAT	response to endogenous stimulus	8	5.7E-1	1.0E0
<input type="checkbox"/> GOTERM_BP_FAT	Enrichment Score: 0.63	Count	P-Value	Benjamini
<input type="checkbox"/> GOTERM_BP_FAT	K1C	3	1.4E-1	9.9E-1
<input type="checkbox"/> GOTERM_BP_FAT	Kinase, motor region, conserved site	3	1.5E-1	1.0E0
<input type="checkbox"/> GOTERM_BP_FAT	Kinase, motor region	3	1.5E-1	1.0E0
<input type="checkbox"/> GOTERM_BP_FAT	domain:Kinase_motor	3	1.5E-1	1.0E0

<https://david.ncifcrf.gov/m2term.jsp?rand=52,9,78,85,25,32,39,1,3,47,46,63,78¤tList=0>

Annotation Cluster	Enrichment Score	RT	RT	Count	P-Value	Benjamini
GOTERM_BP_FAT		RT	■	3	4.0E-1	9.9E-1
Annotation Cluster 48						
SP_PIR_KEYWORDS	Enrichment Score: 0.47	G	■	13	2.4E-1	8.8E-1
UP_SEQ_FEATURE	ubt catalation	RT	■	5	4.0E-1	1.0E0
SP_PIR_KEYWORDS	cross-link:Glycyl lysine isopeptide (Lys-Gly) (interchain with G-Cter in ubiquitin)	RT	■	7	4.1E-1	9.4E-1
Annotation Cluster 49						
UP_SEQ_FEATURE	leucoridin band	RT	■	3	1.2E-1	1.0E0
Annotation Cluster 49	Enrichment Score: 0.46	G	■	3	1.2E-1	1.0E0
UP_SEQ_FEATURE	repeat:ANK 9	RT	■	3	1.5E-1	1.0E0
UP_SEQ_FEATURE	repeat:ANK 8	RT	■	3	2.4E-1	1.0E0
UP_SEQ_FEATURE	repeat:ANK 7	RT	■	4	3.6E-1	1.0E0
UP_SEQ_FEATURE	repeat:ANK 4	RT	■	5	3.9E-1	1.0E0
UP_SEQ_FEATURE	repeat:ANK 5	RT	■	3	4.4E-1	1.0E0
UP_SEQ_FEATURE	repeat:ANK 3	RT	■	4	2.5E-1	1.0E0
UP_SEQ_FEATURE	repeat:ANK 6	RT	■	5	5.0E-1	1.0E0
SMART	ANK	RT	■	5	5.2E-1	1.0E0
UP_SEQ_FEATURE	repeat:ANK 1	RT	■	5	5.2E-1	1.0E0
UP_SEQ_FEATURE	repeat:ANK 2	RT	■	5	5.4E-1	1.0E0
INTERPRO	Ablucrin	RT	■	5	5.4E-1	1.0E0
SP_PIR_KEYWORDS	zlk:crank	RT	■	5	5.4E-1	9.7E-1
Annotation Cluster 60	Enrichment Score: 0.46	G	■	6	1.1E-1	6.5E-1
GOTERM_CC_FAT	denticle	RT	■	6	4.3E-1	9.3E-1
SP_PIR_KEYWORDS	cell oxidation	RT	■	7	4.5E-1	9.5E-1
GOTERM_CC_FAT	neuron projection	RT	■	11	6.6E-1	9.9E-1
GOTERM_CC_FAT	cell projection	RT	■	8	2.9E-1	9.9E-1
Annotation Cluster 61	Enrichment Score: 0.45	G	■	5	3.6E-1	9.9E-1
GOTERM_BP_FAT	embryonic organ development	RT	■	5	3.7E-1	9.9E-1
GOTERM_BP_FAT	sensory organ development	RT	■	4	4.1E-1	9.9E-1
GOTERM_BP_FAT	embryonic organ morphogenesis	RT	■	3	2.1E-1	1.0E0
Annotation Cluster 62	Enrichment Score: 0.44	G	■	3	4.0E-1	1.0E0
UP_SEQ_FEATURE	zinc finger region:PHD-type	RT	■	3	4.0E-1	1.0E0
INTERPRO	Zinc finger: PHD-finger	RT	■	3	4.0E-1	1.0E0
SMART	PHD	RT	■	3	4.3E-1	1.0E0
INTERPRO	Zinc finger: PHD-type	RT	■	3	4.3E-1	1.0E0
INTERPRO	Zinc finger: BHD-type, conserved site	RT	■	3	4.4E-1	1.0E0
Annotation Cluster 63	Enrichment Score: 0.4	G	■	5	1.2E-1	9.5E-1
KEGG_PATHWAY	Sulfocysteine	RT	■	14	1.6E-1	9.8E-1
GOTERM_BP_FAT	RNA processing	RT	■	8	4.8E-1	1.0E0
GOTERM_BP_FAT	mRNA metabolic process	RT	■	7	5.0E-1	1.0E0
GOTERM_BP_FAT	tRNA processing	RT	■	5	6.1E-1	9.8E-1
SP_PIR_KEYWORDS	mRNA processing	RT	■	4	6.6E-1	9.9E-1
SP_PIR_KEYWORDS	mRNA splicing	RT	■	4	8.9E-1	1.0E0
GOTERM_BP_FAT	RNA splicing	RT	■	4	8.9E-1	1.0E0
Annotation Cluster 64	Enrichment Score: 0.38	G	■	5	2.0E-1	9.8E-1
GOTERM_BP_FAT	eye development	RT	■	4	2.9E-1	9.9E-1
GOTERM_BP_FAT	cartilage type: eye development	RT	■	6	3.7E-1	9.9E-1
GOTERM_BP_FAT	sensory organ development	RT	■	8	6.5E-1	1.0E0
GOTERM_BP_FAT	neuron differentiation	RT	■	5	8.5E-1	1.0E0
GOTERM_BP_FAT	neuron development	RT	■	6	1.4E-1	9.8E-1
Annotation Cluster 65	Enrichment Score: 0.35	G	■	6	2.9E-1	9.9E-1
GOTERM_BP_FAT	oligonucleon biosynthetic process	RT	■	3	6.6E-1	1.0E0
GOTERM_BP_FAT	oligonucleon metabolic process	RT	■	3	6.6E-1	1.0E0
GOTERM_BP_FAT	blood vessel: oligonucleon	RT	■	3	6.6E-1	1.0E0
GOTERM_BP_FAT	uric acid: amino acid oligonucleon	RT	■	3	6.6E-1	1.0E0
GOTERM_BP_FAT	oligonucleon	RT	■	7	6.8E-1	9.9E-1
SP_PIR_KEYWORDS	Signal anchor	RT	■	3	1.1E-1	7.5E-1
Annotation Cluster 66	Enrichment Score: 0.35	G	■	3	4.7E-1	1.0E0
SP_PIR_KEYWORDS	amino acid transport	RT	■	3	4.7E-1	1.0E0
GOTERM_BP_FAT	amino acid transport	RT	■	3	4.7E-1	1.0E0
GOTERM_BP_FAT	amino acid transport	RT	■	3	4.7E-1	1.0E0

<https://david.ncifcrf.gov/term.jsp?amot=62.9,79.85,26,32,39,1,3,47,48,63,78&cursorList=0>

Annotation	Enrichment Score	Count	P_Value	Benjamini
GOTERM_BP_FAT		4	4.5E-1	9.9E-1
GOTERM_BP_FAT	arterio/posterior pattern formation	4	4.5E-1	9.9E-1
GOTERM_BP_FAT	cellularization	5	4.5E-1	9.9E-1
GOTERM_BP_FAT	pattern specification process	5	6.9E-1	1.0E0
Annotation Cluster 65				
SMART	Enrichment Score: 0.28	Count	P_Value	Benjamini
SMART		6	4.2E-1	9.9E-1
INTERPRO	Dlx3strn homology	6	4.6E-1	1.0E0
UP_SEQ_FEATURE	domain:PH	6	5.4E-1	1.0E0
INTERPRO	Dlx3strn homology-type	5	7.2E-1	1.0E0
Annotation Cluster 66				
SP_PR_KEYWORDS	Enrichment Score: 0.28	Count	P_Value	Benjamini
GOTERM_MF_FAT	helicase	4	3.7E-1	9.3E-1
GOTERM_MF_FAT	helicase activity	4	4.0E-1	9.9E-1
GOTERM_MF_FAT	nucleic NTP-dependent helicase activity	3	4.7E-1	1.0E0
GOTERM_MF_FAT	ATP-dependent helicase activity	3	4.7E-1	1.0E0
SMART	HELIC	3	4.9E-1	1.0E0
SMART	DEXK	3	5.0E-1	9.9E-1
UP_SEQ_FEATURE	domain:Helicase C-terminal	3	5.1E-1	1.0E0
INTERPRO	Helicase, superfamily 1 and 7, ATP-binding	3	5.2E-1	1.0E0
INTERPRO	DNA/RNA helicase, C-terminal	3	5.2E-1	1.0E0
INTERPRO	DEAD-like helicase, N-terminal	3	5.3E-1	1.0E0
UP_SEQ_FEATURE	domain:Helicase ATP-binding	3	5.4E-1	1.0E0
GOTERM_MF_FAT	ATPase activity	5	8.0E-1	1.0E0
GOTERM_MF_FAT	ATPase activity, coupled	3	9.4E-1	1.0E0
Annotation Cluster 67				
SP_PR_KEYWORDS	Enrichment Score	Count	P_Value	Benjamini
GOTERM_BP_FAT	hblt transport	3	2.6E-1	9.0E-1
GOTERM_BP_FAT	hblt transport	3	7.3E-1	1.0E0
GOTERM_BP_FAT	hblt localization	3	7.6E-1	1.0E0
Annotation Cluster 68				
GOTERM_BP_FAT	Enrichment Score	Count	P_Value	Benjamini
GOTERM_BP_FAT	positive regulation of spermatid	4	7.8E-2	9.8E-1
GOTERM_BP_FAT	positive regulation of transcription from RNA polymerase II promoter	4	2.0E-1	9.9E-1
GOTERM_BP_FAT	transcription	4	2.3E-1	9.8E-1
GOTERM_BP_FAT	regulation of specific transcription	4	4.2E-1	9.9E-1
GOTERM_BP_FAT	regulation of RNA polymerase II promoter	16	5.4E-1	1.0E0
GOTERM_BP_FAT	positive regulation of macrocyclic metabolic process	12	6.0E-1	1.0E0
GOTERM_BP_FAT	positive regulation of macromolecule biosynthetic process	10	6.6E-1	1.0E0
GOTERM_BP_FAT	sequence-specific DNA binding	11	6.6E-1	1.0E0
GOTERM_BP_FAT	positive regulation of nucleoside, nucleotide and nucleic acid metabolic process	11	6.6E-1	1.0E0
GOTERM_BP_FAT	positive regulation of cellular biosynthetic process	12	6.6E-1	1.0E0
GOTERM_BP_FAT	positive regulation of biosynthetic process	12	6.6E-1	1.0E0
GOTERM_BP_FAT	positive regulation of nitrogen compound metabolic process	12	6.8E-1	1.0E0
GOTERM_BP_FAT	metabolic process	11	7.0E-1	1.0E0
GOTERM_BP_FAT	positive regulation of transcription from RNA polymerase II promoter	6	7.9E-1	1.0E0
GOTERM_BP_FAT	positive regulation of transcription, DNA-dependent	7	8.5E-1	1.0E0
GOTERM_BP_FAT	positive regulation of RNA metabolic process	7	8.5E-1	1.0E0
GOTERM_BP_FAT	positive regulation of transcription	8	8.7E-1	1.0E0
GOTERM_BP_FAT	positive regulation of gene expression	8	8.9E-1	1.0E0
GOTERM_BP_FAT	transcription factor activity	12	9.3E-1	1.0E0
Annotation Cluster 69				
INTERPRO	Enrichment Score: 0.27	Count	P_Value	Benjamini
SMART	Helix-loop-helix DNA binding	3	3.9E-1	1.0E0
SMART	HLH	3	5.2E-1	9.9E-1
INTERPRO	Basic Helix-Loop-Helix dimerization region	3	5.5E-1	1.0E0
INTERPRO	BHLH	3	5.5E-1	1.0E0
UP_SEQ_FEATURE	domain:Helix-loop-helix motif	3	5.5E-1	1.0E0
UP_SEQ_FEATURE	DNA-binding region:Basic motif	3	7.4E-1	1.0E0
Annotation Cluster 70				
GOTERM_BP_FAT	Enrichment Score: 0.28	Count	P_Value	Benjamini
GOTERM_BP_FAT	response to toxin	4	9.1E-2	9.8E-1
GOTERM_BP_FAT	cell migration	4	3.0E-1	9.9E-1
GOTERM_BP_FAT	positive regulation of growth	7	3.5E-1	9.9E-1
GOTERM_BP_FAT		3	4.1E-1	9.9E-1

<https://david.ncifcr.gov/terms.jsp?rank=52.9.73.85.25.32.39.1.3.47.46.63.78¤tList=0>

2/29/2016 DAVID: Database for Annotation, Visualization, and Integrated Discovery (Laboratory of Immunopathogenesis and Bioinformatics (LBI), National Inst...

<input type="checkbox"/>	GOTERM_BP_FAT	cell motility	RT	■	7	4.5E-1	9.9E-1
<input type="checkbox"/>	GOTERM_BP_FAT	localization of cell	RT	■	7	4.5E-1	9.9E-1
<input type="checkbox"/>	GOTERM_BP_FAT	regulation of growth	RT	■	7	5.5E-1	1.0E0
<input type="checkbox"/>	GOTERM_BP_FAT	regulation of cell growth	RT	■	4	6.6E-1	1.0E0
<input type="checkbox"/>	GOTERM_BP_FAT	regulation of cell size	RT	■	4	7.0E-1	1.0E0
<input type="checkbox"/>	GOTERM_BP_FAT	positive regulation of developmental process	RT	■	5	7.2E-1	1.0E0
<input type="checkbox"/>	GOTERM_BP_FAT	cell motion	RT	■	8	7.3E-1	1.0E0
<input type="checkbox"/>	GOTERM_BP_FAT	regulation of cellular component size	RT	■	4	8.6E-1	1.0E0
<input type="checkbox"/>	GOTERM_BP_FAT	blood vessel morphogenesis	RT	■	3	8.9E-1	1.0E0
<input type="checkbox"/>	GOTERM_BP_FAT	positive regulation of cell differentiation	RT	■	3	9.1E-1	1.0E0
<input type="checkbox"/>	GOTERM_BP_FAT	blood vessel development	RT	■	3	9.3E-1	1.0E0
<input type="checkbox"/>	GOTERM_BP_FAT	vasculature development	RT	■	3	9.4E-1	1.0E0
Annotation Cluster71							
<input type="checkbox"/>	SP_PR_KEYWORDS	luciferase	G	■	7	3.7E-1	9.3E-1
<input type="checkbox"/>	GOTERM_MF_FAT	acid amino acid lyase activity	RT	■	4	6.4E-1	1.0E0
<input type="checkbox"/>	GOTERM_MF_FAT	lyase activity, ferrioxo-carbonate-iron bonds	RT	■	4	7.3E-1	1.0E0
Annotation Cluster72							
<input type="checkbox"/>	GOTERM_BP_FAT	histone modification	G	■	4	3.6E-1	9.9E-1
<input type="checkbox"/>	GOTERM_BP_FAT	covalent chromatin modification	RT	■	4	3.8E-1	9.9E-1
<input type="checkbox"/>	SP_PR_KEYWORDS	chromatin regulator	RT	■	4	6.7E-1	9.9E-1
<input type="checkbox"/>	GOTERM_BP_FAT	chromatin modification	RT	■	5	7.1E-1	1.0E0
<input type="checkbox"/>	GOTERM_BP_FAT	chromosome organization	RT	■	8	7.5E-1	1.0E0
<input type="checkbox"/>	GOTERM_BP_FAT	chromatin organization	RT	■	6	8.0E-1	1.0E0
Annotation Cluster73							
<input type="checkbox"/>	GOTERM_CC_FAT	soluble fraction	G	■	8	2.2E-1	8.6E-1
<input type="checkbox"/>	GOTERM_BP_FAT	response to insulin stimulus	RT	■	3	5.3E-1	1.0E0
<input type="checkbox"/>	GOTERM_BP_FAT	response to endogenous stimulus	RT	■	8	5.7E-1	1.0E0
<input type="checkbox"/>	GOTERM_BP_FAT	response to steroid hormone stimulus	RT	■	4	6.6E-1	1.0E0
<input type="checkbox"/>	GOTERM_BP_FAT	cellular response to hormone stimulus	RT	■	3	6.8E-1	1.0E0
<input type="checkbox"/>	GOTERM_BP_FAT	response to genetic hypersensitive stimulus	RT	■	3	7.6E-1	1.0E0
<input type="checkbox"/>	GOTERM_BP_FAT	response to hormone stimulus	RT	■	6	7.7E-1	1.0E0
<input type="checkbox"/>	GOTERM_BP_FAT	response to organic substance	RT	■	9	9.4E-1	1.0E0
Annotation Cluster74							
<input type="checkbox"/>	GOTERM_BP_FAT	regulation of protein transport	G	■	3	6.0E-1	1.0E0
<input type="checkbox"/>	GOTERM_BP_FAT	regulation of establishment of protein localization	RT	■	3	6.3E-1	1.0E0
<input type="checkbox"/>	GOTERM_BP_FAT	regulation of protein localization	RT	■	3	7.0E-1	1.0E0
<input type="checkbox"/>	GOTERM_BP_FAT	regulation of cellular localization	RT	■	4	8.1E-1	1.0E0
Annotation Cluster75							
<input type="checkbox"/>	INTERPRO	ETB/POZ	G	■	3	6.1E-1	1.0E0
<input type="checkbox"/>	UP_SEQ_FEATURE	domain: BTB	RT	■	3	6.7E-1	1.0E0
<input type="checkbox"/>	SMART	BTB	RT	■	3	7.6E-1	1.0E0
<input type="checkbox"/>	INTERPRO	ETB/POZ-like	RT	■	3	7.9E-1	1.0E0
<input type="checkbox"/>	INTERPRO	ETB/POZ fold	RT	■	3	7.9E-1	1.0E0
Annotation Cluster76							
<input type="checkbox"/>	UP_SEQ_FEATURE	repeat: WD 6	G	■	4	6.1E-1	1.0E0
<input type="checkbox"/>	INTERPRO	WD40 repeat 2	RT	■	4	7.1E-1	1.0E0
<input type="checkbox"/>	INTERPRO	WD40/YVTN repeat-like	RT	■	5	7.1E-1	1.0E0
<input type="checkbox"/>	UP_SEQ_FEATURE	repeat: WD 5	RT	■	4	7.3E-1	1.0E0
<input type="checkbox"/>	INTERPRO	WD40 repeat, region	RT	■	4	7.4E-1	1.0E0
<input type="checkbox"/>	INTERPRO	WD40 repeat, subdomain	RT	■	4	7.5E-1	1.0E0
<input type="checkbox"/>	UP_SEQ_FEATURE	repeat: WD 4	RT	■	4	7.8E-1	1.0E0
<input type="checkbox"/>	SMART	WD40	RT	■	4	7.8E-1	1.0E0
<input type="checkbox"/>	INTERPRO	WD40 repeat	RT	■	4	8.0E-1	1.0E0
<input type="checkbox"/>	UP_SEQ_FEATURE	repeat: WD 3	RT	■	4	8.1E-1	1.0E0
<input type="checkbox"/>	UP_SEQ_FEATURE	repeat: WD 2	RT	■	4	8.2E-1	1.0E0
<input type="checkbox"/>	UP_SEQ_FEATURE	repeat: WD 1	RT	■	4	8.2E-1	1.0E0
<input type="checkbox"/>	SP_PR_KEYWORDS	wd repeat	RT	■	4	8.2E-1	1.0E0
<input type="checkbox"/>	INTERPRO						

https://david.ncifcr.gov/terms.jsp?and=52,9,79,85,25,32,39,1,3,47,45,63,76&source=0

2/29/2016 DAVID: Database for Annotation, Visualization, and Integrated Discovery (Laboratory of Immunopathogenesis and Biinformatics (LBI): National Inst...

Annotation	Enrichment Score	Count	P-Value	Benjamini
WICD1 repeat, conserved site	0.11	4	8.3E-1	1.0E0
SMART	0.11	Count	P-Value	Benjamini
SMART		3	6.0E-1	1.0E0
INTERPRO		3	6.3E-1	1.0E0
INTERPRO		4	6.7E-1	1.0E0
UP_SEQ_FEATURE		4	7.3E-1	1.0E0
UP_SEQ_FEATURE		4	7.8E-1	1.0E0
UP_SEQ_FEATURE		3	8.6E-1	1.0E0
UP_SEQ_FEATURE		4	8.7E-1	1.0E0
UP_SEQ_FEATURE		4	8.9E-1	1.0E0
UP_SEQ_FEATURE		4	8.9E-1	1.0E0
SP_PIR_KEYWORDS		4	8.9E-1	1.0E0
Annotation Cluster 78	Enrichment Score: 0.11	Count	P-Value	Benjamini
GOTERM_MF_FAT		6	5.9E-1	1.0E0
GOTERM_BP_FAT		13	6.3E-1	1.0E0
GOTERM_BP_FAT		5	6.9E-1	1.0E0
GOTERM_BP_FAT		6	7.5E-1	1.0E0
GOTERM_BP_FAT		6	7.6E-1	1.0E0
GOTERM_BP_FAT		9	7.9E-1	1.0E0
GOTERM_BP_FAT		8	8.0E-1	1.0E0
GOTERM_BP_FAT		8	8.1E-1	1.0E0
GOTERM_BP_FAT		7	8.2E-1	1.0E0
GOTERM_BP_FAT		8	8.5E-1	1.0E0
GOTERM_BP_FAT		8	8.7E-1	1.0E0
GOTERM_BP_FAT		7	8.8E-1	1.0E0
GOTERM_BP_FAT		9	9.5E-1	1.0E0
Annotation Cluster 79	Enrichment Score: 0.1	Count	P-Value	Benjamini
GOTERM_BP_FAT		3	6.0E-1	1.0E0
GOTERM_BP_FAT		3	8.9E-1	1.0E0
GOTERM_BP_FAT		3	9.7E-1	1.0E0
Annotation Cluster 80	Enrichment Score: 0.08	Count	P-Value	Benjamini
GOTERM_CC_FAT		4	7.2E-1	9.9E-1
GOTERM_CC_FAT		4	7.4E-1	9.9E-1
GOTERM_CC_FAT		15	8.1E-1	1.0E0
GOTERM_CC_FAT		9	9.4E-1	1.0E0
GOTERM_CC_FAT		9	9.6E-1	1.0E0
Annotation Cluster 81	Enrichment Score: 0.07	Count	P-Value	Benjamini
GOTERM_BP_FAT		4	5.4E-1	1.0E0
GOTERM_BP_FAT		6	9.1E-1	1.0E0
GOTERM_BP_FAT		5	9.2E-1	1.0E0
GOTERM_BP_FAT		5	9.7E-1	1.0E0
GOTERM_BP_FAT		5	9.7E-1	1.0E0
Annotation Cluster 82	Enrichment Score: 0.07	Count	P-Value	Benjamini
GOTERM_BP_FAT		4	7.8E-1	1.0E0
GOTERM_BP_FAT		4	8.9E-1	1.0E0
GOTERM_BP_FAT		4	8.9E-1	1.0E0
Annotation Cluster 83	Enrichment Score: 0.07	Count	P-Value	Benjamini
GOTERM_BP_FAT		5	7.6E-1	1.0E0
GOTERM_BP_FAT		4	8.0E-1	1.0E0
GOTERM_BP_FAT		3	8.4E-1	1.0E0
GOTERM_BP_FAT		3	9.2E-1	1.0E0
GOTERM_BP_FAT		5	9.7E-1	1.0E0
Annotation Cluster 84	Enrichment Score: 0.06	Count	P-Value	Benjamini
UP_SEQ_FEATURE		3	5.0E-1	1.0E0

<http://www.ebi.ac.uk/QuickGO/GTerm?id=GO:0051247>

2292016 DAVID: Database for Annotation, Visualization, and Integrated Discovery (Laboratory of Immunopathogenesis and Bioinformatics (LB) National Inst...									
	SMART	15	RT	■	9.6E-1	1.0E0			
	INTERPRO		RT	■	9.7E-1	1.0E0			
	INTERPRO	Immunoglobulin subbase	RT	■	9.8E-1	1.0E0			
	SP_PIR_KEYWORDS	Immunoglobulin-like fold	RT	■	9.8E-1	1.0E0			
	INTERPRO	Immunoglobulin domain	RT	■	9.8E-1	1.0E0			
	INTERPRO	Immunoglobulin-like	RT	■	9.9E-1	1.0E0			
	Annotation Cluster 85	Enrichment Score: 0.06	G	■			3		
	GOTERM_BP_FAT	activation of protein kinase activity	RT	■	6.0E-1	1.0E0			
	GOTERM_BP_FAT	regulation of protein modification process	RT	■	7.6E-1	1.0E0			
	GOTERM_BP_FAT	regulation of protein amino acid phosphorylation	RT	■	8.1E-1	1.0E0			
	GOTERM_BP_FAT	regulation of protein kinase activity	RT	■	8.6E-1	1.0E0			
	GOTERM_BP_FAT	regulation of kinase activity	RT	■	8.8E-1	1.0E0			
	GOTERM_BP_FAT	regulation of transferase activity	RT	■	8.9E-1	1.0E0			
	GOTERM_BP_FAT	positive regulation of protein kinase activity	RT	■	9.1E-1	1.0E0			
	GOTERM_BP_FAT	regulation of phosphorylation	RT	■	9.2E-1	1.0E0			
	GOTERM_BP_FAT	positive regulation of kinase activity	RT	■	9.2E-1	1.0E0			
	GOTERM_BP_FAT	positive regulation of transferase activity	RT	■	9.3E-1	1.0E0			
	GOTERM_BP_FAT	regulation of biosynthetic process	RT	■	9.3E-1	1.0E0			
	GOTERM_BP_FAT	regulation of cellular protein metabolic process	RT	■	9.3E-1	1.0E0			
	GOTERM_BP_FAT	positive regulation of catalytic activity	RT	■	9.7E-1	1.0E0			
	GOTERM_BP_FAT	positive regulation of molecular function	RT	■	9.8E-1	1.0E0			
	Annotation Cluster 86	Enrichment Score: 0.05	G	■			5		
	GOTERM_MF_FAT	cysteine-heme oxidase activity	RT	■	6.7E-1	1.0E0			
	GOTERM_MF_FAT	oxidase activity, acting on L-amino acid residues	RT	■	9.8E-1	1.0E0			
	GOTERM_MF_FAT	oxidase activity	RT	■	9.9E-1	1.0E0			
	GOTERM_MF_FAT	oxidoreductase activity	RT	■	9.9E-1	1.0E0			
	Annotation Cluster 87	Enrichment Score: 0.05	G	■			7		
	GOTERM_MF_FAT	actin filament organization activity	RT	■	8.8E-1	1.0E0			
	GOTERM_MF_FAT	identical protein binding	RT	■	9.0E-1	1.0E0			
	GOTERM_MF_FAT	protein homodimerization activity	RT	■	9.1E-1	1.0E0			
	Annotation Cluster 88	Enrichment Score: 0.05	G	■			3		
	GOTERM_MF_FAT	GTPase activity	RT	■	8.6E-1	1.0E0			
	GOTERM_MF_FAT	guanyl ribonucleotide binding	RT	■	8.7E-1	1.0E0			
	GOTERM_MF_FAT	guanyl nucleotide binding	RT	■	8.7E-1	1.0E0			
	GOTERM_MF_FAT	GTP binding	RT	■	9.0E-1	1.0E0			
	GOTERM_MF_FAT	nucleotide phosphate-binding region:GTP	RT	■	9.5E-1	1.0E0			
	Annotation Cluster 89	Enrichment Score: 0.03	G	■			4		
	GOTERM_CC_FAT	endoplasmic reticulum part	RT	■	9.1E-1	1.0E0			
	GOTERM_CC_FAT	endoplasmic reticulum membrane	RT	■	9.3E-1	1.0E0			
	GOTERM_CC_FAT	nuclear envelope endoplasmic reticulum network	RT	■	9.4E-1	1.0E0			
	Annotation Cluster 90	Enrichment Score: 0.02	G	■			4		
	GOTERM_MF_FAT	metal ion transport/channe transporter activity	RT	■	9.1E-1	1.0E0			
	GOTERM_MF_FAT	channel activity	RT	■	9.4E-1	1.0E0			
	GOTERM_MF_FAT	ion channel activity	RT	■	9.5E-1	1.0E0			
	GOTERM_MF_FAT	substrate specific channel activity	RT	■	9.6E-1	1.0E0			
	GOTERM_MF_FAT	channel activity	RT	■	9.7E-1	1.0E0			
	GOTERM_MF_FAT	passive transmembrane transporter activity	RT	■	9.7E-1	1.0E0			
	Annotation Cluster 91	Enrichment Score: 0.02	G	■			3		
	SP_PIR_KEYWORDS	synapse	RT	■	8.6E-1	1.0E0			
	GOTERM_CC_FAT	synapse	RT	■	9.8E-1	1.0E0			
	GOTERM_CC_FAT	cell junction	RT	■	9.9E-1	1.0E0			
	SP_PIR_KEYWORDS	cell junction	RT	■	9.9E-1	1.0E0			
	Annotation Cluster 92	Enrichment Score: 0.02	G	■			3		
	GOTERM_BP_FAT	cellular di-, tri-valent inorganic cation homeostasis	RT	■	9.1E-1	1.0E0			
	GOTERM_BP_FAT	di-, tri-valent inorganic cation homeostasis	RT	■	9.2E-1	1.0E0			
	GOTERM_BP_FAT	cellular cation homeostasis	RT	■	9.4E-1	1.0E0			

<https://david.ncifcrf.gov/terms2term.jsp?anndt=52,9,79,85,25,32,39,1,3,4,7,45,63,78¤tList=0>

2292016 DAVID: Database for Annotation, Visualization, and Integrated Discovery (Laboratory of Immunopathogenesis and Biinformatics (LIB): National Inst...

<input type="checkbox"/>	GOTERM_BP_FAT	chemical homeostasis	RT		6	9.5E-1	1.0E0
<input type="checkbox"/>	GOTERM_BP_FAT	cellular ion homeostasis	RT		4	9.6E-1	1.0E0
<input type="checkbox"/>	GOTERM_BP_FAT	cation homeostasis	RT		3	9.6E-1	1.0E0
<input type="checkbox"/>	GOTERM_BP_FAT	cellular chemical homeostasis	RT		4	9.6E-1	1.0E0
<input type="checkbox"/>	GOTERM_BP_FAT	cellular homeostasis	RT		5	9.7E-1	1.0E0
<input type="checkbox"/>	GOTERM_BP_FAT	ion homeostasis	RT		4	9.8E-1	1.0E0
<input type="checkbox"/>	GOTERM_BP_FAT	homeostatic process	RT		8	9.8E-1	1.0E0
Annotation Cluster 93							
<input type="checkbox"/>	SP_PRR_KEYWORDS	extracellular matrix	RT		3	9.0E-1	1.0E0
<input type="checkbox"/>	GOTERM_CC_FAT	perithelous extracellular matrix	RT		3	9.6E-1	1.0E0
<input type="checkbox"/>	GOTERM_CC_FAT	extracellular matrix	RT		3	9.7E-1	1.0E0
<input type="checkbox"/>	GOTERM_CC_FAT	extracellular region part	RT		7	1.0E0	1.0E0
Enrichment Score: 0.01							
<input type="checkbox"/>	SP_PRR_KEYWORDS	membrane	RT		88	9.6E-1	1.0E0
<input type="checkbox"/>	GOTERM_CC_FAT	intrinsic to membrane	RT		75	9.6E-1	1.0E0
<input type="checkbox"/>	GOTERM_CC_FAT	integral to membrane	RT		70	9.8E-1	1.0E0
<input type="checkbox"/>	UP_SEQ_FEATURE	transmembrane region	RT		63	9.9E-1	1.0E0
<input type="checkbox"/>	SP_PRR_KEYWORDS	transmembrane	RT		63	9.9E-1	1.0E0
<input type="checkbox"/>	UP_SEQ_FEATURE	topological domain: Cytoplasmic	RT		36	1.0E0	1.0E0
<input type="checkbox"/>	UP_SEQ_FEATURE	glycosylation site: N-linked (GlcNAc...)	RT		36	1.0E0	1.0E0
<input type="checkbox"/>	SP_PRR_KEYWORDS	oligosaccharide	RT		38	1.0E0	1.0E0
Enrichment Score: 0							
<input type="checkbox"/>	SP_PRR_KEYWORDS	cell adhesion	RT		3	9.9E-1	1.0E0
<input type="checkbox"/>	GOTERM_BP_FAT	cell adhesion	RT		5	1.0E0	1.0E0
<input type="checkbox"/>	GOTERM_BP_FAT	biological adhesion	RT		5	1.0E0	1.0E0
Enrichment Score: 0							
<input type="checkbox"/>	GOTERM_CC_FAT	integral to plasma membrane	RT		10	1.0E0	1.0E0
<input type="checkbox"/>	GOTERM_CC_FAT	intrinsic to plasma membrane	RT		10	1.0E0	1.0E0
<input type="checkbox"/>	GOTERM_CC_FAT	plasma membrane part	RT		18	1.0E0	1.0E0
Enrichment Score: 0							
<input type="checkbox"/>	GOTERM_CC_FAT	extracellular space	RT		5	1.0E0	1.0E0
<input type="checkbox"/>	GOTERM_CC_FAT	extracellular region part	RT		7	1.0E0	1.0E0
<input type="checkbox"/>	SP_PRR_KEYWORDS	secreted	RT		13	1.0E0	1.0E0
<input type="checkbox"/>	GOTERM_CC_FAT	extracellular region	RT		13	1.0E0	1.0E0
Enrichment Score: 0							
<input type="checkbox"/>	GOTERM_BP_FAT	behavior	RT		3	1.0E0	1.0E0
<input type="checkbox"/>	GOTERM_BP_FAT	cohesion	RT		5	1.0E0	1.0E0
<input type="checkbox"/>	GOTERM_BP_FAT	sensory perception	RT		3	1.0E0	1.0E0
<input type="checkbox"/>	GOTERM_BP_FAT	neurological system process	RT		6	1.0E0	1.0E0
Enrichment Score: 0							
<input type="checkbox"/>	SP_PRR_KEYWORDS	trans-steroid	RT		5	1.0E0	1.0E0
<input type="checkbox"/>	SP_PRR_KEYWORDS	G-protein coupled receptor	RT		4	1.0E0	1.0E0
<input type="checkbox"/>	GOTERM_BP_FAT	G-protein coupled receptor domain	RT		5	1.0E0	1.0E0
<input type="checkbox"/>	GOTERM_BP_FAT	signaling pathway	RT		5	1.0E0	1.0E0
Enrichment Score: 0							
<input type="checkbox"/>	UP_SEQ_FEATURE	topological domain: Cytoplasmic	RT		36	1.0E0	1.0E0
<input type="checkbox"/>	SP_PRR_KEYWORDS	signal peptide	RT		28	1.0E0	1.0E0
<input type="checkbox"/>	UP_SEQ_FEATURE	topological domain: Extracellular	RT		28	1.0E0	1.0E0
<input type="checkbox"/>	UP_SEQ_FEATURE	disulfide bond	RT		21	1.0E0	1.0E0
<input type="checkbox"/>	SP_PRR_KEYWORDS	disulfide bond	RT		22	1.0E0	1.0E0
<input type="checkbox"/>	UP_SEQ_FEATURE	glycosylation site: N-linked (GlcNAc...)	RT		23	1.0E0	1.0E0
<input type="checkbox"/>	SP_PRR_KEYWORDS	glycosylation	RT		36	1.0E0	1.0E0
<input type="checkbox"/>	SP_PRR_KEYWORDS	glycoprotein	RT		38	1.0E0	1.0E0

234 terms were not clustered.

Please cite [Nature Protocols 2009, 4\(1\):44 & Genome Biology 2003, 4\(5\):P3](https://doi.org/10.1093/nar/gkz121) within any publication that makes use of any methods inspired by DAVID.

8.4 Rabbit IPA analysis

INGENUITY[®] PATHWAY ANALYSIS

Analysis Name: Rabbit - 2016-03-14 10:57 AM
Analysis Creation Date: 2016-03-14
Build version: 366632M
Content version: 26127183 (Release Date: 2015-11-30)



Analysis Settings

Reference set: Ingenuity Knowledge Base (Genes Only)
Relationship to include: Direct and Indirect
Includes Endogenous Chemicals
Optional Analyses: My Pathways My List

Filter Summary:
Consider only relationships where
confidence = Experimentally Observed

Summary of Analysis - Rabbit - 2016-03-14 10:57 AM

Top Canonical Pathways

Name	p-value	Overlap
Ceramide Signaling	9.18E-05	8.8 % 7/80
Induction of Apoptosis by HIV1	1.40E-04	10.0 % 6/60
Death Receptor Signaling	2.21E-04	7.6 % 7/92
Tec Kinase Signaling	2.51E-04	5.7 % 9/157
NF-B Activation by Viruses	4.12E-04	8.2 % 6/73

Top Upstream Regulators

Upstream Regulator	p-value of overlap	Predicted Activation
MAX	1.20E-05	
SREBF1	4.07E-05	Inhibited
SATB1	4.38E-05	
amiodarone	9.08E-05	
WHSC1	1.04E-04	

Top Diseases and Bio Functions**Diseases and Disorders**

Name	p-value	#Molecules
Gastrointestinal Disease	1.32E-02 - 1.05E-04	207
Hepatic System Disease	1.28E-02 - 1.05E-04	13
Inflammatory Disease	1.32E-02 - 1.05E-04	44
Organismal Injury and Abnormalities	1.32E-02 - 1.82E-04	245
Immunological Disease	1.32E-02 - 2.23E-04	58

Molecular and Cellular Functions

Summary of Analysis - Rabbit - 2016-03-14 10:57 AM

Name	p-value	#Molecules
Cell Death and Survival	1.32E-02 - 9.08E-06	98
Cellular Function and Maintenance	1.32E-02 - 9.08E-06	49
Cellular Development	1.32E-02 - 1.34E-05	66
Cellular Growth and Proliferation	1.32E-02 - 1.34E-05	95
Lipid Metabolism	1.32E-02 - 3.65E-05	31

Physiological System Development and Function

Name	p-value	#Molecules
Embryonic Development	1.32E-02 - 9.08E-06	24
Hematological System Development and Function	1.32E-02 - 4.41E-05	41
Humoral Immune Response	1.32E-02 - 4.41E-05	19
Immune Cell Trafficking	1.32E-02 - 4.41E-05	13
Lymphoid Tissue Structure and Development	1.14E-02 - 2.09E-04	25

Top Tox Functions**Assays: Clinical Chemistry and Hematology**

Name	p-value	#Molecules
Increased Levels of AST	1.81E-01 - 1.32E-02	1
Increased Levels of Alkaline Phosphatase	2.37E-01 - 1.32E-02	2
Decreased Levels of Albumin	5.19E-02 - 2.63E-02	1
Increased Levels of CRP	2.63E-02 - 2.63E-02	1
Increased Levels of ALT	2.34E-01 - 6.45E-02	1

Cardiotoxicity

Summary of Analysis - Rabbit - 2016-03-14 10:57 AM

Name	p-value	#Molecules
Cardiac Inflammation	4.21E-01 - 2.53E-03	5
Cardiac Damage	1.02E-01 - 1.32E-02	2
Cardiac Necrosis/Cell Death	5.21E-01 - 1.32E-02	6
Congenital Heart Anomaly	4.80E-01 - 3.39E-02	6
Cardiac Stress Response	3.92E-02 - 3.92E-02	1

Hepatotoxicity

Name	p-value	#Molecules
Liver Damage	5.63E-01 - 1.82E-04	6
Liver Degeneration	2.63E-02 - 8.57E-03	3
Liver Necrosis/Cell Death	2.44E-01 - 8.61E-03	7
Liver Inflammation/Hepatitis	5.63E-01 - 1.24E-02	9
Liver Enlargement	1.03E-01 - 2.63E-02	4

Nephrotoxicity

Name	p-value	#Molecules
Renal Necrosis/Cell Death	3.02E-01 - 1.25E-03	14
Glomerular Injury	4.87E-01 - 3.42E-03	8
Renal Damage	3.25E-01 - 1.13E-02	6
Nephrosis	2.13E-01 - 1.32E-02	3
Renal Fibrosis	4.87E-01 - 2.63E-02	3

Top Regulator Effect Networks

ID	Regulators	Diseases & Functions	Consistency Score
1	SREBF1	synthesis of cholesterol ester	1.732
2	STAT1	cell death of tumor cell lines	-6.5

(c) 2000-2016 QIAGEN. All rights reserved.

Summary of Analysis - Rabbit - 2016-03-14 10:57 AM

3	ARNT	cell death of tumor cell lines	-7.0
4	STAT1	cell death of leukocyte cell lines	-8.083
5	SREBF1	necrosis	-11.431

Top Networks

ID	Associated Network Functions	Score
1	Antimicrobial Response, Cell Morphology, Cellular Assembly and Organization	51
2	Cancer, Organismal Injury and Abnormalities, Gastrointestinal Disease	41
3	Auditory and Vestibular System Development and Function, Cellular Development, Cellular Growth and Proliferation	35
4	Lymphoid Tissue Structure and Development, Organ Development, DNA Replication, Recombination, and Repair	33
5	Cell Death and Survival, Cancer, Organismal Injury and Abnormalities	30

Top Tox Lists

Name	p-value	Overlap
Decreases Transmembrane Potential of Mitochondria and Mitochondrial Membrane	1.67E-04	6.8 % 8/117
Increases Liver Hepatitis	6.69E-04	9.4 % 5/53
Anti-Apoptosis	8.06E-04	12.5 % 4/32
Increases Liver Steatosis	9.87E-04	7.0 % 6/86
Increases Permeability Transition of Mitochondria and Mitochondrial Membrane	4.64E-03	25.0 % 2/8

Top My Lists

Name	p-value	Overlap
Colorectal cancer	1.57E-02	1.7 % 73/4364
dysregulated FDR p=0.05 010216	2.64E-01	4.3 % 1/23
Hu downreg	3.30E-01	2.0 % 3/153
EDN1 p=0.01	3.89E-01	2.7 % 1/37
CD40LG p=0.01	5.20E-01	1.8 % 1/55

Top Analysis-Ready Molecules

Exp Fold Change up-regulated

Molecules	Exp. Value	Exp. Chart
CD3D	↑ 23.528	
ITGB1	↑ 17.225	
TMEM127	↑ 14.373	
RCAN3	↑ 12.205	
RAB40AL	↑ 11.558	
SRSF10	↑ 10.717	
MRPL38	↑ 10.485	
LMBR1	↑ 8.205	
TAF9B	↑ 7.659	
UCKL1	↑ 6.825	

Exp Fold Change down-regulated

Molecules	Exp. Value	Exp. Chart
SLC2A3	↓ -12.324	
FADS2	↓ -11.672	
SCD	↓ -11.341	
AK4	↓ -10.804	
BNIP1	↓ -8.996	
EXOSC4	↓ -7.970	
TNF	↓ -6.723	
PRKD3	↓ -6.407	
MIF	↓ -6.105	
PIK3AP1	↓ -5.433	

8.5 Cattle IPA analysis

INGENUITY[®] PATHWAY ANALYSIS



Analysis Name: Cow2 - 2016-03-15 11:00 AM
Analysis Creation Date: 2016-03-15
Build version: 366632M
Content version: 26127183 (Release Date: 2015-11-30)

Analysis Settings

Reference set: Ingenuity Knowledge Base (Genes Only)
Relationship to include: Direct and Indirect
Includes Endogenous Chemicals
Optional Analyses: My Pathways My List

Filter Summary:

Consider only relationships where
confidence = Experimentally Observed

Summary of Analysis - Cow2 - 2016-03-15 11:00 AM

Top Canonical Pathways		
Name	p-value	Overlap
Regulation of eIF4 and p70S6K Signaling	2.35E-04	6.8 % 10/146
EIF2 Signaling	1.43E-03	5.4 % 10/184
mTOR Signaling	1.61E-03	5.3 % 10/187
2-oxobutanoate Degradation I	2.89E-03	40.0 % 2/5
Oxidative Phosphorylation	2.89E-03	6.4 % 7/109

Top Upstream Regulators		
Upstream Regulator	p-value of overlap	Predicted Activation
NUPR1	1.22E-06	Activated
E2f	6.76E-06	
TP53	1.23E-05	
ST1926	1.65E-05	Activated
RRP1B	4.15E-05	

Top Diseases and Bio Functions		
Diseases and Disorders		
Name	p-value	#Molecules
Cancer	2.52E-02 - 1.10E-06	319
Organismal Injury and Abnormalities	2.52E-02 - 1.10E-06	324
Developmental Disorder	2.49E-02 - 2.98E-05	65
Endocrine System Disorders	1.73E-02 - 3.54E-05	22
Gastrointestinal Disease	1.73E-02 - 1.70E-04	273

Molecular and Cellular Functions

Summary of Analysis - Cow2 - 2016-03-15 11:00 AM

Name	p-value	#Molecules
Cellular Assembly and Organization	2.41E-02 - 2.67E-06	43
Gene Expression	1.73E-02 - 1.52E-04	62
RNA Damage and Repair	1.33E-02 - 1.52E-04	7
RNA Post-Transcriptional Modification	1.52E-04 - 1.52E-04	6
DNA Replication, Recombination, and Repair	2.24E-02 - 1.71E-04	35

Physiological System Development and Function

Name	p-value	#Molecules
Embryonic Development	2.37E-02 - 2.98E-05	53
Organismal Survival	5.15E-03 - 2.98E-05	77
Connective Tissue Development and Function	1.73E-02 - 8.86E-04	24
Tissue Development	2.37E-02 - 8.86E-04	48
Organismal Development	2.37E-02 - 1.02E-03	55

Top Tox Functions**Assays: Clinical Chemistry and Hematology**

Name	p-value	#Molecules
Decreased Levels of Hematocrit	1.30E-01 - 1.30E-01	1
Increased Levels of Hematocrit	4.91E-01 - 4.91E-01	2
Increased Levels of Creatinine	4.94E-01 - 4.94E-01	1
Increased Levels of Red Blood Cells	5.24E-01 - 5.24E-01	2

Cardiotoxicity

Name	p-value	#Molecules
Cardiac Degeneration	1.73E-02 - 1.73E-02	1
Congenital Heart Anomaly	5.75E-01 - 1.73E-02	2

(c) 2000-2016 QIAGEN. All rights reserved.

Summary of Analysis - Cow2 - 2016-03-15 11:00 AM

Cardiac Arrythmia	4.01E-01 - 3.43E-02	3
Cardiac Dilatation	1.77E-01 - 6.98E-02	3
Cardiac Arteriopathy	5.18E-01 - 9.95E-02	6

Hepatotoxicity

Name	p-value	#Molecules
Liver Fibrosis	3.19E-01 - 8.76E-03	7
Hepatocellular Peroxisome Proliferation	1.73E-02 - 1.73E-02	1
Liver Hyperplasia/Hyperproliferation	5.97E-01 - 1.73E-02	128
Hepatocellular Carcinoma	5.97E-01 - 3.11E-02	124
Liver Inflammation/Hepatitis	5.55E-01 - 3.43E-02	6

Nephrotoxicity

Name	p-value	#Molecules
Nephrosis	1.73E-02 - 1.73E-02	1
Renal Dilatation	1.73E-02 - 1.73E-02	1
Glomerular Injury	3.31E-01 - 4.62E-02	6
Renal Hyperplasia/Hyperproliferation	4.62E-02 - 4.62E-02	2
Renal Atrophy	1.75E-01 - 1.60E-01	1

Top Networks

ID	Associated Network Functions	Score
1	Cancer, Organismal Injury and Abnormalities, Gastrointestinal Disease	53
2	Cancer, Organismal Injury and Abnormalities, Gastrointestinal Disease	41
3	Cell Cycle, DNA Replication, Recombination, and Repair, Gene Expression	36
4	Ophthalmic Disease, Organismal Injury and Abnormalities, Skeletal and Muscular Disorders	36
5	Cell Cycle, DNA Replication, Recombination, and Repair, Developmental Disorder	34

(c) 2000-2016 QIAGEN. All rights reserved.

Top Tox Lists

Name	p-value	Overlap
Mitochondrial Dysfunction	3.39E-02	4.0 % 7/176
Long-term Renal Injury Anti-oxidative Response Panel (Rat)	3.81E-02	11.1 % 2/18
VDR/RXR Activation	4.64E-02	5.1 % 4/78
Mechanism of Gene Regulation by Peroxisome Proliferators via PPAR	8.29E-02	4.2 % 4/95
Increases Cardiac Dilation	8.41E-02	7.1 % 2/28

Top My Lists

Name	p-value	Overlap
CCL5 p=0.01	3.46E-03	16.7 % 3/18
CSF2 p=0.01	6.87E-03	7.2 % 5/69
CSF1 p=0.01	2.41E-02	8.3 % 3/36
CXCL8 p=0.01	3.05E-02	12.5 % 2/16
CSF3 p=0.01	1.00E-01	6.5 % 2/31

Top My Pathways

Name	p-value	Overlap
CCL5 p=0.01	3.46E-03	16.7 % 3/18
CSF2 p=0.01	6.87E-03	7.2 % 5/69
CSF1 p=0.01	2.41E-02	8.3 % 3/36
CXCL8 p=0.01	3.05E-02	12.5 % 2/16
HGF mechanistic network p0.01	5.81E-02	3.3 % 8/240

Top Analysis-Ready Molecules

Summary of Analysis - Cow2 - 2016-03-15 11:00 AM

Exp Fold Change up-regulated

Molecules	Exp. Value	Exp. Chart
CFHR3	↑ 34.156	
PSMD11	↑ 30.737	
NME3	↑ 22.407	
UNC5B	↑ 19.885	
MUM1	↑ 16.392	
WNT5A	↑ 13.694	
SLC36A4	↑ 12.970	
VASH1	↑ 12.130	
NATD1	↑ 11.199	
SMOC1	↑ 10.862	

Exp Fold Change down-regulated

Molecules	Exp. Value	Exp. Chart
HMGA2	↓ -80.890	
CEP55	↓ -12.382	
UHRF1	↓ -11.811	
KIF2C	↓ -8.982	
PBK	↓ -8.369	
ESPL1	↓ -8.023	
MT-CYB	↓ -7.237	
MT-ND3	↓ -7.147	
KIF22	↓ -7.069	
CCNF	↓ -7.000	

8.6 Rabbit to human with gene description

1	Transcript_Name	Human Ensembl Gene ID	CLUSTER 1	CLUSTER 2	CLUSTER 3	CLUSTER 6	CLUSTER 7	FC	pval	Log_FC	strand	start	end	num_exons	length	gene_id	Description	gene_name
1	ENSCOUT00000008948	ENS00000010958		YES	YES			0.513835471	0.016451238	-0.960621609	-	402300879	40231361	1	483	ENSC0UG000000022356	Uncharacterized protein [Source:UniProtKB/EMBL,Acc:G1SS21]	0
2	ENSCOUT000000023770	ENS000000100294		YES				0.918355717	0.040357954	-0.122875018	+	16562	26899	4	4784	ENSC0UG000000015843	malonyl CoA:ACP acyltransferase [mitochondrial] [Source:HGNC Symbol,Acc:G1SS21]	MCA1
3	ENSCOUT000000024031	ENS000000138381		YES				1.232731108	0.0245595	0.301858143	+	9303819	9305696	1	1878	ENSC0UG000000024832	Uncharacterized protein [Source:UniProtKB/EMBL,Acc:G1TX10]	0
4	ENSCOUT000000015376	ENS000000151093		YES				0.434145939	0.018146202	-1.203748005	+	12327109	12331612	2	2548	ENSC0UG000000015384	3-oxoacyl-ACP synthase, mitochondrial [Source:HGNC Symbol,Acc:HGNC:15884]	OXSM
5	ENSCOUT000000024169	ENS000000172232		YES		YES		1.270737712	0.007420982	0.34566628	+	108176894	108506100	11	1467	ENSC0UG000000057222	ceramide synthase 6 [Source:HGNC Symbol,Acc:HGNC:23826]	CERS6
6	ENSCOUT000000003499	ENS000000134824		YES		YES		0.085672586	0.01453431	-3.545022558	-	2874101	2906618	12	1353	ENSC0UG000000003499	fatty acid desaturase 2 [Source:UniProtKB/EMBL,Acc:G1T847]	FADS2
7	ENSCOUT000000004794	ENS000000093194		YES		YES		0.088172741	0.035263001	-3.503523475	-	48425105	48437117	6	1129	ENSC0UG000000014801	Uncharacterized protein [Source:UniProtKB/EMBL,Acc:G1T847]	0
8	ENSCOUT000000004547	ENS000000001630		YES		YES		0.560022688	0.040601664	-0.836442819	+	36634694	36654515	10	1527	ENSC0UG000000004549	cytochrome P450, family 51, subfamily A, polypeptide 1 [Source:HGNC Symbol,Acc:G1T847]	CYP51A1
9	ENSCOUT000000025399	ENS00000011669		YES		YES		0.231695789	0.00350146	-2.109636273	+	32890155	32893009	7	923	ENSC0UG000000025649	ribosephosphate isomerase 1 [Source:HGNC Symbol,Acc:HGNC:12009]	TRP1
10	ENSCOUT000000008644	ENS000000073246	YES		YES	YES		1.102514047	0.024364476	0.140797037	+	157535923	157466113	21	5250	ENSC0UG000000008642	X-ray repair complementing defective repair in Chinese hamster cells 5 [Source:HGNC Symbol,Acc:HGNC:15884]	XRCC5
11	ENSCOUT000000021649	ENS000000172115	YES		YES	YES		0.73269075	0.043449515	-0.448723692	-	82231495	82231612	1	318	ENSC0UG000000027391	Uncharacterized protein [Source:UniProtKB/EMBL,Acc:G1TY21]	0
12	ENSCOUT000000014272	ENS000000020426	YES		YES	YES		1.058996363	0.003234823	0.082700386	+	9315539	8542359	8	1415	ENSC0UG000000014274	MNAT1 CDK-activating kinase assembly factor 1 [Source:HGNC Symbol,Acc:HGNC:15884]	MNAT1
13	ENSCOUT000000002540	ENS000000176171	YES		YES	YES	YES	0.19389392	0.010643207	-2.36666053	-	90716	95350	5	1033	ENSC0UG000000002541	BCL2 adenovirus E1B 19kDa interacting protein 3 [Source:HGNC Symbol,Acc:HGNC:15884]	BNIP3
14	ENSCOUT000000005276	ENS000000196575	YES		YES	YES		1.174228086	0.042310157	0.23171267	+	27255414	2874309	16	2349	ENSC0UG000000005276	neurofibromin 2 [merlin] [Source:HGNC Symbol,Acc:HGNC:7773]	NF2
15	ENSCOUT000000028328	ENS000000112592	YES		YES	YES		0.325968243	0.045046504	0.407046223	-	21719	40912	7	3011	ENSC0UG000000007979	TATA box binding protein [Source:HGNC Symbol,Acc:HGNC:11588]	TBP
16	ENSCOUT000000015150	ENS000000166484	YES		YES	YES		1.73707855	0.018904004	0.796661332	-	323191	327527	6	2750	ENSC0UG000000015154	mitogen-activated protein kinase 7 [Source:HGNC Symbol,Acc:HGNC:6696]	MAPK7
17	ENSCOUT000000006977	ENS000000177463	YES		YES	YES		0.782668317	0.023524254	-0.353527049	+	10502766	10566683	16	2058	ENSC0UG000000006975	nuclear receptor subfamily 2, group C, member 2 [Source:HGNC Symbol,Acc:HGNC:15884]	NR2C2
18	ENSCOUT000000006606	ENS000000090316	YES		YES	YES		0.553806453	0.021660036	-0.85254623	-	541	750	1	210	ENSC0UG000000006606	macrophage erythroblast attachment [Source:HGNC Symbol,Acc:HGNC:1317]	MAEA
19	ENSCOUT000000004714	ENS000000187325	YES		YES	YES		7.659413773	0.013058727	2.937233977	-	69877434	69884179	7	819	ENSC0UG000000014717	Uncharacterized protein [Source:UniProtKB/EMBL,Acc:G1TY78]	0
20	ENSCOUT000000004604	ENS000000154320	YES		YES	YES		1.123278903	0.00905367	0.278554458	-	37333315	37340228	8	2171	ENSC0UG000000004604	essential meiotic structure-specific endonuclease 1 [Source:HGNC Symbol,Acc:HGNC:15884]	EME1
21	ENSCOUT000000004772	ENS000000123562	YES		YES	YES		1.243844152	0.008386517	0.524553396	+	86448916	86449782	1	867	ENSC0UG000000014778	mortality factor 4 like 2 [Source:HGNC Symbol,Acc:HGNC:15884]	MOF4L2
22	ENSCOUT000000011947	ENS000000105496	YES		YES	YES		0.12874143	0.000736923	-1.676345662	+	518	24350	22	5416	ENSC0UG000000011941	ligase I, DNA, ATP-dependent [Source:HGNC Symbol,Acc:HGNC:6598]	LIG1
23	ENSCOUT000000010693	ENS000000161332	YES		YES	YES		1.126132245	0.021917446	0.787542999	-	55912363	55935420	3	4996	ENSC0UG00000011091	MAPK12 binding inhibitory protein 1 [Source:HGNC Symbol,Acc:HGNC:23826]	MBIP
24	ENSCOUT000000005398	ENS000000175305	YES		YES	YES		0.55320702	0.040346282	0.854855005	-	10448503	10500646	12	1326	ENSC0UG000000005398	cyclin E2 [Source:HGNC Symbol,Acc:HGNC:15884]	CN2E
25	ENSCOUT000000002807	ENS000000143354	YES		YES	YES		0.660821298	0.042852429	-0.59766791	-	153720	240687	44	5418	ENSC0UG000000002802	Fanconi anemia, complementation group D2 [Source:HGNC Symbol,Acc:HGNC:15884]	FANCD2
26	ENSCOUT000000003622	ENS000000109119	YES		YES	YES		0.843671168	0.015444366	-0.245247295	+	4595342	4615895	9	2898	ENSC0UG000000003624	replication factor C (activator 1) 3, 38kDa [Source:HGNC Symbol,Acc:HGNC:15884]	RFC3
27	ENSCOUT000000012216	ENS000000125901	YES		YES	YES		0.905904761	0.015520212	-0.14256871	+	10339298	10041261	4	1304	ENSC0UG000000012218	mitochondrial ribosomal protein S26 [Source:HGNC Symbol,Acc:HGNC:15884]	MPPS26
28	ENSCOUT000000025560	ENS00000013356	YES		YES	YES		1.088044048	0.024445079	-0.104602624	+	10247401	10269842	6	724	ENSC0UG000000010624	polymerase (RNA) III (DNA directed) polypeptide G (32kD) [Source:HGNC Symbol,Acc:HGNC:15884]	POLR3G
29	ENSCOUT00000000324	ENS000000140634	YES		YES	YES		0.87502785	0.042931808	-0.196768358	-	7433345	7667457	23	1905	ENSC0UG000000003222	poly(A)-specific ribonuclease [Source:HGNC Symbol,Acc:HGNC:8609]	PARN
30	ENSCOUT000000008034	ENS000000163682	YES		YES	YES		0.941032153	0.01108972	-0.087684078	-	3788180	3788758	1	579	ENSC0UG000000025072	Uncharacterized protein [Source:UniProtKB/EMBL,Acc:G1SUB3]	0
31	ENSCOUT000000027010	ENS000000108175	YES		YES	YES		1.209761617	0.048564533	0.274722793	+	438368	538550	21	6902	ENSC0UG000000003587	zinc finger, MIZ-type containing 1 [Source:HGNC Symbol,Acc:HGNC:1645]	ZNF21
32	ENSCOUT000000005170	ENS000000186814	YES		YES	YES		0.66053788	0.01961141	-0.598286796	-	76619089	76634379	4	1799	ENSC0UG000000005172	zinc finger and SCAN domain containing 30 [Source:HGNC Symbol,Acc:HGNC:15884]	ZNF30
33	ENSCOUT000000008345	ENS000000169732	YES		YES	YES		1.441915589	0.001056105	0.52796771	+	23445508	23433787	4	1712	ENSC0UG000000008346	protein serine kinase H1 [Source:HGNC Symbol,Acc:HGNC:3523]	PSKH1
34	ENSCOUT000000011703	ENS000000102103	YES		YES	YES		2.24568798	0.02090071	1.548223988	+	33551942	33559604	6	827	ENSC0UG000000011703	polyglutamine binding protein 1 [Source:HGNC Symbol,Acc:HGNC:9330]	PQBP1
35	ENSCOUT000000009375	ENS000000196298	YES		YES	YES		0.30460252	0.02344638	-1.714053263	-	701293	7024361	8	2703	ENSC0UG000000009375	protein phosphatase 1, catalytic subunit, gamma isozyme [Source:HGNC Symbol,Acc:HGNC:15884]	PPP1CC
36	ENSCOUT000000024194	ENS000000147130	YES		YES	YES		1.132362549	0.049674327	0.17933594	-	49710474	49726020	25	6078	ENSC0UG000000012396	zinc finger, MYM-type 3 [Source:HGNC Symbol,Acc:HGNC:13054]	ZMYM3
37	ENSCOUT000000010093	ENS000000162433	YES		YES	YES		0.032555	0.01610221	-3.433545267	-	10181454	10125502	6	1500	ENSC0UG000000010091	adenylate kinase 4 [Source:HGNC Symbol,Acc:HGNC:363]	AK4
38	ENSCOUT000000008576	ENS000000206560	YES		YES	YES		0.691831054	0.042355193	-0.531508321	-	1755795	1868227	28	6250	ENSC0UG000000008568	ankyrin repeat domain 28 [Source:HGNC Symbol,Acc:HGNC:23024]	ANKRD28
39	ENSCOUT000000004934	ENS000000166502	YES		YES	YES		0.930610683	0.024445079	-0.104602624	-	17539978	17568564	15	4206	ENSC0UG000000004933	SUV3-like helicase [Source:HGNC Symbol,Acc:HGNC:11471]	SUPV3L1
40	ENSCOUT000000003856	ENS000000070814	YES		YES	YES		1.12858538	0.074936362	0.278411291	+	32115536	32150424	28	6245	ENSC0UG000000003848	Treacher Collins-Franceschetti syndrome 1 [Source:HGNC Symbol,Acc:HGNC:15884]	TCDF1
41	ENSCOUT000000024418	ENS000000101685	YES		YES	YES		1.633338546	0.002215582	0.707823853	-	89924494	89950849	4	3534	ENSC0UG000000024309	SMAD family member 7 [Source:HGNC Symbol,Acc:HGNC:6773]	SMAD7
42	ENSCOUT000000004123	ENS000000103231	YES		YES	YES		0.690724499	0.048373815	-0.5338177	-	91888326	91923462	10	3238	ENSC0UG000000014124	SUMO1/sentrin specific peptidase 5 [Source:HGNC Symbol,Acc:HGNC:23826]	SENP5
43	ENSCOUT0000000015063	ENS000000119716	YES		YES	YES		1.456968656	0.008231044	0.54296984	+	730203	826058	11	3639	ENSC0UG000000015063	URF1, prefolin-like chaperone [Source:HGNC Symbol,Acc:HGNC:13236]	URF1
44	ENSCOUT000000017149	ENS000000163945	YES		YES	YES		1.487709194	0.022723742	0.573092547	-	1097171	1104740	13	1407	ENSC0UG000000017150	heterogeneous nuclear ribonucleoprotein H1 [H] [Source:HGNC Symbol,Acc:HGNC:15884]	HNRNP1H
45	ENSCOUT000000008238	ENS000000198529	YES		YES	YES		10.71630331	0.010132538	3.421816193	+	129565575	129586425	3	515	ENSC0UG000000023326	Sin3A-associated protein, 30kDa [Source:HGNC Symbol,Acc:HGNC:1053]	SAP30
46	ENSCOUT000000010417	ENS000000164105	YES		YES	YES		0.351549812	0.015689712	-1.508199972	+	51236221	51244206	4	2247	ENSC0UG000000010418	exosome component 10 [Source:HGNC Symbol,Acc:HGNC:18189]	EXOSC10
47	ENSCOUT000000027951	ENS000000178896	YES		YES	YES		0.125465243	0.026038242	-2.394640332	-	10554	11771	3	738	ENSC0UG000000027949	exosome component 4 [Source:HGNC Symbol,Acc:HGNC:18189]	EXOSC4
48	ENSCOUT000000003879	ENS000000080069	YES		YES	YES		1.204146629	0.013843083	0.26801108	-	66143	102352	12	3665	ENSC0UG000000003873	CTD (carboxy-terminal domain, RNA polymerase II, polypeptide A) phosphatase 1 [Source:HGNC Symbol,Acc:HGNC:15884]	CTDP1
49	ENSCOUT000000000407	ENS000000125256	YES		YES	YES		0.279642946	0.018583122	-1.838342669	+	112251933						

61	ENSDCUT00000024642	ENSG000000087088		YES	YES	YES	2.027111268	0.03360173	1.01942528	-	90719	93528	5	579	ENSDCUG00000006423	BCL2-associated X protein [Source:HGNC Symbol;Acc:HGNC:959]	BAX
62	ENSDCUT00000032048	ENSG00000019630		YES			1.274447604	0.032233476	0.349872061	+	30172447	30180160	6	489	ENSDCUG00000026354	placental growth factor [Source:HGNC Symbol;Acc:HGNC:8893]	PGF
63	ENSDCUT00000015230	ENSG000000145643		YES			0.304866331	0.021765952	-1.713656624	+	71073774	71082596	5	792	ENSDCUG00000015236	Uncharacterized protein [Source:UniProtKB/TrEMBL;Acc:G1T902]	0
64	ENSDCUT00000031433	ENSG000000075790		YES	YES		0.859000883	0.020262515	-0.219268481	-	125566	127231	1	726	ENSDCUG00000028156	Uncharacterized protein [Source:UniProtKB/TrEMBL;Acc:G1T924]	0
65	ENSDCUT00000008309	ENSG000000100234		YES			2.51224051	0.00366106	1.328974998	-	68307960	88362257	5	5335	ENSDCUG000000009310	metalloproteinase inhibitor 3 precursor [Source:RefSeq peptide;Acc:NP_001100000]	TIMP3
66	ENSDCUT00000007940	ENSG000000184254		YES			1.125648237	0.010062358	0.110715372	-	21	32016	12	6932	ENSDCUG00000007938	aldehyde dehydrogenase 11 family, member A3 [Source:HGNC Symbol;Acc:HGNC:27962]	ALDH1A3
67	ENSDCUT00000001542	ENSG000000104312		YES			0.662776092	0.001105467	-0.593406534	+	105172432	105208358	11	4818	ENSDCUG000000001542	receptor-interacting serine-threonine kinase 2 [Source:HGNC Symbol;Acc:HGNC:27962]	RIPK2
68	ENSDCUT00000006956	ENSG000000184584		YES	YES		1.436087749	0.039155328	0.522143905	+	21717532	21721600	6	1143	ENSDCUG00000006958	transmembrane protein 173 [Source:HGNC Symbol;Acc:HGNC:27962]	TMEM173
69	ENSDCUT00000000040	ENSG000000113734		YES	YES		0.11164894	0.025573732	-3.163226838	+	54179323	54191736	6	687	ENSDCUG00000000040	BCL2/adenovirus E1B 19kDa interacting protein 1 [Source:HGNC Symbol;Acc:HGNC:27962]	BNIP1
70	ENSDCUT00000000172	ENSG000000134215		YES			2.201697586	0.006062542	1.138616321	+	56144498	56550635	27	6134	ENSDCUG00000000172	vav 3 guanine nucleotide exchange factor [Source:HGNC Symbol;Acc:HGNC:27962]	VAV3
71	ENSDCUT00000006278	ENSG000000140239		YES	YES		1.237276578	0.034451832	0.307168034	+	12711305	12731422	11	1285	ENSDCUG00000006277	BCL2/adenovirus E1B 19kDa interacting protein 2 [Source:HGNC Symbol;Acc:HGNC:27962]	BNIP2
72	ENSDCUT00000004623	ENSG000000138613		YES			1.342191638	0.020785756	0.424590674	-	8941946	8981823	6	774	ENSDCUG00000004627	APH1B gamma secretase subunit [Source:HGNC Symbol;Acc:HGNC:240]	APH1B
73	ENSDCUT00000015411	ENSG000000114209		YES			1.076805208	0.008326844	0.106757293	-	62397127	62443385	8	823	ENSDCUG00000015413	programmed cell death 10 [Source:HGNC Symbol;Acc:HGNC:8761]	PDCD10
74	ENSDCUT00000004132	ENSG000000028157		YES			0.418770231	0.049761638	-1.255763206	-	1901647	1932164	9	2459	ENSDCUG00000004127	tumor necrosis factor receptor superfamily, member 1B [Source:HGNC Symbol;Acc:HGNC:8893]	TNFRSF1B
75	ENSDCUT00000012027	ENSG000000137193		YES			1.318439568	0.019969398	0.339631467	+	27027210	27031509	6	1514	ENSDCUG00000012026	Pim-1 proto-oncogene, serine/threonine kinase [Source:HGNC Symbol;Acc:HGNC:27962]	PIM1
76	ENSDCUT00000015956	ENSG000000135755		YES			1.065324802	0.007485036	0.092105664	-	17013509	17040696	7	1424	ENSDCUG00000015961	Serine/threonine-protein phosphatase 2A catalytic subunit alpha isoform	PPP2CA
77	ENSDCUT00000001921	ENSG000000185825		YES	YES		0.765459382	0.043508814	-0.385602227	+	694531	727417	8	831	ENSDCUG00000001921	B-cell receptor-associated protein 31 [Source:HGNC Symbol;Acc:HGNC:27962]	BPCA31
78	ENSDCUT00000002187	ENSG000000196230		YES			0.77320004	0.038959603	-0.371086382	+	22748030	22752315	4	2641	ENSDCUG00000002187	tubulin, beta class I [Source:HGNC Symbol;Acc:HGNC:20778]	TUBB
79	ENSDCUT00000006052	ENSG000000152895		YES			0.776087549	0.022884741	-0.365708686	+	14294137	14304532	3	1862	ENSDCUG00000006054	GIN5 complex subunit 3 [Psf3 homolog] [Source:HGNC Symbol;Acc:HGNC:27962]	GIN5
80	ENSDCUT00000025334	ENSG000000198924		YES			1.06243205	0.003148041	0.087370573	-	61409924	61437082	9	4172	ENSDCUG00000004921	DNA cross-link repair 1A [Source:HGNC Symbol;Acc:HGNC:17660]	DCLRE1A
81	ENSDCUT000000017632	ENSG000000174943		YES			0.77371366	0.006671638	-0.370766745	-	18314268	18323818	6	390	ENSDCUG000000017636	potassium channel tetramerization domain containing 13 [Source:HGNC Symbol;Acc:HGNC:27962]	KCTD13
82	ENSDCUT00000000013	ENSG000000070950		YES			0.5860789	0.026107386	-0.770833196	+	42530	146086	13	1537	ENSDCUG00000000013	RAD18 E3 ubiquitin protein ligase [Source:HGNC Symbol;Acc:HGNC:1827]	RAD18
83	ENSDCUT000000031279	ENSG000000031279				YES	0.054120272	0.001695629	-4.207687089	-	119951100	119951563	1	464	ENSDCUG000000031279	Uncharacterized protein [Source:UniProtKB/TrEMBL;Acc:G1U116]	0
84	ENSDCUT00000015392	ENSG000000181938					1.089854141	0.002391647	0.123870293	+	33349371	33362270	13	2596	ENSDCUG00000015393	Small nucleolar RNA SNORD30 [Source:RFAM;Acc:RF00068]	SNORD30
85	ENSDCUT00000019648	ENSG000000277846					0.832794559	0.002532464	-0.263367453	+	1503980	1510049	1	89	ENSDCUG00000019648	Uncharacterized protein [Source:UniProtKB/TrEMBL;Acc:G1U116]	0
86	ENSDCUT00000017551	ENSG00000017551					0.98037903	0.004855068	-0.028588469	+	71836473	71896381	1	509	ENSDCUG00000017552	aldehyde dehydrogenase 1 family, member L2 [Source:HGNC Symbol;Acc:HGNC:27962]	ALDH1L2
87	ENSDCUT00000006365	ENSG000000136010					0.643275676	0.013769814	-0.636490598	+	91263358	91325818	23	6154	ENSDCUG00000006362	Small nucleolar RNA SNORD29 [Source:RFAM;Acc:RF00070]	SNORD29
88	AIHV1gp18.1						1.035905543	0.01510364	0.05089246	+	38345	40030	1	1686	AIHV1gp18	aglynyltransferase 1 [Source:HGNC Symbol;Acc:HGNC:782]	ATE1
89	ENSDCUT00000019581	ENSG00000019581					0.942382639	0.021954861	-0.085615042	+	1509745	1509809	1	65	ENSDCUG00000019581	mitogen-activated protein kinase kinase kinase 4 [Source:HGNC Symbol;Acc:HGNC:27962]	MAP4K4
90	ENSDCUT00000003374	ENSG000000107663					0.491244869	0.021964763	-1.025485757	-	68671085	68850046	13	5208	ENSDCUG00000003373	Uncharacterized protein [Source:UniProtKB/TrEMBL;Acc:G1U116]	0
91	ENSDCUT00000008192	ENSG000000071054					0.488702868	0.02780959	-1.003747534	-	90545948	90731059	32	7249	ENSDCUG00000008180	Uncharacterized protein [Source:UniProtKB/TrEMBL;Acc:G1U116]	0
92	ENSDCUT000000031018	ENSG000000031018					0.009074781	0.030517064	-6.783244567	+	23171050	23171457	1	408	ENSDCUG000000031018	Uncharacterized protein [Source:UniProtKB/TrEMBL;Acc:G1U116]	0
93	ENSDCUT00000028495	ENSG00000028495					0.121575049	0.017050447	-3.042456211	-	242	336	1	95	ENSDCUG00000028495	phosphatidylinositol-specific phospholipase C, X domain containing 2 [Source:HGNC Symbol;Acc:HGNC:27962]	PLCXD2
94	ENSDCUT00000022824	ENSG000000240891					2.450840084	0.021877649	1.293158817	-	107473747	107533072	4	1630	ENSDCUG00000022825	Uncharacterized protein [Source:UniProtKB/TrEMBL;Acc:U3KNC9]	0
95	ENSDCUT000000033691	ENSG000000033691					1.484330878	0.015547678	0.569812725	-	249501	252516	4	1192	ENSDCUG00000003369	Uncharacterized protein [Source:UniProtKB/TrEMBL;Acc:U3KNC9]	0
96	ENSDCUT000000025140	ENSG000000025140					0.993587712	0.010742514	-0.009280763	-	22803292	22804049	1	758	ENSDCUG00000002514	Uncharacterized protein [Source:UniProtKB/TrEMBL;Acc:U3KNC9]	0
97	AIHV1gp08.1						1.013526685	0.020804324	0.019384074	+	14725	16767	1	2043	AIHV1gp08	leucine rich repeat neuronal 3 [Source:HGNC Symbol;Acc:HGNC:17200]	LRRN3
98	ENSDCUT00000013565	ENSG000000173114					1.024956285	0.0126394	0.035562379	+	47981727	47983853	1	2127	ENSDCUG00000013571	GRB2-binding adaptor protein, transmembrane [Source:HGNC Symbol;Acc:HGNC:27962]	GAPT
99	ENSDCUT00000023234	ENSG000000175857					1.022768321	0.006802398	0.032507593	+	74425245	74425718	1	474	ENSDCUG00000023235	Uncharacterized protein [Source:UniProtKB/TrEMBL;Acc:U3KNH4]	0
100	ENSDCUT000000033736	ENSG000000033736					1.03951913	0.041509753	0.055916307	+	143548	144798	1	1251	ENSDCUG00000003373	serine/arginine-rich splicing factor 3 [Source:HGNC Symbol;Acc:HGNC:27962]	SRSF3
101	ENSDCUT00000028806	ENSG000000211535					1.027606111	0.002479401	0.039287375	-	16278486	16278558	1	73	ENSDCUG00000028806	Uncharacterized protein [Source:UniProtKB/TrEMBL;Acc:U3KNH4]	0
102	ENSDCUT00000033317	ENSG000000112081					1.036278329	0.034092733	0.051411541	+	28545708	28553942	5	4519	ENSDCUG00000033317	potassium channel, inwardly rectifying subfamily J, member 14 [Source:HGNC Symbol;Acc:HGNC:27962]	KCNJ14
103	ENSDCUT00000002404	ENSG000000101972					1.034878887	0.02287232	0.049493149	+	14689862	14690171	1	310	ENSDCUG00000002404	apolipoprotein L domain containing 1 [Source:HGNC Symbol;Acc:HGNC:27962]	APOLD1
104	ENSDCUT00000008995	ENSG000000182324					1.037878849	0.010078283	0.053635268	+	96090	98925	2	1302	ENSDCUG00000008998	Uncharacterized protein [Source:UniProtKB/TrEMBL;Acc:G1T2U1]	0
105	ENSDCUT000000023471	ENSG000000178878					1.038444187	0.010994665	0.054423678	-	26945542	26946288	1	747	ENSDCUG00000002348	Uncharacterized protein [Source:UniProtKB/TrEMBL;Acc:G1T2U1]	0
106	ENSDCUT000000029967	ENSG000000180935					1.03552974	0.000823818	0.050368988	+	110738755	110739432	1	678	ENSDCUG00000002997	Uncharacterized protein [Source:UniProtKB/TrEMBL;Acc:G1T2U1]	0
107	ENSDCUT000000021607	ENSG000000021607					1.034461539	0.009711978	0.048880008	+	6776859	6777764	1	906	ENSDCUG00000002196	Uncharacterized protein [Source:UniProtKB/TrEMBL;Acc:G1T2U1]	0
108	ENSDCUT000000013264	ENSG000000013264					0.964560403	0.022262767	-0.052056509	+	15896219	15897556	1	1338	ENSDCUG00000013266	Small nucleolar RNA SNORA58 [Source:RFAM;Acc:RF00048]	SNORA58
109	ENSDCUT000000010785	ENSG000000010785					1.03511882	0.03556771	0.049786713	-	1828855	1829584	1	730	ENSDCUG00000010788	PDS5 cohesin associated factor A [Source:HGNC Symbol;Acc:HGNC:27962]	PDS5A
110	ENSDCUT000000025731	ENSG000000025731					1.516043944	0.029816454	0.600311572	-	38289165	38289301	1	137	ENSDCUG000000024097	cohesin subunit SA-2 [Source:RefSeq peptide;Acc:NP_00164797]	STAG2
111	ENSDCUT00000005987	ENSG000000121692					1.83913245	0.046663098	0.879025383	-	23073525	23206002	32	7044	ENSDCUG00000005980	fibronectin leucine rich transmembrane protein 3 [Source:HGNC Symbol;Acc:HGNC:27962]	FLRT3
112	ENSDCUT00000033492	ENSG000000176338					1.114230484	0.0178789	0.231979332	-	46445	476206	3	552			

8.8 Cattle to human with gene description

1	Transcript Name	Human Ensembl Gene ID	CLUSTER 1	CLUSTER 2	CLUSTER 3	CLUSTER 4	CLUSTER 5	FC	pval	Log_FC	strand	start	end	num_exons	length	gene_id	Description	gene_name
1	ENSBTAT00000015873	ENSNG00000120053				YES	YES	1.3294164	0.0097024	0.4107931		20285687	20310044	9	1974	ENSBTAG000000011960	glutamic-oxaloacetic transaminase 1, soluble [Source:HGNC Symb]	GOTT1
2	ENSBTAT00000043780	ENSNG000000065057	YES		YES		YES	1.4380666	0.017064	0.5241305	-	1590252	1595934	6	1029	ENSBTAG000000006272	nth-like DNA glycosylase 1 [Source:HGNC Symb;Acc:HGNC:602]	NTHL1
3	ENSBTAT00000011619	ENSNG00000132664			YES		YES	0.3082448	0.0380734	-1.637852	+	38841092	38855175	9	1839	ENSBTAG00000008825	polymerase (RNA) III (DNA directed) polypeptide F, 39 kDa [Source:POLR3F]	
4	ENSBTAT00000020336	ENSNG00000006695	YES				YES	0.6505892	0.0162541	-0.620181	+	32696437	32804796	7	2845	ENSBTAG00000015294	COX10 heme A:farnesyltransferase cytochrome c oxidase assembl	COX10
5	ENSBTAT000000064176	ENSNG00000014919	YES				YES	20.259094	0.0188731	4.3404977	-	20533690	20550733	9	1585	ENSBTAG000000045703	cytochrome c oxidase assembly homolog 15 [yeast] [Source:HGNC]	COX15
6	ENSBTAT000000039643	ENSNG00000167283	YES				YES	0.0062025	0.0239109	-7.332933	+	29521980	29531009	3	474	ENSBTAG00000007332	uroporphyrinogen III synthase [Source:HGNC Symb;Acc:HGNC: UROS]	
7	ENSBTAT00000007615	ENSNG00000188690	YES				YES	0.0347346	0.0361015	-4.847484	-	45635844	45660024	10	1714	ENSBTAG000000005791	Uncharacterized protein [Source:UniProtKB/TrEMBL;Acc:G3NOR]	
8	ENSBTAT000000064252	ENSNG00000128951	YES				YES	0.1885056	0.0453446	-2.40732	+	14267911	14267962	1	582	ENSBTAG000000047462	Uncharacterized protein [Source:UniProtKB/TrEMBL;Acc:G3NOR]	
9	ENSBTAT000000020608	ENSNG00000105835					YES	74.309429	0.0001398	6.2154734	-	47597860	47635332	11	1814	ENSBTAG00000015509	nicotinamide phosphoribosyltransferase [Source:HGNC Symb;Acc:HGNC: NAMPT]	
10	ENSBTAT00000025662	ENSNG00000138363					YES	1445.9097	0.0064757	10.497762	+	10384780	103870755	16	2042	ENSBTAG00000019274	5-aminimidazole-4-carboxamide ribonucleotide formyltransferase ATIC	
11	ENSBTAT000000120204	ENSNG00000112541					YES	23.233443	0.0112433	4.8725059	-	101987619	102068001	19	2362	ENSBTAG000000017759	phosphodiesterase 10A [Source:HGNC Symb;Acc:HGNC:8772]	PDE10A
12	ENSBTAT00000018301	ENSNG00000125877					YES	0.5248596	0.0138623	-0.330052	-	52449560	52462382	8	934	ENSBTAG000000137716	inosine triphosphatase (nucleoside triphosphate pyrophosphatase) ITPA	
13	ENSBTAT00000003935	ENSNG00000172113					YES	34.281313	0.0321761	5.0993505	+	52126504	52133264	6	1086	ENSBTAG00000003025	NME/NM23 nucleoside diphosphate kinase 6 [Source:HGNC Symb; NME6]	
14	ENSBTAT000000022012	ENSNG00000103024					YES	23371.596	0.0363354	14.842134	-	1348415	1349600	5	813	ENSBTAG00000016552	NME/NM23 nucleoside diphosphate kinase 3 [Source:HGNC Symb; NME3]	
15	ENSBTAT00000005978	ENSNG00000194944					YES	0.0268973	0.0374393	-5.216395	-	80939906	80970032	8	1131	ENSBTAG000000004549	uracil phosphoribosyltransferase (FUR1) homolog (S. cerevisiae) [Source:UPRT]	
16	ENSBTAT00000018370	ENSNG000000069362					YES	11.837396	0.044216	3.5652798	+	85480247	85537788	11	2258	ENSBTAG00000013825	branched chain amino-acid transaminase 1, cytosolic [Source:HGNC:BCAT1]	
17	ENSBTAT000000046902	ENSNG00000143156					YES	0.6948802	0.0485144	-0.525164	-	37533775	37838172	12	1413	ENSBTAG00000002689	NME/NM23 family member 7 [Source:HGNC Symb;Acc:HGNC:2C: NME7]	
18	ENSBTAT000000065618	ENSNG00000069374	YES	YES		YES		2.086328	0.0238884	1.060966	-	35101143	35101808	1	666	ENSBTAG000000046690	Uncharacterized protein [Source:UniProtKB/TrEMBL;Acc:G3MYK]	
19	ENSBTAT00000015829	ENSNG00000158204	YES	YES		YES		0.7963207	0.0289074	-0.327492	+	57854278	57857485	8	850	ENSBTAG00000011931	CD63 antigen [Source:UniProtKB/Swiss-Prot;Acc:Q9XSK2]	CD63
20	ENSBTAT000000021426	ENSNG00000123643	YES	YES		YES		0.1249039	0.0269532	-3.00111	+	64650884	64684500	10	1531	ENSBTAG00000016034	solute carrier family 36 (proton/amino acid symporter), member 1 [S. SLC36A1]	
21	ENSBTAT000000024228	ENSNG00000162144	YES	YES		YES		0.1076718	0.0136631	-3.802451	-	40551223	40562584	7	1868	ENSBTAG00000018202	cytochrome b5f1 family, member A3 [Source:HGNC Symb;Acc:CYB5F1A3]	
22	ENSBTAT00000028656	ENSNG00000155039		YES		YES		8.631973	0.0237126	3.1096914	+	75708345	75780623	7	1024	ENSBTAG00000039968	transmembrane protein 55A [Source:HGNC Symb;Acc:HGNC:2E: TMEM55A]	
23	ENSBTAT000000049326	ENSNG00000186187		YES		YES		2.2605669	0.0362335	1.1766846	+	2396335	2482363	4	1389	ENSBTAG000000034689	zinc and ring finger 1, E3 ubiquitin protein ligase [Source:HGNC Symb; ZNF1F1]	
24	ENSBTAT000000044878	ENSNG00000114742		YES		YES		1.6529749	0.0377671	0.7285849	+	12416319	12468477	19	3957	ENSBTAG000000037445	W/D repeat domain 48 [Source:HGNC Symb;Acc:HGNC:30594]	WD48
25	ENSBTAT000000052079	ENSNG00000068001		YES		YES		0.5070393	0.0425012	-0.37983	+	50553227	50597453	4	1876	ENSBTAG000000000484	hyaluronoglucosaminidase 2 [Source:HGNC Symb;Acc:HGNC:5:HYAL2]	
26	ENSBTAT000000007967	ENSNG00000132646	YES		YES		YES	0.2321709	0.0482774	-2.106741	+	47788530	47794802	6	1988	ENSBTAG000000006085	proliferating cell nuclear antigen [Source:HGNC Symb;Acc:HGNC:PCNA]	PCNA
27	ENSBTAT00000019379	ENSNG00000174547	YES	YES		YES		0.3654304	0.009037	-1.452331	-	45127205	45130554	5	827	ENSBTAG00000015006	mitochondrial ribosomal protein L11 [Source:HGNC Symb;Acc:HM:MRPL11]	
28	ENSBTAT000000064878	ENSNG00000171421	YES	YES		YES		1.0488679	0.0155609	0.068833	+	70995214	70998377	2	775	ENSBTAG000000047906	mitochondrial ribosomal protein L36 [Source:HGNC Symb;Acc:HM:MRPL36]	
29	ENSBTAT000000020681	ENSNG00000104980	YES	YES		YES		0.5560291	0.016638	-0.846768	-	17907314	17920304	13	1816	ENSBTAG00000015567	translocase of inner mitochondrial membrane 44 homolog (yeast) [Source:TIMM44]	
30	ENSBTAT000000030623	ENSNG00000132153	YES	YES		YES		0.0038182	0.0176716	-8.03291	-	52465093	52480017	19	3743	ENSBTAG00000015833	DEAH (Asp-Glu-Ala-His) box helicase 30 [Source:HGNC Symb;Acc:DEAH30]	
31	ENSBTAT000000032066	ENSNG00000104835	YES	YES		YES		0.3985734	0.0198164	-1.327083	-	48896564	48905591	16	1888	ENSBTAG00000001780	serine--tRNA ligase, mitochondrial precursor [Source:RefSeq pep]	
32	ENSBTAT000000023334	ENSNG00000104835	YES	YES		YES		0.443606	0.0235088	-1.153267	-	48896564	48905510	16	1907	ENSBTAG00000001780	serine--tRNA ligase, mitochondrial precursor [Source:RefSeq pep]	
33	ENSBTAT000000044248	ENSNG00000135823	YES	YES		YES		3.3865515	0.0366613	1.7938169	+	65097628	65115555	7	2779	ENSBTAG00000003091	ribonuclease L [2',5'-oligoadenylate synthetase-dependent] [Source:RNASEL]	
34	ENSBTAT000000001464	ENSNG00000116161	YES	YES		YES		1.1358608	0.040665	0.1837861	+	57694739	57705495	6	1200	ENSBTAG000000011017	calyculin binding protein [Source:HGNC Symb;Acc:HGNC:3042: CACYBP]	
35	ENSBTAT000000009173	ENSNG00000133635	YES	YES		YES		1.4336715	0.0464338	0.519745	+	35662559	35763653	24	2611	ENSBTAG000000006978	hydroxysteroid (17-beta) dehydrogenase 4 [Source:HGNC Symb;Acc:HGNC:HSD17B4]	
36	ENSBTAT000000012969	ENSNG00000197448	YES	YES		YES		0.6163564	0.0436358	-0.639159	+	107466164	107473271	8	951	ENSBTAG000000009839	glutathione S-transferase kappa 3 [Source:HGNC Symb;Acc:HGNC:GSTK1]	
37	ENSBTAT000000015019	ENSNG00000176324	YES	YES		YES		0.316109	0.014603	-1.861506	-	17696953	17696398	19	2624	ENSBTAG00000011360	pre-mRNA-splicing factor SYF1 [Source:RefSeq peptide;Acc:NP_X482]	
38	ENSBTAT00000005018	ENSNG00000134637	YES	YES		YES		0.0839459	0.0056007	-3.484455	-	108882202	108918432	16	2302	ENSBTAG00000003849	guanine nucleotide binding protein-like 2 (nucleolar) [Source:HGNC:GNL2]	
39	ENSBTAT000000022090	ENSNG00000115283	YES	YES		YES		132.65435	0.005198	7.0515282	+	10113121	10115411	9	906	ENSBTAG000000016806	polycomb group ring finger 1 [Source:HGNC Symb;Acc:HGNC:17:PCGF1]	
40	ENSBTAT000000026265	ENSNG00000117905	YES	YES		YES		0.8147415	0.007854	-0.235586	+	60016985	60024586	6	3021	ENSBTAG00000019707	GATA binding protein 1 [Source:HGNC Symb;Acc:HGNC:4171: GATA2]	
41	ENSBTAT000000050636	ENSNG00000116035	YES	YES		YES		2.7875308	0.0087621	1.4789878	-	44765461	44793485	10	2123	ENSBTAG00000007323	cleavage and polyadenylation specific factor 8, 68kDa [Source:HGNC:CPSP6]	
42	ENSBTAT00000016381	ENSNG00000112658	YES	YES		YES		0.3260660	0.0088613	-1.616752	+	16747958	16754754	7	1905	ENSBTAG00000012777	serum response factor [Source:HGNC Symb;Acc:HGNC:11291] SRF	
43	ENSBTAT000000012578	ENSNG00000142684	YES	YES		YES		0.3103642	0.0126996	-1.687966	-	127523710	127524790	3	748	ENSBTAG000000009562	zinc finger protein 593 [Source:HGNC Symb;Acc:HGNC:30943] ZNF593	
44	ENSBTAT000000021725	ENSNG00000171243	YES	YES		YES		0.1764751	0.0158515	-2.502464	+	86211497	86237574	12	1380	ENSBTAG00000016332	inhibitor of growth factor, member 3 [Source:HGNC Symb;Acc:HGNC:ING3]	
45	ENSBTAT000000016693	ENSNG000000090316	YES	YES		YES		2.9013876	0.016016	1.536743	+	103330259	103343607	9	1243	ENSBTAG000000012575	macrophage erythroid attachment [Source:RefSeq peptide;Acc:MAEA]	
46	ENSBTAT000000010773	ENSNG00000129103	YES	YES		YES		0.6730517	0.0175	-0.71211	+	27995066	28005720	3	1773	ENSBTAG000000008190	sulfatase modifying factor 2 [Source:HGNC Symb;Acc:HGNC:20:SUMF2]	
47	ENSBTAT000000004477	ENSNG00000109622	YES	YES		YES		437.50236	0.0189091	8.773147	+	45354486	45359172	7	3101	ENSBTAG000000007480	cold inducible RNA binding protein [Source:HGNC Symb;Acc:HGNC:CRBP]	
48	ENSBTAT000000003926	ENSNG0000017655	YES	YES		YES		0.5235298	0.01934	-0.333857	-	45577377	45579723	4	615	ENSBTAG000000038409	methyl-CpG binding domain protein 3 [Source:HGNC Symb;Acc:HGNC:MBD3]	
49	ENSBTAT000000037847	ENSNG0000011007	YES	YES		YES		3.5039487	0.0198284	1.8008795	+	123743823	123752821	4	1255	ENSBTAG000000028595	transcription elongation factor B (TIF) polypeptide 3 (TIF3) elong. TCEB3	
50	ENSBTAT00000008252	ENSNG00000120948	YES	YES		YES		0.0090479	0.0213198	-6.788205	-	43491408	43498458	6	1351	ENSBTAG000000008937	TAR DNA binding protein [Source:HGNC Symb;Acc:HGNC:11571: TARDBP]	
51	ENSBTAT000000021204	ENSNG00000117222	YES	YES		YES		3.466082	0.0215429	1.7933058	-	2634854	2733979	14	2536	ENSBTAG00000015946		

61	ENSBAT00000024621	ENSG00000102103		YES	0.0267102	0.031957	-5.226466 +	92092355	92098095	6	1397	ENSBTAG00000018498	polyglutamine binding protein 1 [Source:HGNC Symbol,Acc:HGNC: PQBP1]
62	ENSBAT00000023380	ENSG00000143554		YES	26.956389	0.0320107	4.7525553 +	29402369	29420344	13	2261	ENSBTAG00000017582	checkpoint kinase 1 [Source:HGNC Symbol,Acc:HGNC:1925] CHEK1
63	ENSBAT00000011723	ENSG00000183733		YES	0.569136	0.0322039	-0.813155 +	13612910	13619093	3	582	ENSBTAG00000008905	folliculogenesis specific bHLH transcription factor [Source:HGNC: FLS1]
64	ENSBAT00000016879	ENSG00000171311		YES	0.2789132	0.0343448	-1.842112 -	18522239	18528239	8	885	ENSBTAG00000012639	exosome component 1 [Source:HGNC Symbol,Acc:HGNC:17286] EXOSC1
65	ENSBAT00000011468	ENSG00000182263		YES	0.3510973	0.0388047	-1.510057 +	32850155	32852428	1	2274	ENSBTAG00000008704	fidgetin [Source:HGNC Symbol,Acc:HGNC:13285] FIGN
66	ENSBAT00000026442	ENSG00000189046		YES	2725.705	0.0396397	11.412414 +	66234084	66239899	4	2047	ENSBTAG00000019846	alkB homolog 2, alpha-ketoglutarate-dependent dioxygenase [Sc ALKBH2]
67	ENSBAT00000022893	ENSG00000185163		YES	10.103807	0.0448581	3.3368271 +	46015020	46021726	15	1660	ENSBTAG00000017219	DEAD (Asp-Glu-Ala-Asp) box polypeptide 51 [Source:HGNC Sym: DDX51]
68	ENSBAT00000027125	ENSG00000136626		YES	0.0011422	0.0452157	-3.773967 -	98843684	98847740	4	2343	ENSBTAG00000020355	Kruppel-like factor 4 [gut] [Source:HGNC Symbol,Acc:HGNC:634] KLF4
69	ENSBAT00000005194	ENSG00000121390		YES	44.301962	0.0470105	5.4632967 +	36523631	36579763	9	1983	ENSBTAG00000003934	Rab3 effector protein with kelch motifs [Source:HGNC Symbol,Acc:RABEPK]
70	ENSBAT00000020093	ENSG00000136933	YES	YES	130.46996	0.0083122	7.0275517 +	36032496	36113995	7	1149	ENSBTAG00000015098	premelanosome protein [Source:HGNC Symbol,Acc:HGNC:10880] PMEL
71	ENSBAT00000005250	ENSG00000185664	YES	YES	0.4501991	0.0205022	-1.151365 +	57669835	57677941	11	2046	ENSBTAG000000004019	protein tyrosine phosphatase type IVA, member 3 [Source:HGNC: PTP4A3]
72	ENSBAT000000064455	ENSG00000184489	YES	YES	0.1634948	0.0097756	-2.612772 -	3578346	3586015	5	1532	ENSBTAG000000046467	WASH complex subunit 2 [Source:RefSeq peptide,Acc:NP_119511]
73	ENSBAT000000025173	ENSG00000172661		YES	12.908443	0.0162201	3.6302431 +	44495476	44542213	31	4104	ENSBTAG00000018915	membrane magnesium transporter 1 [Source:HGNC Symbol,Acc:HMMG11]
74	ENSBAT000000035505	ENSG00000163446		YES	1361.3805	0.018348	10.410855 +	19576179	19585346	5	923	ENSBTAG000000025297	tripartite motif containing 3 [Source:HGNC Symbol,Acc:HGNC:100] TRIM3
75	ENSBAT00000004636	ENSG00000110171		YES	16.418434	0.0222347	4.0372446 +	47193828	47219561	12	2792	ENSBTAG000000003565	activity-regulated cytoskeleton-associated protein [Source:HGNC AIC]
76	ENSBAT000000028836	ENSG000001198576		YES	0.8829855	0.0403111	-0.179538 +	2892788	2893378	1	1191	ENSBTAG000000021639	SRA stem-loop-interacting RNA-binding protein, mitochondrial [S: mitochondrial ribosomal protein L14 [Source:HGNC Symbol,Acc:Hi MRPL14]
77	ENSBAT000000043035	ENSG00000119705	YES	YES	0.1176846	0.0048966	-3.087003 +	89914334	89923167	4	378	ENSBTAG000000008135	MAD1 mitotic arrest deficient-like 1 (yeast) [Source:HGNC Symbol,Acc: MADM1]
78	ENSBAT00000015619	ENSG00000180992	YES	YES	0.1378779	0.0113643	-2.858537 -	17644487	17647839	2	1270	ENSBTAG000000011760	nudix (nucleoside diphosphate linked moiety X)-type motif 8 [Source: NUDT8]
79	ENSBAT000000003210	ENSG00000002822	YES	YES	0.2958212	0.0123786	-1.757202 +	41535263	41778055	18	2711	ENSBTAG000000002474	carbohydrate (chondroitin 4) sulfotransferase 12 [Source:HGNC: S: CHST12]
80	ENSBAT000000044604	ENSG00000167799	YES	YES	18.411771	0.014342	4.2025565 -	46123752	46126289	4	917	ENSBTAG000000011809	hydroxysteroid dehydrogenase like 1 [Source:HGNC Symbol,Acc: HSD17B10]
81	ENSBAT000000027841	ENSG00000136213		YES	23.321624	0.0146728	4.5435963 -	41732194	41309545	2	1839	ENSBTAG000000020898	spinster homolog 1 (Drosophila) [Source:HGNC Symbol,Acc:HGNC: SPNS1]
82	ENSBAT000000024993	ENSG00000103160		YES	6.4229422	0.015835	2.6832343 -	10439489	10451245	6	3223	ENSBTAG000000018770	LDC532995 protein; Uncharacterized protein [Source:UniProtKB/TrEMBL: Q95982]
83	ENSBAT00000019510	ENSG00000169682		YES	2.4628588	0.0167286	1.3003339 -	26126253	26134744	12	2189	ENSBTAG000000014653	sideroflexin 4 [Source:HGNC Symbol,Acc:HGNC:16088] SFXM4
84	ENSBAT00000012771	ENSG00000100890	YES	YES	0.0395397	0.0175643	-4.660555 +	45821718	45353661	7	1936	ENSBTAG000000009682	solute carrier family 37 (glucose-6-phosphate transporter), member 3 [Source:HGNC Symbol,Acc:HGNC:16088] SLC37A4
85	ENSBAT00000011502	ENSG00000183605	YES	YES	1.2602546	0.019208	0.3337152 -	39653449	39663981	14	1937	ENSBTAG000000008730	ATP-binding cassette, sub-family E (ABC1), member 1 [Source:HGNC: ABCE1]
86	ENSBAT000000061244	ENSG00000137700	YES	YES	0.0685236	0.0204713	-3.867255 -	30122001	30127150	8	2110	ENSBTAG000000006077	SCD1 cytochrome c oxidase assembly protein [Source:HGNC Sym: SCD1]
87	ENSBAT000000061070	ENSG00000145431	YES	YES	0.0267573	0.0205277	-5.223922 +	49348702	43457620	5	938	ENSBTAG000000043959	solute carrier family 25 (pyrimidine nucleotide carrier), member 33 [S: SLC25A33]
88	ENSBAT000000048747	ENSG00000164163	YES	YES	0.2678889	0.0219552	-1.796416 -	13333870	13384710	18	2391	ENSBTAG00000019854	tankyrase, TRF1-interacting ankyrin-related ADP-ribose polymerase: TNKS
89	ENSBAT000000023032	ENSG00000133028	YES	YES	0.7918704	0.0231404	-0.336664 -	30276156	30236404	6	3793	ENSBTAG000000021780	ST6 (alpha-N-acetyl-neuraminyl-2,3-beta-galactosyl-1,3)-N-acetylglucosaminyl 6-sulfatase [Source:HGNC Symbol,Acc:HGNC:11875] ST6GALNAC
90	ENSBAT00000004127	ENSG00000171612	YES	YES	0.7054251	0.0237531	-0.503435 -	44801770	44831904	7	1447	ENSBTAG000000003177	39S ribosomal protein L17, mitochondrial [Source:UniProtKB/Swiss-Prot: P0C100]
91	ENSBAT00000001917	ENSG00000132723	YES	YES	3.2702694	0.0242947	1.7094095 +	24632930	24789416	27	4308	ENSBTAG000000014663	mitochondrial fission regulator 1 [Source:HGNC Symbol,Acc:HGNC: MTFFR1]
92	ENSBAT000000042557	ENSG00000170731	YES	YES	1.6026506	0.0310710	0.6804599 +	55803307	55822126	8	1825	ENSBTAG00000015255	thymopoietin [Source:HGNC Symbol,Acc:HGNC:11875] TMPO
93	ENSBAT000000034505	ENSG00000158042	YES	YES	0.7484915	0.0319107	-0.418019 +	47004019	47005492	3	831	ENSBTAG000000024781	translocase of outer mitochondrial membrane 7 homolog (yeast) [S: TOMM7]
94	ENSBAT00000011379	ENSG00000006885	YES	YES	0.864997	0.0360488	-0.203233 +	31735268	31794502	8	1852	ENSBTAG000000008623	Glycerol kinase; Uncharacterized protein [Source:UniProtKB/TrEMBL: Q95982]
95	ENSBAT000000005553	ENSG00000120802	YES	YES	0.0318515	0.0376983	-4.972497 +	63027194	63052802	7	2356	ENSBTAG000000004240	mitochondrial ribosomal protein S27 [Source:HGNC Symbol,Acc: HMRP57]
96	ENSBAT00000008388	ENSG00000136683	YES	YES	0.0261096	0.0379617	-5.253275 -	89692607	89693271	1	165	ENSBTAG000000006398	apolipoprotein O-like [Source:HGNC Symbol,Acc:HGNC:24009] APOOL
97	ENSBAT000000003378	ENSG000001198814	YES	YES	0.8095261	0.0381665	-0.30485 +	111538716	11160550	1	1835	ENSBTAG000000000301	NADH dehydrogenase [ubiquinone] 1 alpha subcomplex subunit 2 [Source:HGNC Symbol,Acc:HGNC:11875] NDH1
98	ENSBAT00000002549	ENSG00000113048	YES	YES	0.8375143	0.0400667	-0.255814 +	3211237	3195274	11	2179	ENSBTAG00000001962	ADP-ribosylation factor interacting protein 1 [Source:HGNC Symbol: AFRP1]
99	ENSBAT000000023044	ENSG00000155008	YES	YES	0.2425345	0.0405268	-2.043738 -	75160536	75265102	9	1236	ENSBTAG000000021790	solute carrier family 25 (mitochondrial iron transporter), member 28 [S: SLC25A28]
100	ENSBAT000000064188	ENSG00000131495	YES	YES	6.3962646	0.0418814	2.6772236 -	64586967	64587266	1	300	ENSBTAG000000047836	low density lipoprotein receptor-related protein 5 [Source:HGNC: LRP5]
101	ENSBAT000000029627	ENSG00000164144	YES	YES	6.5216893	0.0424265	2.7052457 -	4732242	4868678	9	3026	ENSBTAG000000008438	NADH dehydrogenase (ubiquinone) Fe-S protein 8, 23kDa (NADH) [Source:HGNC: NDUFS8]
102	ENSBAT00000018063	ENSG00000155287	YES	YES	0.0560773	0.0424577	-4.15644 -	20466104	20476402	4	1146	ENSBTAG000000012107	platelet derived growth factor D [Source:HGNC Symbol,Acc:HGNC:18547] PDGFRD
103	ENSBAT000000007756	ENSG00000162337	YES	YES	9.135145	0.0425081	3.191476 +	46485172	46573460	22	5030	ENSBTAG000000005903	semaphorin 4B [Source:HGNC Symbol,Acc:HGNC:18547] SEMA4B
104	ENSBAT00000016013	ENSG00000110171	YES	YES	0.2316219	0.0469012	-2.110156 +	46205045	46208795	7	886	ENSBTAG000000012072	semaphorin 4B [Source:HGNC Symbol,Acc:HGNC:18547] SEMA4B
105	ENSBAT000000020333	ENSG00000119392	YES	YES	0.89965	0.0464764	-0.515295 +	39077978	39103990	16	2436	ENSBTAG000000030566	semaphorin 4B [Source:HGNC Symbol,Acc:HGNC:18547] SEMA4B
106	ENSBAT000000043232	ENSG00000170962	YES	YES	122.11325	0.0467381	6.932076 +	4501435	4788300	7	2055	ENSBTAG000000034827	nucleolar envelope membrane protein [Source:HGNC Symbol,Acc:HGNC:18547] NECAP2
107	ENSBAT000000035896	ENSG000001317404	YES	YES	0.0796308	0.0489574	-3.850529 -	28111675	28114705	4	1538	ENSBTAG000000006366	Wolfram syndrome 1 (wolframin) [Source:HGNC Symbol,Acc:HGNC: WFS1]
108	ENSBAT000000017663	ENSG00000157191	YES	YES	0.8662606	0.0485823	-0.207127 -	136252384	136266397	8	2019	ENSBTAG000000013282	Uncharacterized protein [Source:UniProtKB/TrEMBL: Acc:G3N353]
109	ENSBAT000000066249	ENSG00000103501	YES	YES	5.6467589	0.0492745	2.497423 +	104673701	104696495	7	2667	ENSBTAG000000046671	Uncharacterized protein [Source:UniProtKB/TrEMBL: Acc:G3N353]
110	ENSBAT00000011044	ENSG000001002071	YES	YES	10.977035	0.0020713	3.4564165 +	219743	220147	1	405	ENSBTAG000000032198	1-acylglycerol-3-phosphate O-acyltransferase 4 [Source:HGNC: AGPAT4]
111	ENSBAT000000065516	ENSG00000026652		YES	0.9621405	0.0003172	-0.055681 -	71676362	71677651	1	1290	ENSBTAG000000046463	autophagy related 2A [Source:HGNC Symbol,Acc:HGNC:29028] ATG2A
112	ENSBAT0000000010089	ENSG00000110046		YES	0.0494256	0.0005049	-4.338537 -	98239672	98376380	9	1886	ENSBTAG000000007688	ESC2 protein; Uncharacterized protein [Source:UniProtKB/TrEMBL: Q95982]
113	ENSBAT000000003283	ENSG00000110046		YES	0.1667031	0.0012762	-2.584647 -	43752917	43757930	9	1224	ENSBTAG000000007058	semaphorin 4B [Source:HGNC Symbol,Acc:HGNC:18547] SEMA4B
114	ENSBAT000000008606	ENSG00000117320		YES	0.4819603	0.0013901	-1.053014 -	10859329	10859722	10	2372	ENSBTAG000000006551	semaphorin 4B [Source:HGNC Symbol,Acc:HGNC:18547] SEMA4B
115	ENSBAT000000024759	ENSG00000095539		YES	2.2374255	0.0019569	1.1618396 +	21677156	21690795	16	4269	ENSBTAG00000018604	CDC42 small effector 2 [Source:HGNC Symbol,Acc:HGNC:18547] CDC42SE2
116	ENSBAT000000052263	ENSG00000158985		YES	0.4781896	0.0018425	-1.064345 -	24318564	24436629	6	3306	ENSBTAG000000005361	Uncharacterized protein [Source:UniProtKB/TrEMBL: Acc:G3N353]
117	ENSBAT000000064006	ENSG00000137720		YES	5.1974376	0.0025845	2.3778005 +	22550859	22552378	3	609	ENSBTAG000000045821	small glutamine-rich tetrapeptide repeat (TPR)-containing, member 2 [Source:HGNC Symbol,Acc:HGNC:28522] RNF182
118	ENSBAT000000022481	ENSG00000197860		YES	6.0090595	0.0029296	2.5871932 +	13805928	13851473	11	1115	ENSBTAG00000016902	ring finger protein 182 [Source:HGNC Symbol,Acc:HGNC:28522] RNF182
119	ENSBAT00000006401	ENSG00000180537		YES	0.2878961	0.0030021	-1.79638 -	42467107	42467856	1	750	ENSBTAG000000045884	HISTH3B
120	ENSBAT000000045045	ENSG000001003004		YES	0.8290912	0.0030034	-0.270397 -	31497480	31497890	1	411	ENSBTAG000000031766	

61	ENSG00000103024, ENSG00000143156, ENSG00000172113	GO:0046131	pyrimidine ribonucleotide metabolic process	3	0.928793	0.034965	10.03065	0.952558	
62	ENSG00000103024, ENSG00000143156, ENSG00000172113	GO:0006227	pyrimidine nucleotide biosynthetic process	3	0.928793	0.056109	7.750595	0.965369	
63	ENSG00000006695, ENSG00000167283, ENSG00000103024, ENSG00000138363, ENSG00000060382, ENSG00000105835, ENSG00000120053, ENSG0000014919, ENSG00000172113	GO:0044271	nitrogen compound biosynthetic process	11	3.405573	0.059318	1.923827	0.968574	
64	ENSG00000103024, ENSG00000143156, ENSG00000172113	GO:0016776	phosphotransferase activity, phosphate group a	3	0.928793	0.10001	5.567324	0.903171	
65	ENSG00000128951, ENSG00000103024, ENSG00000143156, ENSG00000172113	GO:0009116	nucleotide metabolic process	4	1.23839	0.101857	3.552521	0.983692	
66	ENSG00000167283, ENSG00000103024, ENSG00000138363, ENSG00000143156, ENSG00000172113	GO:0009152	purine ribonucleotide biosynthetic process	5	1.547988	0.149619	2.429074	0.976379	
67	ENSG00000103024, ENSG00000143156, ENSG00000172113	GO:0019205	nucleobase, nucleoside, nucleotide kinase activity	3	0.928793	0.154345	4.272596	0.933764	
68	ENSG00000167283, ENSG00000103024, ENSG00000138363, ENSG00000143156, ENSG00000172113	GO:0003260	ribonucleotide biosynthetic process	5	1.547988	0.173047	2.291949	0.962695	
69	ENSG00000103024, ENSG00000143156, ENSG00000172113	GO:0009119	nucleotide metabolic process	3	0.928793	0.152561	3.706978	0.905363	
70	ENSG00000167283, ENSG00000128951, ENSG00000103024, ENSG00000143156, ENSG00000172113	GO:0009141	nucleotide triphosphate metabolic process	5	1.547988	0.197644	2.169478	0.985281	
71	ENSG00000167283, ENSG00000103024, ENSG00000138363, ENSG00000143156, ENSG00000172113	GO:0009150	purine ribonucleotide metabolic process	5	1.547988	0.22323	2.059432	0.985413	
72	ENSG00000167283, ENSG00000103024, ENSG00000138363, ENSG00000105835, ENSG00000143156, ENSG00000172113	GO:0009165	nucleotide biosynthetic process	6	1.857585	0.227444	1.833553	0.985325	
73	ENSG00000167283, ENSG00000103024, ENSG00000143156, ENSG00000172113	GO:0009206	purine ribonucleotide triphosphate biosynthetic process	4	1.23839	0.246274	2.320014	0.985012	
74	ENSG00000167283, ENSG00000103024, ENSG00000138363, ENSG00000105835, ENSG00000143156, ENSG00000172113	GO:0034404	nucleobase, nucleoside and nucleotide biosynthesis	6	1.857585	0.250047	1.767057	0.985475	
75	ENSG00000167283, ENSG00000103024, ENSG00000138363, ENSG00000105835, ENSG00000143156, ENSG00000172113	GO:0034654	nucleobase, nucleoside, nucleotide and nucleotide triphosphate biosynthetic process	6	1.857585	0.250047	1.767057	0.985475	
76	ENSG00000167283, ENSG00000103024, ENSG00000143156, ENSG00000172113	GO:0009145	purine nucleoside triphosphate biosynthetic process	4	1.23839	0.250371	2.296579	0.984484	
77	ENSG00000167283, ENSG00000103024, ENSG00000143156, ENSG00000172113	GO:0009201	ribonucleoside triphosphate biosynthetic process	4	1.23839	0.250371	2.296579	0.984484	
78	ENSG00000167283, ENSG00000103024, ENSG00000138363, ENSG00000143156, ENSG00000172113	GO:0009253	ribonucleotide metabolic process	5	1.547988	0.257286	1.933345	0.983823	
79	ENSG00000167283, ENSG00000103024, ENSG00000138363, ENSG00000143156, ENSG00000172113	GO:0006164	purine nucleotide biosynthetic process	5	1.547988	0.261155	1.920282	0.983726	
80	ENSG00000167283, ENSG00000103024, ENSG00000143156, ENSG00000172113	GO:0009142	nucleotide triphosphate biosynthetic process	4	1.23839	0.285159	2.226033	0.984288	
81	ENSG00000167283, ENSG00000103024, ENSG00000143156, ENSG00000172113	GO:0009205	purine ribonucleotide triphosphate metabolic process	4	1.23839	0.336936	1.943259	0.988103	
82	ENSG00000167283, ENSG00000103024, ENSG00000143156, ENSG00000172113	GO:0009199	ribonucleoside triphosphate metabolic process	4	1.23839	0.341737	1.926791	0.987867	
83	ENSG00000167283, ENSG00000103024, ENSG00000143156, ENSG00000172113	GO:0009144	purine nucleoside triphosphate metabolic process	4	1.23839	0.36091	1.863618	0.987778	
84	ENSG00000167283, ENSG00000103024, ENSG00000138363, ENSG00000143156, ENSG00000172113	GO:0006163	purine nucleotide metabolic process	5	1.547988	0.410751	1.527966	0.931877	
85									
86									
87	Genes	Annotation Cluster 6	Enrichment Score: 1.2634076030382662						
88	ENSG00000006695, ENSG00000133028, ENSG00000014919	Category	Term	Count	%	PValue	Fold Enrich	Benjamini	
89	ENSG00000006695, ENSG00000133028, ENSG00000145431, ENSG00000110717, ENSG00000171368, ENSG00000167552, ENSG00000014919	GOTERM_BP_FAT	GO:0008535 respiratory chain complex IV assembly	3	0.928793	0.007982	21.31513	0.979548	
90	ENSG00000006695, ENSG00000133028, ENSG00000162144, ENSG00000167283, ENSG00000110717, ENSG00000131495, ENSG00000120053, ENSG00000014919	GOTERM_BP_FAT	GO:0043823 cellular protein complex assembly	7	2.167183	0.065603	2.456064	0.970647	
91		GOTERM_BP_FAT	GO:0006097 generation of precursor metabolites and energy	8	2.47678	0.309545	1.452788	0.987084	
92									
93	Genes	Annotation Cluster 7	Enrichment Score: 1.2598047353013444						
94	ENSG00000146587, ENSG00000175895, ENSG00000071243, ENSG00000183605, ENSG00000213588, ENSG00000180537, ENSG00000100722, ENSG0000010539, ENSG00000172113	Category	Term	Count	%	PValue	Fold Enrich	Benjamini	
95	ENSG00000146587, ENSG00000175895, ENSG00000071243, ENSG00000103024, ENSG00000213588, ENSG00000180537, ENSG00000100722, ENSG0000010539, ENSG00000172113	GOTERM_MF_FAT	GO:0046914 transition metal ion binding	62	19.19505	0.006175	1.363345	0.728527	
96	ENSG00000146587, ENSG00000175895, ENSG00000071243, ENSG00000186167, ENSG00000213588, ENSG00000180537, ENSG00000187147, ENSG00000172059, ENSG00000172113	SP_PIR_KEYWORDS	metal-binding	65	20.12384	0.006338	1.352684	0.278586	
97	ENSG00000146587, ENSG00000175895, ENSG00000071243, ENSG00000186167, ENSG00000213588, ENSG00000180537, ENSG00000187147, ENSG00000142303, ENSG00000172113	SP_PIR_KEYWORDS	zinc-finger	40	12.3839	0.08422	1.44002	0.40985	
98	ENSG00000146587, ENSG00000175895, ENSG00000071243, ENSG00000186167, ENSG00000213588, ENSG00000180537, ENSG00000187147, ENSG00000172113	SP_PIR_KEYWORDS	zinc	43	13.31269	0.131972	1.214939	0.770517	
99	ENSG00000146587, ENSG00000175895, ENSG00000071243, ENSG00000186167, ENSG00000213588, ENSG00000180537, ENSG00000187147, ENSG00000172113	GOTERM_MF_FAT	GO:0008270 zinc ion binding	45	13.93189	0.140998	1.192482	0.930474	
100	ENSG00000146587, ENSG00000175895, ENSG00000071243, ENSG00000186167, ENSG00000103024, ENSG00000213588, ENSG00000180537, ENSG00000100722, ENSG00000172113	GOTERM_MF_FAT	GO:0046872 metal ion binding	76	23.52941	0.141487	1.124223	0.923388	
101	ENSG00000146587, ENSG00000175895, ENSG00000071243, ENSG00000186167, ENSG00000103024, ENSG00000213588, ENSG00000180537, ENSG00000100722, ENSG00000172113	GOTERM_MF_FAT	GO:0043169 cation binding	76	23.52941	0.16393	1.117371	0.938686	
102	ENSG00000146587, ENSG00000175895, ENSG00000071243, ENSG00000186167, ENSG00000103024, ENSG00000213588, ENSG00000180537, ENSG00000100722, ENSG00000172113	GOTERM_MF_FAT	GO:0043167 ion binding	76	23.52941	0.20392	1.097449	0.945494	
103									
104	Genes	Annotation Cluster 8	Enrichment Score: 1.18480932573949434						
105	ENSG00000103024, ENSG00000132153, ENSG00000112541, ENSG00000164896, ENSG00000089737, ENSG00000132466, ENSG00000185163, ENSG00000106799, ENSG00000172113	Category	Term	Count	%	PValue	Fold Enrich	Benjamini	
106	ENSG00000103024, ENSG00000132153, ENSG00000112541, ENSG00000164896, ENSG00000089737, ENSG00000132466, ENSG00000185163, ENSG00000106799, ENSG00000172113	GOTERM_MF_FAT	GO:0030554 adenylyl nucleotide binding	37	11.45511	0.021524	1.436843	0.839927	
107	ENSG00000103024, ENSG00000132153, ENSG00000112541, ENSG00000164896, ENSG00000089737, ENSG00000132466, ENSG00000185163, ENSG00000106799, ENSG00000172113	GOTERM_MF_FAT	GO:0001883 purine nucleoside binding	37	11.45511	0.026417	1.415304	0.847188	
108	ENSG00000103024, ENSG00000132153, ENSG00000112541, ENSG00000164896, ENSG00000089737, ENSG00000132466, ENSG00000185163, ENSG00000106799, ENSG00000172113	GOTERM_MF_FAT	GO:0032553 adenylyl ribonucleotide binding	35	10.83591	0.027073	1.43181	0.808087	
109	ENSG00000103024, ENSG00000132153, ENSG00000112541, ENSG00000164896, ENSG00000089737, ENSG00000132466, ENSG00000185163, ENSG00000106799, ENSG00000172113	GOTERM_MF_FAT	GO:0001882 nucleoside binding	37	11.45511	0.028936	1.405646	0.786734	
110	ENSG00000103024, ENSG00000132153, ENSG00000112541, ENSG00000164896, ENSG00000089737, ENSG00000132466, ENSG00000185163, ENSG00000106799, ENSG00000172113	UP_SEQ_FEATURE	binding site:ATP	16	4.93556	0.031787	1.841217	0.937074	
111	ENSG00000103024, ENSG00000132153, ENSG00000112541, ENSG00000164896, ENSG00000089737, ENSG00000132466, ENSG00000185163, ENSG00000106799, ENSG00000172113	GOTERM_MF_FAT	GO:0005524 ATP binding	34	10.52632	0.035861	1.409735	0.818828	
112	ENSG00000103024, ENSG00000132153, ENSG00000112541, ENSG00000164896, ENSG00000089737, ENSG00000132466, ENSG00000185163, ENSG00000106799, ENSG00000172113	SP_PIR_KEYWORDS	atp-binding	31	9.597523	0.037833	1.445339	0.528605	
113	ENSG00000103024, ENSG00000132153, ENSG00000112541, ENSG00000164896, ENSG00000089737, ENSG00000132466, ENSG00000185163, ENSG00000106799, ENSG00000172113	GOTERM_MF_FAT	GO:0001666 nucleotide binding	47	14.55108	0.052078	1.282096	0.870869	
114	ENSG00000103024, ENSG00000132153, ENSG00000112541, ENSG00000164896, ENSG00000089737, ENSG00000132466, ENSG00000185163, ENSG00000106799, ENSG00000172113	UP_SEQ_FEATURE	nucleotide phosphate-binding region:ATP	23	7.120743	0.065142	1.463336	0.938839	
115	ENSG00000103024, ENSG00000132153, ENSG00000112541, ENSG00000164896, ENSG00000089737, ENSG00000132466, ENSG00000185163, ENSG00000106799, ENSG00000172113	GOTERM_MF_FAT	GO:0017076 purine nucleotide binding	40	12.3839	0.078786	1.271776	0.915224	
116	ENSG00000103024, ENSG00000132153, ENSG00000112541, ENSG00000164896, ENSG00000089737, ENSG00000132466, ENSG00000185163, ENSG00000106799, ENSG00000172113	GOTERM_MF_FAT	GO:0032555 purine ribonucleotide binding	38	11.76471	0.094774	1.267506	0.915063	
117	ENSG00000103024, ENSG00000132153, ENSG00000112541, ENSG00000164896, ENSG00000089737, ENSG00000132466, ENSG00000185163, ENSG00000106799, ENSG00000172113	GOTERM_MF_FAT	GO:0032553 ribonucleotide binding	38	11.76471	0.094774	1.267506	0.915063	
118	ENSG00000103024, ENSG00000132153, ENSG00000112541, ENSG00000164896, ENSG00000089737, ENSG00000132466, ENSG00000185163, ENSG00000106799, ENSG00000172113	SP_PIR_KEYWORDS	nucleotide-binding	35	10.83591	0.102445	1.283933	0.740461	
119	ENSG00000103024, ENSG00000132153, ENSG00000112541, ENSG00000164896, ENSG00000089737, ENSG00000132466, ENSG00000185163, ENSG00000106799, ENSG00000172113	SP_PIR_KEYWORDS	kinase	16	4.93556	0.147726	1.438346	0.78955	
120	ENSG00000103024, ENSG00000132153, ENSG00000112541, ENSG00000164896, ENSG00000089737, ENSG00000132466, ENSG00000185163, ENSG00000106799, ENSG00000172113	GOTERM_MF_FAT	GO:0004672 protein kinase activity	14	4.334365	0.187879	1.414799	0.940763	
121	ENSG00000103024, ENSG00000132153, ENSG00000112541, ENSG00000164896, ENSG00000089737, ENSG00000132466, ENSG00000185163, ENSG00000106799, ENSG00000172113	INTERPRO	IPRO17441:Protein kinase, ATP binding site	11	3.405573	0.199174	1.497194	0.999287	

123			Annotation Cluster 9	Enrichment Score: 1.1297027188409117					
124	Genes		Category	Term	Count	%	PValue	Fold Enrich	Benjamini
125	ENSG00000006695, ENSG00000185664, ENSG00000014919, ENSG00000188690		GOTERM_BP_FAT	GO:0046148 pigment biosynthetic process	4	1.23839	0.03054	5.823778	0.969003
126	ENSG00000006695, ENSG00000014919, ENSG00000188690		GOTERM_BP_FAT	GO:0006783 heme biosynthetic process	3	0.928793	0.034965	10.03065	0.952558
127	ENSG00000006695, ENSG00000185664, ENSG00000014919, ENSG00000188690		GOTERM_BP_FAT	GO:0042440 pigment metabolic process	4	1.23839	0.043962	5.052474	0.955711
128	ENSG00000006695, ENSG00000014919, ENSG00000188690		GOTERM_BP_FAT	GO:0006779 porphyrin biosynthetic process	3	0.928793	0.047208	8.52605	0.953258
129	ENSG00000006695, ENSG00000014919, ENSG00000188690		GOTERM_BP_FAT	GO:0033014 tetrapyrrole biosynthetic process	3	0.928793	0.047208	8.52605	0.953258
130	ENSG00000006695, ENSG00000014919, ENSG00000188690		GOTERM_BP_FAT	GO:0042168 heme metabolic process	3	0.928793	0.056109	7.750955	0.965368
131	ENSG00000006695, ENSG00000014919, ENSG00000188690		KEGG_PATHWAY	hsa00860: Porphyrin and chlorophyll metabolism	3	0.928793	0.089433	5.926573	0.967477
132	ENSG00000006695, ENSG00000105835, ENSG00000014919, ENSG00000188690, ENSG00000023909		GOTERM_BP_FAT	GO:0051188 cofactor biosynthetic process	5	1.547968	0.090662	2.929914	0.984902
133	ENSG00000006695, ENSG00000014919, ENSG00000188690		GOTERM_BP_FAT	GO:0033013 tetrapyrrole metabolic process	3	0.928793	0.091141	5.880035	0.983302
134	ENSG00000006695, ENSG00000014919, ENSG00000188690		GOTERM_BP_FAT	GO:0006778 porphyrin metabolic process	3	0.928793	0.091141	5.880035	0.983302
135	ENSG00000006695, ENSG00000105835, ENSG00000197448, ENSG00000014919, ENSG00000188690, ENSG00000023909		GOTERM_BP_FAT	GO:0051186 cofactor metabolic process	6	1.857585	0.256691	1.748933	0.984904
136	ENSG00000006695, ENSG00000014919, ENSG00000188690		GOTERM_BP_FAT	GO:0018130 heterocycle biosynthetic process	3	0.928793	0.276725	2.890187	0.985729
137									
138									
139	Genes		Annotation Cluster 10	Enrichment Score: 1.093631290268119					
140	ENSG000000087263, ENSG00000189046, ENSG00000178467		Category	Term	Count	%	PValue	Fold Enrich	Benjamini
141	ENSG000000087263, ENSG00000189046, ENSG00000178467		INTERPRO	IPR005123: Oxoglutarate and iron-dependent oxygenase	3	0.928793	0.029311	10.32871	0.996639
142	ENSG000000087263, ENSG00000189046, ENSG00000178467		UP_SEQ_FEATURE	domain Fe2O2 dioxygenase	3	0.928793	0.044962	8.779513	0.997354
143	ENSG000000087263, ENSG00000189046, ENSG00000132510, ENSG00000178467		GOTERM_MF_FAT	GO:0018702 oxidoreductase activity, acting on single donors	4	1.23839	0.092167	3.711549	0.921447
144	ENSG000000087263, ENSG00000189046, ENSG00000132510, ENSG00000178467		GOTERM_MF_FAT	GO:0018701 oxidoreductase activity, acting on single donors	4	1.23839	0.095377	3.656153	0.904039
145	ENSG000000087263, ENSG00000189046, ENSG00000178467		SP_PIR_KEYWORDS	dioxygenase	3	0.928793	0.287868	2.811312	0.909942
146									
147	Genes		Annotation Cluster 11	Enrichment Score: 1.0526031513223535					
148	ENSG00000103024, ENSG00000112541, ENSG00000106799, ENSG00000136159, ENSG00000172113, ENSG00000127334, ENSG000000064655, ENSG00000169446, ENSG000001		Category	Term	Count	%	PValue	Fold Enrich	Benjamini
149	ENSG00000127334, ENSG00000167799, ENSG00000119414, ENSG00000106799, ENSG00000154237, ENSG00000136159		GOTERM_MF_FAT	GO:0000287 magnesium ion binding	13	4.024768	0.06554	1.761344	0.90728
150	ENSG00000127334, ENSG00000167799, ENSG00000119414, ENSG00000106799, ENSG00000154237, ENSG00000136159		SP_PIR_KEYWORDS	manganese	6	1.857585	0.093765	2.441403	0.744348
			GOTERM_MF_FAT	GO:0030145 manganese ion binding	6	1.857585	0.106343	2.385996	0.895023

8.10 Scripts

8.10.1 EdgeR

```

#source("http://bioconductor.org/biocLite.R")
#biocLite("edgeR")
library(edgeR)
library(limma)
library(gtools)

#####
#####
## SET THE WORKING DIRECTORY

setwd('/home/svztg/Desktop/David_haig_Rabbit_vs_Cattle/RABBIT/Edge
R_DE')

directory <- getwd()
filenames <- list.files(directory, pattern="*.counts")

for (file in filenames)
{

x <- read.delim(file,row.names="GENE")
group <- factor(c(2,2,1,1))

all_results_table = paste(file,"_all_Results_edgeR.xls")
FDR.lt0.05_table = paste(file,"_FDR_p0.05_edgeR.xls")
PValue.lt0.05_table = paste(file,"_PValue_p0.05_edgeR.xls")
mds.plot.name = paste(file,".MDS.plot.pdf")
smear.plot.name = paste(file,".smear.plot.pdf")
volcano.plot.name = paste(file,".volcano.plot.pdf")

#####
#####

y <- DGEList(counts=x,group=group)
z <- DGEList(counts=x,group=group)
## Since the smallest group size is TWO, we keep genes that
achieve at least one count per million (cpm) in at least TWO
samples:\n";
keep <- rowSums(cpm(y)>1) >= 1
y <- y[keep,]
# Re-compute the library sizes
y$samples$lib.size <- colSums(y$counts)
z$samples$lib.size <- colSums(z$counts)
# Compute effective library sizes using TMM normalization:\n";
y <- calcNormFactors(y)
z <- calcNormFactors(z)
y$samples
# Output plot as a pdf
pdf(mds.plot.name)
plotMDS(y)
dev.off()

```

```

y <- estimateCommonDisp(y)
z <- estimateCommonDisp(z)
y <- estimateTagwiseDisp(y)
z <- estimateTagwiseDisp(z)
#plotBCV(y)
et <- exactTest(y)
etz <- exactTest(z)
top <- topTags(et)

pdf(smear.plot.name)
plotSmear(y, de.tags=top, main="Differential expression using
the common dispersion")
dev.off()

## Check the individual cpm values for the top genes:
cpm(y)[rownames(top), ]
## The total number of DE genes at 5% FDR is given by:
summary(de <- decideTestsDGE(et))
## Plot the log-fold-changes, highlighting the DE genes:
detags <- rownames(y)[as.logical(de)]

## Get LogFC values
LogFCvalues <- etz$table$logFC
## Get the Genenames
RownamesforLogFC <- rownames(etz)

## Convert LogFC to FC
FC <- logratio2foldchange(LogFCvalues, base=2)
## Convert FC list to dataframe with Genenames
FClist <- data.frame( RownamesforLogFC, FC )

# volcano plot
pdf(volcano.plot.name)
plot(et$table$logFC, -log10(et$table$PValue), pch=19, cex=0.2,
main = "Volcano Plot", xlab = "LogFC", ylab = "-log10 pvalue")
dev.off()

## Generate an EdgeR results table
EdgeRResults <- topTags( et , n = nrow( et$table ) )$table
## Generate an counts table
gene.counts <- z$counts
## Merge tables
most.results <- merge(gene.counts, EdgeRResults, by=0, all=TRUE)
combined.results <- merge(most.results, FClist, by=1, all=TRUE)

## Identify if a gene is up or down regulated
#combined.results.UP.G2 <- subset(combined.results, logFC > 0)
# combined.results.DOWN.G2 <- subset(combined.results, logFC <=
0)
# combined.results.UP.G2[, "G2vsG1"] <- "UP"
#combined.results.DOWN.G2[, "G2vsG1"] <- "DOWN"

## Add Up or Down to combined results
#combined.results <-
rbind(combined.results.UP.G2, combined.results.DOWN.G2)

```

```
## Filter combined.results to identify significant genes
significant.results0.05FDR <- subset(combined.results, FDR <=
0.05)
significant.results0.05 <- subset(combined.results, PValue <=
0.05)
## Write tables
write.table(combined.results,
file=all_results_table,row.names=FALSE,col.names=TRUE,quote=FALSE)
write.table(significant.results0.05, file=
PValue.lt0.05_table,row.names=FALSE,col.names=TRUE,quote=FALSE)
write.table(significant.results0.05FDR,
file=FDR.lt0.05_table,row.names=FALSE,col.names=TRUE,quote=FALSE)

}
```

8.10.2 Ballgown

```

## ----loadmethods, echo=FALSE, message=FALSE, warning=FALSE-----
-----
## source("http://bioconductor.org/biocLite.R")
## biocLite("ballgown")

library(edgeR)
library(limma)
library(ballgown)
library(gtools)

## ----Variables-----
-----

group = factor(c(1,1,2,2))
data_directory
='/home/svztg/Desktop/David_haig_Rabbit_vs_Cattle/COW/assemblies'

## ----makebg, message=FALSE-----
-----

setwd(data_directory)
directory <- getwd()
bg = ballgown(dataDir=data_directory, samplePattern='assembly',
meas='all')

## ----getexpr-----
-----

gene_expression = texpr(bg, 'FPKM')
transcript_values = texpr(bg, 'all')
transcript_names = transcriptNames(bg)

## ----pData-----
-----

pData(bg) = data.frame(id=sampleNames(bg), group)
phenotype_results = pData(bg)

## ----getStats-----
-----

stats_results = statstest(bg, feature='transcript',
gexpr=gene_expression, getFC=TRUE, meas='FPKM', covariate='group')
stats_results <- merge(transcript_names, stats_results, by=0,
all=TRUE)
stats_results = subset(stats_results,
select=c("x", "fc", "pval", "qval"))
colnames(stats_results)[1] <- "t_name"
colnames(stats_results)[2] <- "Ratio"
Log_FC <- log2(stats_results$Ratio)
FC <- logratio2foldchange(Log_FC, base=2)
stats_results <- cbind(stats_results, Log_FC, FC)
stats_results = subset(stats_results,
select=c("t_name", "Ratio", "FC", "Log_FC", "pval", "qval"))
stats_results <- merge(stats_results, transcript_values)
colnames(stats_results)[1] <- "Transcript_Name"

```

```
stats_results <- stats_results[ order(stats_results$pval) ,]

## ----writeTable-----
-----

#transcript_table = paste("transcript_table", sep="" )
#write.table(transcript_values,
file=transcript_table,row.names=FALSE,col.names=TRUE,quote=FALSE,s
ep="\t")

phenotype_results_table = paste("phenotype_results_table", sep =
"" )
write.table(phenotype_results,
file=phenotype_results_table,row.names=FALSE,col.names=TRUE,quote=
FALSE,sep="\t")

stats_results_table = paste("stats_results_table", sep="" )
write.table(stats_results,
file=stats_results_table,row.names=FALSE,col.names=TRUE,quote=FALS
E,sep="\t")

## ----sessioninfo, results='markup'-----
-----
#sessionInfo()
```

8.10.3 Hisat

```
#!/usr/bin/bash

#HISAT and StringTie wrapper script v0.0.1
#Tom Giles
#09.12.14
#thomas.giles@nottingham.ac.uk

#####
# FUNCTIONS:
#####

help_readme() {

# Help Section

    echo "

HISAT and StringTie wrapper script v1.0.1 by Tom Giles (21.10.15)
(thomas.giles@nottingham.ac.uk) `basename $0`

This pipeline aligns reads to a genome sequence using Hisat v2
(Kim D, Langmead B and Salzberg SL. HISAT: a fast spliced aligner
with low memory requirements. Nature Methods 2015). Technical
replicates from different lanes are merged using samtools (Heng
Li, Et Al, The Sequence Alignment/Map format and SAMtools.
Bioinformatics 2009) and then assembled to identify transcript
level expression using stringtie (Pertea M, Et Al. StringTie
enables improved reconstruction of a transcriptome from RNA-seq
reads Nature Biotechnology 2015).

Usage:

Hisat_Wrapper.sh <genome_directory> <read_directory>

The genome_directory should contain the following 2 files:

    # GENOME_SEQUENCE=      genome_name.fa
    # GENOME_ANNOTATIONS  =      genome_name.gtf

if you wish to use the SNP aware indexer the genome folder should
also contain:

    # GENOME_SNPS      =      genome_name.vcf

The read_directory should contain trimmed.gz reads in pairs:

You will be prompted to enter the number of CPUS's to use, the
amount of RAM and the unique read suffixes

The number of cores and amount of RAM should be specified as whole
numbers (eg 20 = 20gb)

The read suffixes should be unique:

    # *_R1_001.fq.gz
    # *_R2_001.fq.gz
```

for optimum compatibility we recommend that the reads are formatted as follows:

```
# SAMPLE_REPLICATE_LANE_READSUFFIX
```

If the reads are not formatted in this manner it is likely that the script will crash whilst merging of the sorted bamfiles.

This script assumes that the reads were generated across multiple lane (eg: L001, L002).

If the reads were not generated across multiple lanes then the script will crash whilst merging of the sorted bamfiles. In this instance you may need to re-write the Merge_bam_files function or rename your reads so that the technical replicates are defined after the second underscore in the readname.

Dependencies (The following tools must be installed at \$/PATH):

```
# HISAT (tested with version 2.0.0-beta)
# samtools (tested with version 0.1.19)
# HTSeq_count (tested with version 0.6.1)
# StringTie (tested with version 1.0.4)
```

If not set, the CPU and RAM settings determined automatically based on the available system resources

```
"
exit 0
}
#-----#
Extract_Splice_sites(){
# Extract Splice sites from GFF

START=$(date +%s)

if [ -f $SPLICE_SITES ];

then
echo "Splice site file $SPLICE_SITES exists"
else
echo "Extracting splice sites from $GENOME_GTF"
python $HISAT2_DIRECTORY/extract_splice_sites.py $GENOME_GTF
> $SPLICE_SITES

fi;
wait

END=$(date +%s)
TIME_SPLICE_SITES=$((END-START))
```

```

    echo "Time to extract Splice sites from GFF: $TIME_SPLICE_SITES
seconds"

}

#-----#

Extract_Exons(){

# Extract Exons from GFF

    START=$(date +%s)

    if [ -f $EXONS ];

        then
            echo "Exon file $EXONS exists"
        else
            echo "Extracting exons sites from $GENOME_GTF"
            python $HISAT2_DIRECTORY/extract_exons.py $GENOME_GTF >
$EXONS

        fi;
        wait

        END=$(date +%s)
        TIME_EXONS=$((END-START))
        echo "Time to extract Exons from GFF: $TIME_EXONS  seconds"

    }

#-----#

Extract_SNPs(){

# Extract Exons from VCF

    START=$(date +%s)

    if [ -f $SNPS ];

        then
            echo "Exon file $SNPS exists"
        else
            echo "Extracting SNPs from $GENOME_VCF"

            cat $GENOME_VCF | awk -F $'\t' 'BEGIN {OFS = FS}{
                if (index($8, "deletion")) { print
$3,"deletion"$1,$2,length($5);}
                else if (index($8, "SNV")) { print
$3,"single"$1,$2,$5;}
                else if (index($8,"insertion")) { print
$3,"insertion"$1,$2,$5;}
            }' | tr '[],' '[\t]' | awk -F $'\t' 'BEGIN {OFS = FS}{
                if ($6=="") { print $1,$2,$3,$4,"$5;}
                else { for (i=4; i<=NF; i++) print
$1,$2,$3,$4,"$i;
            }' > $SNPS

```

```

    fi;
    wait

    END=$(date +%s)
    TIME_EXONS=$((END-START))
    echo "Time to extract SNPs from GFF: $TIME_SNPs seconds"
}

#-----#

Index_reference_genome_no_SNPs(){

# Build the reference genome without the SNP aware indexer

    START=$(date +%s)

    if [ -f $INDEX_NAME.1.ht2 ] ;

        then
            echo "GENOME_SEQUENCE $INDEX_NAME Exists. If you need to re-
index the genome please remove current version in
$GENOME_DIRECTORY"
        else
            echo "Indexing $GENOME_SEQUENCE with splice site aware
algorithm";
            hisat2-build --verbose -p $NPROC --ss $SPLICE_SITES --exon
$EXONS $GENOME_SEQUENCE $INDEX_NAME

        fi;
        wait

        END=$(date +%s)
        TIME_INDEXING=$((END-START))
        echo "Time to index the reference sequence: $TIME_INDEXING
seconds"

    }

#-----#

Index_reference_genome_with_SNPs(){

# Build the reference genome with the SNP aware indexer

    START=$(date +%s)

    if [ -f $INDEX_NAME.1.ht2 ] ;

        then
            echo "GENOME_SEQUENCE $INDEX_NAME Exists. If you need to re-
index please remove current version"
        else
            echo "Indexing $GENOME_SEQUENCE with splice site aware
algorithm";

```

```

        hisat2-build --verbose -p $NPROC --snp $SNP --ss
        $SPLICE_SITES --exon $EXONS $GENOME_SEQUENCE $INDEX_NAME

        fi;
        wait

        END=$(date +%s)
        TIME_INDEXING=$((END-START))
        echo "Time to index the reference sequence: $TIME_INDEXING
seconds"

    }

#-----#

Run_alignment() {

#Run hisat on all read pairs

    START=$(date +%s)

    for fq_pair_1 in $WORKING_DIRECTORY/*$READ1_SUFFIX ;

        do

            filename=${fq_pair_1}$READ1_SUFFIX}
            fq_pair_2=${filename}$READ2_SUFFIX

            samfile=$filename.$SAMFILE
            mapping_statistics=$filename.$MAPPING_STATISTICS
            novel_splice_sites=$filename.$NOVEL_SPLICE_SITES
            unaligned_singletons=$filename.$UNMAPPED_SINGLETONS
            unaligned_pairs=$filename.$UNMAPPED_PAIRS

            if [ -f $samfile ] ;
                then
                    echo "$samfile Exists"
                else
                    echo "now aligning $fq_pair_1 and $fq_pair_2"
                    hisat2 -x $INDEX_NAME -p $NPROC --known-splicesite-
infile $SPLICE_SITES --novel-splicesite-outfile
$novel_splice_sites -1 $fq_pair_1 -2 $fq_pair_2 -S $samfile --met-
file $mapping_statistics --un-gz $unaligned_singletons --un-conc-
gz $unaligned_pairs;
                    fi
                done;
                wait

            END=$(date +%s)
            TIME_ALLGINING=$((END-START))
            echo "Time to run hisat: $TIME_ALLGINING seconds"

        }

#-----#

Convert_SAM_to_BAM() {

```

```

#Convert all .sam files to sorted .bam files in batches of NPROC

START=$(date +%s)

for samfile in $WORKING_DIRECTORY/*.SAMFILE;

do

    bamfile="${samfile%.sam}.alignment"

    if [ -f $bamfile.bam ];
    then
        echo "$bamfile.bam Exists"
    else
        echo "Now sorting $samfile."
        samtools view -bS $samfile | samtools sort - $bamfile
&

        PROC=$((PROC+6))

        if [ "$PROC" -ge "$NPROC" ];
        then
            wait
            PROC=0
        fi

    fi
done;
wait

END=$(date +%s)
TIME_SORTING=$((END-START))
echo "Time to convert .sam files to sorted .bam files:
$TIME_SORTING seconds"

}

#-----#

Merge_bam_files(){

#merge the sorted .bam files

    START=$(date +%s)

    grouped_sample_ID=$(find "$WORKING_DIRECTORY" -name
"*.*.alignment.bam" -exec echo "{}" \;)
    echo "$grouped_sample_ID" >
$WORKING_DIRECTORY/list_of_alignments.tmp
    sample_IDS=$(cat $WORKING_DIRECTORY/list_of_alignments.tmp | rev
| cut -d"/" -f1 | rev | cut -d"_" -f1-2 | sort | uniq)

    for sample in $sample_IDS;
    do
        list=$(find "$WORKING_DIRECTORY" -name
"$sample*.alignment.bam");

        echo "merging sorted bam files"
        echo " $list"
    done
}

```

```

        samtools merge
$WORKING_DIRECTORY/"$sample".merged_alignment.bam $list
done;

wait

END=$(date +%s)
TIME_MERGING=$((END-START))
echo "Time to merge .bam files: $TIME_MERGING seconds"
}

#-----#

Generate_assembly(){

#Run stringtie on sorted .bam files

START=$(date +%s)

for bamfile in $WORKING_DIRECTORY/*merged_alignment.bam;

do
    results_summary="${bamfile%.merged_alignment.bam}_assembly/r
esults_summary.txt"
    results_folder="${bamfile%.merged_alignment.bam}_assembly"

    if [ -f $results_summary ];
    then
        echo "$results_summary Exists"
    else
        echo "Now running StringTie on $bamfile."
        mkdir $results_folder
        stringtie $bamfile -G $GENOME_GTF -p $NPROC -b
$results_folder > $results_summary
    fi
done;
wait

END=$(date +%s)
TIME_ASSEMBLING=$((END-START))
echo "Time to run StringTie: $TIME_ASSEMBLING seconds"
}

#-----#

Generate_counts(){

#Run HTSeq on sorted .bam files

START=$(date +%s)

for bamfile in $WORKING_DIRECTORY/*merged_alignment.bam;

do
    results_counts="${bamfile%.bam}.counts"

```

```

if [ -f $results_counts ];
then
    echo "$results_summary Exists"
else
    echo "Now running HTSeq on $bamfile."
    samtools view $bamfile | htseq-count - $GENOME_GTF >
$results_counts &

    PROC=$((PROC+2))

    if [ "$PROC" -ge "$NPROC" ];
    then
        wait
        PROC=0
    fi
fi
done;
wait

END=$(date +%s)
TIME_COUNTING=$((END-START))
echo "Time to count alignments with HTSeq counts: $TIME_COUNTING
seconds"

}

#-----#

Generate_statistics(){

#Calculate total runtime, the number of reads and Mapping
Statistics

START=$(date +%s)

echo "Generating statistics"

for fq_pair_1 in $WORKING_DIRECTORY/*$READ1_SUFFIX;
do

    filename=${fq_pair_1}$READ1_SUFFIX
    fq_pair_2=${filename}$READ2_SUFFIX
    samfile=$filename.$SAMFILE
    bamfile=$filename.alignment.$BAMFILE
    sample_name=${filename##*/}

    number_of_R1_input_reads=$(zcat "$fq_pair_1" | echo $((`wc
-1`/4)))
    number_of_R2_input_reads=$(zcat "$fq_pair_2" | echo $((`wc -
1`/4)))
    flagstat=$(samtools flagstat $bamfile)

    echo "Filename = $sample_name
number of reads = $number_of_R1_input_reads +
$number_of_R2_input_read
Samtools flagstats ="

```

```

$flagstat

"
done > "$WORKING_DIRECTORY/Run_statistics.tsv"

END=$(date +%s)
TIME_GENERATE_STATISTICS=$((END-START))
}

#-----#

Move_files(){

#Make new directories and move files accordingly

if [ ! -d "$WORKING_DIRECTORY/reads" ]; then
    mkdir $WORKING_DIRECTORY/reads
fi;

if [ ! -d "$WORKING_DIRECTORY/reads/trimmed" ]; then
    mkdir $WORKING_DIRECTORY/reads/trimmed
    mv $WORKING_DIRECTORY/*$READ1_SUFFIX
$WORKING_DIRECTORY/reads/trimmed
    mv $WORKING_DIRECTORY/*$READ2_SUFFIX
$WORKING_DIRECTORY/reads/trimmed
fi;

if [ ! -d "$WORKING_DIRECTORY/reads/unmapped_singletons" ]; then
    mkdir $WORKING_DIRECTORY/reads/unmapped_singletons
    mv $WORKING_DIRECTORY/*$UNMAPPED_SINGLETONS
$WORKING_DIRECTORY/reads/unmapped_singletons
fi;

if [ ! -d "$WORKING_DIRECTORY/reads/unmapped_pairs" ]; then
    mkdir $WORKING_DIRECTORY/reads/unmapped_pairs
    mv $WORKING_DIRECTORY/*.unmapped.pairs.fq.*.gz
$WORKING_DIRECTORY/reads/unmapped_pairs
fi;

if [ ! -d "$WORKING_DIRECTORY/alignments" ]; then
    mkdir $WORKING_DIRECTORY/alignments
fi;

if [ ! -d "$WORKING_DIRECTORY/alignments/merged_alignment" ];
then
    mkdir $WORKING_DIRECTORY/alignments/merged_alignment
    mv $WORKING_DIRECTORY/*.merged_alignment.bam
$WORKING_DIRECTORY/alignments/merged_alignment
fi;

if [ ! -d "$WORKING_DIRECTORY/alignments/samfiles" ]; then
    mkdir $WORKING_DIRECTORY/alignments/samfiles
    mv $WORKING_DIRECTORY/*$SAMFILE
$WORKING_DIRECTORY/alignments/samfiles
fi;

if [ ! -d "$WORKING_DIRECTORY/alignments/sorted_bamfiles" ]; then

```

```

    mkdir $WORKING_DIRECTORY/alignments/sorted_bamfiles
    mv $WORKING_DIRECTORY/*$BAMFILE
$WORKING_DIRECTORY/alignments/sorted_bamfiles
fi;

if [ ! -d "$WORKING_DIRECTORY/alignments/statistics" ]; then
    mkdir $WORKING_DIRECTORY/alignments/statistics
    mv $WORKING_DIRECTORY/*$MAPPING_STATISTICS
$WORKING_DIRECTORY/alignments/statistics
fi;

if [ ! -d "$WORKING_DIRECTORY/alignments/novel_splice_sites" ];
then
    mkdir $WORKING_DIRECTORY/alignments/novel_splice_sites
    mv $WORKING_DIRECTORY/*$NOVEL_SPLICE_SITES
$WORKING_DIRECTORY/alignments/novel_splice_sites
fi;

if [ ! -d "$WORKING_DIRECTORY/assemblies" ]; then
    mkdir $WORKING_DIRECTORY/assemblies
    mv $WORKING_DIRECTORY/*assembly
$WORKING_DIRECTORY/assemblies
fi;
if [ ! -d "$WORKING_DIRECTORY/counts" ]; then
    mkdir $WORKING_DIRECTORY/counts
    mv $WORKING_DIRECTORY/*counts $WORKING_DIRECTORY/counts
fi;

}

#####
# Either run the pipeline or exit based on input variables
#####

GENOME_DIRECTORY=$1;
WORKING_DIRECTORY=$2;

if [ "$1" = -h ];
then

    help_readme

elif [ "$1" = --help ];
then

    help_readme

elif [ -d "$1" ] && [ -d "$2" ];
then

    gtf=$(ls $GENOME_DIRECTORY/*.gtf | wc -l)
    fa=$(ls $GENOME_DIRECTORY/*.fa | wc -l)
    vcf=$(ls $GENOME_DIRECTORY/*.vcf | wc -l)

    if [ "$gtf" = "1" ] && [ "$fa" = "1" ];
    then

```

```

        echo "Run Started"
        echo "HISAT and StringTie wrapper script v1.0.1 by Tom
Giles (21.10.15) (thomas.giles@nottingham.ac.uk)"
        echo "for more information on how to run this script
please use -h or --help"
        echo ""
        echo "Genome folder = $1"
        echo "Read folder = $2"

#-----#

# Set global variables

echo -n "Enter the number of CPU cores to use > "
read number_of_cores
echo -n "Enter the amount of RAM (in GB) to use > "
read amount_of_ram
echo -n "Enter the unique read_1 suffix > "
read READ1_SUFFIX
echo -n "Enter the unique read_2 suffix > "
read READ2_SUFFIX

#-----#

# Define the status of the system

NPROC=$(grep -c ^processor /proc/cpuinfo)

if [ "$number_of_cores" -lt "$NPROC" ];
then

        NPROC=$number_of_cores
    else
        echo "$number_of_cores is greater than the
available number of cores. \n Using $NPROC cores"
    fi

KB_RAM=$(head -1 /proc/meminfo | awk '{ print $2 }');
GB_RAM=$(echo "scale=2; $KB_RAM /1048576" | bc);
GB_RAM_ROUNDED=$(echo ${GB_RAM%.*});
RAM=$((GB_RAM_ROUNDED-2));

if [ "$amount_of_ram" -lt "$RAM" ];
then

        RAM=$amount_of_ram
    else
        echo "$amount_of_ram is greater than the
available amount of RAM. \n Using $RAM GB of RAM"
    fi

echo "Using $RAM GB of RAM and $NPROC cores"

```

```

#~~~~~
~#

# Automatically define the additional core variables

GENOME_SEQUENCE=$(find $GENOME_DIRECTORY -type f -name
*.fa)
GENOME_GTF=$(find $GENOME_DIRECTORY -type f -name
*.gtf)

INDEX_NAME="${GENOME_SEQUENCE%.fa}"
SPLICE_SITES="${GENOME_GTF%.gtf}.splice_sites"
EXONS="${GENOME_GTF%.gtf}.exons"
HISAT2_DIRECTORY=$(which hisat2 | sed
's,/*[^/]\+/*$,,' )
SAMFILE="sam"
BAMFILE="bam"
MAPPING_STATISTICS="mapping_statistics.txt"
NOVEL_SPLICE_SITES="novel_splice_sites.tsv"
UNMAPPED_SINGLETONS="unmapped.singletons.fq.gz"
UNMAPPED_PAIRS="unmapped.pairs.fq.gz"

if [ "$vcf" = "1" ];
then

$GENOME_VCF=$(find $GENOME_DIRECTORY -type f -
name *.vcf)

$SNPS="${GENOME_VCF%.vcf}.snps"
echo "SNP file present - will attempt to
generate a SNP sensitive genome index"
else
echo "SNP file not present - will not attempt to
generate a SNP sensitive genome index"
fi

#~~~~~
~#

# call functions

Extract_Splice_sites;
Extract_Exons;

if [ "$vcf" = "1" ];
then

Extract_SNPs;
fi

if [ "$vcf" = "1" ];
then

Index_reference_genome_with_SNPs;
else

Index_reference_genome_no_SNPs;

```

```

        fi
        Run_alignment;
        Convert_SAM_to_BAM;
        Merge_bam_files;
        Generate_counts;
        Generate_assembly;
        Generate_statistics;
        Move_files;

#~~~~~
~#

        # Collect Statistics

        echo "Run Finished"
        rm $WORKING_DIRECTORY/*.tmp

        Run_date=$(date);

        TIME_SPLICE_SITES=$(echo $TIME_SPLICE_SITES | awk
' {print int($1/60) "m:"int($1%60)}"s"')
        TIME_EXONS=$(echo $TIME_EXONS | awk '{print
int($1/60) "m:"int($1%60)}"s"')
        TIME_INDEXING=$(echo $TIME_INDEXING | awk '{print
int($1/60) "m:"int($1%60)}"s"')
        TIME_ALLGINING=$(echo $TIME_ALLGINING | awk '{print
int($1/60) "m:"int($1%60)}"s"')
        TIME_SORTING=$(echo $TIME_SORTING | awk '{print
int($1/60) "m:"int($1%60)}"s"')
        TIME_MERGING=$(echo $TIME_MERGING | awk '{print
int($1/60) "m:"int($1%60)}"s"')
        TIME_COUNTS=$(echo $TIME_COUNTS | awk '{print
int($1/60) "m:"int($1%60)}"s"')
        TIME_ASSEMBLING=$(echo $TIME_ASSEMBLING | awk '{print
int($1/60) "m:"int($1%60)}"s"')
        TIME_GENERATE_STATISTICS=$(echo
$TIME_GENERATE_STATISTICS | awk '{print
int($1/60) "m:"int($1%60)}"s"')

        echo ""
        echo "PERFORMANCE STATISTICS:"
        echo "Number of CPUs = $NPROC | Amount of Ram used =
$RAM"

        if [ "$TIME_SPLICE_SITES" != "0m:0s" ];
        then
                echo "Time to extract splice sites from GFF:
$TIME_SPLICE_SITES"
        else
                echo "splice sites file existed";
        fi
        if [ "$TIME_EXONS" != "0m:0s" ]; then echo "Time to
extract exons from GFF: $TIME_EXONS";
        else
                echo "Exon file already existed";
        fi
        if [ "$TIME_INDEXING" != "0m:0s" ]; then

```

```

        echo "Time to index the reference sequence:
$TIME_INDEXING";
    else
        echo "Genome was already indexed"
    fi
    if [ "$TIME_ALLGINING" != "0m:0s" ];
    then
        echo "Time to run HISAT: $TIME_ALLGINING";
    fi
    if [ "$TIME_SORTING" != "0m:0s" ];
    then
        echo "Time to convert .sam files to sorted .bam
files: $TIME_SORTING";
    fi
    if [ "$TIME_MERGING" != "0m:0s" ];
    then
        echo "Time to merge .bam files: $TIME_MERGING";
    fi
    if [ "$TIME_COUNTS" != "0m:0s" ];
    then
        echo "Time to count alignments with HTSeq
counts: $TIME_COUNTS";
    fi
    if [ "$TIME_ASSEMBLING" != "0m:0s" ];
    then
        echo "Time to run StringTie: $TIME_ASSEMBLING";
    fi
    if [ "$TIME_GENERATE_STATISTICS" != "0m:0s" ];
    then
        echo "Time to generate statistics:
$TIME_GENERATE_STATISTICS";
    fi
    exit 0

    else
        help_readme

    fi
else
    help_readme

fi

```

References

References

- ABU ELZEIN, E. M., HOUSAWI, F. M., GAMEEL, A. A., AL-AFALEQ, A. I. & EL-BASHIR, A. M. 2003. Sheep-associated malignant catarrhal fever involving 3-5-week-old calves in Saudi Arabia. *J Vet Med B Infect Dis Vet Public Health*, 50, 53-9.
- ABUHAMMAD, S. & ZIHLIF, M. 2013. Gene expression alterations in doxorubicin resistant MCF7 breast cancer cell line. *Genomics*, 101, 213-220.
- Ackermann, M. (2006). "Pathogenesis of gammaherpesvirus infections." *Veterinary Microbiology* **113**(3): 211-222.
- ANASTASIADOU, E., BOCCELLATO, F., CIRONE, M., KIS, L. L., KLEIN, E., FRATI, L., FAGGIONI, A. & TRIVEDI, P. 2005. Epigenetic mechanisms do not control viral latency III in primary effusion lymphoma cells infected with a recombinant Epstein-Barr virus. *Leukemia*, 19, 1854-6.
- ANDERSON, I. E., BUXTON, D., CAMPBELL, I., RUSSELL, G., DAVIS, W. C., HAMILTON, M. J. & HAIG, D. M. 2007. Immunohistochemical study of experimental malignant catarrhal fever in rabbits. *J Comp Pathol*, 136, 156-66.
- ANDERSON, I. E., DEANE, D., SWA, S., THOMSON, J., CAMPBELL, I., BUXTON, D., WEI, X. Q., STEWART, J., RUSSELL, G. & HAIG, D. M. 2008. Production and utilization of interleukin-15 in malignant catarrhal fever. *J Comp Pathol*, 138, 131-44.
- ANDERSON, I. E., REID, H. W., NETTLETON, P. F., MCINNES, C. J. & HAIG, D. M. 2001. Detection of cellular cytokine mRNA expression during orf virus infection in sheep: differential interferon-gamma mRNA expression by cells in primary versus reinfection skin lesions. *Vet Immunol Immunopathol*, 83, 161-76.
- BARTEL, D. P. 2009. MicroRNAs: target recognition and regulatory functions. *Cell*, 136, 215-33.
- BARTON, E., MANDAL, P. & SPECK, S. H. 2011. Pathogenesis and host control of gammaherpesviruses: lessons from the mouse. *Annu Rev Immunol*, 29, 351-97.
- BENJAMIN, A. M., NICHOLS, M., BURKE, T. W., GINSBURG, G. S. & LUCAS, J. E. 2014. Comparing reference-based RNA-Seq mapping methods for non-human primate data. *BMC genomics*, 15, 1.
- BLAKE, N. 2010. Immune evasion by gammaherpesvirus genome maintenance proteins. *J Gen Virol*, 91, 829-46.
- Borodovsky, Alexandra; et al. (2013). "5-azacytidine reduces methylation, promotes differentiation and induces tumor regression in a patient-

- derived IDH1 mutant glioma xenograft". *Oncotarget*. 4 (10): 1737–1747.
- BOUDRY, C., MARKINE-GORIAYNOFF, N., DELFORGE, C., SPRINGAEL, J. Y., DE LEVAL, L., DRION, P., RUSSELL, G., HAIG, D. M., VANDERPLASSCHEN, A. F. & DEWALS, B. 2007. The A5 gene of alcelaphine herpesvirus 1 encodes a constitutively active G-protein-coupled receptor that is non-essential for the induction of malignant catarrhal fever in rabbits. *J Gen Virol*, 88, 3224-33.
- BOYLE, J. P. & MONIE, T. P. 2012. Computational analysis predicts the Kaposi's sarcoma-associated herpesvirus tegument protein ORF63 to be alpha helical. *Proteins*, 80, 2063-70.
- BOYMAN, O. & SPRENT, J. 2012. The role of interleukin-2 during homeostasis and activation of the immune system. *Nat Rev Immunol*, 12, 180-90.
- BRIDGEN, A., MUNRO, R. & REID, H. W. 1992. The detection of Alcelaphine herpesvirus-1 DNA by in situ hybridization of tissues from rabbits affected with malignant catarrhal fever. *J Comp Pathol*, 106, 351-9.
- BULLARD, J. H., PURDOM, E., HANSEN, K. D. & DUDOIT, S. 2010. Evaluation of statistical methods for normalization and differential expression in mRNA-Seq experiments. *BMC bioinformatics*, 11, 94.
- BURRELLS, C. & REID, H. W. 1991. Phenotypic analysis of lymphoblastoid cell lines derived from cattle and deer affected with "sheep-associated" malignant catarrhal fever. *Vet Immunol Immunopathol*, 29, 151-61.
- BUXTON, D. & REID, H. W. 1980. Transmission of malignant catarrhal fever to rabbits. *Vet Rec*, 106, 243-5.
- BUXTON, D., REID, H. W., FINLAYSON, J. & POW, I. 1984. Pathogenesis of 'sheep-associated' malignant catarrhal fever in rabbits. *Res Vet Sci*, 36, 205-11.
- CFSP. 2012. Malignant catarrhal fever Available: http://www.cfsph.iastate.edu/Factsheets/pdfs/malignant_catarrhal_fever.pdf [Accessed 28/08/2015].
- CHANG, H. W., WANG, H. C., CHEN, C. Y., HUNG, T. W., HOU, M. F., YUAN, S. S., HUANG, C. J. & TSENG, C. N. 2014. 5-azacytidine induces anoikis, inhibits mammosphere formation and reduces metalloproteinase 9 activity in MCF-7 human breast cancer cells. *Molecules*, 19, 3149-59.
- CHEN, Z. & DUAN, X. 2011. Ribosomal RNA depletion for massively parallel bacterial RNA-sequencing applications. *Methods Mol Biol*, 733, 93-103.

- CHRISTMAN, J. K. 2002. 5-Azacytidine and 5-aza-2'-deoxycytidine as inhibitors of DNA methylation: mechanistic studies and their implications for cancer therapy. *Oncogene*, 21, 5483-95.
- CHU, Y. & COREY, D. R. 2012. RNA sequencing: platform selection, experimental design, and data interpretation. *Nucleic Acid Ther*, 22, 271-4.
- CLEAVELAND, S., KUSILUKA, L., OLE KUWAI, J., BELL, C. & KAZWALA, R. 2001. Assessing the impact of malignant catarrhal fever in Ngorongoro District, Tanzania. Department for international development, animal health programme, 1-57.
- COSCOY, L. 2007. Immune evasion by Kaposi's sarcoma-associated herpesvirus. *Nat Rev Immunol*, 7, 391-401.
- COULTER, L. J., WRIGHT, H. & REID, H. W. 2001. Molecular genomic characterization of the viruses of malignant catarrhal fever. *J Comp Pathol*, 124, 2-19.
- CUNHA, C. W., GAILBREATH, K. L., O'TOOLE, D., KNOWLES, D. P., SCHNEIDER, D. A., WHITE, S. N., TAUS, N. S., DAVIES, C. J., DAVIS, W. C. & LI, H. 2012. Ovine herpesvirus 2 infection in American bison: virus and host dynamics in the development of sheep-associated malignant catarrhal fever. *Veterinary microbiology*, 159, 307-319.
- CUNHA, C. W., O'TOOLE, D., TAUS, N. S., KNOWLES, D. P. & LI, H. 2013. Are rabbits a suitable model to study sheep-associated malignant catarrhal fever in susceptible hosts? *Vet Microbiol*, 163, 358-63.
- CUNHA, C. W., TRAU, D. L., TAUS, N. S., OAKS, J. L., O'TOOLE, D., DAVITT, C. M. & LI, H. 2008. Detection of ovine herpesvirus 2 major capsid gene transcripts as an indicator of virus replication in shedding sheep and clinically affected animals. *Virus Res*, 132, 69-75.
- CZABOTAR, P. E., LESSENE, G., STRASSER, A. & ADAMS, J. M. 2014. Control of apoptosis by the BCL-2 protein family: implications for physiology and therapy. *Nature reviews Molecular cell biology*, 15, 49-63.
- DAVIS, W. C., BROWN, W. C., HAMILTON, M. J., WYATT, C. R., ORDEN, J. A., KHALID, A. M. & NAESSENS, J. 1996. Analysis of monoclonal antibodies specific for the gamma delta TcR. *Vet Immunol Immunopathol*, 52, 275-83.
- DAVISON, A. J., EBERLE, R., EHLERS, B., HAYWARD, G. S., MCGEOCH, D. J., MINSON, A. C., PELLETT, P. E., ROIZMAN, B., STUDDERT, M. J. & THIRY, E. 2009. The order Herpesvirales. *Arch Virol*, 154, 171-7.
- DEWALS, B. G. & VANDERPLASSCHEN, A. 2011. Malignant catarrhal fever induced by Alcelaphine herpesvirus 1 is characterized by an expansion of activated CD3+CD8+CD4- T cells expressing a cytotoxic phenotype in both lymphoid and non-lymphoid tissues. *Vet Res*, 42, 95.

- DEWALS, B., BOUDRY, C., FARNIR, F., DRION, P. V. & VANDERPLASSCHEN, A. 2008. Malignant catarrhal fever induced by alcelaphine herpesvirus 1 is associated with proliferation of CD8+ T cells supporting a latent infection. *PLoS One*, 3, e1627.
- DEWALS, B., BOUDRY, C., GILLET, L., MARKINE-GORIAYNOFF, N., DE LEVAL, L., HAIG, D. & VANDERPLASSCHEN, A. 2006a. Cloning of the genome of Alcelaphine herpesvirus 1 as an infectious and pathogenic bacterial artificial chromosome. *Journal of general virology*, 87, 509-517.
- DEWALS, B., MYSTER, F., PALMEIRA, L., GILLET, L., ACKERMANN, M. & VANDERPLASSCHEN, A. 2011. Ex vivo bioluminescence detection of alcelaphine herpesvirus 1 infection during malignant catarrhal fever. *J Virol*, 85, 6941-54.
- DRY, I., HAIG, D. M., INGLIS, N. F., IMRIE, L., STEWART, J. P. & RUSSELL, G. C. 2008. Proteomic analysis of pathogenic and attenuated alcelaphine herpesvirus 1. *J Virol*, 82, 5390-7.
- DRY, I., TODD, H., DEANE, D., PERCIVAL, A., MCLEAN, K., INGLIS, N. F., MANSON, E. D., HAIG, D. M., NAYUNI, S., HUTT-FLETCHER, L. M., GRANT, D. M., BARTLEY, K., STEWART, J. P. & RUSSELL, G. C. 2016. Alcelaphine herpesvirus 1 glycoprotein B: recombinant expression and antibody recognition. *Arch Virol*, 161, 613-9.
- EDINGTON, N. & PLOWRIGHT, W. 1980. The protection of rabbits against the herpesvirus of malignant catarrhal fever by inactivated vaccines. *Research in veterinary science*, 28, 384-386.
- ENSSER, A. & FLECKENSTEIN, B. 2005. T-Cell Transformation and Oncogenesis by γ 2-Herpesviruses. In: GEORGE, F. V. W. & GEORGE, K. (eds.) *Advances in Cancer Research*. Academic Press.
- ENSSER, A., PFLANZ, R. & FLECKENSTEIN, B. 1997a. Primary structure of the alcelaphine herpesvirus 1 genome. *Journal of virology*, 71, 6517-6525.
- FENG, W. H., HONG, G., DELECLUSE, H. J. & KENNEY, S. C. 2004. Lytic induction therapy for Epstein-Barr virus-positive B-cell lymphomas. *J Virol*, 78, 1893-902.
- FERRIS, D., HAMDY, F. & DARDIRI, A. 1976. Detection of African malignant catarrhal fever virus antigens in cell cultures by immunofluorescence. *Veterinary Microbiology*, 1, 437-448.
- FLINT, S. J., ENQUIST, L. W., RACANIELLO, V. R. & SKALA, A. 2009. *Principles of Virology volume I: Molecular Biology*, Washington, USA: American Society for Microbiology Press.
- FRAME, F. M. & DALZIEL, R. G. 2008. Transcriptional control by the R-transactivator protein of alcelaphine herpesvirus-1. *Vet Res Commun*, 32, 215-23.

- FRAME, F. M. & DALZIEL, R. G. 2008. Transcriptional control by the R-transactivator protein of alcelaphine herpesvirus-1. *Vet Res Commun*, 32, 215-23.
- FRASER, S. J., NETTLETON, P. F., DUTIA, B. M., HAIG, D. M. & RUSSELL, G. C. 2006. Development of an enzyme-linked immunosorbent assay for the detection of antibodies against malignant catarrhal fever viruses in cattle serum. *Vet Microbiol*, 116, 21-8.
- FRAZEE, A. C., PERTEA, G., JAFFE, A. E., LANGMEAD, B., SALZBERG, S. L. & LEEK, J. T. 2014. Flexible isoform-level differential expression analysis with Ballgown. *bioRxiv*.
- GAILBREATH, K. L., TAUS, N. S., CUNHA, C. W., KNOWLES, D. P. & LI, H. 2008. Experimental infection of rabbits with ovine herpesvirus 2 from sheep nasal secretions. *Vet Microbiol*, 132, 65-73.
- GARDELLA, T., MEDVECZKY, P., SAIRENJI, T. & MULDER, C. 1984. Detection of circular and linear herpesvirus DNA molecules in mammalian cells by gel electrophoresis. *Journal of Virology*, 50, 248-254.
- GASPER, D., BARR, B., LI, H., TAUS, N., PETERSON, R., BENJAMIN, G., HUNT, T. & PESAVENTO, P. A. 2012. Ibex-associated malignant catarrhal fever-like disease in a group of bongo antelope (*Tragelaphus eurycerus*). *Vet Pathol*, 49, 492-7.
- GOODWIN, D. J., WALTERS, M. S., SMITH, P. G., THURAU, M., FICKENSCHER, H. & WHITEHOUSE, A. 2001. Herpesvirus saimiri open reading frame 50 (Rta) protein reactivates the lytic replication cycle in a persistently infected A549 cell line. *J Virol*, 75, 4008-13.
- GRABSTEIN, K. H., EISENMAN, J., SHANEBECK, K., RAUCH, C., SRINIVASAN, S., FUNG, V., BEERS, C., RICHARDSON, J., SCHOENBORN, M. A., AHDIEH, M. & ET AL. 1994. Cloning of a T cell growth factor that interacts with the beta chain of the interleukin-2 receptor. *Science*, 264, 965-8.
- GRIFFITHS-JONES, S., SAINI, H. K., VAN DONGEN, S. & ENRIGHT, A. J. 2008. miRBase: tools for microRNA genomics. *Nucleic acids research*, 36, D154-D158.
- GRUNDHOFF, A. & SULLIVAN, C. S. 2011. Virus-encoded microRNAs. *Virology*, 411, 325-43.
- HAAF, T. 1995. The effects of 5-azacytidine and 5-azadeoxycytidine on chromosome structure and function: implications for methylation-associated cellular processes. *Pharmacol Ther*, 65, 19-46.
- HAIG, D. M., GRANT, D., DEANE, D., CAMPBELL, I., THOMSON, J., JEPSON, C., BUXTON, D. & RUSSELL, G. C. 2008. An immunisation strategy for the protection of cattle against alcelaphine herpesvirus-1-induced malignant catarrhal fever. *Vaccine*, 26, 4461-8.

- HAIR, J. R., LYONS, P. A., SMITH, K. G. C. & EFSTATHIOU, S. 2007. Control of Rta expression critically determines transcription of viral and cellular genes following gammaherpesvirus infection. *J Gen Virol*, 88, 1689-97.
- HANDLEY, J. A., SARGAN, D. R., HERRING, A. J. & REID, H. W. 1995. Identification of a region of the alcelaphine herpesvirus-1 genome associated with virulence for rabbits. *Vet Microbiol*, 47, 167-81.
- HART, J., ACKERMANN, M., JAYAWARDANE, G., RUSSELL, G., HAIG, D. M., REID, H. & STEWART, J. P. 2007b. Complete sequence and analysis of the ovine herpesvirus 2 genome. *J Gen Virol*, 88, 28-39.
- Henry J. Kaminski (2008). *Myasthenia Gravis and Related Disorders*. Springer. p. 163. Cyclosporine is derived from a fungus and is a cyclic undecapeptide with actions directed exclusively on T cells.
- HENRY, M. L., ELKHAMMAS, E. A., DAVIES, E. A. & FERGUSON, R. M. 1995. A clinical trial of cyclosporine G in cadaveric renal transplantation. *Pediatr Nephrol*, 9 Suppl, S49-51.
- HEUSCHELE, W. 1988. Malignant catarrhal fever: a review of a serious disease hazard for exotic and domestic ruminants. *Zoologische Garten*, 58, 123-133.
- HOUSE, A. E. & LYNCH, K. W. 2008. Regulation of alternative splicing: more than just the ABCs. *J Biol Chem*, 283, 1217-21.
- HU, J., GARBER, A. C. & RENNE, R. 2002. The latency-associated nuclear antigen of Kaposi's sarcoma-associated herpesvirus supports latent DNA replication in dividing cells. *J Virol*, 76, 11677-87.
- HUSSY, D., STAUBER, N., LEUTENEGGER, C. M., RIEDER, S. & ACKERMANN, M. 2001. Quantitative fluorogenic PCR assay for measuring ovine herpesvirus 2 replication in sheep. *Clin Diagn Lab Immunol*, 8, 123-8.
- INGOLIA, N. T., BRAR, G. A., ROUSKIN, S., MCGEACHY, A. M. & WEISSMAN, J. S. 2012. The ribosome profiling strategy for monitoring translation in vivo by deep sequencing of ribosome-protected mRNA fragments. *Nat Protoc*, 7, 1534-50.
- JACOBY, R. O., BUXTON, D. & REID, H. W. 1988. The pathology of wildebeest-associated malignant catarrhal fever in hamsters, rats and guinea-pigs. *J Comp Pathol*, 98, 99-109.
- JIN, L. & LLOYD, R. V. 1997. In situ hybridization: methods and applications. *J Clin Lab Anal*, 11, 2-9.
- JONES, P. A. 1985. Altering gene expression with 5-azacytidine. *Cell*, 40, 485-6.

- JONGBLOETS, B. C., RAMAKERS, G. M. J. & PASTERKAMP, R. J. 2013. Semaphorin7A and its receptors: Pleiotropic regulators of immune cell function, bone homeostasis, and neural development. *Seminars in Cell & Developmental Biology*, 24, 129-138.
- Joshi NA, Fass JN. (2011). Sickle: A sliding-window, adaptive, quality-based trimming tool for FastQ files (Version 1.33) [Software]. Available at <https://github.com/najoshi/sickle>.
- Kaur, Keerat; Yang, Jinpu; Eisenberg, Carol; Eisenberg, Leonard (2014). "5-azacytidine promotes the transdifferentiation of cardiac cells to skeletal myocytes." (PDF). *Cellular Reprogramming*. 16: 324–30.
- KEEL, M. K., GAGE, P. J., NOON, T. H., BRADLEY, G. A. & COLLINS, J. K. 2003. Caprine herpesvirus-2 in association with naturally occurring malignant catarrhal fever in captive sika deer (*Cervus nippon*). *Journal of Veterinary Diagnostic Investigation*, 15, 179-183.
- KENT, W. J. 2002. BLAT--the BLAST-like alignment tool. *Genome Res*, 12, 656-64.
- KIM, D., LANGMEAD, B. & SALZBERG, S. L. 2015. HISAT: a fast spliced aligner with low memory requirements. *Nat Meth*, 12, 357-360.
- KINCAID, R. P. & SULLIVAN, C. S. 2012. Virus-encoded microRNAs: an overview and a look to the future. *PLoS Pathog*, 8, e1003018.
- KLIEFORTH, R., MAALOUF, G., STALIS, I., TERIO, K., JANSSEN, D. & SCHRENZEL, M. 2002. Malignant catarrhal fever-like disease in Barbary red deer (*Cervus elaphus barbarus*) naturally infected with a virus resembling alcelaphine herpesvirus 2. *Journal of clinical microbiology*, 40, 3381-3390.
- KUMAR, R., ICHIHASHI, Y., KIMURA, S., CHITWOOD, D. H., HEADLAND, L. R., PENG, J., MALOOF, J. N. & SINHA, N. R. 2012. A High-Throughput Method for Illumina RNA-Seq Library Preparation. *Front Plant Sci*, 3, 202.
- LANKESTER, F., LUGELO, A., KAZWALA, R., KEYYU, J., CLEAVELAND, S. & YODER, J. 2015a. The economic impact of malignant catarrhal fever on pastoralist livelihoods. *PLoS one*, 10, e0116059.
- LANKESTER, F., LUGELO, A., MNYAMBWA, N., NDABIGAYE, A., KEYYU, J., KAZWALA, R., GRANT, D. M., RELF, V., HAIG, D. M., CLEAVELAND, S. & RUSSELL, G. C. 2015b. Alcelaphine Herpesvirus-1 (Malignant Catarrhal Fever Virus) in Wildebeest Placenta: Genetic Variation of ORF50 and A9.5 Alleles. *PLoS One*, 10, e0124121.
- LI, H., CUNHA, C. W. & TAUS, N. S. 2011b. Malignant catarrhal fever: understanding molecular diagnostics in context of epidemiology. *International journal of molecular sciences*, 12, 6881-6893.

- LI, H., CUNHA, C. W., DAVIES, C. J., GAILBREATH, K. L., KNOWLES, D. P., OAKS, J. L. & TAUS, N. S. 2008a. Ovine herpesvirus 2 replicates initially in the lung of experimentally infected sheep. *J Gen Virol*, 89, 1699-708.
- LI, H., CUNHA, C. W., GAILBREATH, K. L., O'TOOLE, D., WHITE, S. N., VANDERPLASSCHEN, A., DEWALS, B., KNOWLES, D. P. & TAUS, N. S. 2011a. Characterization of ovine herpesvirus 2-induced malignant catarrhal fever in rabbits. *Veterinary microbiology*, 150, 270-277.
- LI, H., CUNHA, C. W., TAUS, N. S. & KNOWLES, D. P. 2014. Malignant Catarrhal Fever: Inching Toward Understanding. *Annu. Rev. Anim. Biosci.*, 2, 209-233.
- LI, H., DYER, N., KELLER, J. & CRAWFORD, T. B. 2000. Newly recognized herpesvirus causing malignant catarrhal fever in white-tailed deer (*Odocoileus virginianus*). *Journal of Clinical Microbiology*, 38, 1313-1318.
- LI, H., GAILBREATH, K., BENDER, L. C., WEST, K., KELLER, J. & CRAWFORD, T. B. 2003. Evidence of three new members of malignant catarrhal fever virus group in muskox (*Ovibos moschatus*), Nubian ibex (*Capra nubiana*), and gemsbok (*Oryx gazella*). *J Wildl Dis*, 39, 875-80.
- LI, H., GAILBREATH, K., FLACH, E. J., TAUS, N. S., COOLEY, J., KELLER, J., RUSSELL, G. C., KNOWLES, D. P., HAIG, D. M., OAKS, J. L., TRAU, D. L. & CRAWFORD, T. B. 2005. A novel subgroup of rhadinoviruses in ruminants. *J Gen Virol*, 86, 3021-6.
- LI, H., HANDSAKER, B., WYSOKER, A., FENNEL, T., RUAN, J., HOMER, N., MARTH, G., ABECASIS, G. & DURBIN, R. 2009. The Sequence Alignment/Map format and SAMtools. *Bioinformatics*, 25, 2078-9.
- LI, H., KARNEY, G., O'TOOLE, D. & CRAWFORD, T. B. 2008b. Long distance spread of malignant catarrhal fever virus from feedlot lambs to ranch bison. *The Canadian Veterinary Journal*, 49, 183.
- LI, H., MCGUIRE, T. C., MULLER-DOBLIES, U. U. & CRAWFORD, T. B. 2001. A simpler, more sensitive competitive inhibition enzyme-linked immunosorbent assay for detection of antibody to malignant catarrhal fever viruses. *J Vet Diagn Invest*, 13, 361-4.
- LI, H., SHEN, D. T., KNOWLES, D. P., GORHAM, J. R. & CRAWFORD, T. B. 1994. Competitive inhibition enzyme-linked immunosorbent assay for antibody in sheep and other ruminants to a conserved epitope of malignant catarrhal fever virus. *Journal of Clinical Microbiology*, 32, 1674-1679.
- LI, H., SNOWDER, G., O'TOOLE, D. & CRAWFORD, T. B. 1998. Transmission of ovine herpesvirus 2 in lambs. *J Clin Microbiol*, 36, 223-6.

- LI, H., TAUS, N. S., JONES, C., MURPHY, B., EVERMANN, J. F. & CRAWFORD, T. B. 2006. A devastating outbreak of malignant catarrhal fever in a bison feedlot. *J Vet Diagn Invest*, 18, 119-23.
- LIGGITT, H. D. & DEMARTINI, J. C. 1980a. The pathomorphology of malignant catarrhal fever. I. Generalized lymphoid vasculitis. *Vet Pathol*, 17, 58-72.
- LIGGITT, H. D. & DEMARTINI, J. C. 1980b. The pathomorphology of malignant catarrhal fever. II. Multisystemic epithelial lesions. *Vet Pathol*, 17, 73-83.
- LINDGREEN, S. 2012. AdapterRemoval: easy cleaning of next-generation sequencing reads. *BMC Res Notes*, 5, 337.
- LODOLCE, J. P., BURKETT, P. R., KOKA, R. M., BOONE, D. L. & MA, A. 2002. Regulation of lymphoid homeostasis by interleukin-15. *Cytokine & growth factor reviews*, 13, 429-439.
- LUSCOMBE, N. M., GREENBAUM, D. & GERSTEIN, M. 2001. What is bioinformatics? A proposed definition and overview of the field. *Methods Inf Med*, 40, 346-58.
- MAHER, C. A., KUMAR-SINHA, C., CAO, X., KALYANA-SUNDARAM, S., HAN, B., JING, X., SAM, L., BARRETTE, T., PALANISAMY, N. & CHINNAIYAN, A. M. 2009. Transcriptome sequencing to detect gene fusions in cancer. *Nature*, 458, 97-101.
- MALARKEY, D. E. & MARONPOT, R. R. 1996. Polymerase chain reaction and in situ hybridization: applications in toxicological pathology. *Toxicol Pathol*, 24, 13-23.
- MATSUDA, S. & KOYASU, S. 2000. Mechanisms of action of cyclosporine. *Immunopharmacology*, 47, 119-125.
- MCKINNEY, W. P., YOUNG, M. J., HARTZ, A. & LEE, M. B. 1989. The inexact use of Fisher's Exact Test in six major medical journals. *JAMA*, 261, 3430-3.
- M Dunowska (2014) A review of equid herpesvirus 1 for the veterinary practitioner. Part A: Clinical presentation, diagnosis and treatment, *New Zealand Veterinary Journal*, 62:4, 179-188,
- MEIER-TRUMMER, C. S., REHRAUER, H., FRANCHINI, M., PATRIGNANI, A., WAGNER, U. & ACKERMANN, M. 2009a. Malignant catarrhal fever of cattle is associated with low abundance of IL-2 transcript and a predominantly latent profile of ovine herpesvirus 2 gene expression. *PLoS One*, 4, e6265.
- MEIER-TRUMMER, C. S., TOBLER, K., HILBE, M., STEWART, J. P., HART, J., CAMPBELL, I., HAIG, D. M., GLAUSER, D. L., EHRENSPERGER, F. & ACKERMANN, M. 2009b. Ovine herpesvirus 2 structural proteins in

- epithelial cells and M-cells of the appendix in rabbits with malignant catarrhal fever. *Vet Microbiol*, 137, 235-42.
- MESRI, E. A., CESARMAN, E., ARVANITAKIS, L., RAFII, S., MOORE, M. A., POSNETT, D. N., KNOWLES, D. M. & ASCH, A. S. 1996. Human herpesvirus-8/Kaposi's sarcoma-associated herpesvirus is a new transmissible virus that infects B cells. *J Exp Med*, 183, 2385-90.
- METTENLEITER, T. C., KLUPP, B. G. & GRANZOW, H. 2009. Herpesvirus assembly: an update. *Virus Res*, 143, 222-34.
- MICHEL, A. L. 1993. Generation of a nucleic acid probe specific for the alcelaphine herpesvirus 1 and its use for the detection of malignant catarrhal fever virus DNA in blue wildebeest calves (*Connochaetes taurinus*). *Onderstepoort J Vet Res*, 60, 87-93.
- MILLS, R., ROZANOV, M., LOMSADZE, A., TATUSOVA, T. & BORODOVSKY, M. 2003. Improving gene annotation of complete viral genomes. *Nucleic acids research*, 31, 7041-7055.
- MILNE, E. M. & REID, H. W. 1990. Recovery of a cow from malignant catarrhal fever. *Vet Rec*, 126, 640-1.
- MIRANGI, P. K. 1991. Attempts to immunize cattle against virulent African malignant catarrhal fever virus (alcelaphine herpesvirus-1) with a herpesvirus isolated from American cattle. *Vet Microbiol*, 28, 129-39.
- MORIN, R., BAINBRIDGE, M., FEJES, A., HIRST, M., KRZYWINSKI, M., PUGH, T., MCDONALD, H., VARHOL, R., JONES, S. & MARRA, M. 2008. Profiling the HeLa S3 transcriptome using randomly primed cDNA and massively parallel short-read sequencing. *Biotechniques*, 45, 81-94.
- MORIZANE, Y., HONDA, R., FUKAMI, K. & YASUDA, H. 2005. X-linked inhibitor of apoptosis functions as ubiquitin ligase toward mature caspase-9 and cytosolic Smac/DIABLO. *J Biochem*, 137, 125-32.
- MORTAZAVI, A., WILLIAMS, B. A., MCCUE, K., SCHAEFFER, L. & WOLD, B. 2008. Mapping and quantifying mammalian transcriptomes by RNA-Seq. *Nat Methods*, 5, 621-8.
- MOSSMAN, S. P., LEIB, D. A., MCCARTHY, K. & HART, C. A. 1989. The effects of 5-azacytidine, 12-O-tetradecanoylphorbol 13-acetate and sodium n-butylate on reactivation of alphaherpesvirus saimiri from explant cultures of latently infected rabbit dorsal root ganglia. *J Gen Virol*, 70 (Pt 9), 2507-12.
- MOTT, J. L., ZHANG, D., FREEMAN, J. C., MIKOLAJCZAK, P., CHANG, S. W. & ZASSENHAUS, H. P. 2004. Cardiac disease due to random mitochondrial DNA mutations is prevented by cyclosporin A. *Biochemical and Biophysical Research Communications*, 319, 1210-1215.

- MUSHI, E. & RURANGIRWA, F. 1981. Epidemiology of bovine malignant catarrhal fevers, a review. *Veterinary research communications*, 5, 127-142.
- MUSHI, E., KARSTAD, L. & JESSETT, D. 1980. Isolation of bovine malignant catarrhal fever virus from ocular and nasal secretions of wildebeest calves. *Research in Veterinary Science*, 29, 168-171.
- MUSHI, E., RURANGIRWA, F. & KARSTAD, L. 1981. Shedding of malignant catarrhal fever virus by wildebeest calves. *Veterinary Microbiology*, 6, 281-286.
- MYSTER, F., PALMEIRA, L., SOREL, O., BOUILLENNE, F., DEPAUW, E., SCHWARTZ-CORNIL, I., VANDERPLASSCHEN, A. & DEWALS, B. G. 2015. Viral semaphorin inhibits dendritic cell phagocytosis and migration but is not essential for gammaherpesvirus-induced lymphoproliferation in malignant catarrhal fever. *J Virol*, 89, 3630-47.
- Navada, Shyamala C.; Steinmann, Juliane; Lübbert, Michael; Silverman, Lewis R. (2014). "Clinical development of demethylating agents in hematology". *Journal of Clinical Investigation*. 124 (1): 4-46.
- NELSON, D. D., DAVIS, W. C., BROWN, W. C., LI, H., O'TOOLE, D. & OAKS, J. L. 2010. CD8(+)/perforin(+)/WC1(-) gammadelta T cells, not CD8(+) alphabeta T cells, infiltrate vasculitis lesions of American bison (*Bison bison*) with experimental sheep-associated malignant catarrhal fever. *Vet Immunol Immunopathol*, 136, 284-91.
- NELSON, D. D., TAUS, N. S., SCHNEIDER, D. A., CUNHA, C. W., DAVIS, W. C., BROWN, W. C., LI, H., O'TOOLE, D. & OAKS, J. L. 2013. Fibroblasts express OvHV-2 capsid protein in vasculitis lesions of American bison (*Bison bison*) with experimental sheep-associated malignant catarrhal fever. *Vet Microbiol*, 166, 486-92.
- NICOLL, M. P., PROENÇA, J. T. & EFSTATHIOU, S. 2012. The molecular basis of herpes simplex virus latency. *FEMS microbiology reviews*, 36, 684-705.
- NOURI-ARIA, K. T. 2008. In situ Hybridization. *Methods Mol Med*, 138, 331-47.
- OIE. 2013. Malignant catarrhal fever. Available: http://www.oie.int/fileadmin/Home/eng/Health_standards/tahm/2.04.15_MCF.pdf [Accessed 14/08/2015].
- O'TOOLE, D., LI, H., MILLER, D., WILLIAMS, W. & CRAWFORD, T. 1997. Chronic and recovered cases of sheep-associated malignant catarrhal fever in cattle. *The Veterinary Record*, 140, 519-524.
- OWENS, G. C., ERICKSON, K. L., MALONE, C. C., PAN, C., HUYNH, M. N., CHANG, J. W., CHIRWA, T., VINTERS, H. V., MATHERN, G. W. & KRUSE, C. A. 2015. Evidence for the involvement of gamma delta T cells in the immune response in Rasmussen encephalitis. *J Neuroinflammation*, 12, 134.

- PALMEIRA, L., SOREL, O., VAN CAMPE, W., BOUDRY, C., ROELS, S., MYSTER, F., RESCHNER, A., COULIE, P. G., KERKHOFS, P., VANDERPLASSCHEN, A. & DEWALS, B. G. 2013. An essential role for gamma-herpesvirus latency-associated nuclear antigen homolog in an acute lymphoproliferative disease of cattle. *Proc Natl Acad Sci U S A*, 110, E1933-42.
- PARAMESWARAN, N., DEWALS, B. G., GILES, T. C., DEPPMANN, C., BLYTHE, M., VANDERPLASSCHEN, A., EMES, R. D. & HAIG, D. 2014. The A2 gene of alcelaphine herpesvirus-1 is a transcriptional regulator affecting cytotoxicity in virus-infected T cells but is not required for malignant catarrhal fever induction in rabbits. *Virus Res*, 188, 68-80.
- PELLETT, P. E. & ROZIMAN, B. 2007. Herpesviridae A Brief Introduction *In: KNIPE, D. M. & HOWLEY, P. M. (eds.) Fields Virology*. 5th ed. Philadelphia, USA: Lippincott Williams & wilkins.
- PENG, L., RYAZANTSEV, S., SUN, R. & ZHOU, Z. H. 2010. Three-dimensional visualization of gammaherpesvirus life cycle in host cells by electron tomography. *Structure*, 18, 47-58.
- PERTEA, M., PERTEA, G. M., ANTONESCU, C. M., CHANG, T. C., MENDELL, J. T. & SALZBERG, S. L. 2015. StringTie enables improved reconstruction of a transcriptome from RNA-seq reads. *Nat Biotechnol*, 33, 290-5.
- Pfaffl MW (2004) Quantification strategies in real-time PCR. In: Bustin SA (ed), A-Z of Quantitative PCR, pp. 87-120. La Jolla, CA: IUL Biotechnology Series, International University Line
- PFEFFER, S., ZAVOLAN, M., GRASSER, F. A., CHIEN, M., RUSSO, J. J., JU, J., JOHN, B., ENRIGHT, A. J., MARKS, D., SANDER, C. & TUSCHL, T. 2004. Identification of virus-encoded microRNAs. *Science*, 304, 734-6.
- PFEFFER, S., SEWER, A., LAGOS-QUINTANA, M., SHERIDAN, R., SANDER, C., GRASSER, F. A., VAN DYK, L. F., HO, C. K., SHUMAN, S., CHIEN, M., RUSSO, J. J., JU, J., RANDALL, G., LINDENBACH, B. D., RICE, C. M., SIMON, V., HO, D. D., ZAVOLAN, M. & TUSCHL, T. 2005. Identification of microRNAs of the herpesvirus family. *Nat Methods*, 2, 269-76.
- PLOWRIGHT, W. 1965. MALIGNANT CATARRHAL FEVER IN EAST AFRICA. I. BEHAVIOUR OF THE VIRUS IN FREE-LIVING POPULATIONS OF BLUE WILDEBEEST (GORGON TAURINUS TAURINUS, BURCHELL). *Res Vet Sci*, 6, 56-68.
- PLOWRIGHT, W. 1965. MALIGNANT CATARRHAL FEVER IN EAST AFRICA. II. OBSERVATIONS ON WILDEBEEST CALVES AT THE LABORATORY AND CONTACT TRANSMISSION OF THE INFECTION TO CATTLE. *Res Vet Sci*, 6, 69-83.
- PLOWRIGHT, W., FERRIS, R. D. & SCOTT, G. R. 1960. Blue wildebeest and the aetiological agent of bovine malignant catarrhal fever. *Nature*, 188, 1167-9.

- PLOWRIGHT, W., HERNIMAN, K. A., JESSETT, D. M., KALUNDA, M. & RAMPTON, C. S. 1975. Immunisation of cattle against the herpesvirus of malignant catarrhal fever: failure of inactivated culture vaccines with adjuvant. *Res Vet Sci*, 19, 159-66.
- POLLOCK, J. S., FÖRSTERMANN, U., MITCHELL, J. A., WARNER, T. D., SCHMIDT, H., NAKANE, M. & MURAD, F. 1991. Purification and characterization of particulate endothelium-derived relaxing factor synthase from cultured and native bovine aortic endothelial cells. *Proceedings of the National Academy of Sciences*, 88, 10480-10484.
- POULOS, M. G., BATRA, R., CHARIZANIS, K. & SWANSON, M. S. 2011. Developments in RNA splicing and disease. *Cold Spring Harbor perspectives in biology*, 3, a000778.
- QIU, X., HOTHER, C., RALFKIAER, U. M., SOGAARD, A., LU, Q., WORKMAN, C. T., LIANG, G., JONES, P. A. & GRONBAEK, K. 2010. Equitoxic doses of 5-azacytidine and 5-aza-2'deoxyctidine induce diverse immediate and overlapping heritable changes in the transcriptome. *PLoS One*, 5.
- RAHMAN, A., ALAM, M., RAO, S., CAI, L., LUTHER T, C., SHAFIQ, S. & SIDDIQUI, M. 2001. Differential effects of doxorubicin on atrial natriuretic peptide expression in vivo and in vitro. *Biological research*, 34, 195-206.
- REID, H. W., BUXTON, D., POW, I. & FINLAYSON, J. 1986. Malignant catarrhal fever: experimental transmission of the 'sheep-associated' form of the disease from cattle and deer to cattle, deer, rabbits and hamsters. *Res Vet Sci*, 41, 76-81.
- REID, H. W., BUXTON, D., POW, I., FINLAYSON, J. & BERRIE, E. L. 1983. A cytotoxic T-lymphocyte line propagated from a rabbit infected with sheep associated malignant catarrhal fever. *Res Vet Sci*, 34, 109-13.
- REID, H., BUXTON, D., POW, I. & FINLAYSON, J. 1989. Isolation and characterisation of lymphoblastoid cells from cattle and deer affected with 'sheep-associated' malignant catarrhal fever. *Research in veterinary science*, 47, 90-96.
- ROBERT, N., WONG, G. W. & WRIGHT, J. M. 2010. Effect of cyclosporine on blood pressure. *Cochrane Database Syst Rev*, Cd007893.
- ROMERO, I. G., PAI, A. A., TUNG, J. & GILAD, Y. 2014. RNA-seq: impact of RNA degradation on transcript quantification. *BMC biology*, 12, 42.
- ROSBOTTOM, J., DALZIEL, R. G., REID, H. W. & STEWART, J. P. 2002. Ovine herpesvirus 2 lytic cycle replication and capsid production. *Journal of general virology*, 83, 2999-3002.
- ROSSITER, P. B., MUSHI, E. Z. & PLOWRIGHT, W. 1977. The development of antibodies in rabbits and cattle infected experimentally with an

- african strain of malignant catarrhal fever virus. *Veterinary Microbiology*, 2, 57-66.
- RUSSELL, G. C., BENAVIDES, J., GRANT, D. M., TODD, H., THOMSON, J., PURI, V., NATH, M. & HAIG, D. M. 2012b. Host gene expression changes in cattle infected with Alcelaphine herpesvirus 1. *Virus Res*, 169, 246-54.
- RUSSELL, G. C., BENAVIDES, J., GRANT, D., TODD, H., DEANE, D., PERCIVAL, A., THOMSON, J., CONNELLY, M. & HAIG, D. M. 2012a. Duration of protective immunity and antibody responses in cattle immunised against alcelaphine herpesvirus-1-induced malignant catarrhal fever. *Vet Res*, 43, 51.
- RUSSELL, G. C., SCHOLE, S. F., TWOMEY, D. F., COURTENAY, A. E., GRANT, D. M., LAMOND, B., NORRIS, D., WILLOUGHBY, K., HAIG, D. M. & STEWART, J. P. 2014. Analysis of the genetic diversity of ovine herpesvirus 2 in samples from livestock with malignant catarrhal fever. *Vet Microbiol*, 172, 63-71.
- RUSSELL, G. C., STEWART, J. P. & HAIG, D. M. 2009. Malignant catarrhal fever: a review. *Vet J*, 179, 324-35.
- RUSSELL, G. C., TODD, H., DEANE, D., PERCIVAL, A., DAGLEISH, M. P., HAIG, D. M. & STEWART, J. P. 2013. A novel spliced gene in alcelaphine herpesvirus 1 encodes a glycoprotein which is secreted in vitro. *J Gen Virol*, 94, 2515-23.
- RUSSELL, P. H. 1980. Malignant catarrhal fever virus in rabbits—Reproduction of clinical disease by cell-free virus and partial protection against such disease by vaccination with inactivated virus. *Veterinary Microbiology*, 5, 161-163.
- SCHAEFER, B. C., PAULSON, E., STROMINGER, J. L. & SPECK, S. H. 1997. Constitutive activation of Epstein-Barr virus (EBV) nuclear antigen 1 gene transcription by IRF1 and IRF2 during restricted EBV latency. *Mol Cell Biol*, 17, 873-86.
- SCHALL, T. J., LEWIS, M., KOLLER, K. J., LEE, A., RICE, G. C., WONG, G. H., GATANAGA, T., GRANGER, G. A., LENTZ, R., RAAB, H. & ET AL. 1990. Molecular cloning and expression of a receptor for human tumor necrosis factor. *Cell*, 61, 361-70.
- SCHOCK, A. & REID, H. W. 1996. Characterisation of the lymphoproliferation in rabbits experimentally affected with malignant catarrhal fever. *Vet Microbiol*, 53, 111-9.
- SCHOCK, A., COLLINS, R. A. & REID, H. W. 1998. Phenotype, growth regulation and cytokine transcription in Ovine Herpesvirus-2 (OHV-2)-infected bovine T-cell lines. *Vet Immunol Immunopathol*, 66, 67-81.

- SCHROEDER, A., MUELLER, O., STOCKER, S., SALOWSKY, R., LEIBER, M., GASSMANN, M., LIGHTFOOT, S., MENZEL, W., GRANZOW, M. & RAGG, T. 2006. The RIN: an RNA integrity number for assigning integrity values to RNA measurements. *BMC Mol Biol*, 7, 3.
- SCHULTHEISS, P. C., COLLINS, J. K., AUSTGEN, L. E. & DEMARTINI, J. C. 1998. Malignant catarrhal fever in bison, acute and chronic cases. *J Vet Diagn Invest*, 10, 255-62.
- Schultheiss, P. C., et al. (2000). "Epizootic malignant catarrhal fever in three bison herds: differences from cattle and association with ovine herpesvirus-2." *J Vet Diagn Invest* **12**(6): 497-502.
- SETO, E., MOOSMANN, A., GRÖMMINGER, S., WALZ, N., GRUNDHOFF, A. & HAMMERSCHMIDT, W. 2010. Micro RNAs of Epstein-Barr virus promote cell cycle progression and prevent apoptosis of primary human B cells. *PLoS Pathog*, 6, e1001063.
- SI, H. & ROBERTSON, E. S. 2006. Kaposi's sarcoma-associated herpesvirus-encoded latency-associated nuclear antigen induces chromosomal instability through inhibition of p53 function. *Journal of virology*, 80, 697-709.
- SIMON, S., LI, H., O'TOOLE, D., CRAWFORD, T. B. & OAKS, J. L. 2003. The vascular lesions of a cow and bison with sheep-associated malignant catarrhal fever contain ovine herpesvirus 2-infected CD8(+) T lymphocytes. *J Gen Virol*, 84, 2009-13.
- SMITH, X. G., BOLTON, E. M., RUCHATZ, H., WEI, X., LIEW, F. Y. & BRADLEY, J. A. 2000. Selective blockade of IL-15 by soluble IL-15 receptor alpha-chain enhances cardiac allograft survival. *J Immunol*, 165, 3444-50.
- STAUDT, M. R. & DITTMER, D. P. 2007. The Rta/Orf50 transactivator proteins of the gamma-herpesviridae. *Curr Top Microbiol Immunol*, 312, 71-100.
- STÜBIG, T., BADBARAN, A., LUETKENS, T., HILDEBRANDT, Y., ATANACKOVIC, D., BINDER, T., FEHSE, B. & KRÖGER, N. 2014. 5-Azacytidine promotes an inhibitory T-cell phenotype and impairs immune mediated antileukemic activity. *Mediators of inflammation*, 2014.
- SWA, S., WRIGHT, H., THOMSON, J., REID, H. & HAIG, D. 2001. Constitutive activation of Lck and Fyn tyrosine kinases in large granular lymphocytes infected with the gamma-herpesvirus agents of malignant catarrhal fever. *Immunology*, 102, 44-52.
- SZYF, M., ELIASSON, L., MANN, V., KLEIN, G. & RAZIN, A. 1985. Cellular and viral DNA hypomethylation associated with induction of Epstein-Barr virus lytic cycle. *Proceedings of the National Academy of Sciences*, 82, 8090-8094.
- TAUS, N. S., HERNDON, D. R., TRAU, D. L., STEWART, J. P., ACKERMANN, M., LI, H., KNOWLES, D. P., LEWIS, G. S. & BRAYTON, K. A. 2007.

- Comparison of ovine herpesvirus 2 genomes isolated from domestic sheep (*Ovis aries*) and a clinically affected cow (*Bos bovis*). *J Gen Virol*, 88, 40-5.
- TAUS, N. S., SCHNEIDER, D. A., OAKS, J. L., YAN, H., GAILBREATH, K. L., KNOWLES, D. P. & LI, H. 2010. Sheep (*Ovis aries*) airway epithelial cells support ovine herpesvirus 2 lytic replication in vivo. *Veterinary microbiology*, 145, 47-53.
- TAUS, N. S., TRAU, D. L., OAKS, J. L., CRAWFORD, T. B., LEWIS, G. S. & LI, H. 2005. Experimental infection of sheep with ovine herpesvirus 2 via aerosolization of nasal secretions. *J Gen Virol*, 86, 575-9.
- THONUR, L., RUSSELL, G. C., STEWART, J. P. & HAIG, D. M. 2006. Differential transcription of ovine herpesvirus 2 genes in lymphocytes from reservoir and susceptible species. *Virus Genes*, 32, 27-35.
- TRAU, D. L., ELIAS, S., TAUS, N. S., HERRMANN, L. M., OAKS, J. L. & LI, H. 2005. A real-time PCR assay for measuring alcelaphine herpesvirus-1 DNA. *J Virol Methods*, 129, 186-90.
- TSUJIMOTO, Y. 1998. Role of Bcl-2 family proteins in apoptosis: apoptosomes or mitochondria? *Genes to Cells*, 3, 697-707.
- UPPAL, T., BANERJEE, S., SUN, Z., VERMA, S. C. & ROBERTSON, E. S. 2014. KSHV LANA—The Master Regulator of KSHV Latency. *Viruses*, 6, 4961-98.
- VIRGIN, H. W. T., PRESTI, R. M., LI, X. Y., LIU, C. & SPECK, S. H. 1999. Three distinct regions of the murine gammaherpesvirus 68 genome are transcriptionally active in latently infected mice. *J Virol*, 73, 2321-32.
- WANG, Z., GERSTEIN, M. & SNYDER, M. 2009. RNA-Seq: a revolutionary tool for transcriptomics. *Nat Rev Genet*, 10, 57-63.
- WILHELM, B. T. & LANDRY, J. R. 2009. RNA-Seq-quantitative measurement of expression through massively parallel RNA-sequencing. *Methods*, 48, 249-57.
- WILSON, E., HEDGES, J. F., BUTCHER, E. C., BRISKIN, M. & JUTILA, M. A. 2002. Bovine gamma delta T cell subsets express distinct patterns of chemokine responsiveness and adhesion molecules: a mechanism for tissue-specific gamma delta T cell subset accumulation. *J Immunol*, 169, 4970-5.
- WIYONO, A., BAXTER, S. I., SAEPULLOH, M., DAMAYANTI, R., DANIELS, P. & REID, H. W. 1994. PCR detection of ovine herpesvirus-2 DNA in Indonesian ruminants--normal sheep and clinical cases of malignant catarrhal fever. *Vet Microbiol*, 42, 45-52.

- WRIGHT, H., STEWART, J. P., IRERI, R. G., CAMPBELL, I., POW, I., REID, H. W. & HAIG, D. M. 2003. Genome re-arrangements associated with loss of pathogenicity of the gamma-herpesvirus alcelaphine herpesvirus-1. *Res Vet Sci*, 75, 163-8.
- XU, X., NG, S., WU, Z. L., NGUYEN, D., HOMBURGER, S., SEIDEL-DUGAN, C., EBENS, A. & LUO, Y. 1998. Human semaphorin K1 is glycosylphosphatidylinositol-linked and defines a new subfamily of viral-related semaphorins. *J Biol Chem*, 273, 22428-34.
- YI, H., CHO, Y. J., WON, S., LEE, J. E., JIN YU, H., KIM, S., SCHROTH, G. P., LUO, S. & CHUN, J. 2011. Duplex-specific nuclease efficiently removes rRNA for prokaryotic RNA-seq. *Nucleic Acids Res*, 39, e140.
- YOUN, T. J., PIAO, H., KWON, J. S., CHOI, S. Y., KIM, H. S., PARK, D. G., KIM, D. W., KIM, Y. G. & CHO, M. C. 2002. Effects of the calcineurin dependent signaling pathway inhibition by cyclosporin A on early and late cardiac remodeling following myocardial infarction. *Eur J Heart Fail*, 4, 713-8.
- ZEMLJIC, T., POT, S. A., HAESSIG, M. & SPIESS, B. M. 2012. Clinical ocular findings in cows with malignant catarrhal fever: ocular disease progression and outcome in 25 cases (2007-2010). *Vet Ophthalmol*, 15, 46-52.